In vitro metabolism of tetrazole aminoquinolines and derivatives of metergoline and fusidic acid

Mathew Njoroge

Supervisor: **Professor Kelly Chibale**

Department of Chemistry, University of Cape Town

Thesis presented for the degree of Doctor of Philosophy in the Department of Chemistry,

University of Cape Town

December 2014

UNIVERSITY OF CAPE TOWN

IYUNIVESITHI YASEKAPA • UNIVERSITEIT VAN KAAPSTAD

DECLARATION

I, **Mathew Njoroge**, declare that:

i) this thesis is my own unaided work, both in conception and execution, and that apart from the normal guidance of my supervisors, I have received no assistance apart from that acknowledged;

ii) neither the substance nor any part of the thesis has been submitted in the past, or is being, or is to be submitted for a degree in the University of Cape Town or any other University.

Signed: _____ Date: _____

To all those who believed in me, even when I didn't

Acknowledgements

This PhD work and the associated thesis is the work of many hands.

I'm grateful to Professor Kelly Chibale for his patience, guidance and advice without which this work would not have been possible.

I also thank Elaine Rutherfoord-Jones, whose administrative support has been invaluable, as well as the rest of the departmental and faculty administrative staff.

This journey would have started very slowly without the patience and hard work of my first teachers, Dr. Stefan Louw and Dr. Nyaradzo Chigorimbo-Tsikiwa, who went beyond the call of duty to ensure that I mastered the basics of LC-MS and biotransformation work. I'm also grateful to Drs Matshawe Tukulula, Marlene Espinoza, Kawaljit Singh and to Gurminder Singh and Faith Mjambili whose efforts in synthetic chemistry provided the compounds and the ideas for this work. I also thank the rest of our research group, both present and past generations, for stimulating conversations, encouragement and for the probing questions on metabolism and pharmacokinetics that encouraged me to explore the subject further.

I'm also grateful for the wonderful company of my Kenyan colleagues in Cape Town, both at UCT and elsewhere, for continually setting the bar so high, and for the many warm meals, laughter and words of encouragement which made the journey so much easier.

I also thank to Prof. Pete Smith and Dr. Lubbe Wiesner, of UCT Pharmacology, and their colleagues at the Pharmacokinetics lab for many words of advice, and for logistical support regarding LC-MS work. I'm particularly greatful to Nina Lawrence for many discussions on the setting up and validation of ADME assays, and also for logistical support with this work

I acknowledge the kind support of Dr. Digby Warner and Dr. Vinayak Singh, of the Molecular Mycobacteriology Research Unit, Insitute of Infectious Disease and Molecular Medicine, UCT, for discussions on the *Mycobacterial* lysate work and for production of lysate and supernatant.

The hepatocyte MetID and CYP450 inhibition work was performed during a research internship at the Novartis Institute of Biomedical Research, Basel. I'm grateful to my internship mentors, Olivier Heudi and Jacques Kameni-Tcheudji both for their patience and guidance during the internship. I also thank Hilmar Schiller, Judith Streckfuss for assistance

with the CYP450 inhibition assays; Ulrike Glaenzel and Robert Nuffer for the hepatocyte metabolite identification work, and the rest of their colleagues in the Drug Metabolism and Pharmacokinetics department for their kind assistance. I sincerely thank the Diversity and Inclusion department, especially Colin Pillai and Rita Michel for organising the program and for their inspiration both during and after the program.

I'm grateful to the funders – the Department of Science and Technology, through the MRC Research Chairs program and the Department of Chemistry, University of Cape Town.

Finally, I end at the beginning. One of the big questions about this PhD journey is why anyone would possibly want to go through it. While a variety of answers exist, for me, its my love of science and my curiosity of its mysteries that drives me. This were inculcated into me by my parents and reinforced by growing up with my siblings. I don't think I have the words, or indeed that the words exist, that would express my gratitude for their love, support, encouragement throughout my studies, and beyond. My interest in science was further reinforced by two great teachers, one in primary school and one in highschool, both co-incidentally called Mr. Macharia. I'm grateful to them and their colleagues over the ages for getting me to where I am. I'm also grateful for the inspiration of another teacher, this time a lecturer I met in the 4th year at School of Pharmacy, Dr. Faith Okalebo for encouraging me to dream big and for getting me started on this journey.

And the ultimate beginning and end, to God be all honor and praise

Abstract

Drug metabolism is recognised as a key component of the drug discovery and development process. It exerts an influence on the action, duration of action and toxicity of a drug *in vivo.* The integration of drug metabolism studies is therefore crucial to compound progression through the various stages of the development process. This work details the *in vitro* metabolism work conducted during the early development of aminoquinoline tetrazoles, and derivatives of metergoline and fusidic acid as potential antiplasmodial and/or antimycobacterial agents.

An investigation of the *in vitro* metabolism of a series of deoxyamodiaquine tetrazoles found that the most active compounds were rapidly metabolised by oxidation and dealkylation on the tertiary nitrogen substituents. The compounds were also potent CYP450 inhibitors, with submicromolar IC_{50}s for CYP450 2C8 and 3A4 and moderate inhibition of most other CYP450s. While these compounds did not show glutathione adduct formation as reported for amodiaquine, compounds with cycloalkyl substituents on the tertiary nitrogen formed cyanide adducts.

The chloroquine tetrazole analogues were in general less metabolically stable than chloroquine. The main metabolic pathway for these derivatives was aminoquinoline *N*-oxidation and *tert*-butyl hydroxylation. While the P450 inhibition potency of these compounds was lower than that of the deoxyamodiaquine tetrazoles, they displayed submicromolar inhibition of CYP3A4. Interestingly, for a series of chloroquine analogues, these compounds also show evidence of glutathione adduct formation on the 4-aminoquinoline nucleus. This is hypothesised to result from the ‘masked aniline’ nature of the aminoquinoline ring.

The metergoline analogues investigated were in general more metabolically stable than metergoline. This was attributable to the better stability of the amide linker relative to its carbamate counterpart in metergoline, as evidenced by the lack of formation of 8β-aminomethyl-1,6-dimethylergoline in incubations of the amide derivatives. Metabolism was mainly on the ergoline nucleus by hydroxylation and *N*-demethylation. However, alkyl hydroxylation was also observed among derivatives with alkyl chains longer than ethyl, either substituted directly on the amide bond, or substituted on a phenyl ring.

Fusidic acid underwent species specific metabolism to a metabolite tentatively identified as 3-epifusidic acid that was only formed in rat and mouse liver microsomes. This metabolite was detected in all derivatives with a free C-3 OH and in 3-ketofusidic acid. The formation of this metabolite is hypothesised to result from C-3 oxidation followed by non-stereoselective reduction to give fusidic acid and 3-epifusidic acid. Fusidic acid and most of its derivatives were also metabolised by C-3 oxidation to the respective 3-keto- derivatives and by hydroxylation. C-3 esters but not their C-21 counterparts were hydrolysed in microsomes and plasma to fusidic acid. Fusidic acid was also found to undergo metabolism in a *Mycobacterium smegmatis* lysate but not in *Mycobacterium tuberculosis* supernatant or in the buffer control, to form fusidic acid lactone. This process has been associated with fusidic acid resistance in certain species of *Nocardia* and *Streptomyces.*

These findings will be useful in the further exploration of these compounds as antiplasmodial and/or antimycobacterial agents.

List of abbreviations

PK	Pharmacokinetics
AO	Aldehyde oxidase
CES	Carboxylesterase
CYP450	Cytochrome P450
GSH	Reduced glutathione
GST	Glutathione S-transferases
HLM	Human Liver Microsomes
MLM	Mouse Liver Microsomes
RLM	Rat Liver Microsomes
NADPH	Reduced β-Nicotinamide Adenine Dinucleotide 2'-Phosphate
UDPGA	Uridine-5'-diphosphate Glucuronosyl Transferases
UGT	Uridine-5'-diphosphate-α-D-glucuronic acid
LC	Liquid Chromatography
MS	Mass Spectrometry
XIC	Extracted Ion Chromatogram
TIC	Total Ion Chromatogram
CID	Collision Induced Dissociation
H/D	Hydrogen/Deuterium exchange
ESI	Electrospray ionisation
EPI	Enhanced Product Ion spectrum
EMS	Enhanced Mass Spectrum
MRM	Multiple Reaction Monitoring

PI	Precursor Ion
NL	Neutral Loss
QSAR	Quantitative Structure Activity Relationship
TPSA	Total Polar Surface Area
SAR	Structure Activity Relationship
DMSO	Dimethyl Sulfoxide
PBS	Phosphate Buffered Saline
NAPQI	N-acetyl-*para*-quinoneimine
KCN	Potassium Cyanide
MTC	Minimum Toxic Concentration
MEC	Minimum Effective Concentration

Table of contents

List of figures

List of tables

Publications

Publications arising from this thesis

(1) Tukulula, M.; **Njoroge, M**.; Mugumbate, G. C.; Gut, J.; Rosenthal, P. J.; Barteau, S.; Streckfuss, J.; Heudi, O.; Kameni-Tcheudji, J.; Chibale, K. Tetrazole-Based Deoxyamodiaquines: Synthesis, ADME/PK Profiling and Pharmacological Evaluation as Potential Antimalarial Agents. *Bioorg. Med. Chem.* **2013**, *21*, 4904–4913.

(2) Tukulula, M.; **Njoroge, M**.; Abay, E. T.; Mugumbate, G. C.; Wiesner, L.; Taylor, D.; Gibhard, L.; Norman, J.; Swart, K. J.; Gut, J.; et al. Synthesis and in Vitro and in Vivo Pharmacological Evaluation of New 4-Aminoquinoline-Based Compounds. *ACS Med. Chem. Lett.* **2013**, *4*, 1198–1202.

Other Publications

(3) **Njoroge, M**.; Njuguna, N. M.; Mutai, P.; Ongarora, D. S. B.; Smith, P. W.; Chibale, K. Recent Approaches to Chemical Discovery and Development Against Malaria and the Neglected Tropical Diseases Human African Trypanosomiasis and Schistosomiasis. *Chem. Rev.* **2014**, *114 (22)*, 11138

(4) Kigondu, E. M.; **Njoroge, M**.; Singh, K.; Njuguna, N.; Warner, D. F.; Chibale, K. Synthesis and Synergistic Antimycobacterial Screening of Chlorpromazine and Its Metabolites. *Medchemcomm* **2014**, *5*, 502.

(5) Denti, P.; Sharp, S.-K.; Kröger, W. L.; Schwager, S. L.; Mahajan, A.; **Njoroge, M**.; Gibhard, L.; Smit, I.; Chibale, K.; Wiesner, L.; et al. Pharmacokinetic Evaluation of Lisinopril-Tryptophan, a Novel C-Domain ACE Inhibitor. *Eur. J. Pharm. Sci.* **2014**, *56*, 113–119.

(6) Mjambili, F.; **Njoroge, M**.; Naran, K.; De Kock, C.; Smith, P. J.; Mizrahi, V.; Warner, D.; Chibale, K. Synthesis and Biological Evaluation of 2-Aminothiazole Derivatives as Antimycobacterial and Antiplasmodial Agents. *Bioorg. Med. Chem. Lett.* **2014**, *24*, 560–564.

(7) Chigorimbo-Murefu, N. T. L.; **Njoroge, M**.; Louw, S.; Mugumbate, G.; Chibale, K. Drug Metabolite Generation Using a Laboratory Evolved NADPH Independent Cytochrome P450: Application of in Vitro and in Silico Approaches. *Drug Metab. Lett.* **2013**, *7*, 68–77.

(8) Chigorimbo-Murefu, N. T. L.; **Njoroge, M**.; Nzila, A.; Louw, S.; Masimirembwa, C.; Chibale, K. Biotransformation and Biocatalysis: Roles and Applications in the Discovery of Antimalarials. *Future Med. Chem.* **2012**, *4*, 2325–2336.

(9) Louw, S.; **Njoroge, M**.; Chigorimbo-Murefu, N.; Chibale, K. Comparison of Electrospray Ionisation, Atmospheric Pressure Chemical Ionisation and Atmospheric Pressure Photoionisation for the Identification of Metabolites from Labile Artemisinin-Based Anti-Malarial Drugs Using a QTRAP® Mass Spectrometer. *Rapid Commun. Mass Spectrom.* **2012**, *26*, 2431–2442.

Conference attendance

1. 1st H3D symposium. October 15th – 18th, **2012**. Cape Town, South Africa. (Poster presentation)

2. 10th International ISSX meeting. September 29th – October 3rd, **2013.** Toronto, Canada. (Poster presentation)

3. 17th World Congress of Basic and Clinical Pharmacology. July 13th – 18th, **2014**. Cape Town, South Africa. (Poster presentation)

4. 2nd H3D symposium. August 27th – 29th, **2014**. Livingstone, Zambia. (Poster presentation)

“The Road goes ever on and on
Down from the door where it began.
Now far ahead the Road has gone,
And I must follow, if I can,
Pursuing it with eager feet,
Until it joins some larger way
Where many paths and errands meet.
And whither then? I cannot say.”

“Still round the corner there may wait
A new road or a secret gate,
And though we pass them by today,
Tomorrow we may come this way
And take the hidden paths that run
Towards the Moon or to the Sun.”

(The Lord of the rings)

J.R.R TOLKIEN

Chapter 1

INTRODUCTION & LITERATURE REVIEW

"*In order to understand the actions of drugs it is an absolute necessity to have knowledge of the transformations they undergo in the body. It is obvious that we must not judge drugs according to the form and amount administered, but rather according to the form and amount which actually is eliciting the action*." **Bucheim 1859**[1]

1.1 Chapter overview

In this chapter, a broad introduction on the relevance of metabolism to xenobiotic clearance is provided. The major classes involved in the metabolism of drugs and drug-like compounds are presented and their relevance to the medicinal chemistry process in drug discovery discussed, followed by a discussion on drug metabolism systems. An overview of LC-MS as an analytical tool in early drug metabolism studies is also provided. Finally, the justification and aims of this work are provided.

1.2 Absorption Distribution Metabolism and Excretion (ADME)

The activity of a drug *in vivo* is dependent not only on its ability to act at the relevant target but on the concentration of the drug that is available at the site of action and the duration for which it is available. For many drugs, these factors are determined by the interplay of four processes - Absorption, Distribution, Metabolism and Excretion, also referred to by the acronym ADME. [2]

Orally administered drugs first undergo dissolution in the gastrointestinal tract and are then either passively or actively absorbed through the gastrointestinal walls into the systemic circulation. They then distribute into various body compartments based on the drug's physicochemical characteristics. Drugs in systemic circulation are also subject to metabolic and excretory processes. The interaction of all these processes results in a change in drug concentration over time and this has been referred to as the pharmacokinetics of the drug. [2]

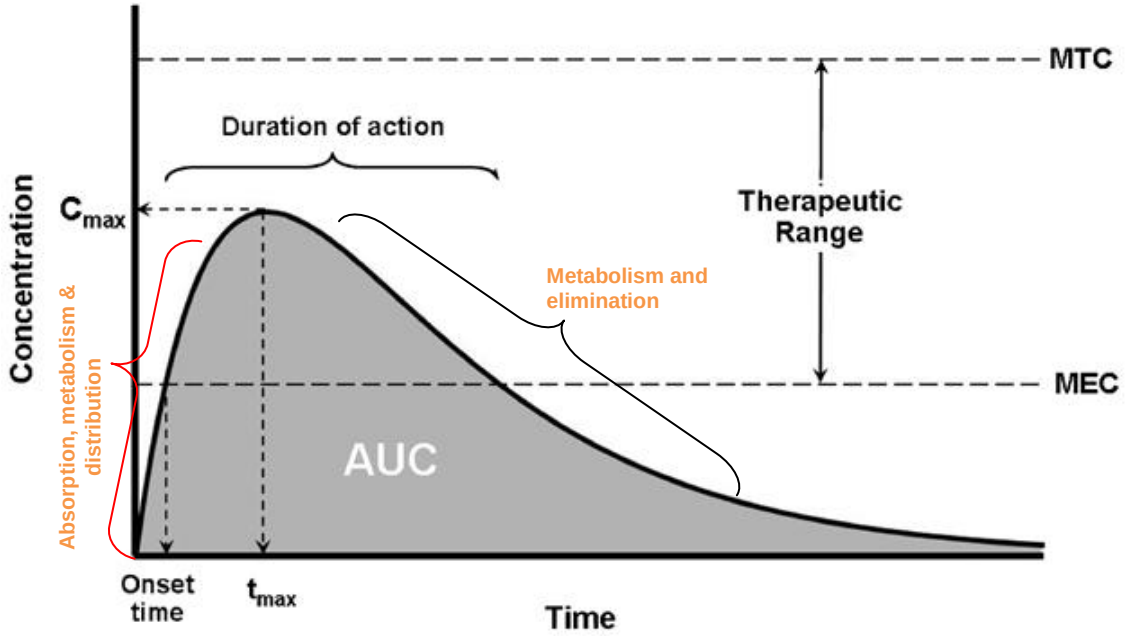

Figure 1.1: Drug pharmacokinetics following oral dosing[3]

The pharmacokinetics of a drug will determine whether the minimum effective concentration is reached, how long it is maintained for and whether toxic effects are produced. From this perspective, it is unsurprising that failure rates of 40% were observed in drug discovery eras where pharmacokinetic studies were not closely integrated into the development process (Figure 1.2).[4] This figure has been suggested to be even higher because pharmacokinetics may be a major contributor to failures attributed to efficacy and toxicity. [5]

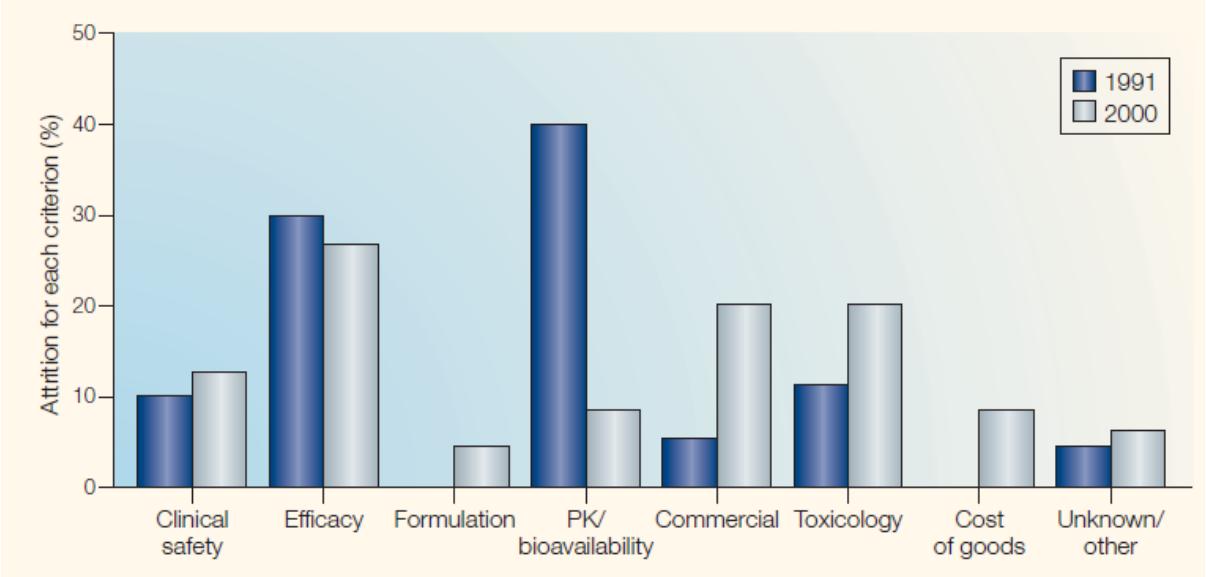

Figure 1.2: Reasons for attrition from clinical drug development[4]

1.3 Drug metabolism

Xenobiotics, foreign compounds present in living systems, pose a continuing danger to the organism and constantly need to be eliminated to maintain life.[6] Metabolism is the process by which xenobiotics are chemically modified so as to facilitate their elimination and/or to detoxify them. The same enzymes systems are also involved in the biosynthesis and homeostasis of various endogenous molecules required to maintain normal function e.g. steroid hormones. Metabolism is thus important in preventing accumulation of xenobiotics and endogenous molecules.[7] As will be discussed later, metabolism, while primarily a detoxifying process, is also implicated in the formation of toxic species which may adversely affect biological processes.

Metabolism usually proceeds by reducing the lipophilicity of the targeted xenobiotic therefore preventing its reabsorption during excretion. This point underlies an important relationship – the physicochemical characteristic of a drug are important in determining the route of its excretion. This knowledge has been distilled into various predictive systems most of all the Biopharmaceutics Drug Disposition Classification System (BDCS) – an extension

of the previously reported Biopharmaceutics Classification System (BCSD) – which attempts to predict the elimination route of compounds based on their solubility and permeability.[8]

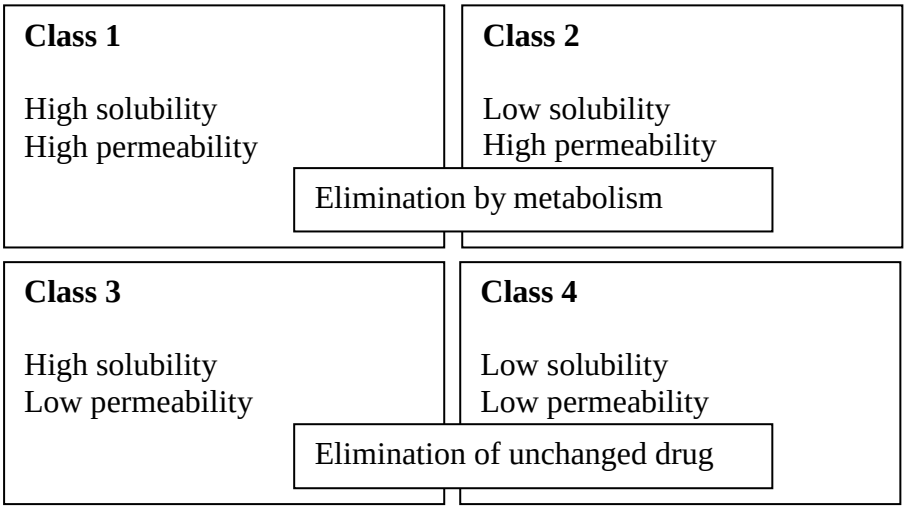

Figure 1.3: Relationship between solubility and permeability and excretion[8]

This relationship exists because highly permeable drugs – usually lipophilic as well – will tend to diffuse more efficiently into drug metabolising cells like hepatocytes and will also be more efficiently reabsorbed following renal excretion ensuring that they stay in circulation until metabolic processes make them hydrophilic enough for excretion.

Metabolism has traditionally been divided into phase I metabolism, consisting mostly of oxidoreductive and hydrolytic processes and phase II metabolism which mainly involves conjugation of endogenous molecules to polar functional groups in the drug either originally present in the drug, or introduced/unmasked during phase I metabolism.[9,10] These phases are not necessarily sequential and will not necessarily occur on the same compound. Testa and co-workers reported that redox reactions account for up to 70% of first generation metabolites with the importance of conjugation reactions increasing with the generation until they account for almost 50% of metabolites in the third and subsequent generations.[11]

1.4 Drug metabolising enzymes

Drug metabolism mainly occurs in the liver though other organs like skin, lungs and blood (both cells and plasma) make important contributions to the biotransformation of certain drugs. In line with the role of metabolism in the clearance of xenobiotics, many drug metabolising enzymes with widely differing substrate specificities are expressed in man. A recent review of over 1000 xenobiotics, cytochrome P450 enzymes were found to account for up to 40% of metabolites formed, with uridine diphosphate-glucuronyl transferases (UGTs), dehydrogenases, hydrolases, glutathione transferases and sulfotransferases also making significant contributions.[11] An overview of the major classes follows.

1.4.1 Cytochrome P450 enzymes

1.4.1.1 Nomenclature

The Cytochrome P450 enzymes (P450s) are a super-family of haem containing mono-oxygenases with more than 21000 named members across different species.[12,13] The 'P450' name was ascribed based on a characteristic spectrophotometric absorbance maximum at 450nm.[14] The human genome contains at least 57 genes involved in P450 expression.[12,13] The P450s are expressed as membrane-bound enzymes in almost all tissues, usually in the endoplasmic reticulum but also in mitochondria. They are classified based on amino acid sequence identity, with those sharing at least 40% identity being grouped into a family denoted by a number e.g. CYP1. These families are further divided into subfamilies denoted by a letter – members of a subfamily have at least 55% sequence identity for example CYP1A. Finally, a number is assigned to each isoform in a subfamily e.g. CYP1A1 and CYP1A2.[15] Mammals have 18 families and 43 subfamilies of P450s.[12,13] Families 1-3 are the most involved in xenobiotic metabolism, while the others are predominantly involved in the biosynthesis of sterols, fatty acids and other endogenous compounds.[16] In mice, it has been shown that deletion of *Cyp2c, Cyp2d, and Cyp3a* gene clusters results in viable and fertile

individuals with minor phenotypic changes, showing that these genes are mostly involved in xenobiotic metabolism. A review of the primary clearance mechanism for 200 drugs showed that CYP 3A4, 2C9, 2C19, 2D6 and 1A2 in that order are the most important for drug metabolism, accounting for the metabolism of more than 90% of the reviewed drugs that were metabolised by CYP450s.[17]

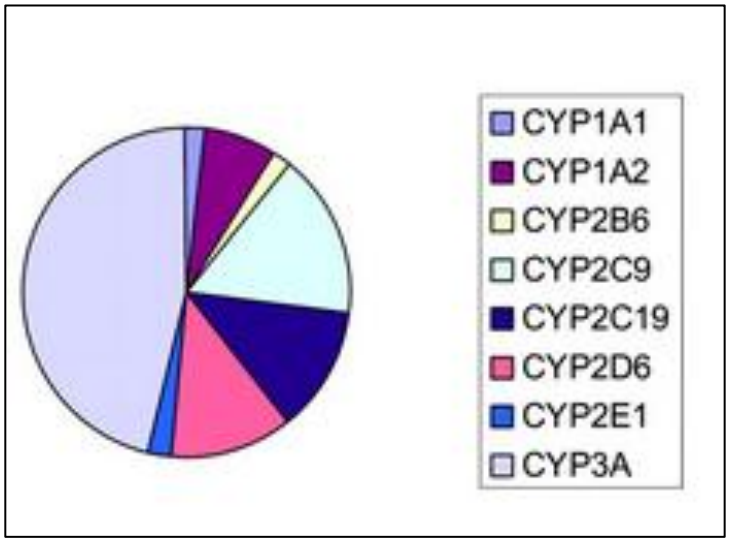

Figure 1.4: CYP450s most commonly involved in drug metabolism[17]

1.4.1.2 Structure

P450s usually consist of 480 – 560 amino acids and a ferriprotoporphyrin-9 prosthetic group anchored to the protein by a cysteine residue. As already mentioned, variations in the amino acid sequence lead to the different isoforms while the FP-9 is preserved across all P450s. FP-9 in its resting state consists of iron as Fe^{3+} in a hexacooordinated state with 4 pyrrole nitrogens, the sulfur from the cysteine residue and a molecule of water, which is displaced by substrate binding.[18]

1.4.1.3 Mechanism

In general, P450s act by activating molecular oxygen to reactive species which can participate in reactions with less active reaction centres in their substrates leading to their chemical transformation. The general catalytic cycle is shown in Figure 1.5.

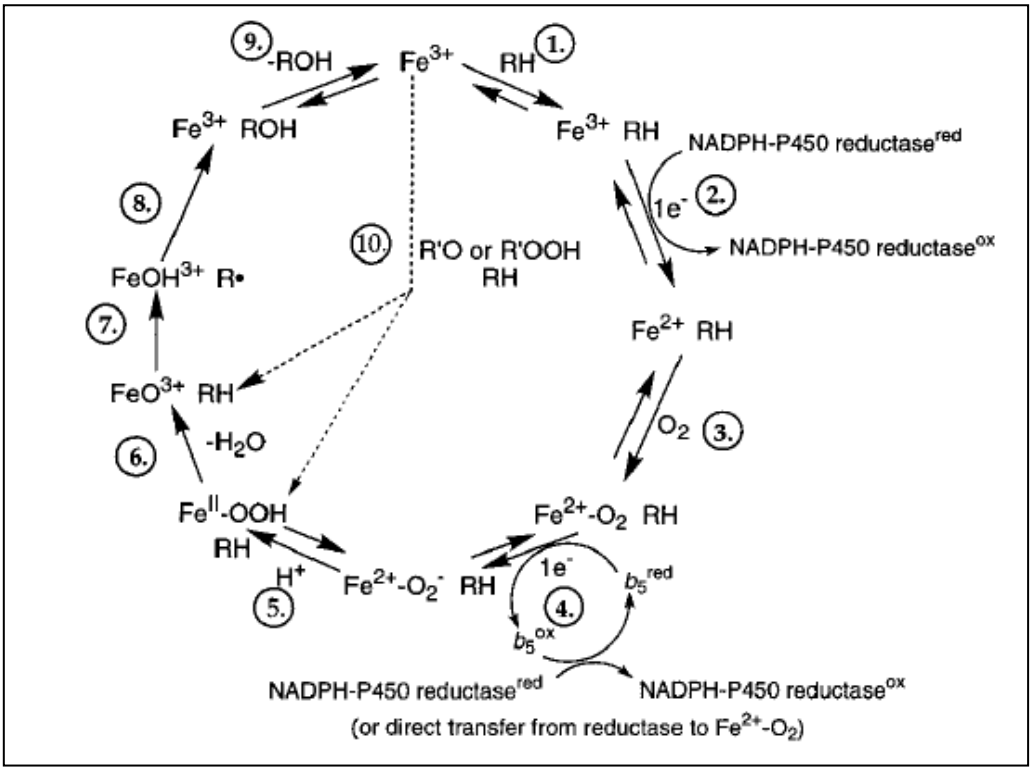

Figure 1.5: General catalytic cycle for P450 metabolism[19]

The cycle begins by the binding of the substrate to the enzyme displacing a molecule of water and resulting in changes in the electronic configuration of the iron to its high spin pentacoordinated form. This low to high spin change facilitates the electron transfer from NADPH in the second step by increasing the redox potential of heme.[20] The ferrous intermediate produced from the second step is also responsible for the characteristic spectrophotometric absorbance of P450s through reversible binding to carbon monoxide. This ferrous intermediate binds to oxygen (step 3) producing an unstable complex which receives the second electron from NADPH reductase (step 4). This is followed by protonation

(step 5) and then heterolytic cleavage of the O-O bond (step 6) to yield a highly reactive FeO^{3+} complex which is the oxidising species in most P450 reactions. This complex abstracts an electron or proton from the substrate (step 7) and the subsequent rebound leads to oxidation of the substrate (step 8). The cycle then ends with the release of the metabolised susbtrate.[21–23]

Several points arising from this catalytic cycle are of relevance to subsequent discussions on drug metabolism and to its prediction by *in silico* tools. First, binding of the substrate in step 1 is governed by the 3D structure of the substrate and the enzyme. However, the structure of the metabolite formed is not necessarily discernible from this step as it is more dependent on the geometry and chemical reactivity of the complex formed in step 7.[24] Secondly the high reactivity of the $(FeO)^{3+}$ species means that unlike in other enzymes, the structure of the protein is not important in determining the mechanism of metabolism. This accounts for the high substrate and reaction promiscuity observed with P450s relative to other enzymes.[25] Thirdly, when considering a particular reaction by a specific P450 enzyme on a group of related substrates, step 7, i.e. the abstraction of hydrogen or an electron, is the rate limiting step.[23] Reaction regioselectivity is thus partially controlled by the energy involved in hydrogen abstraction and by the stability of the resulting carbon radical. It should be emphasised though that as mentioned under the first point, the orientation of the substrate, as determined by its 3-dimensional interaction with the active site and nearby amino acids is also crucial to the determination of regioselectivity.

Based on variations in the structure and subsequent rearrangement of the $(FeO)^{3+}$ - substrate complex formed in step 7, P450 reactions may be divided into six categories; carbon (sp^3) hydroxylation, heteroatom release, heteroatom oxygenation, epoxidation, oxidative group transfer and olefinic suicide destruction.

Carbon hydroxylation involves abstraction of a hydrogen radical by $(FeO)^{3+}$ with the resulting 'oxygen rebound' – reaction of the carbon radical with the –OH on the iron – leading to the hydroxylated product.[23] The implications of this mechanism is that a C-H bond is required on the carbon to be hydroxylated although a C-H bond on an adjacent carbon may rearrange after hydrogen radical abstraction to form a more stable intermediate.[26] In addition, subject to the orientation of the substrate in the active site, the reactivity of the C-H bond will determine the regioselectivity. Based on the energy required for hydrogen abstraction, benzylic carbons are the most easily hydroxylated, followed by allylic and then aliphatic carbons. Branching increases the stability of the radical intermediate and tertiary carbons are therefore more susceptible than secondary carbons.[26] For long chain hydrocarbons with no activated positions, substrate orientation in relation to the active site leads to ω and ω-1 hydroxylation despite the less favourable energetics. The basic features of this mechanism (hydrogen abstraction followed by oxygen rebound) are also implicated in alcohol oxidation to carbonyl and subsequently carboxylic acid.[19,27]

Heteroatom oxygenation occurs with substrates containing N, S, P and I. The mechanism is thought to involve sequential electron abstraction from the heteroatom followed by oxygen rebound to form the heteroatom oxide.

Heteroatom release may be seen as a mix of heteroatom oxygenation and carbon hydroxylation. It occurs by electron abstraction from the heteroatom with subsequent radical delocalisation and proton abstraction on the carbon α to the heteroatom yielding a carbon radical. This is then hydroxylated to form an unstable carbinol which rearranges to release the alkyl group.[19,23]

Epoxidation, oxidative group migration and olefinic suicide inactivation all occur when the substrate has double bonds or is aromatic in nature. The mechanism of oxidation of these

groups of compounds is thought to involve an epoxide intermediate. With alkenes the reactivity of this epoxide leads to reaction with the home leading to inactivation of the enzyme (olefinic suicide inactivation). In some cases though, the epoxide is stable enough to be observed as a metabolite. In most cases it rearranges through protonation to form a phenol (in the case of phenyl rings) or other hydroxylated aromatic group. With aromatic groups, the observation of a 3,4 hydrogen shift was previously thought to be evidence of the epoxide intermediate. However, other mechanisms, for example electrophilic addition of FeO^{3+} to the aromatic group have also been shown to be plausible. Based on these mechanistic considerations, aromatic hydroxylation is driven both by steric and electronic considerations.[28,29]

The reactions discussed above and relevant examples from marketed drugs are summarised in Table 1.1.

Table 1.1: Reactions catalysed by Cytochrome P450 enzymes

Mechanistic category	Reaction	Example
Carbon (sp3) hydroxylation	Aliphatic hydroxylation[30]	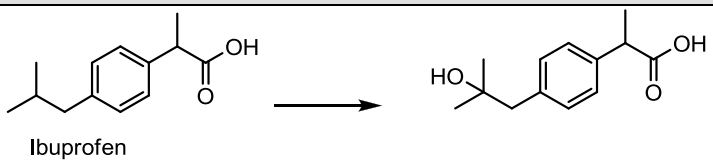 Ibuprofen
	Benzylic oxidation[31]	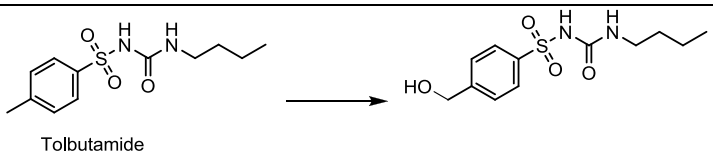 Tolbutamide
	Alcohol/Aldehyde oxidation[27]	$CH_3CH_2OH \longrightarrow CH_3CHO \longrightarrow CH_3COOH$
Heteroatom oxygenation	*N*-oxidation[32]	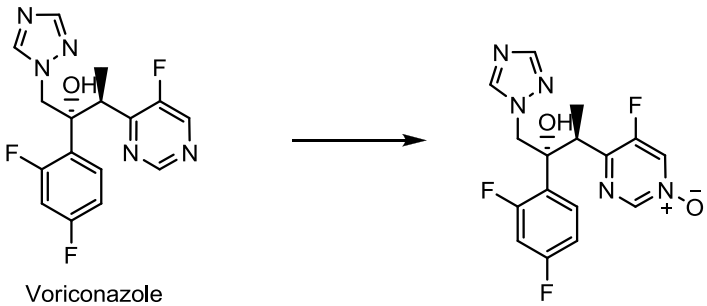 Voriconazole
	S-oxidation[33]	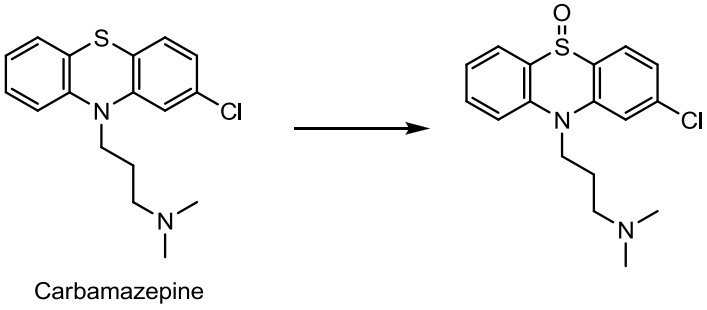 Carbamazepine
Mechanistic category	Reaction	Example

Heteroatom release	O-dealkylation[34]	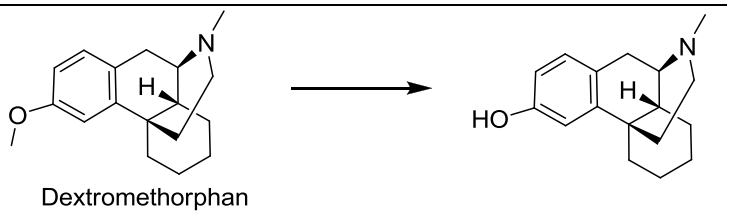 Dextromethorphan
	N-dealkylation[34]	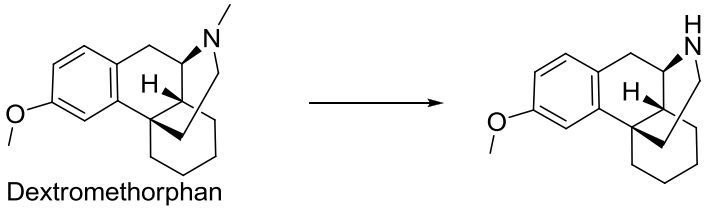 Dextromethorphan
	Oxidative cleavage of esters[35] (and amides, carbamates, ureas etc)	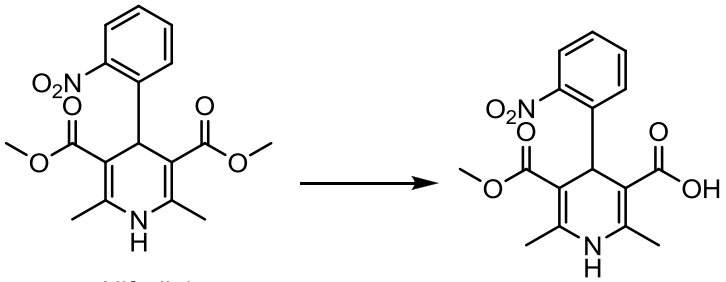 Nifedipine
Epoxidation	Aromatic oxidation[36]	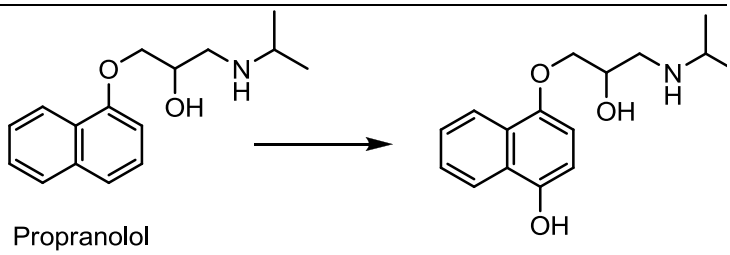 Propranolol
	Alkene epoxidation[37]	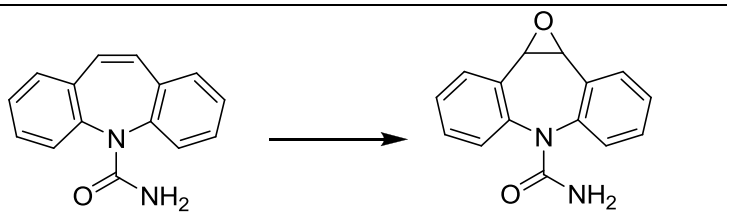 Carbamazepine

1.4.1.4 Prediction of CYP450 metabolism

The role of CYP450s in the metabolism of drugs has led to a high level of interest in predicting such metabolism *in silico.* The ultimate aim of such work is to improve the efficiency of medicinal chemistry programs by identifying such metabolically labile sites before synthesis, leading to production of metabolically stable compounds from the beginning. *In silico* models for CYP450 metabolism prediction can be broadly classified into quantitative structure activity relationship-(QSAR)-based and structure-based methods. QSAR-based models are statistical relationships between calculated molecular properties and the rate of metabolism or an equivalent surrogate.[38] They are by their nature heavily dependent on the robustness of the data used in their creation and this may sometimes limit their application. In contrast, structure-based methods consider the structure of the compound and/or enzyme, either in its entirety as 2D or 3D model or as fragments derived from the parent structure. These methods will often use rule-based, docking, quantum mechanical criteria or a combination of some or all of these (sometimes in combination with QSAR models) to predict CYP450 metabolism.[39]

StarDrop, the *in silico* tool used in this work, uses a quantum mechanical-based model for the prediction of metabolism by CYP3A4, CYP2D6 and CYP2C9, which together account for the metabolism of more than 90% of clinical compounds.[40] The software predicts the regioselectivity of metabolism for the three CYP450s and in addition gives a measure of the lability of the site of metabolism for CYP3A4. The regioselectivity is calculated based on the intrinsic vulnerability to metabolism of a given site and the accessibility of the site as determined from the 3D structure of the compound. Since the rate limiting step in CYP450 metabolism is often the hydrogen atom abstraction, the Arrhenius equation can be applied to relate the rate of metabolism at a particular site to the negative exponent of the activation energy of hydrogen atom abstraction at the site. This activation energy must be calculated for

each site of metabolism, and the calculations are, therefore, computationally intensive if done *ab initio.* Instead, StarDrop uses the AM1 semi-empirical technique, and corrects for systematic errors using data from *ab initio* calculations.[41,42] This dramatically lowers the computational resources required for the prediction but still requires a few minutes per compound on an ordinary desktop. This was about 5 – 10min for compounds reported in this work. As discussed earlier, the similarity in oxidising species (FeO^{3+}) between CYP450s, implies that the mechanistic aspects of metabolism are independent of the enzyme and can be determined using the structure of the compound only. However, the relative contribution of intrinsic reactivity and accessibility for a given site of metabolism will vary based on the structure of the CYP450 being considered and the model parameters in StarDrop are therefore trained using a set of experimentally observed metabolites. The overall success of StarDrop in predicting the top 3 metabolites formed is comparable to that of docking-based algorithms like MetaSite.[39] StarDrop was selected for this work because it offers an integrated tool, able to perform not only P450 modelling, but a range of ADME predictions, de novo design and library management, allowing more efficient collaboration between the chemistry and ADME-DMPK teams.

1.4.2 Molybdenum hydroxylases

1.4.2.1 Structure and occurrence

Molybdenum hydroxylases are a family of molybdenum-containing flavoenzymes found in almost all organisms.[43,44] In higher organisms, the molybdenum is typically present in the form of a tetracyclic pterin-based complex referred to as molybdenum-cofactor (MoCo).[43–45] In human and experimental animal drug metabolism, the most relevant of the molybdoflavoenzymes are aldehyde oxidase and xanthine oxidase. The physiological role of aldehyde oxidase is still unclear though vitamin and serotonin catabolism have been proposed, xanthine oxidase has a clearer role in the catabolism of purine nucleotides.[45] Both enzymes share a similar protein structure and are located in the cell cytosol predominantly in the liver, but also in plasma, lungs, gastrointestinal tract and kidneys.[46] While xanthine oxidase activity is similar across species, there are significant differences in the activity of aldehyde oxidase across common lab species, complicating inter-species extrapolation of pharmacokinetic data.[46–48] Aldehyde oxidase activity is highest in monkeys and humans, lower in rodents and completely absent in dogs. There are also significant inter-strain and inter-individual differences in rats and even sex differences in mice.[46,47,49] Aldehyde oxidase is of greater importance amongst the molybdenum hydroxylases and the discussions that follow therefore centre on it.

1.4.2.2 Mechanism

The general mechanism for the metabolism of substrates by aldehyde and xanthine oxidase is broadly similar and involves the nucleophilic attack of the substrate by Mo-Co followed by substrate release through a reaction between water and the tetrahedral substrate enzyme complex. An example of this mechanism for the oxidation of phtalazine by aldehyde oxidase is shown in Figure 1.6

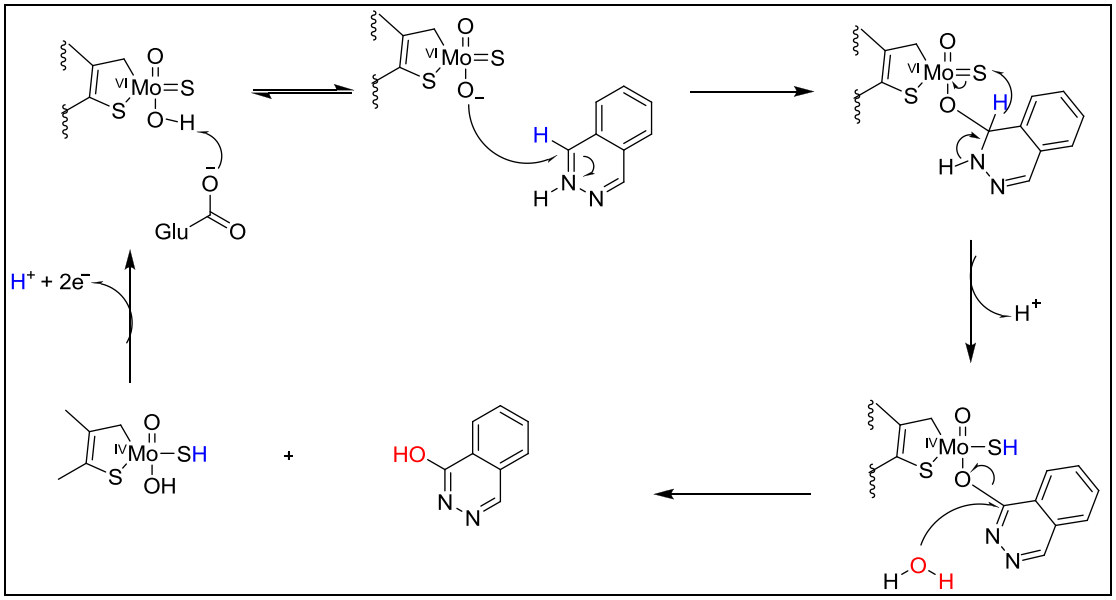

Figure 1.6: Oxidation of phthalazine by aldehyde oxidase (Modified from Pryde et al[47])

The catalytic cycle starts with base-catalysed deprotonation of the Mo-OH. This has been proposed to occur through a glutamate residue, with Glu-1261 being the most obvious by nature of its position in the active site of the enzyme. This facilitates nucleophilic attack of the substrate to form a tetrahedral substrate-enzyme complex.[43,46–48] The free energy of this intermediate has been reported to be predictive of the metabolite formed for AO but not XO.[50] Hydride transfer from the substrate to the enzyme then occurs changing the oxidation state of molybdenum from +6 to +4. A nucleophilic attack by water releases the oxidised substrate and the enzyme is regenerated by a transfer of $2e^-$ to FAD and by loss of a proton.[43,46–48] The net reaction is:

$$RH + H_2O \longrightarrow ROH + 2H^+ + 2e^-$$

This catalytic cycle differs from that of P450s in two key aspects: first the oxygen atom incorporated into substrates arises from water and not from molecular oxygen; secondly, reducing equivalents are generated as a result of the reaction whereas they are consumed during metabolism by CYP450s.[43,46,48]

1.4.2.3 Medicinal chemistry relevance

A possible unintended effect of the literature trove that exists for CYP450 metabolism has been the growth in medicinal chemistry approaches to minimise or avoid P450 metabolism, resulting in a growing importance of otherwise minor metabolic pathways.[47] As an example, the synthesis of electron deficient heterocycles reduces the potential for P450 metabolism but increases the potential of metabolism by aldehyde oxidase, which relies upon nucleophilic attack. A recent review found that up to 56% of compounds in selected libraries contain substructures that could predispose them to aldehyde oxidase metabolism.[47]

1.4.2.3.1 Oxidation of aromatic heterocycles

From a medicinal chemistry point of view, the most important reaction of aldehyde oxidase is the oxidation of aromatic heterocyclic moieties, usually on a carbon next to nitrogen.[47] This is particularly important because of the increasing presence of nitrogen containing aromatic heterocycles in drug discovery. As would be expected based on the nucleophilic mechanism, the rate of metabolism of these compounds correlates with the electron density of the ring; electron withdrawing groups will therefore increase the rate of metabolism while electron donating groups will reduce it.[51,52]

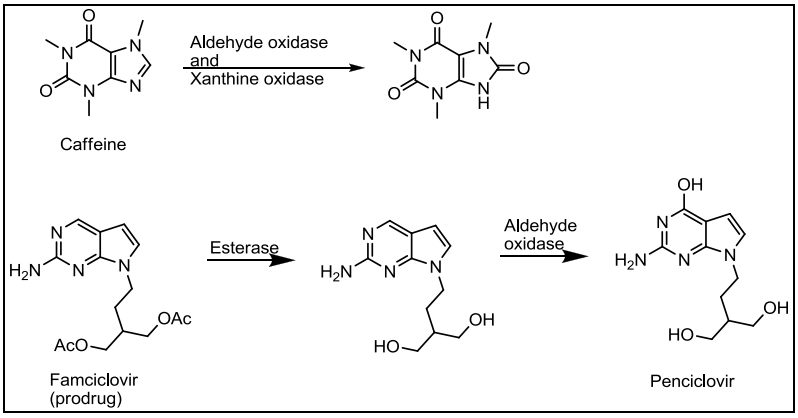

Figure 1.7: Examples of the oxidation of aromatic heterocycles by the Aldehyde oxidase and Xanthine oxidase[47]

1.4.2.3.2 Oxidation of aldehydes and iminium ions

Aldehyde oxidase is involved in the oxidation of aldehyde groups and iminium ions, usually as a secondary step in the metabolism of alcohols and cyclic amines respectively.[46,47,49] Aldehydes are converted to the respective carboxylic acids while iminium ions are converted to lactams. In general the activity of this enzyme in this reactions has been reported to be lower than that during aromatic heterocycle oxidation.[49] The production of reactive oxygen species by the aldehyde oxidase-mediated metabolism of acetaldehyde, derived from alcohol metabolism, has been reported as a possible cause of alcohol-induced liver injury.

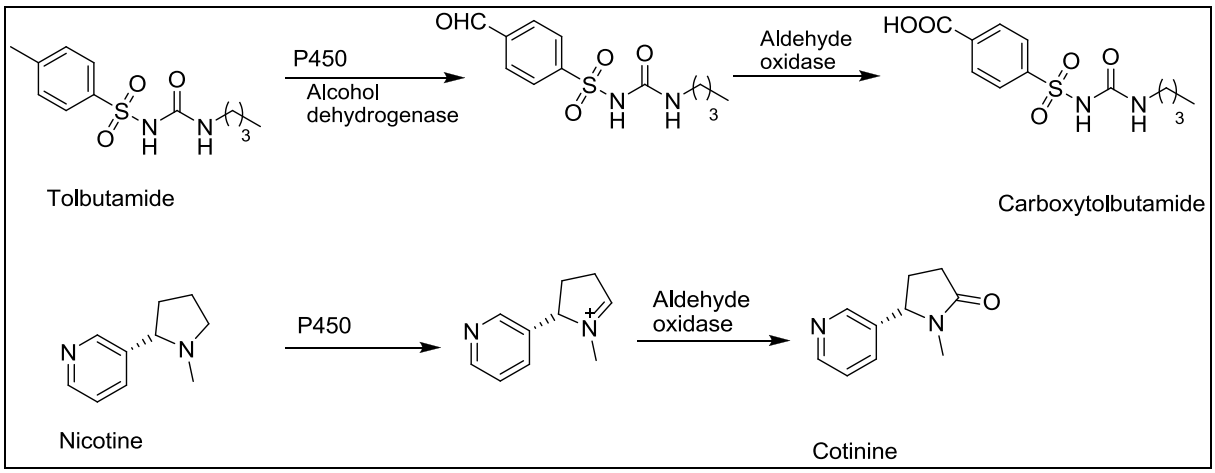

Figure 1.8: Examples of oxidation of aldehydes and iminium ions by aldehyde oxidase[47,53,54]

1.4.3 Esterases

1.4.3.1 Structure and occurrence

Hydrolases – enzymes which catalyse the water-catalysed breakdown of susceptible compounds are comprised of many structurally and mechanistically diverse members. Amongst the most important of these are esterases which primarily hydrolyse esters but are also involved in the hydrolysis of amides, carbamates and other related molecules.[25,55,56] Their distribution varies in different tissues. In plasma for example, butyrylcholinesterase, paraoxonase, albumin and acetylcholinesterase are the main ones present. While the catalytic activity of albumin is low, it is present in amounts of up to 50-60 g/l in plasma leading to significant catalytic activity.[57] The membranes of red blood cells contain additional esterases particularly esterase D and acetylcholinesterase and drug hydrolysis will therefore differ between plasma and whole blood.[57,58] In the liver and small intestines, the main hydrolases present are the carboxylesterases (human carboxylesterase-1, -2) with human carboxylesterase-1 (hCE1) being predominant in the liver and hCE-2 being predominant in the small intestines.[59,60] Species differences in esterase distribution and activity have been reported. For example, in human blood, the esterase activity is mainly due to cholinesterases while in rat and mouse blood, carboxylesterases are more predominant. Rodent blood also has higher total esterase activities than human blood and this should therefore be taken into account when extrapolating esterase hydrolysis between these models and man.[61] Ester hydrolysis by carboxylesterases is more substrate specific and the discussion that follows therefore focuses more on these enzymes.

The active site of carboxylesterases is characterised by a catalytic triad containing serine, histamine and glutamate which participate in the mechanism of these enzymes.[62–64] While the catalytic site is mostly conserved, differences in other parts of the enzymes result in different substrate specificities between hCE-1 and hCE-2. hCE-1 is mostly involved in the hydrolysis

of compounds containing a large acyl group and a small alcohol moiety while hCE-2 hydrolyses substrates with small acyl groups and large alcohol groups.[59,64]

1.4.3.2 Mechanism

Carboxylesterase hydrolysis of esters proceeds by nucleophilic attack of the substrate by a serine residue at the active site. This attack is facilitated by deprotonation of the serine by a histidine residue, which is in turn facilitated by hydrogen bond-mediated stabilisation by glutamate. This catalytic triad Serine – Histidine – Glutamate is highly conserved and is a feature of other serine esterases e.g. cholinesterases.[55,64]

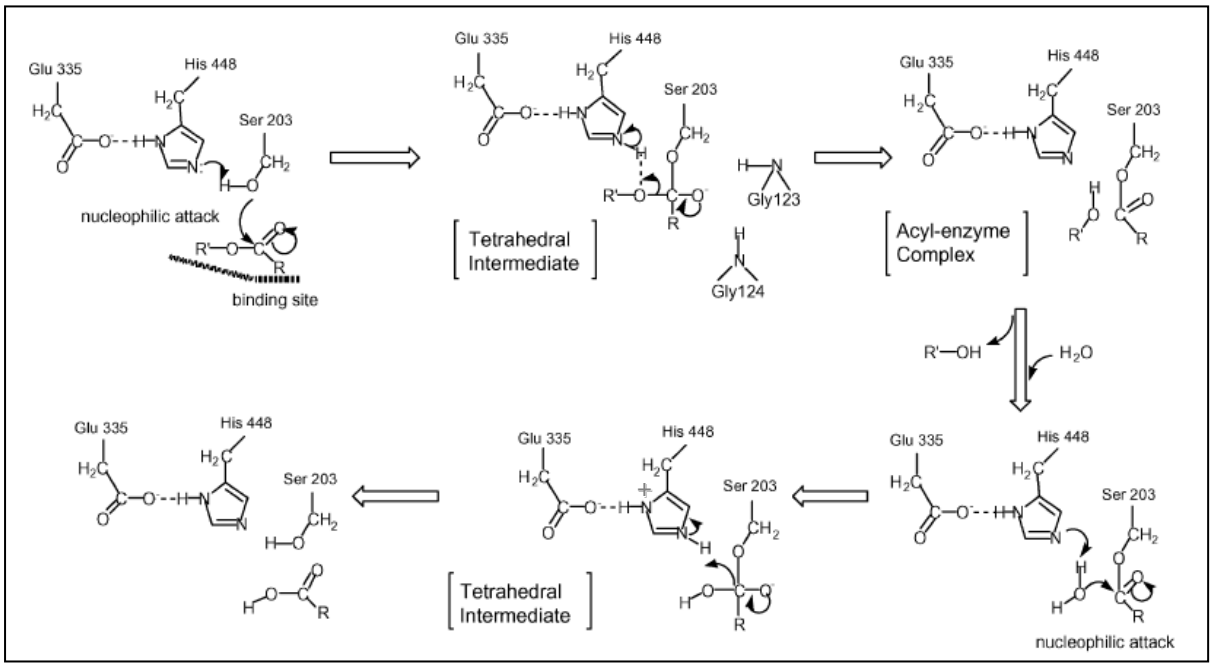

Figure 1.9: Mechanism of ester hydrolysis by carboxyesterases[55]

The resulting rearrangement of the intermediate releases the alcohol and gives an acyl enzyme complex. The alcohol formed or any other alcohol present in a high enough concentration may attack this complex leading to transesterification.[64] An analogous process then occurs with the histidine catalysed nucleophilic attack of the acyl enzyme complex to release the carboxylic acid and regenerate the serine.

1.4.3.3 Medicinal chemistry relevance

Esterases are often involved in activation of prodrugs, usually designed to facilitate absorption by masking more polar groups. A number of compounds are, however, only active as their ester forms and they are therefore deactivated by these enzymes. The transesterification reactions may also have relevance as in the example of cocaine, where transesterification with ethanol, either from the hydrolysis of cocaine or from co-ingested liquor, has been reported.[65–68]

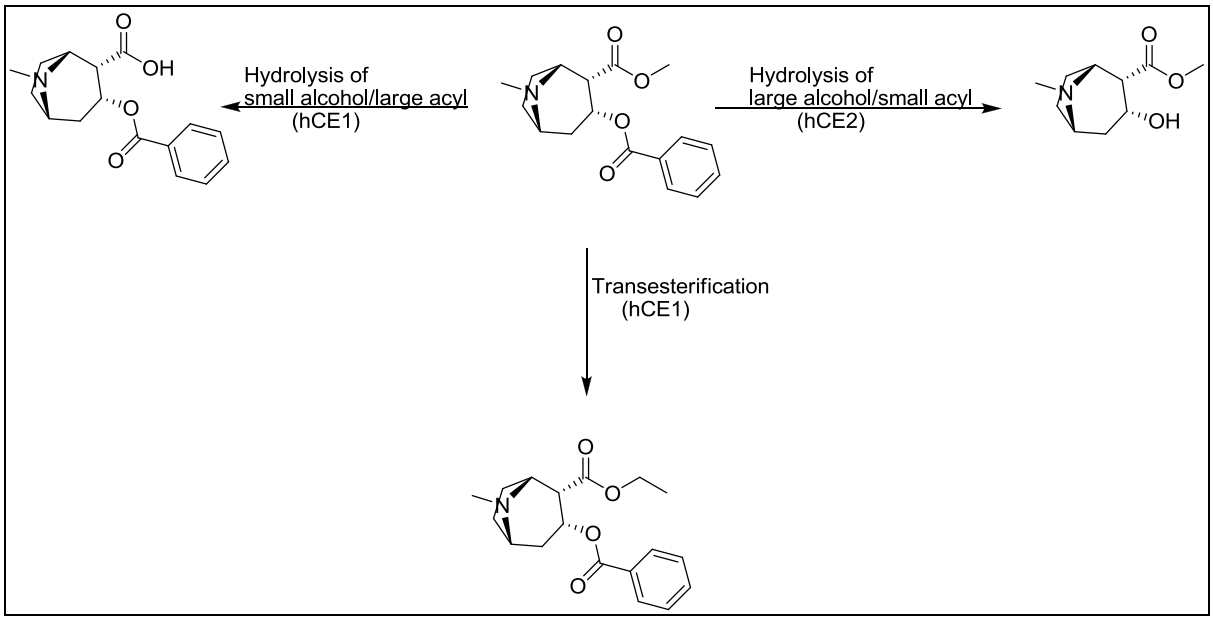

Figure 1.10: Reactions catalysed by carboxylesterases as exemplified by cocaine. The predominant enzyme involved is shown in brackets

1.4.4 UDP Glucuronosyl transferases

1.4.4.1 Structure and occurrence

Uridine-5'-diphosphate glucuronosyl transferases (UGTs) are a super-family of enzymes, which as their name implies catalyse the transfer of glucuronic acid from their co-factor UDP-α-D-glucuronic acid (UDPGA) to nucleophilic sites of substrates.[69–71] The *UGT* genetic super-family contains 117 genes encoding enzymes that have been divided into four families – UGT1, UGT2, UGT3 and UGT8.[72] In humans and experimental animals the UGT1 and 2 families are the most important for drug metabolism. Like P450s, these enzymes are membrane-bound and are found bound to the endoplasmic reticulum, though they are mostly lumenal – incorporated within the endoplasmic reticulum (≈95%), in contrast to P450s which have a significant cytosolic portion.[70,73] This subcellular location is also responsible for the latency in activity seen in drug metabolism studies with hepatocytes and microsomes because the endoplasmic reticulum represents a diffusion barrier for the substrate, co-factor, metabolite and by-product.[71,74]

UGTs have important endogenous substrates, bilirubin being one of the better known ones. Because of their broad and overlapping substrate specificity, drugs sometimes compete with endogenous molecules for glucuronidation leading to physiological disturbances.[69,75] UGTs are referred to as low affinity, high capacity enzymes which means that at low doses in the presence of a competing pathway, the drug will probably be metabolised by the competing pathway with glucuronidation only gaining preference at higher concentrations.[76]

1.4.4.2 Mechanism

Glucuronidation proceeds through a nucleophilic (S_N2) attack of C_1 on UDPGA, displacing UDP and forming the glucuronide. The mechanism necessitates an inversion of configuration from α- in UDPGA to β in glucuronides. While the specific aspects of this mechanism are

still under investigation, it has been proposed that a histidine, aspartate or glutamate residue is involved in activating the substrate by deprotonation.[70,77]

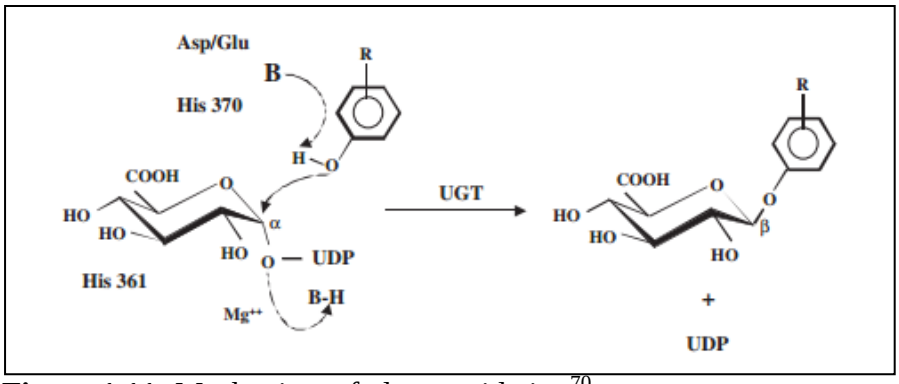

Figure 1.11: Mechanism of glucuronidation[70]

1.4.4.3 Medicinal chemistry relevance

Glucuronidation is the most important conjugation reaction and UGTs rank second to P450s in the number of drugs they metabolise. Based on their mechanism, substrates must contain a nucleophilic atom usually O, N or S but also C if nucleophilic enough. This functional group can be introduced as part of phase I metabolism or may be already present in the molecule. *O*-glucuronides can be formed from alcohols, carboxylic acids and even hydroxylamines/hydroxylamides.[25,78] *O*-glucuronides formed from carboxylic acids are referred to as acyl glucuronides and are potentially reactive towards nucleophilic cell constituents leading to toxicity.[79] Transesterification with glycerol has also been reported as an artefact *in vitro*.[80] *N*-glucuronides can be formed from amines (1°, 2°, 3°), amides, sulphonamides and even aromatic *N*-heterocycles.[78,81] The formation of quaternary *N*-glucuronides shows wide species differences, being highest in higher primates (man, chimpanzees) and virtually absent in lab animals (dogs and rodents), the formation of non-quaternary glucuronides is less species dependent.[81] C-glucuronides are much rarer and as alluded to, require acidic carbons or enolic acids.[82,83] Selenium-linked glucuronides have also been reported.[84]

1.4.6 Glutathione S-transferases

1.4.6.1 Structure and occurrence

Glutathione S-transferases (GSTs) are an enzyme superfamily found in most aerobic organisms. They typically make up about 1% of the total cellular protein and are involved in the protection of cells against oxidative stress and chemical toxicity due to alkylation of cellular components.[46,85,86] This function is served by catalysis of reactions between the thiol group of reduced glutathione (GSH) and electrophilic centres in substrates. They exist as dimers with each subunit having a hydrophilic site – where GSH is bound through hydrogen bonds – and a hydrophobic site for substrate binding.[87–89] The enzymes exist as two broad families; soluble/cytosolic enzymes and membrane associated proteins. Their detoxification role is mainly associated with the cytosolic family of enzymes. Based on sequence identity, mammalian cytosolic GSTs can be classified into 8 classes – designated α, μ, π etc and 4 additional classes in bacteria insects and plants.[86] In line with their detoxification role, the enzymes have broad and overlapping substrate specificities. In addition, it has been reported that some GSTs directly bind some carcinogenic compounds and also that some classes of GSTs bind the glutathione conjugates therefore maximising the detoxification effect during GSH depletion.[90,91]

1.4.6.2 Mechanism

Glutathione conjugation occurs through nucleophilic attack of the substrate by the thiolate anion of GSH. This implies that conjugation can occur even in the absence of enzyme. GSTs, however, increase the rate of this reaction by activating the GSH through deprotonation of the thiol. This is thought to involve a tyrosine residue at the active site and may either be through a base-mediated mechanism or through hydrogen-bond stabilisation. The result is that the thiol pKa of glutathione bound to GST is about two units lower than the pKa of free

glutathione (pH6.4-6.7 vs pH 9.0), therefore increasing the amount of ionised glutathione available for the conjugation reaction.[87–89]

1.4.6.3 Medicinal chemistry relevance

Glutathione conjugation is primarily a detoxification mechanism and will usually occur following activation of the compound by P450s or other oxidising enzymes to create reactive intermediates. While the primary mechanism is the same, the reaction type may vary based on the nature of the substrate. Common reactions are nucleophilic aromatic substitution, Michael addition, epoxide ring opening and reduction of hydroperoxides. Amodiaquine metabolism, which is discussed in more detail in Chapter 2, is a well-known example of the relevance of glutathione conjugation in the elimination of reactive drug metabolites.

Due to their role in detoxification, GSTs have also been implicated in resistance to anticancer agents.[92]

1.4.6 Other Phase II enzymes

Enzyme	Reactions	Important notes
Sulfotransferases[93]	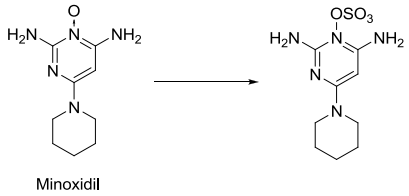 Minoxidil	• Is a high affinity low capacity process and is therefore more relevant at low concentrations and is easily saturated. • Mechanism is similar to glucuronidation with the sulfate donor as 3'-phosphoadenosine-5-phosphosulfate[24]
Acetyltransferases[94]	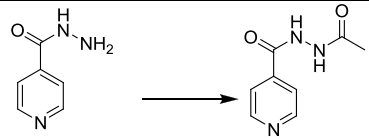 Isoniazid	• Catalyse transfer of an acetyl group from acetyl CoA to usually to primary aromatic amines but also to hydroxylamines and hydrazines
Methyltransferases[95]	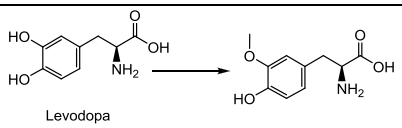 Levodopa	• Catalyse transfer of a methyl group from S-adenosylmethionine to catechols, sulfhydryl and nitrogen containing compounds
Amino acid conjugation enzymes (acyl transferases)[46]	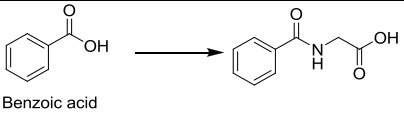 Benzoic acid	• First drug metabolism reaction to be described. • Is a two-step reaction involving formation of an acylCoA thioester followed by acyl transfer to the –NH2 of amino acids.

1.5 Systems for the study of drug metabolism

Drug metabolism studies are an integral part of the drug discovery and development process. Ultimately, the aim of these studies is to identify all metabolic outcomes relevant to a drug

and its metabolites in man and to understand and thus anticipate the interaction of the drug with the metabolism of other drugs or endogenous substrates (FDA guidance). The choice of system depends both on convenience (cost, throughput etc) and biological relevance. The ultimate system is of course *in vivo* studies in man, for drugs being developed for humans. However, cost and ethical concerns mean that this can only realistically be done in later phases of drug discovery, when the safety and efficacy in animal models has been comprehensively demonstrated. Various systems have therefore been developed to model drug metabolism in man and therefore allow for comprehensive metabolism studies before human trials. The systems are discussed in decreasing order of their biological complexity.

1.5.1 Animal models of drug metabolism

While there are occasional species differences in metabolism between man and animal models, experimental animals provide the best picture of drug metabolism *in vivo*. This is partly because metabolism *in vivo* is subject to many processes that are difficult to model *in vitro.* Most regulatory guidelines suggest that metabolism should be studied in at least one rodent and one non-rodent species to allow a better prediction of human metabolism and anticipate potential problems such as metabolic toxicity. The choice of model is dependent on the similarity of pathways between the model and man as predicted from *in vitro* data or literature.

More recently advances in genetics and immunology have allowed development of chimeric mice, which have human livers. These models are created by destroying hepatocytes of immunocompromised mice (e.g. SCID mouse) and repopulating their livers with human hepatocytes.[96–98] The resulting models express most human hepatic enzymes and transporters and the metabolic and excretory processes have been shown to be similar to humans.[99–102] Mice models in which various enzymes have been deleted have also recently been reported

and may offer ways of investigating the importance of these pathways in the clearance of various xenobiotics.[103,104]

1.5.2 *In vitro* models of drug metabolism

While animal models offer a biological complex and relevant model, the cost and ethical concerns that arise with their use means that it is often more practical to study *in vitro* metabolism first. Here again there is a broad variety of choices based on the question to be answered, for example whether the aim is to study the totality of metabolism or to study one particular metabolic process.

Given the central role of the liver in drug metabolism, most *in vitro* models are hepatic. However, equivalents exist for most of these models when another organ is to be studied. The first models were whole organ models where the entire liver or part of it was used, for example the perfused liver model and liver slices. These models offer a biological complex system where the 3D architecture of the cells is maintained and which preserve all relevant metabolic and excretory processes. However, the cost, throughput and difficulty in handling make these unsuited for routine use. In addition, to maintain viability, the models have to be used as soon as they are prepared which means that they are not commercially available. Most routine drug metabolism studies are therefore done on a variety of cellular and sub-cellular fractions depending on the level of complexity required.[105,106]

Hepatocytes provide the most direct way to study hepatic drug metabolism. However, to offer a direct comparison to metabolism *in vivo*, it should be recalled that metabolism i*n vivo* depends not only on a complete enzyme complement but also on transporter activity, cell-cell contact etc. The degree to which hepatocytes model the *in vivo* process is therefore dependent on how close they are to modelling all these processes. Hepatocytes can be freshly isolated (primary hepatocytes) or cultured. Freshly isolated hepatocytes suffer the disadvantage that

they can only be used for several hours following their isolation, making it difficult to perform experiments on demand. Various techniques have therefore emerged for their cryopreservation.[107–109] These cells, however, lack the 3D architecture of hepatocytes *in vivo* and may therefore not adequately model some *in vivo* processes. In addition, the short viability period of hepatocytes in suspension (about 4hours) means that metabolites of slowly metabolised compounds and even secondary metabolites of other compounds are often absent.[110,111] This is of particular concern since a lot of medicinal chemistry work targets reducing the degree of metabolism, therefore increasing the proportion of slowly metabolised compounds in drug discovery. These disadvantages have been overcome by the development of culture technologies which extend viabilities to several days. Recent improvements to culture models include the co-culture of hepatocytes with non-parenchymal cells which improves hepatocyte function and allows enzyme activity to be retained for longer.[112–114]

Subcellular fractions derived from hepatocytes are often the first system used in the screening of compounds in early drug discovery. They give a good representation of the metabolic processes involved for a drug and often give good in vitro/in vivo correlations. They also solve problems with inter-individual variation since they can easily be pooled. Other advantages are their stability in storage, low cost and easy commercial availability. However, they only model the metabolic process and the in vivo scaling may therefore be affected if other processes e.g. transport play important roles in the clearance. Co-factor supplementation e.g. NADPH for P450s and UDPGA for UGTs must be provided since the cellular biosynthetic processes are no longer functional. In addition, their activity reduces during incubation limiting their use for slowly metabolised compounds. They are produced by differential centrifugation of the liver to produce either membranes or supernatant. The S9 fraction is obtained following centrifugation at 9000g and contains most phase I and II enzymes. It is therefore the most complete subcellular fraction based on enzyme activity.

Further ultracentrifugation produces a pellet containing the membrane bound enzymes which is reconstituted to give microsomes, and a supernatant containing the soluble enzymes referred to as the cytosol. Microsomes are the most widely used fractions in early drug discovery due to the significance of P450 metabolism for most drugs.[106] As alluded to earlier, the similar preparative processes can be used to obtain subcellular fractions of other organs for metabolism studies. Intestinal microsomes and S9 have for example been used to model first pass metabolism in the gut wall.[115]

When the aim of the metabolism study is to investigate a particular enzymatic reaction, isolated enzymes offer the most direct strategy. These enzymes are most often used to study kinetic processes (e.g. determination of Km and Vmax) and in the identification of enzymes responsible for formation of specific metabolites. The enzymes are expressed recombinantly in mammalian but more often in yeast, bacteria and insect cells.[116–118]

1.6 Analytical strategies in drug metabolism studies

Analytical methodologies for drug metabolism studies are needed for quantitative reasons for example when monitoring drug concentrations and for qualitative reasons for example when identifying metabolites formed. Both quantitative and qualitative methods must be specific enough because the drugs and metabolites are present in a complex biological matrix, and sensitive enough because drug and/or metabolite concentrations are typically low (pM - μM). The degree of specificity and sensitivity required may increase as a drug advances through the discovery and development chain.

In early drug discovery, the most widely used techniques for drug metabolism studies are liquid-chromatography – mass spectrometry (LC-MS) methods.[119] LC-MS provides high sensitivity and specificity while maintaining the capacity for high throughput required in early drug discovery. The chromatography part of the set-up separates the drug and/or metabolites from the biological matrices allowing for more sensitive detection of the analytes. The mass spectrometer will typically use atmospheric pressure ionisation methods – most commonly electrospray or atmospheric pressure chemical ionisation to ionise the analytes which are then directed further into the MS for sorting and detection based on mass-charge (m/z) ratios.

The first application of LC-MS techniques in drug metabolism studies is usually in the determination of metabolic stability of drug compounds to guide structural modification. Analytically, this involves comparison of the amount of drug remaining at a predetermined time point against the amount of drug at T_0.[120–122] Absolute quantification is therefore not required though a generic internal standard is included to minimise effects due to variations in MS sensitivity. This assay is most often performed using multiple reaction monitoring (MRM), an analysis mode present on triple quadrupole mass spectrometers, which allows for the selective monitoring of the parent precursor ion (M+H) and fragment ion. The results are

reported as percentage compound remaining, half-life or as scaled figures representing whole liver metabolism e.g clearance or hepatic extraction.[123,124]

Metabolic stability assays give an indication of the stability of the compound in the presence of drug metabolising enzymes. The next logical step is the determination of the metabolites responsible for the observed reductions in parent concentrations. The metabolic profiling or metabolite identification studies vary in complexity as the drug development process continues. In early drug discovery, the main objective of these studies is often to identify the major metabolites formed so as to identify the metabolically labile positions in the molecule and guide strategies to block these positions. Broadly, this is accomplished by analysing incubations of the compound in the presence of drug metabolising enzymes and identifying the new peaks present. From an LC-MS perspective, two levels of data are required – first the precursor ions of the metabolites formed and secondly their fragmentation patterns.[125,126] For metabolites forming by direct modification of the molecule by addition or unmasking of functional groups with no rearrangement, the mass shifts between the precursor ions of the parent and metabolite are usually diagnostic of the type of metabolite formed. By this principle a gain of 16 units most commonly indicates oxidation while a loss of 14 units may indicate demethylation.[127] The strength of these assumptions has increased with the growth of high resolution MS (HRMS) where they can be more accurately measured and the molecular formula of the resulting metabolite confirmed from the accurate mass. The second level of data required for MS identification of metabolites is the fragment ion data most commonly obtained through collision-induced dissociation. Comparison of the fragments of the metabolite and parent should allow determination of the region of the molecule modified.[128] The acquisition of these two levels of metabolite data can be done through data dependent acquisition where a survey MS scan, usually the enhanced mass spectrum (EMS) scan is used to trigger the acquisition of product ion data for ions that meet a set of predefined criteria.

The entire approach is then referred to as MS/MS, MS^2 or tandem mass spectrometry because ions identified through one mass scan are fragmented in another scan. Based on instrument capability these can be improved to MS^3 usually in an attempt to understand the fragmentation pathway. These approaches of generating fragmentation data have been referred to as MS^n to account for all possible iterations of the process as defined by the instrument capability.[129] On Quadrupole Time of flight (QTof) instruments, the approach often used to acquire the 2 levels of data is referred to as MS^E. The instrument first operates at low collision energy (5-10V) so that the precursor ions are identified. The collision energy is then ramped up to give the collision induced fragments. A major advantage of this approach is that all ions are therefore fragmented with the resulting advantage that unexpected metabolites may be easier to find. The data set created is potentially quite big, though software approaches have been developed to help in the data mining. [130,131] Where the metabolites are known either from literature or predicted through *in silico* software, MRM can be used for analysis. While the sensitivity of the method is an advantage, the selectivity may be a problem because only metabolite transitions predefined before analysis can be found.[132,133]

The comparison of collision induced dissociation (CID) spectra will often provide a tentative identification of the metabolite and this is often the limit of MS metabolite identification. Based on the fragmentation pattern of the compound, comparison of the CID spectra of the parent and metabolite will often lead to a tentative identification of the region of the molecule undergoing metabolic change. This is often the limit of MS techniques and it is usually more difficult to pinpoint the specific atom modified using MS data alone. This challenge is gradually being overcome with the development of *in silico* metabolite identification techniques.[39,134] These techniques have evolved to consider MS fragmentation and therefore combine data of the most likely sites of metabolism and CID fragmentation to generate

proposed structures of metabolites.[135–137] Early tests on some of the software show correct assignment in about 80% of the model set.[130] Further advances in these approaches should allow automated data processing, greatly increasing the throughput of early metabolite identification studies and improving the detection of unexpected metabolites formed through rearrangement reactions.

While the focus of the earliest studies is in identifying the pathways that contribute to the highest metabolic clearance, there is a gradual shift towards understanding all metabolites and metabolic pathways as the discovery and development process continues. This is essential first in understanding any toxicological consequences of the metabolic processes but also in allowing for a fair inter species extrapolation of data. More advanced studies may therefore require radiolabeling of the drug and mass balance studies to ensure that the entirety of the pathways is known and accounted for[138]. This also necessitates LC-NMR approaches in order to unambiguously assign structures to all metabolites.

1.7 Relevance of metabolism and metabolites in drug discovery and development

1.7.1 Metabolism and pharmacological activity

Drug metabolism is generally a clearance process contributing to the decrease in concentration of the parent drug with time. This generally results in reduction of the pharmacological activity exerted by the parent drug with time, preventing accumulation and toxicity.[2] However, since metabolism results in formation of metabolites, the activity and toxicity of the metabolites is also relevant to the overall evaluation of the drug.[139] Most regulatory authorities prescribe a limit for *in vivo* metabolites beyond which the metabolite must be characterised to the same degree as the parent.[140,141]

Like for the parent drug, the pharmacological activity of the metabolite will depend on its ability to get to the site of action in sufficient concentrations and also on its ability to bind productively to the target.[142] Because metabolism usually involves a slight modification of structure, most metabolites possess a degree of pharmacological activity similar to that of the parent.[142,143] The degree to which this intrinsic activity translates to overall pharmacological activity depends on the extent to which the change in structure influences binding to the drug target and also on the degree to which the change in physicochemical properties influences the concentration at the drug target. Metabolites produced from lipophilic drugs therefore tend to retain some pharmacological activity since the structural changes introduced by metabolism are often minor and because like their respective parent drugs, they retain a good degree of their lipoidal permeability.[142,143] This is, however, very dependent on the respective drug and target involved. An example of these factors is the glucuronidation of morphine to morphine-3-glucuronide and morphine-6-glucuronide (Figure 1.12).

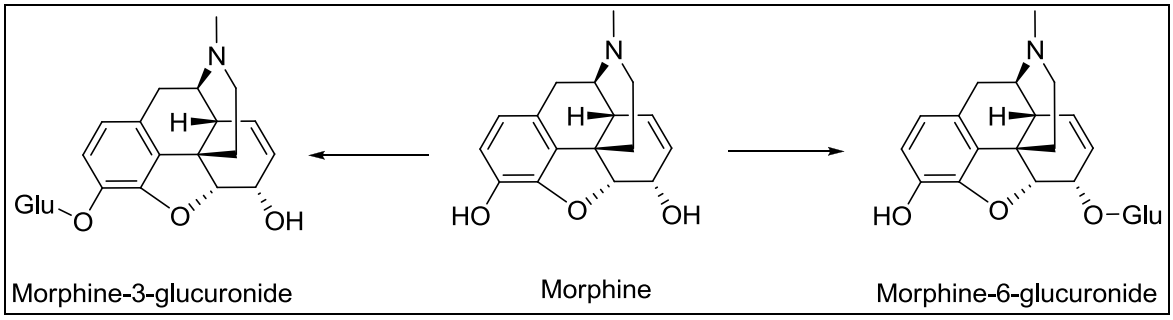

Figure 1.12: Morphine and its glucuronides

While the metabolic change occurring is the same, morphine-6-glucuronide is effective for analgesia in man and shows a better side effect profile than morphine while morphine-3-glucuronide is inactive.[144,145] This implies that the 3 position is less able to tolerate this change than the 6 position, which is supported by intrinsic activity data. The reasons for the better profile of morphine-6-glucuronide compared to morphine are still unclear.[146] However, it is known that the pharmacokinetic profile and brain accumulation of this compound is superior to morphine. It has been suggested that the increased hydrophilicity may reduce protein binding and the resulting increase in free plasma concentration may lead to higher levels of accumulation in the cerebrospinal fluid.[146] This example also demonstrates the potential advantages of pharmacologically active metabolites. These advantages and further examples of pharmacologically active metabolites have been extensively reviewed.[143,147–149]

In summary, metabolism can lead to either pharmacologically active or inactive metabolites depending on the influence of the structural changes on intrinsic activity and physicochemical properties.

1.7.3 Metabolism and toxicity

Many exceptions exist to the role of metabolism as a detoxifying process. The toxicity may result from the interaction of the metabolite with a drug target, either relevant or not to its mechanism of action. This type of toxicity is dose dependent and is predictable based on the known pharmacological activities of the drug. A bigger problem is often the metabolism of drugs to chemically reactive electrophilic species, which may bind to cell macromolecules leading to toxicity either directly by impairing their function or through involvement of the immune system. The time course of such toxicity may vary from immediately the drug is taken to several years after the drug was administered, in the case of teratogenicity and carcinogenicity.[150,151] A common example is acetaminophen. At its usual doses, the compound is metabolised by sulfation and glucuronidation. These pathways become saturated in an overdose increasing the significance of a CYP450-mediated process which produces the quinoneimine (N-acetyl-p-benzoquinoneimine, NAPQI) (Figure 1.13).

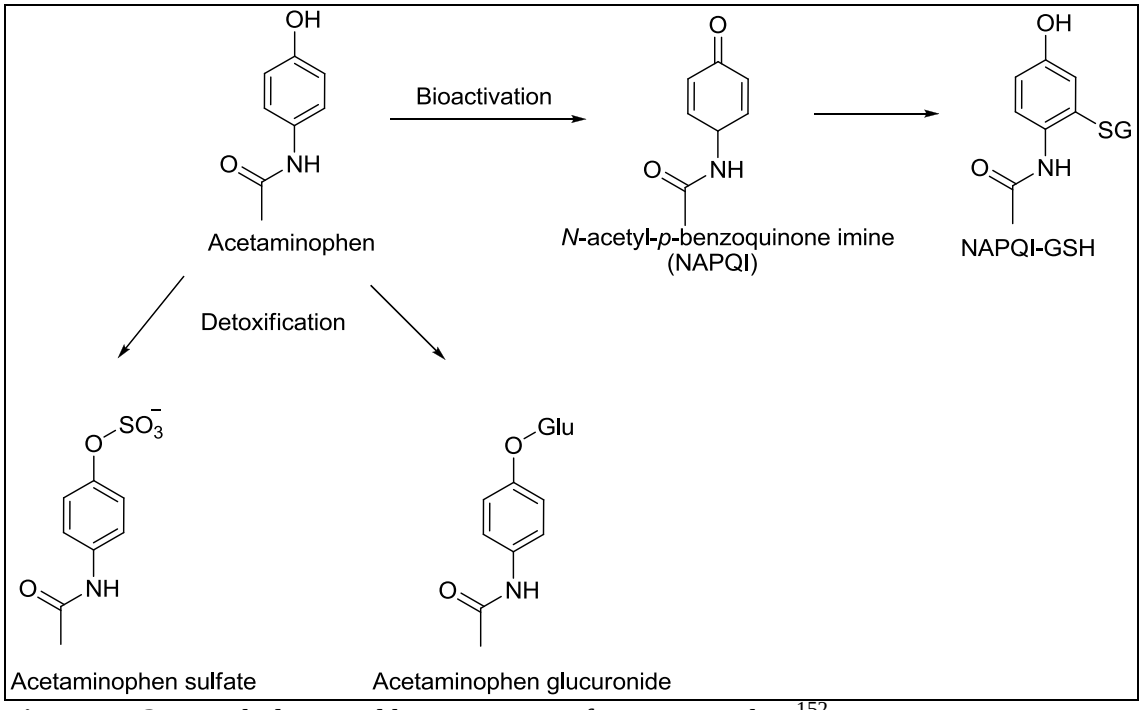

Figure 1.13: Metabolism and bioactivation of acetaminophen[152]

NAPQI is conjugated to glutathione to minimise its toxicity but if the dose is high enough, the glutathione is gradually depleted and at levels above 70% depletion, NAPQI reacts with cellular nucleophiles leading to hepatocyte damage. [153–156]

The toxicity and pharmacological activity of metabolites is therefore a key concern that should be addressed as early as possible in the discovery process.

1.8 Justification

From the foregoing discussions, it is clear that the integration of metabolism studies in early drug discovery and development is an important strategy in minimising the probability of failure in later stages. Further, the proper application of metabolism studies can help guide structural modifications of compounds and explain or predict their activity in the presence of drug metabolising systems. Finally, both the intrinsic activity and physicochemical properties of the metabolites are important in understanding the contribution of metabolites to the overall pharmacological activity of a compound.

This project explores the *in vitro* metabolism of tetrazole aminoquinolines and derivatives of metergoline and fusidic acid. In each chapter, the metabolic stability is considered and metabolite identification studies are used to understand the contribution of various metabolic pathways to the metabolic stability of the compounds. The experimentally observed metabolites are then compared to predicitions from StarDrop to understand whether the sites of metabolism could have been accurately predicted *a priori*. Finally, the predicted physicochemical properties of selected metabolites are compared to those of the parent compound to understand the consequence of the metabolic transformations.

1.9 Objective and specific aims

1.9.1 Objective

To investigate the *in vitro* metabolism of tetrazole deoxyamodiaquines, tetrazole chloroquines, metergoline derivatives and fusidic acid derivatives.

1.9.2 Specific aims

i) To select compounds for drug metabolism studies based on biological activity.

ii) To evaluate the metabolic stability of the selected compounds *in vitro*

iii) To identify the metabolites contributing to the instability of the compounds by LC-MS/MS

1.10 References

(1) Conti, A.; Bickel, M. H. History of Drug Metabolism : Discoveries of the Major Pathways in the 19th Century. *Drug Metab. Rev.* **1977**, *6*, 1–50.

(2) Caldwell, J.; Gardner, I.; Swales, N. An Introduction to Drug Disposition: The Basic Principles of Absorption, Distribution, Metabolism, and Excretion. *Toxicol. Pathol.* **1995**, *23*, 102–114.

(3) Mehrotra, N.; Gupta, M.; Kovar, A.; Meibohm, B. The Role of Pharmacokinetics and Pharmacodynamics in Phosphodiesterase-5 Inhibitor Therapy. *Int. J. Impot. Res.* **2006**, *19*, 253–264.

(4) Kola, I.; Landis, J. Can the Pharmaceutical Industry Reduce Attrition Rates? *Nat. Rev. Drug Discov.* **2004**, *3*, 711–715.

(5) Smith, D. A.; Schmid, E.; Jones, B. Do Drug Metabolism and Pharmacokinetic Departments Make Any Contribution to Drug Discovery? *Clin. Pharmacokinet.* **2002**, *41*, 1005–1019.

(6) Jakoby, W. B.; Ziegler, D. M. The Enzymes of Detoxication. *J. Biol. Chem.* **1990**, *265*, 20715–20718.

(7) Meyer, U. A. Endo-Xenobiotic Crosstalk and the Regulation of Cytochromes P450. *Drug Metab. Rev.* **2007**, *39*, 639–646.

(8) Wu, C.-Y.; Benet, L. Z. Predicting Drug Disposition via Application of BCS: Transport/Absorption/ Elimination Interplay and Development of a Biopharmaceutics Drug Disposition Classification System. *Pharm. Res.* **2005**, *22*, 11–23.

(9) Williams, R. . *Detoxification Mechanisms*; 2nd ed.; Chapman & Hall: London, 1959.

(10) Caldwell, J. Drug Metabolism and Pharmacogenetics: The British Contribution to Fields of International Significance. *Br. J. Pharmacol.* **2006**, *147 Suppl* , S89–99.

(11) Testa, B.; Pedretti, A.; Vistoli, G. Reactions and Enzymes in the Metabolism of Drugs and Other Xenobiotics. *Drug Discov. Today* **2012**, *17*, 549–560.

(12) Cytochrome P450 Homepage http://drnelson.uthsc.edu/CytochromeP450.html (accessed Mar 25, 2014).

(13) Nelson, D. R. The Cytochrome p450 Homepage. *Hum. Genomics* **2009**, *4*, 59–65.

(14) Omura, T.; Sato, R. A New Cytochrome in Liver Microsomes. *J. Biol. Chem.* **1962**, *237*, 1375–1376.

(15) Nelson, D. R. Cytochrome P450 Nomenclature, 2004. *Methods Mol. Biol.* **2006**, *320*, 1–10.

(16) Guengerich, F. P.; Wu, Z.-L.; Bartleson, C. J. Function of Human Cytochrome P450s: Characterization of the Orphans. *Biochem. Biophys. Res. Commun.* **2005**, *338*, 465–469.

(17) Williams, J. A.; Hyland, R.; Jones, B. C.; Smith, D. A.; Hurst, S.; Goosen, T. C.; Peterkin, V.; Koup, J. R.; Ball, S. E. Drug-Drug Interactions for UDP-Glucuronosyltransferase Substrates: A Pharmacokinetic Explanation for Typically Observed Low Exposure (AUCi/AUC) Ratios. *Drug Metab. Dispos.* **2004**, *32*, 1201–1208.

(18) Danielson, P. B. The Cytochrome P450 Superfamily: Biochemistry, Evolution and Drug Metabolism in Humans. *Curr. Drug Metab.* **2002**, *3*, 561–597.

(19) Guengerich, F. P. Common and Uncommon Cytochrome P450 Reactions Related to Metabolism and Chemical Toxicity. *Chem. Res. Toxicol.* **2001**, *14*, 611–650.

(20) Guengerich, F. P.; Johnson, W. W. Kinetics of Ferric Cytochrome P450 Reduction by NADPH-Cytochrome P450 Reductase: Rapid Reduction in the Absence of Substrate and Variations among Cytochrome P450 Systems. *Biochemistry* **1997**, *36*, 14741–14750.

(21) Hamdane, D.; Zhang, H.; Hollenberg, P. Oxygen Activation by Cytochrome P450 Monooxygenase. *Photosynth. Res.* **2008**, *98*, 657–666.

(22) Guengerich, F. P.; Isin, E. M. Mechanisms of Cytochrome P450 Reactions. *Acta Chim. Slov.* **2008**, *55*, 7–19.

(23) Guengerich, F. P.; Macdonald, T. L. Chemical Mechanisms of Catalysis by Cytochromes P-450: A Unified View. *Acc. Chem. Res.* **1984**, *17*, 9–16.

(24) Smith, D. A.; van de Waterbeemd, H.; Walker, D. K. *Pharmacokinetics and Metabolism in Drug Design*; Smith, D. A.; van de Waterbeemd, H.; Mannhold, R.; Kubinyi, H.; Timmerman, H., Eds.; 1st ed.; Wiley-VCH Verlag GmbH & Co. KGaA: Weinheim, 2001.

(25) Uetrecht, J.; Trager, W. *Drug Metabolism: Chemical and Enzymatic Aspects*; Informa Healthcare USA, Inc.: New York, 2007.

(26) *Drug Metabolism Handbook: Concepts and Applications*; Nassar, A. F.; Hollenberg, P. F.; Scatina, J., Eds.; John Wiley & Sons, Inc.: Hoboken, NJ, USA, 2009.

(27) Bell-Parikh, L. C.; Guengerich, F. P. Kinetics of Cytochrome P450 2E1-Catalyzed Oxidation of Ethanol to Acetic Acid via Acetaldehyde. *J. Biol. Chem.* **1999**, *274*, 23833–23840.

(28) Dowers, T. S.; Rock, D. A.; Rock, D. A.; Perkins, B. N. S.; Jones, J. P. An Analysis of the Regioselectivity of Aromatic Hydroxylation and N-Oxygenation by Cytochrome P450 Enzymes. *Drug Metab. Dispos.* **2004**, *32*, 328–332.

(29) Rydberg, P.; Ryde, U.; Olsen, L. Prediction of Activation Energies for Aromatic Oxidation by Cytochrome P450. *J. Phys. Chem. A* **2008**, *112*, 13058–13065.

(30) Hamman, M. A.; Thompson, G. A.; Hall, S. D. Regioselective and Stereoselective Metabolism of Ibuprofen by Human Cytochrome P450 2C. *Biochem. Pharmacol.* **1997**, *54*, 33–41.

(31) Miners, J. O.; Smith, K. J.; Robson, R. A.; McManus, M. E.; Veronese, M. E.; Birkett, D. J. Tolbutamide Hydroxylation by Human Liver Microsomes. *Biochem. Pharmacol.* **1988**, *37*, 1137–1144.

(32) Hyland, R. Identification of the Cytochrome P450 Enzymes Involved in the N-Oxidation of Voriconazole. *Drug Metab. Dispos.* **2003**, *31*, 540–547.

(33) Wójcikowski, J.; Boksa, J.; Daniel, W. A. Main Contribution of the Cytochrome P450 Isoenzyme 1A2 (CYP1A2) to N-Demethylation and 5-Sulfoxidation of the Phenothiazine Neuroleptic Chlorpromazine in Human Liver--A Comparison with Other Phenothiazines. *Biochem. Pharmacol.* **2010**, *80*, 1252–1259.

(34) Blake, M. J.; Gaedigk, A.; Pearce, R. E.; Bomgaars, L. R.; Christensen, M. L.; Stowe, C.; James, L. P.; Wilson, J. T.; Kearns, G. L.; Leeder, J. S. Ontogeny of Dextromethorphan O- and N-Demethylation in the First Year of Life. *Clin. Pharmacol. Ther.* **2007**, *81*, 510–516.

(35) Funaki, T.; Soons, P. A.; Guenoerich, F. P.; Breimer, D. D. In Vivo Oxidative Cleavage of a Pyridinecarboxylic Acid Ester Metabolite of Nifedipine. *Biochem. Pharmacol.* **1989**, *38*, 4213–4216.

(36) Masubuchi, Y.; Hosokawa, S.; Horie, T.; Suzuki, T.; Ohmori, S.; Kitada, M.; Narimatsu, S. Cytochrome P450 Isozymes Involved in Propranolol Metabolism in Human Liver Microsomes. The Role of CYP2D6 as Ring-Hydroxylase and CYP1A2 as N-Desisopropylase. *Drug Metab. Dispos. Biol. fate Chem.* **1994**, *22*, 909–915.

(37) Kerr, B. M.; Thummel, K. E.; Wurden, C. J.; Klein, S. M.; Kroetz, D. L.; Gonzalez, F. J.; Levy, R. Human Liver Carbamazepine Metabolism. *Biochem. Pharmacol.* **1994**, *47*, 1969–1979.

(38) Li, H.; Sun, *Æ*. J.; Fan, *Æ*. X.; Sui, *Æ*. X.; Zhang, *Æ*. L.; Wang, Y.; He, *Æ*. Z. Considerations and Recent Advances in QSAR Models for Cytochrome P450-Mediated Drug Metabolism Prediction. **2008**, 843–855.

(39) T'jollyn, H.; Boussery, K.; Mortishire-Smith, R. J.; Coe, K.; De Boeck, B.; Van Bocxlaer, J. F.; Mannens, G. Evaluation of Three State-of-the-Art Metabolite Prediction Software Packages (Meteor, MetaSite, and StarDrop) through Independent and Synergistic Use. *Drug Metab. Dispos.* **2011**, *39*, 2066–2075.

(40) StarDrop - Optibrium www.optibrium.com/StarDrop (accessed Jun 12, 2014).

(41) Segall, M. D. ISSX 2011: Predicting Regioselectivity and Lability of Cytochrome P450 Metabolism using Quantum Mechanical Simulations

http://www.optibrium.com/news/presentations/ISSX Poster 2011 - P450.pdf (accessed Nov 29, 2014).

(42) Dewar, M.; Zoebisch, E. Development and Use of Quantum Mechanical Molecular Models. 76. AM1: A New General Purpose Quantum Mechanical Molecular Model. *J. Am. Chem. Soc.* **1985**, *107*, 3902–3909.

(43) Kisker, C.; Schindelin, H.; Rees, D. C. Molybdenum-Cofactor-Containing Enzymes: Structure and Mechanism. *Annu. Rev. Biochem.* **1997**, *66*, 233–267.

(44) Schwarz, G.; Mendel, R. R.; Ribbe, M. W. Molybdenum Cofactors, Enzymes and Pathways. *Nature* **2009**, *460*, 839–847.

(45) Garattini, E.; Fratelli, M.; Terao, M. Mammalian Aldehyde Oxidases: Genetics, Evolution and Biochemistry. *Cell. Mol. Life Sci.* **2008**, *65*, 1019–1048.

(46) *Enzyme Systems That Metabolise Drugs and Other Xenobiotics*; Ioannides, C., Ed.; John Wiley & Sons, Ltd: Chichester, UK, 2001.

(47) Pryde, D. C.; Dalvie, D.; Hu, Q.; Jones, P.; Obach, R. S.; Tran, T. Aldehyde Oxidase: An Enzyme of Emerging Importance in Drug Discovery. *J. Med. Chem.* **2010**, *53*, 8441–8460.

(48) Alfaro, J. F.; Joswig-Jones, C. A.; Ouyang, W.; Nichols, J.; Crouch, G. J.; Jones, J. P. Purification and Mechanism of Human Aldehyde Oxidase Expressed in Escherichia Coli. *Drug Metab. Dispos.* **2009**, *37*, 2393–2398.

(49) Kitamura, S.; Sugihara, K.; Ohta, S. Drug-Metabolizing Ability of Molybdenum Hydroxylases. *Drug Metab. Pharmacokinet.* **2006**, *21*, 83–98.

(50) Torres, R. A.; Korzekwa, K. R.; McMasters, D. R.; Fandozzi, C. M.; Jones, J. P. Use of Density Functional Calculations to Predict the Regioselectivity of Drugs and Molecules Metabolized by Aldehyde Oxidase. *J. Med. Chem.* **2007**, *50*, 4642–4647.

(51) Pryde, D. C.; Tran, T.-D.; Jones, P.; Duckworth, J.; Howard, M.; Gardner, I.; Hyland, R.; Webster, R.; Wenham, T.; Bagal, S.; et al. Medicinal Chemistry Approaches to Avoid Aldehyde Oxidase Metabolism. *Bioorg. Med. Chem. Lett.* **2012**, *22*, 2856–2860.

(52) Dalvie, D.; Sun, H.; Xiang, C.; Hu, Q.; Jiang, Y.; Kang, P. Effect of Structural Variation on Aldehyde Oxidase-Catalyzed Oxidation of Zoniporide. *Drug Metab. Dispos.* **2012**, *40*, 1575–1587.

(53) McDaniel, H. G.; Podgainy, H.; Bressler, R. The Metabolism of Tolbutamide in Rat Liver. *J. Pharmacol. Exp. Ther.* **1969**, *167*, 91–97.

(54) Brandänge, S.; Lindblom, L. The Enzyme “Aldehyde Oxidase” Is an Iminium Oxidase. Reaction with Nicotine Delta 1’(5') Iminium Ion. *Biochem. Biophys. Res. Commun.* **1979**, *91*, 991–996.

(55) Satoh, T.; Hosokawa, M. Structure, Function and Regulation of Carboxylesterases. *Chem. Biol. Interact.* **2006**, *162*, 195–211.

(56) Fukami, T.; Yokoi, T. The Emerging Role of Human Esterases. *Drug Metab. Pharmacokinet.* **2012**, *27*, 466–477.

(57) Li, B.; Sedlacek, M.; Manoharan, I.; Boopathy, R.; Duysen, E. G.; Masson, P.; Lockridge, O. Butyrylcholinesterase, Paraoxonase, and Albumin Esterase, but Not Carboxylesterase, Are Present in Human Plasma. *Biochem. Pharmacol.* **2005**, *70*, 1673–1684.

(58) Cossum, P. A. Role of the Red Blood Cell in Drug Metabolism. *Biopharm. Drug Dispos.* **1988**, *9*, 321–336.

(59) Imai, T.; Taketani, M.; Shii, M.; Hosokawa, M.; Chiba, K. Substrate Specificity of Carboxylesterase Isozymes and Their Contribution to Hydrolase Activity in Human Liver and Small Intestine. *Drug Metab. Dispos.* **2006**, *34*, 1734–1741.

(60) Taketani, M.; Shii, M.; Ohura, K.; Ninomiya, S.; Imai, T. Carboxylesterase in the Liver and Small Intestine of Experimental Animals and Human. *Life Sci.* **2007**, *81*, 924–932.

(61) Rudakova, E. V.; Boltneva, N. P.; Makhaeva, G. F. Comparative Analysis of Esterase Activities of Human, Mouse, and Rat Blood. *Bull. Exp. Biol. Med.* **2011**, *152*, 73–75.

(62) Satoh, T.; Taylor, P.; Bosron, W. F.; Sanghani, S. P.; Hosokawa, M.; La Du, B. N. Current Progress on Esterases: From Molecular Structure to Function. *Drug Metab. Dispos.* **2002**, *30*, 488–493.

(63) Bencharit, S.; Morton, C. L.; Hyatt, J. L.; Kuhn, P.; Danks, M. K.; Potter, P. M.; Redinbo, M. R. Crystal Structure of Human Carboxylesterase 1 Complexed with the Alzheimer's Drug Tacrine: From Binding Promiscuity to Selective Inhibition. *Chem. Biol.* **2003**, *10*, 341–349.

(64) Imai, T. Human Carboxylesterase Isozymes: Catalytic Properties and Rational Drug Design. *Drug Metab. Pharmacokinet.* **2006**, *21*, 173–185.

(65) Bencharit, S.; Morton, C. L.; Xue, Y.; Potter, P. M.; Redinbo, M. R. Structural Basis of Heroin and Cocaine Metabolism by a Promiscuous Human Drug-Processing Enzyme. *Nat. Struct. Biol.* **2003**, *10*, 349–356.

(66) Bourland, J. A.; Martin, D. K.; Mayersohn, M. In Vitro Transesterification of Cocaethylene (Ethylcocaine) in the Presence of Ethanol. Esterase-Mediated Ethyl Ester Exchange. *Drug Metab. Dispos.* **1998**, *26*, 203–206.

(67) Pindel, E. V; Kedishvili, N. Y.; Abraham, T. L.; Brzezinski, M. R.; Zhang, J.; Dean, R. A.; Bosron, W. F. Purification and Cloning of a Broad Substrate Specificity Human Liver Carboxylesterase That Catalyzes the Hydrolysis of Cocaine and Heroin. *J. Biol. Chem.* **1997**, *272*, 14769–14775.

(68) Brzezinski, M. R.; Abraham, T. L.; Stone, C. L.; Dean, R. A.; Bosron, W. F. Purification and Characterization of a Human Liver Cocaine Carboxylesterase That Catalyzes the Production of Benzoylecgonine and the Formation of Cocaethylene from Alcohol and Cocaine. *Biochem. Pharmacol.* **1994**, *48*, 1747–1755.

(69) Tukey, R. H.; Strassburg, C. P. Human UDP-Glucuronosyltransferases: Metabolism, Expression, and Disease. *Annu. Rev. Pharmacol. Toxicol.* **2000**, *40*, 581–616.

(70) Ouzzine, M.; Barré, L.; Netter, P.; Magdalou, J.; Fournel-Gigleux, S. The Human UDP-Glucuronosyltransferases: Structural Aspects and Drug Glucuronidation. *Drug Metab. Rev.* **2003**, *35*, 287–303.

(71) Fisher, M. B.; Paine, M. F.; Strelevitz, T. J.; Wrighton, S. A. The Role of Hepatic and Extrahepatic UDP-Glucuronosyltransferases in Human Drug Metabolism. *Drug Metab. Rev.* **2001**, *33*, 273–297.

(72) Mackenzie, P. I.; Bock, K. W.; Burchell, B.; Guillemette, C.; Ikushiro, S.; Iyanagi, T.; Miners, J. O.; Owens, I. S.; Nebert, D. W. Nomenclature Update for the Mammalian UDP Glycosyltransferase (UGT) Gene Superfamily. *Pharmacogenet. Genomics* **2005**, *15*, 677–685.

(73) Radominska-Pandya, A.; Ouzzine, M.; Fournel-Gigleux, S.; Magdalou, J. Structure of UDP-Glucuronosyltransferases in Membranes. *Methods Enzymol.* **2005**, *400*, 116–147.

(74) Hänninen, O.; Alanen, K. The Competitive Inhibition of P-Nitrophenyl-Beta-D-Glucopyranosiduronic Acid Synthesis by Aliphatic Alcohols in Vitro. *Biochem. Pharmacol.* **1966**, *15*, 1465–1467.

(75) Wells, P. G.; Mackenzie, P. I.; Chowdhury, J. R.; Guillemette, C.; Gregory, P. A.; Ishii, Y.; Hansen, A. J.; Kessler, F. K.; Kim, P. M.; Chowdhury, N. R.; et al. Glucuronidation and the UDP-Glucuronosyltransferases in Health and Disease. *Drug Metab. Dispos.* **2004**, *32*, 281–290.

(76) Morris, M. E.; Pang, K. S. Competition between Two Enzymes for Substrate Removal in Liver: Modulating Effects due to Substrate Recruitment of Hepatocyte Activity. *J. Pharmacokinet. Biopharm.* **1987**, *15*, 473–496.

(77) Locuson, C. W.; Tracy, T. S. Comparative Modelling of the Human UDP-Glucuronosyltransferases: Insights into Structure and Mechanism. *Xenobiotica.* **2007**, *37*, 155–168.

(78) Testa, B.; Krämer, S. D. The Biochemistry of Drug Metabolism--an Introduction: Part 4. Reactions of Conjugation and Their Enzymes. *Chem. Biodivers.* **2008**, *5*, 2171–2336.

(79) Grillo, M. P.; Knutson, C. G.; Sanders, P. E.; Waldon, D. J.; Hua, F.; Ware, J. A. Studies on the Chemical Reactivity of Diclofenac Acyl Glucuronide with Glutathione: Identification of Diclofenac-S-Acyl-Glutathione in Rat Bile. *Drug Metab. Dispos.* **2003**, *31*, 1327–1336.

(80) Obach, R. S. Glycerolysis of Acyl Glucuronides as an Artifact of in Vitro Drug Metabolism Incubations. *Drug Metab. Dispos.* **2009**, *37*, 1581–1586.

(81) Chiu, S. H.; Huskey, S. W. Species Differences in N-Glucuronidation. *Drug Metab. Dispos.* **1998**, *26*, 838–847.

(82) Argikar, U. A. Unusual Glucuronides. *Drug Metab. Dispos.* **2012**, *40*, 1239–1251.

(83) Nishiyama, T.; Kobori, T.; Arai, K.; Ogura, K.; Ohnuma, T.; Ishii, K.; Hayashi, K.; Hiratsuka, A. Identification of Human UDP-Glucuronosyltransferase Isoform(s) Responsible for the C-Glucuronidation of Phenylbutazone. *Arch. Biochem. Biophys.* **2006**, *454*, 72–79.

(84) Müller, A.; Gabriel, H.; Sies, H.; Terlinden, R.; Fischer, H.; Römer, A. A Novel Biologically Active Selenooorganic Compound--VII. Biotransformation of Ebselen in Perfused Rat Liver. *Biochem. Pharmacol.* **1988**, *37*, 1103–1109.

(85) Ketterer, B.; Coles, B.; Meyer, D. J. The Role of Glutathione in Detoxication. *Environ. Health Perspect.* **1983**, *49*, 59–69.

(86) Armstrong, R. N. Glutathione S-Transferases: Reaction Mechanism, Structure, and Function. *Chem. Res. Toxicol.* **1991**, *4*, 131–140.

(87) Dirr, H.; Reinemer, P.; Huber, R. X-Ray Crystal Structures of Cytosolic Glutathione S-Transferases. Implications for Protein Architecture, Substrate Recognition and Catalytic Function. *Eur. J. Biochem.* **1994**, *220*, 645–661.

(88) Párraga, A.; García-Sáez, I.; Walsh, S. B.; Mantle, T. J.; Coll, M. The Three-Dimensional Structure of a Class-Pi Glutathione S-Transferase Complexed with Glutathione: The Active-Site Hydration Provides Insights into the Reaction Mechanism. *Biochem. J.* **1998**, *333 (Pt 3*, 811–816.

(89) Ji, X.; Johnson, W. W.; Sesay, M. A.; Dickert, L.; Prasad, S. M.; Ammon, H. L.; Armstrong, R. N.; Gilliland, G. L. Structure and Function of the Xenobiotic Substrate Binding Site of a Glutathione S-Transferase as Revealed by X-Ray Crystallographic Analysis of Product Complexes with the Diastereomers of 9-(S-Glutathionyl)-10-Hydroxy-9,10-Dihydrophenanthrene. *Biochemistry* **1994**, *33*, 1043–1052.

(90) Habig, W. H.; Pabst, M. J.; Fleischner, G.; Gatmaitan, Z.; Arias, I. M.; Jakoby, W. B. The Identity of Glutathione S-Transferase B with Ligandin, a Major Binding Protein of Liver. *Proc. Natl. Acad. Sci. U. S. A.* **1974**, *71*, 3879–3882.

(91) Meyer, D. J. Significance of an Unusually Low Km for Glutathione in Glutathione Transferases of the Alpha, Mu and Pi Classes. *Xenobiotica.* **1993**, *23*, 823–834.

(92) Townsend, D. M.; Tew, K. D. The Role of Glutathione-S-Transferase in Anti-Cancer Drug Resistance. *Oncogene* **2003**, *22*, 7369–7375.

(93) Buhl, A. E.; Waldon, D. J.; Baker, C. A.; Johnson, G. A. Minoxidil Sulfate Is the Active Metabolite That Stimulates Hair Follicles. *J. Invest. Dermatol.* **1990**, *95*, 553–557.

(94) Ellard, G. A. Variations between Individuals and Populations in the Acetylation of Isoniazid and Its Significance for the Treatment of Pulmonary Tuberculosis. *Clin. Pharmacol. Ther.* **1976**, *19*, 610–625.

(95) Dingemanse, J.; Jorga, K.; Zurcher, G.; Schmitt, M.; Sedek, G.; Prada, M.; Brummelen, P. Pharmacokinetic-Pharmacodynamic Interaction between the COMT Inhibitor Tolcapone and Single-Dose Levodopa. *Br. J. Clin. Pharmacol.* **1995**, *40*, 253–262.

(96) Mercer, D. F.; Schiller, D. E.; Elliott, J. F.; Douglas, D. N.; Hao, C.; Rinfret, A.; Addison, W. R.; Fischer, K. P.; Churchill, T. A.; Lakey, J. R.; et al. Hepatitis C Virus Replication in Mice with Chimeric Human Livers. *Nat. Med.* **2001**, *7*, 927–933.

(97) Dandri, M.; Burda, M. R.; Török, E.; Pollok, J. M.; Iwanska, A.; Sommer, G.; Rogiers, X.; Rogler, C. E.; Gupta, S.; Will, H.; et al. Repopulation of Mouse Liver with Human Hepatocytes and in Vivo Infection with Hepatitis B Virus. *Hepatology* **2001**, *33*, 981–988.

(98) Strom, S. C.; Davila, J.; Grompe, M. Chimeric Mice with Humanized Liver: Tools for the Study of Drug Metabolism, Excretion, and Toxicity. *Methods Mol. Biol.* **2010**, *640*, 491–509.

(99) Tateno, C.; Yoshizane, Y.; Saito, N.; Kataoka, M.; Utoh, R.; Yamasaki, C.; Tachibana, A.; Soeno, Y.; Asahina, K.; Hino, H.; et al. Near Completely Humanized Liver in Mice Shows Human-Type Metabolic Responses to Drugs. *Am. J. Pathol.* **2004**, *165*, 901–912.

(100) Foster, J. R.; Lund, G.; Sapelnikova, S.; Tyrrell, D. L.; Kneteman, N. M. Chimeric Rodents with Humanized Liver: Bridging the Preclinical/clinical Trial Gap in ADME/toxicity Studies. *Xenobiotica.* **2014**, *44*, 109–122.

(101) Ohtsuki, S.; Kawakami, H.; Inoue, T.; Nakamura, K.; Tateno, C.; Katsukura, Y.; Obuchi, W.; Uchida, Y.; Kamiie, J.; Horie, T.; et al. Validation of uPA/SCID Mouse with Humanized Liver as a Human Liver Model: Protein Quantification of Transporters, Cytochromes P450, and UDP-Glucuronosyltransferases by LC-MS/MS. *Drug Metab. Dispos.* **2014**, *42*, 1039–1043.

(102) Bateman, T. J.; Reddy, V. G. B.; Kakuni, M.; Morikawa, Y.; Kumar, S. Application of Chimeric Mice with Humanized Liver for Study of Human-Specific Drug Metabolism. *Drug Metab. Dispos.* **2014**, *42*, 1055–1065.

(103) Scheer, N.; McLaughlin, L. A.; Rode, A.; MacLeod, A. K.; Henderson, C. J.; Wolf, C. R. Deletion of Thirty Murine Cytochrome P450 Genes Results in Viable Mice with Compromised Drug Metabolism. *Drug Metab. Dispos.* **2014**, dmd.114.057885–.

(104) Xiang, Z.; Snouwaert, J. N.; Kovarova, M.; Nguyen, M.; Repenning, P. W.; Latour, A. M.; Cyphert, J. M.; Koller, B. H. Mice Lacking Three Loci Encoding 14 Glutathione Transferase Genes: A Novel Tool for Assigning Function to the GSTP, GSTM, and GSTT Families. *Drug Metab. Dispos.* **2014**, *42*, 1074–1083.

(105) Cross, D. M.; Bayliss, M. K. A Commentary on the Use of Hepatocytes in Drug Metabolism Studies during Drug Discovery and Development. *Drug Metab. Rev.* **2000**, *32*, 219–240.

(106) Brandon, E. F. .; Raap, C. D.; Meijerman, I.; Beijnen, J. H.; Schellens, J. H. . An Update on in Vitro Test Methods in Human Hepatic Drug Biotransformation Research: Pros and Cons. *Toxicol. Appl. Pharmacol.* **2003**, *189*, 233–246.

(107) Li, A. P.; Lu, C.; Brent, J. A.; Pham, C.; Fackett, A.; Ruegg, C. E.; Silber, P. M. Cryopreserved Human Hepatocytes: Characterization of Drug-Metabolizing Enzyme Activities and Applications in Higher Throughput Screening Assays for Hepatotoxicity, Metabolic Stability, and Drug-Drug Interaction Potential. *Chem. Biol. Interact.* **1999**, *121*, 17–35.

(108) Lloyd, T. D. R.; Orr, S.; Skett, P.; Berry, D. P.; Dennison, A. R. Cryopreservation of Hepatocytes: A Review of Current Methods for Banking. *Cell Tissue Bank.* **2003**, *4*, 3–15.

(109) McGinnity, D. F.; Soars, M. G.; Urbanowicz, R. A.; Riley, R. J. Evaluation of Fresh and Cryopreserved Hepatocytes as in Vitro Drug Metabolism Tools for the Prediction of Metabolic Clearance. *Drug Metab. Dispos.* **2004**, *32*, 1247–1253.

(110) Skett, P. Problems in Using Isolated and Cultured Hepatocytes for Xenobiotic Metabolism/metabolism-Based Toxicity Testing-Solutions? *Toxicol. In Vitro* **1994**, *8*, 491–504.

(111) Gebhardt, R.; Hengstler, J. G.; Müller, D.; Glöckner, R.; Buenning, P.; Laube, B.; Schmelzer, E.; Ullrich, M.; Utesch, D.; Hewitt, N.; et al. New Hepatocyte in Vitro Systems for Drug Metabolism: Metabolic Capacity and Recommendations for Application in Basic Research and Drug Development, Standard Operation Procedures. *Drug Metab. Rev.* **2003**, *35*, 145–213.

(112) Khetani, S. R.; Bhatia, S. N. Microscale Culture of Human Liver Cells for Drug Development. *Nat. Biotechnol.* **2008**, *26*, 120–126.

(113) Wang, W. W.; Khetani, S. R.; Krzyzewski, S.; Duignan, D. B.; Obach, R. S. Assessment of a Micropatterned Hepatocyte Coculture System to Generate Major Human Excretory and Circulating Drug Metabolites. *Drug Metab. Dispos.* **2010**, *38*, 1900–1905.

(114) Ramsden, D.; Tweedie, D. J.; St George, R.; Chen, L.-Z.; Li, Y. Generating an in Vitro-in Vivo Correlation for Metabolism and Liver Enrichment of a Hepatitis C Virus Drug, Faldaprevir, Using a Rat Hepatocyte Model (HepatoPac). *Drug Metab. Dispos.* **2014**, *42*, 407–414.

(115) Dalvie, D.; Obach, R. S.; Kang, P.; Prakash, C.; Loi, C.-M.; Hurst, S.; Nedderman, A.; Goulet, L.; Smith, E.; Bu, H.-Z.; et al. Assessment of Three Human in Vitro Systems in the Generation of Major Human Excretory and Circulating Metabolites. *Chem. Res. Toxicol.* **2009**, *22*, 357–368.

(116) Friedberg, T. Recombinant in Vitro Tools to Predict Drug Metabolism and Safety. *Pharm. Sci. Technolo. Today* **2000**, *3*, 99–105.

(117) Schroer, K.; Kittelmann, M.; Lütz, S. Recombinant Human Cytochrome P450 Monooxygenases for Drug Metabolite Synthesis. *Biotechnol. Bioeng.* **2010**, *106*, 699–706.

(118) Tang, W.; Wang, R. W.; Lu, A. Y. H. Utility of Recombinant Cytochrome P450 Enzymes□: A Drug Metabolism Perspective. **2005**, 503–517.

(119) Prakash, C.; Shaffer, C. L.; Nedderman, A.; Editor, G.; Baker, T. R. Analytical Strategies for Identifying Drug Metabolites. *Mass Spectrom. Rev.* **2007**, *26*, 340–369.

(120) Korfmacher, W. A. Principles and Applications of LC-MS in New Drug Discovery. *Drug Discov. Today* **2005**, *10*, 1357–1367.

(121) Korfmacher, W. A.; Palmer, C. A.; Nardo, C.; Dunn-Meynell, K.; Grotz, D.; Cox, K.; Lin, C. C.; Elicone, C.; Liu, C.; Duchoslav, E. Development of an Automated Mass Spectrometry System for the Quantitative Analysis of Liver Microsomal Incubation Samples: A Tool for Rapid Screening of New Compounds for Metabolic Stability. *Rapid Commun. Mass Spectrom.* **1999**, *13*, 901–907.

(122) Li, A. P. Screening for Human ADME/Tox Drug Properties in Drug Discovery. *Drug Discov. Today* **2001**, *6*, 357–366.

(123) Di, L.; Kerns, E. H.; Gao, N.; Li, S. Q.; Huang, Y.; Bourassa, J. L.; Huryn, D. M. Experimental Design on Single-Time-Point High-Throughput Microsomal Stability Assay. *J. Pharm. Sci.* **2004**, *93*, 1537–1544.

(124) Obach, R. S. Prediction of Human Clearance of Twenty-Nine Drugs from Hepatic Microsomal Intrinsic Clearance Data: An Examination of in Vitro Half-Life Approach and Nonspecific Binding to Microsomes. *Drug Metab. Dispos.* **1999**, *27*, 1350–1359.

(125) Clarke, N. J.; Rindgen, D.; Korfmacher, W. A.; Cox, K. A. Peer Reviewed: Systematic LC/MS Metabolite Identification in Drug Discovery. *Anal. Chem.* **2001**, *73*, 430 A–439 A.

(126) Kostiainen, R.; Kotiaho, T.; Kuuranne, T.; Auriola, S. Liquid Chromatography/atmospheric Pressure Ionization-Mass Spectrometry in Drug Metabolism Studies. *J. Mass Spectrom.* **2003**, *38*, 357–372.

(127) Baranczewski, P.; Stańczak, A.; Kautiainen, A.; Sandin, P.; Edlund, P.-O. Introduction to Early in Vitro Identification of Metabolites of New Chemical Entities in Drug Discovery and Development. *Pharmacol. Rep.* **2006**, *58*, 341–352.

(128) Prasad, B.; Garg, A.; Takwani, H.; Singh, S. Metabolite Identification by Liquid Chromatography-Mass Spectrometry. *TrAC Trends Anal. Chem.* **2011**, *30*, 360–387.

(129) Tozuka, Z.; Kaneko, H.; Shiraga, T.; Mitani, Y.; Beppu, M.; Terashita, S.; Kawamura, A.; Kagayama, A. Strategy for Structural Elucidation of Drugs and Drug Metabolites Using (MS)n Fragmentation in an Electrospray Ion Trap. *J. Mass Spectrom.* **2003**, *38*, 793–808.

(130) Bonn, B.; Leandersson, C.; Fontaine, F.; Zamora, I. Enhanced Metabolite Identification with MS(E) and a Semi-Automated Software for Structural Elucidation. *Rapid Commun. Mass Spectrom.* **2010**, *24*, 3127–3138.

(131) Bateman, K. P.; Castro-Perez, J.; Wrona, M.; Shockcor, J. P.; Yu, K.; Oballa, R.; Nicoll-Griffith, D. A. MSE with Mass Defect Filtering for in Vitro and in Vivo Metabolite Identification. *Rapid Commun. Mass Spectrom.* **2007**, *21*, 1485–1496.

(132) Huang, J.; Bathena, S. P. R.; Alnouti, Y. Metabolite Profiling of Praziquantel and Its Analogs during the Analysis of in Vitro Metabolic Stability Using Information-Dependent Acquisition on a Hybrid Triple Quadrupole Linear Ion Trap Mass Spectrometer. *Drug Metab. Pharmacokinet.* **2010**, *25*, 487–499.

(133) Gao, H.; Materne, O. L.; Howe, D. L.; Brummel, C. L. Method for Rapid Metabolite Profiling of Drug Candidates in Fresh Hepatocytes Using Liquid Chromatography Coupled with a Hybrid Quadrupole Linear Ion Trap. *Rapid Commun. Mass Spectrom.* **2007**, *21*, 3683–3693.

(134) Pähler, A.; Brink, A. Software Aided Approaches to Structure-Based Metabolite Identification in Drug Discovery and Development. *Drug Discov. Today. Technol.* **2013**, *10*, e207–17.

(135) Zimmerlin, A.; Kiffe, M. Fixing Clearance as Early as Lead Optimization Using High Throughput in Vitro Incubations in Combination with Exact Mass Detection and Automatic Structure Elucidation of Metabolites. *Drug Discov. Today Technol.* **2013**, *10*, e191–e198.

(136) Zamora, I.; Fontaine, F.; Serra, B.; Plasencia, G. High-Throughput, Computer Assisted, Specific MetID. A Revolution for Drug Discovery. *Drug Discov. Today. Technol.* **2013**, *10*, e199–205.

(137) Stranz, D. D.; Miao, S.; Campbell, S.; Maydwell, G.; Ekins, S. Combined Computational Metabolite Prediction and Automated Structure-Based Analysis of Mass Spectrometric Data. *Toxicol. Mech. Methods* **2008**, *18*, 243–250.

(138) Roffey, S. J.; Obach, R. S.; Gedge, J. I.; Smith, D. A. What Is the Objective of the Mass Balance Study? A Retrospective Analysis of Data in Animal and Human Excretion Studies Employing Radiolabeled Drugs. *Drug Metab. Rev.* **2007**, *39*, 17–43.

(139) Smith, D. A.; Obach, R. S. Metabolites and Safety: What Are the Concerns, and How Should We Address Them? *Chem. Res. Toxicol.* **2006**, *19*, 1570–1579.

(140) EMA. *ICH Guideline M3 (R2) on Non-Clinical Safety Studies for the Conduct of Human Clinical Trials and Marketing Authorisation for Pharmaceuticals*; 2009; Vol. 3.

(141) FDA. *Guidance for Industry Safety Testing of Drug Guidance for Industry Safety Testing of Drug Metabolites*; 2008.

(142) Smith, D. A.; Dalvie, D. Why Do Metabolites Circulate? *Xenobiotica.* **2012**, *42*, 107–126.

(143) Obach, R. S. Pharmacologically Active Drug Metabolites: Impact on Drug Discovery and Pharmacotherapy. *Pharmacol. Rev.* **2013**, *65*, 578–640.

(144) Janicki, P. K. Pharmacology of Morphine Metabolites. *Curr. Pain Headache Rep.* **1997**, *1*, 264–270.

(145) Romberg, R.; Sarton, E.; Teppema, L.; Matthes, H. W. D.; Kieffer, B. L.; Dahan, A. Comparison of Morphine-6-Glucuronide and Morphine on Respiratory Depressant and Antinociceptive Responses in Wild Type and Mu-Opioid Receptor Deficient Mice. *Br. J. Anaesth.* **2003**, *91*, 862–870.

(146) Kilpatrick, G. J.; Smith, T. W. Morphine-6-Glucuronide: Actions and Mechanisms. *Med. Res. Rev.* **2005**, *25*, 521–544.

(147) Kang, M. J.; Song, W. H.; Shim, B. H.; Oh, S. Y.; Lee, H. Y.; Chung, E. Y.; Sohn, Y.; Lee, J. Pharmacologically Active Metabolites of Currently Marketed Drugs: Potential Resources for New Drug Discovery and Development. *Yakugaku zasshi J. Pharm. Soc. Japan* **2010**, *130*, 1325–1337.

(148) Fura, A. Role of Pharmacologically Active Metabolites in Drug Discovery and Development. *Drug Discov. Today* **2006**, *11*, 133–142.

(149) Fura, A.; Shu, Y.; Zhu, M.; Hanson, R. L.; Roongta, V.; Humphreys, W. G. Discovering Drugs through Biological Transformation: Role of Pharmacologically Active Metabolites in Drug Discovery. *J. Med. Chem.* **2004**, *47*, 4339–4351.

(150) Edwards, I. R.; Aronson, J. K. Adverse Drug Reactions: Definitions, Diagnosis, and Management. *Lancet* **2000**, *356*, 1255–1259.

(151) Smith, D. A.; Obach, R. S. Seeing through the Mist: Abundance versus Percentage. Commentary on Metabolites in Safety Testing. *Drug Metab. Dispos.* **2005**, *33*, 1409–1417.

(152) Laine, J. E.; Auriola, S.; Pasanen, M.; Juvonen, R. O. Acetaminophen Bioactivation by Human Cytochrome P450 Enzymes and Animal Microsomes. *Xenobiotica.* **2009**, *39*, 11–21.

(153) Bessems, J. G.; Vermeulen, N. P. Paracetamol (acetaminophen)-Induced Toxicity: Molecular and Biochemical Mechanisms, Analogues and Protective Approaches. *Crit. Rev. Toxicol.* **2001**, *31*, 55–138.

(154) Davis, D. C.; Potter, W. Z.; Jollow, D. J.; Mitchell, J. R. Species Differences in Hepatic Glutathione Depletion, Covalent Binding and Hepatic Necrosis after Acetaminophen. *Life Sci.* **1974**, *14*, 2099–2109.

(155) Van de Straat, R.; de Vries, J.; Debets, A. J. J.; Vermeulen, N. P. E. The Mechanism of Prevention of Paracetamol-Induced Hepatotoxicity by 3,5-Dialkyl Substitution. *Biochem. Pharmacol.* **1987**, *36*, 2065–2070.

(156) Vermeulen, N. P.; Bessems, J. G.; Van de Straat, R. Molecular Aspects of Paracetamol-Induced Hepatotoxicity and Its Mechanism-Based Prevention. *Drug Metab. Rev.* **1992**, *24*, 367–407.

Chapter 2

TETRAZOLE AMINOQUINOLINES

2.1 Chapter overview

In this chapter the *in vitro* metabolism of two compound series; tetrazole deoxyamodiaquines and tetrazole chloroquines, is investigated. The tentative structure of the metabolites formed is suggested based on the fragmentation and H/D exchange data. The CYP450 inhibition of selected compounds is evaluated and *in silico* modelling is used to suggest an explanation for the potent CYP450 inhibition. Finally, the StarDrop prediction of the sites of metabolism is compared to the experimentally observed metabolites.

2.2 Tetrazole deoxyamodiaquines

2.2.1 Background

Amodiaquine is a 4-aminoquinoline-based antimalarial compound that was once widely used in prophylaxis and treatment of malaria.[1] However, accumulating evidence on its links to incidents of hepato-toxicity and agranulocytosis led to its withdrawal as a prophylactic and it is now more commonly used in combination therapy in the treatment of acute malaria.[2–4] The toxicity of amodiaquine has been suggested to arise from its metabolic activation to a reactive quinone-imine.[5–7] This reactive metabolite is trapped by glutathione and N-acetylcysteine in the cell and the conjugates have been observed in polymorphonucleocytes and in vivo in rats.[6,8] Once glutathione is depleted, the quinone-imine reacts with other soft nucleophiles in the cell leading to toxicity. Other metabolites of amodiaquine with the 4-aminophenol feature have also been suggested as contributors to the toxicity.[9]

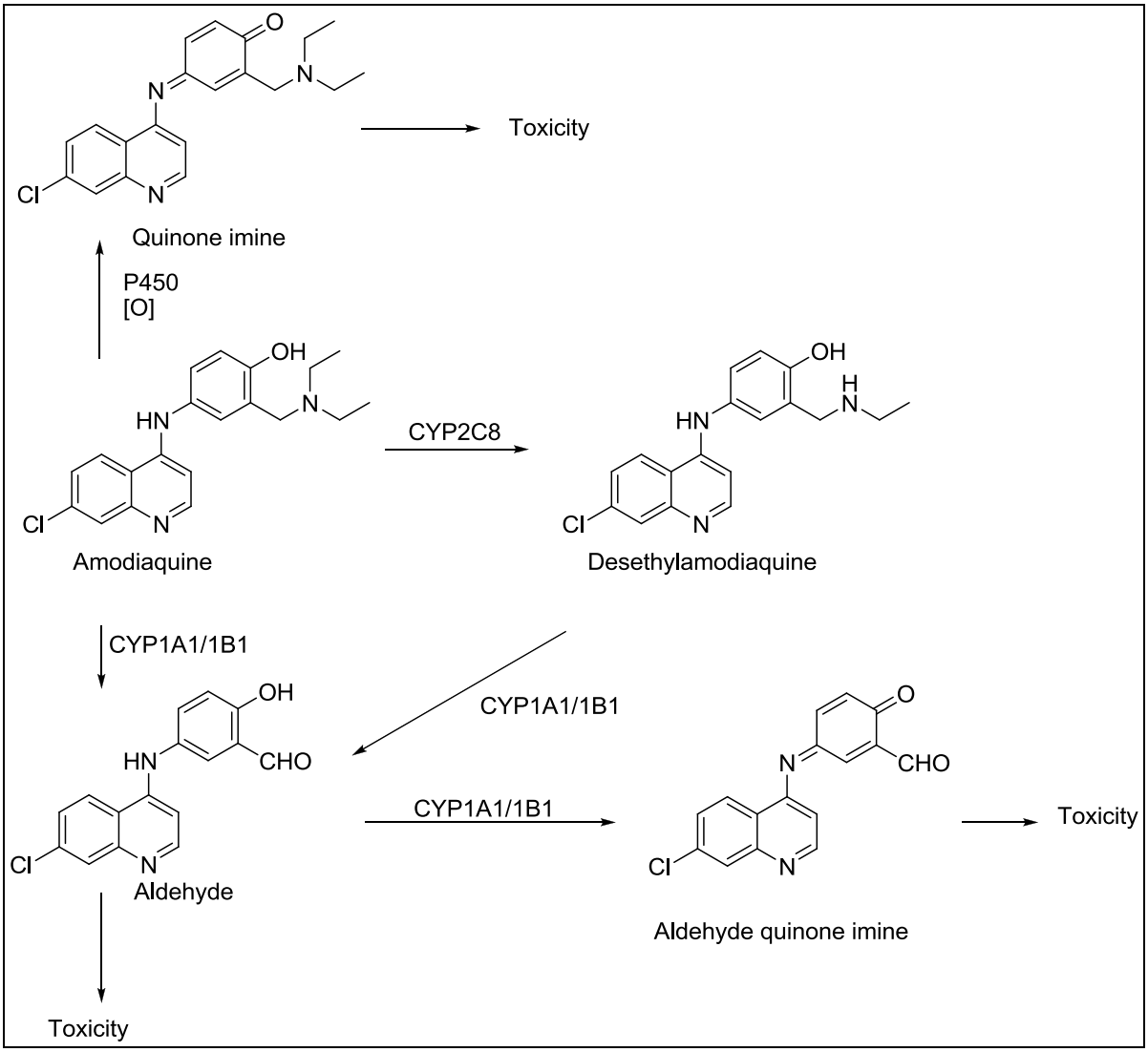

Figure 2.1: Metabolic bioactivation of amodiaquine[10]

Various chemical approaches have been explored to reduce the toxicity while retaining the good antimalarial activity associated with amodiaquine. The earliest modifications involved fluorine substitution at the 4'-position replacing the –OH group. The fluoroamodiaquine derivative thus derived does not form the quinoneimine metabolite and is metabolised primarily by N-dealkylation.[11] The more metabolically stable *tert*-butyl derivative, in which the diethyl side chain is replaced with a *tert*-butyl group, has been suggested as a candidate for clinical evaluation.[12] Another approach has involved the switching of the 3' and 4'-groups to give isoquine. This compound retains the antiplasmodial activity of amodiaquine and does not form the quinone-imine but was shown to have low bioavailability, attributable to its

rapid first pass metabolism by dealkylation. The *tert*-butyl substituted derivative is more stable and was evaluated as a clinical candidate.[13] Its development has been recently discontinued due to its inability to show superiority over chloroquine.[1]

The approach presented in this work considers deoxyamodiaquine derivatives, where the 4'-hydroxyl group is removed.[14] The compounds are further fused to a *tert*-butyl substituted tetrazole ring, to improve their physicochemical characteristics. The metabolism of the most active compounds was evaluated and their corresponding derivatives without a *tert*-butyl group, was evaluated. The antiplasmodial activity of these derivatives against chloroquine susceptible and chloroquine resistant strains is shown in Table 2.1 below.[14]

Table 2.1: Biological activity of selected tetrazole deoxyamodiaquines[14]

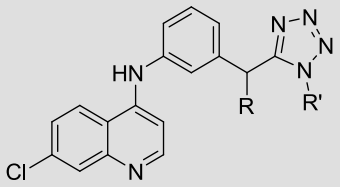

Code	R	R'	*P. falciparum IC50 (µM)*		
			3D7	**K1**	**W2**
TK1		t-Bu	0.052 ± 0.003	0.150 ± 0.030	0.227 ± 0.003
TK2	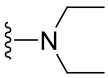	t-Bu	0.100 ± 0.014	0.006 ± 0.004	0.066 ± 0.003
TK3	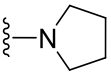	t-Bu	0.010 ± 0.002	0.0096 ± 0.003	0.077 ± 0.0002
TK4	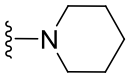	t-Bu	0.050 ± 0.004	0.170 ± 0.014	0.082 ± 0.006
TK1B3		H	0.487 ± 0.066	2.979 ± 0.307	1.168 ± 0.105
TK2B3	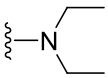	H	0.164 ± 0.012	0.054 ± 0.009	0.475 ± 0.011
TK3B3	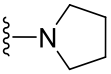	H	1.097 ± 0.058	0.049 ± 0.014	0.181 ± 0.036
TK4B3	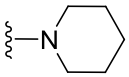	H	0.286 ± 0.024	1.264 ± 0.088	0.487 ± 0.017
	Amodiaquine		0.001 ± 0.0002	0.027 ± 0.0007	0.401 ± 0.0009

2.2.2 Metabolism studies

2.2.2.1 Microsomal Metabolic stability

The microsomal metabolic stability of the eight derivatives was assessed in human and rat liver microsomes using a single point assay. **TK1 –TK4** were rapidly metabolised with less than 5% of the parent remaining after a 30 minutemin incubation at 0.1mg/ml microsomal protein. This rate of metabolism was comparable to amodiaquine in human, but not in rat microsomes, where amodiaquine was more stable.

Table 2.2: Metabolic stability of tetrazole deoxyamodiaquines

Compound	**Microsomal stability (% remaining at 30 min)**		**Log P***
	HLM	RLM	
TK1	<5	<5	4.31
TK2	<5	<5	4.96
TK3	<5	<5	4.52
TK4	<5	<5	5.02
TK1B3	91	>99	2.89
TK2B3	92	>99	3.57
TK3B3	>99	>99	3.14
TK4B3	83	>99	3.68
Amodiaquine	<5	55	4.24

*Predicted using StarDrop v.5.5

The removal of the *tert*-butyl group leads to about a 1 unit drop in predicted log P, and this reduction in lipophilicity may explain the better microsomal stability of these compounds. Another possible explanation is that the *tert*- butyl group is metabolically labile, but this was discounted, as discussed in the sections below.

2.2.2.2 Metabolite identification in microsomes

To further understand the structural issues underlying the metabolism of these derivatives, two representative compounds, **TK2** and **TK3** and their respective B3 derivatives were selected for metabolite identification experiments.

A typical extracted ion chromatogram of **TK2** and its metabolites in HLMs is shown below.

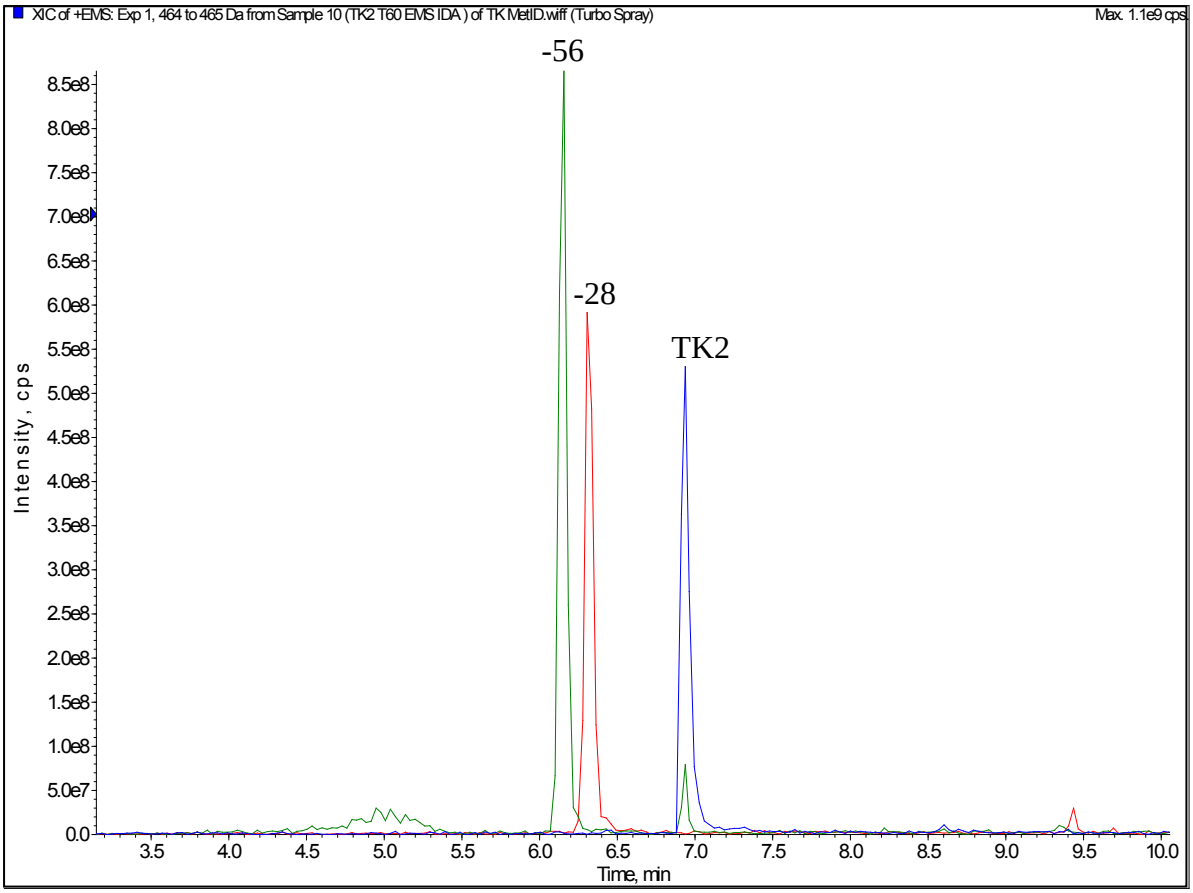

Figure 2.2: Extracted ion chromatogram of TK2 and its metabolites in HLMs

Two metabolites were detected which were -28Da and -56Da respectively, compared to the precursor ion of the parent. No metabolism occurred in the absence of NADPH or microsomes. These losses suggest deethylation and di-deethylation and the product ion spectra are consistent with this.

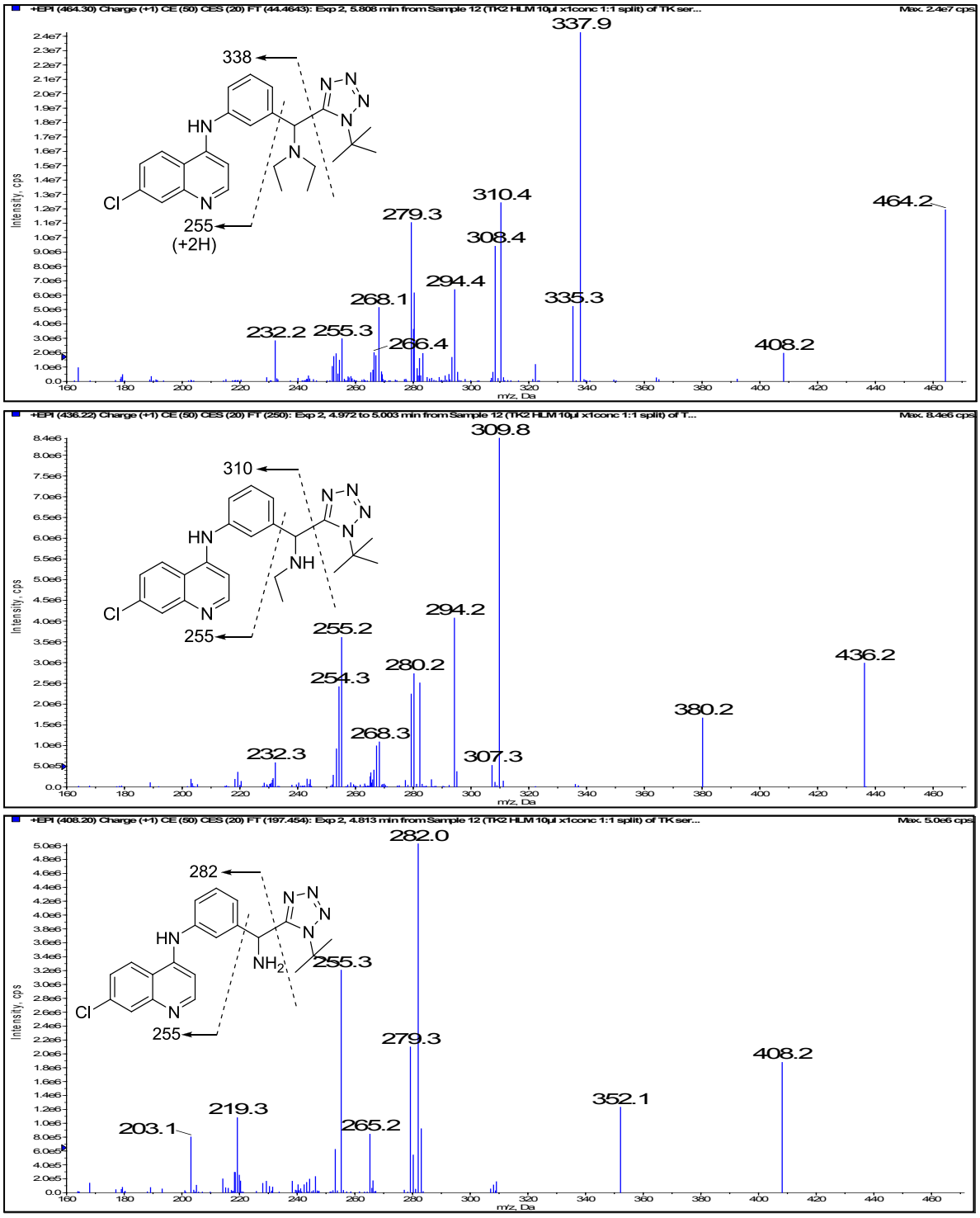

Figure 2.3: Product ion spectra of **TK2** and its metabolites

The metabolism of **TK3** appears to be more complex and at least 8 phase I metabolites were detected in human and rat liver microsomal experiments. The fragmentation pathway of **TK3** was considered in more detail in order to better assign the tentative structures of the metabolites.

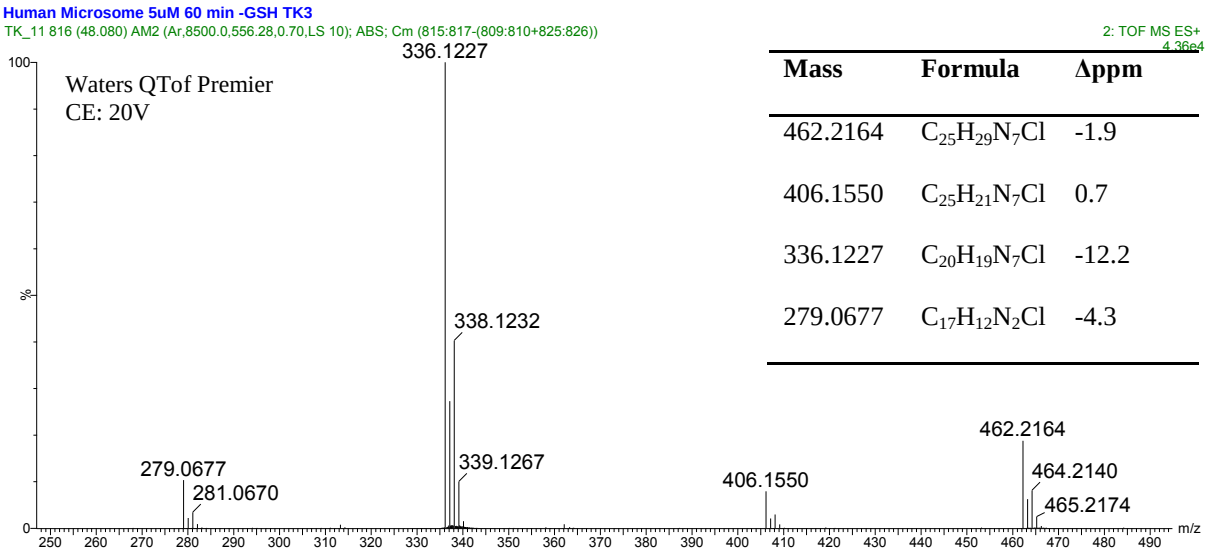

Mass	Formula	Δppm
462.2164	$C_{25}H_{29}N_7Cl$	-1.9
406.1550	$C_{25}H_{21}N_7Cl$	0.7
336.1227	$C_{20}H_{19}N_7Cl$	-12.2
279.0677	$C_{17}H_{12}N_2Cl$	-4.3

Figure 2.4: Product ion spectrum of **TK3**

The m/z 406 fragment is suggested to arise from a loss of the *tert*-butyl group followed by protonation of the tetrazole nitrogen. The proposed molecular formula for the m/z 336 fragment suggests that it arises from heterolytic cleavage of the tetrazole ring. A different fragmentation pathway involving loss of the pyrrolidine ring and loss of the tetrazole nitrogens likely produces the m.z 279 fragment, as suggested by its molecular formula. The precursor ion and the fragments shown, display the typical chlorine isotope pattern, giving an extra criterion for assessing metabolites.

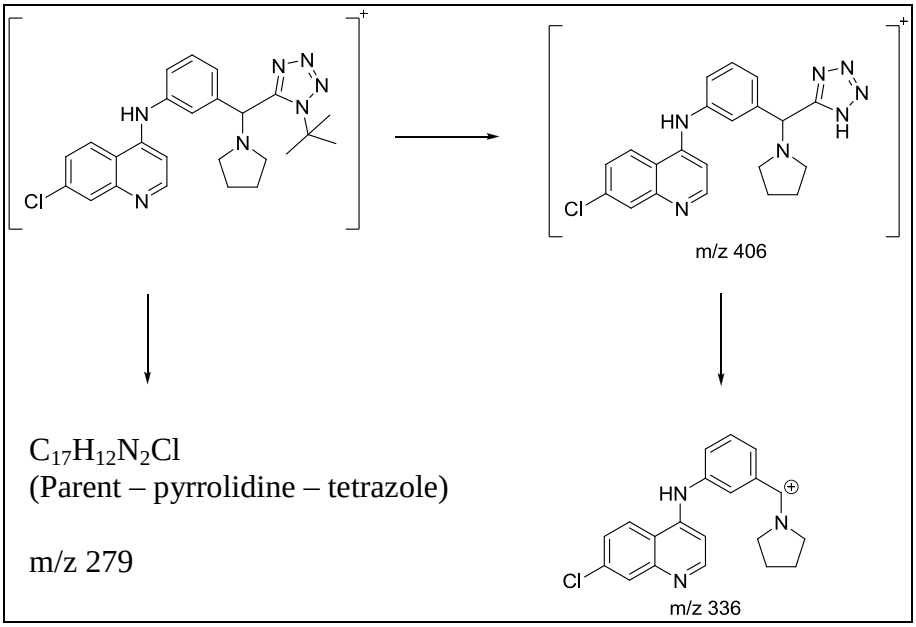

Figure 2.5: Key fragments of **TK3**

This fragmentation pathway is common to all derivatives in the series and the analogous fragments (-56Da, -126Da, m/z 279) can be seen in **TK2** and its metabolites in Figure 2.3 above. Depending on the ease with which substitutions on the nitrogen can be cleaved, a fragment with m/z 282 (or 280 following loss of 2H through double bond formation) may also form by loss of the substituted tetrazole ring accompanied by heterolytic cleavage of the substitutions on the nitrogen.

Based on this fragmentation pathway, a neutral loss (NL) scan of 126Da was performed, in addition to the other scan modes discussed in the methods, to detect the metabolites.

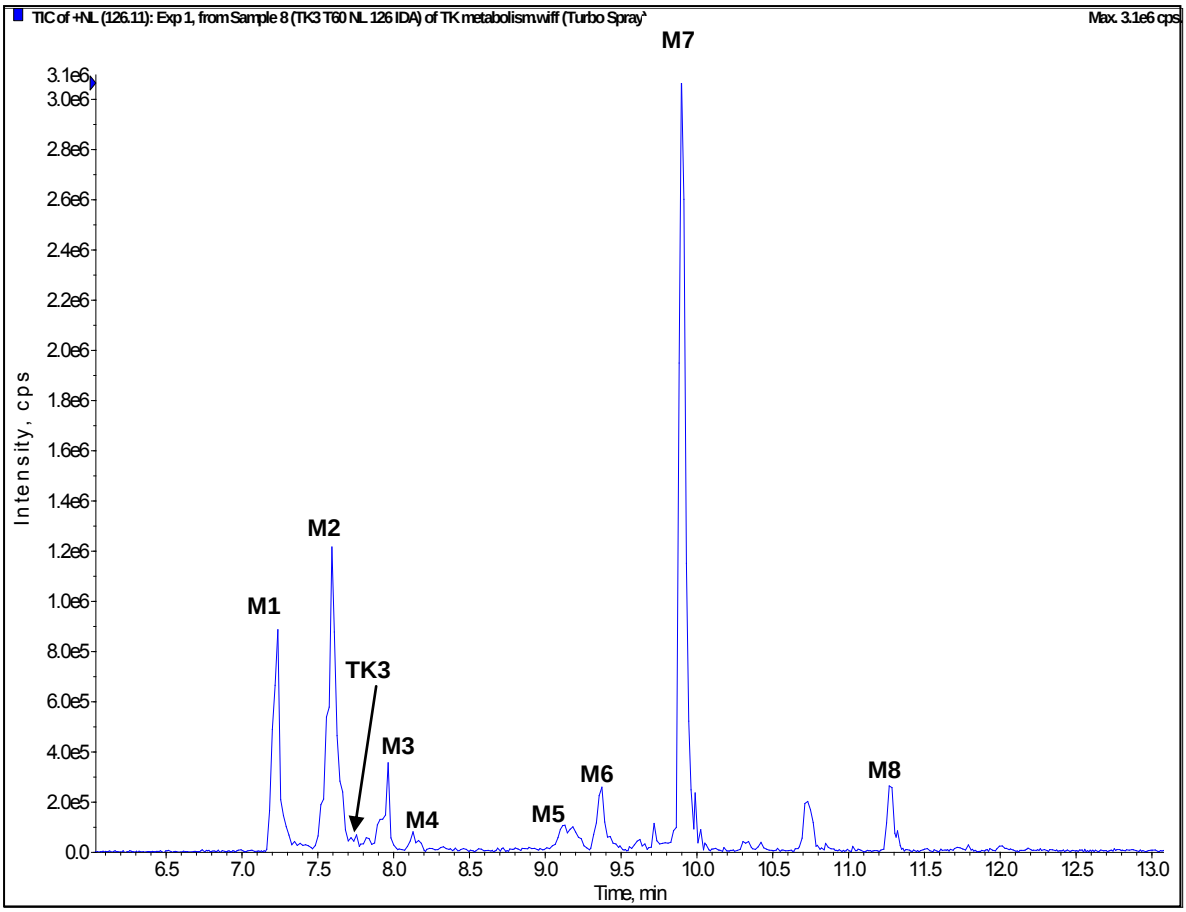

Figure 2.6: Neutral loss scan of 126Da showing HLM metabolites of **TK3**

The rapid metabolism of **TK3** is evident here since almost no parent remains after a 60 minute incubation. A similar metabolite profile was observed in rat liver microsomes. The product ion spectra of all the metabolites contain the same neutral losses as the parent (-56Da, -126Da) suggesting that metabolism does not occur on substituted tetrazole. In addition, the metabolites have the m/z 279 fragment (or m/z 280/282) implying that the N-phenyl-7-chloroaminoquinoline core remains unchanged. A summary of the MS/MS data of **TK3** and the metabolites is presented below.

Table 2.3: Summary of HLM metabolites of **TK3**

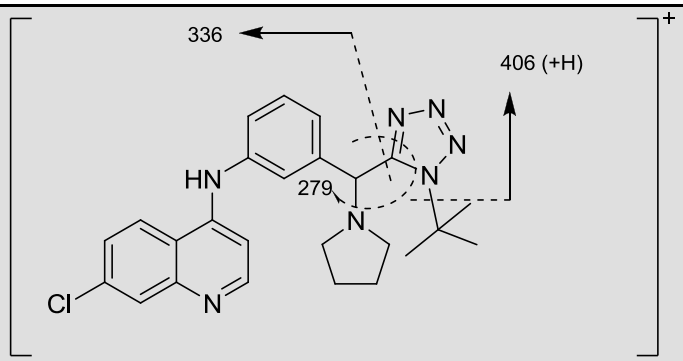

Code	Rt	m/z	Fragments		
			A	B	C
			406	336	279
M1	7.23	408	352	282	279
M2	7.60	478	422	352	279
M3	7.96	494	438	368	279
M4	8.13	480	424	354	279
M5	9.17	492	436	366	279
M6	9.37	492	436	366	279
M7	9.90	476	420	350	279
M8	11.28	458	402	332	279
TK3	7.66	462	406	336	279

The data therefore strongly suggest that metabolism occurs on the pyrrolidine ring. Further experimental work was therefore carried out to verify this hypothesis.

2.2.2.2.1 Further investigations into pyrrolidine ring metabolism

The analysis of the incubations was conducted using a NL scan of 27Da to detect the cyanide adducts and, as in the other metabolite identification experiments, using an enhanced mass spectrum scan coupled to enhanced product ion scans using information dependent

acquisition (EMS-IDA-EPI). When **TK3** was incubated with cyanide in HLMs, three adducts with m/z 503 (A1) and 487 (A2 and A3) were detected in the NL scan. No adducts were detected in the absence of NADPH or microsomes. A2 and A3 were, however, formed even in the absence of cyanide.

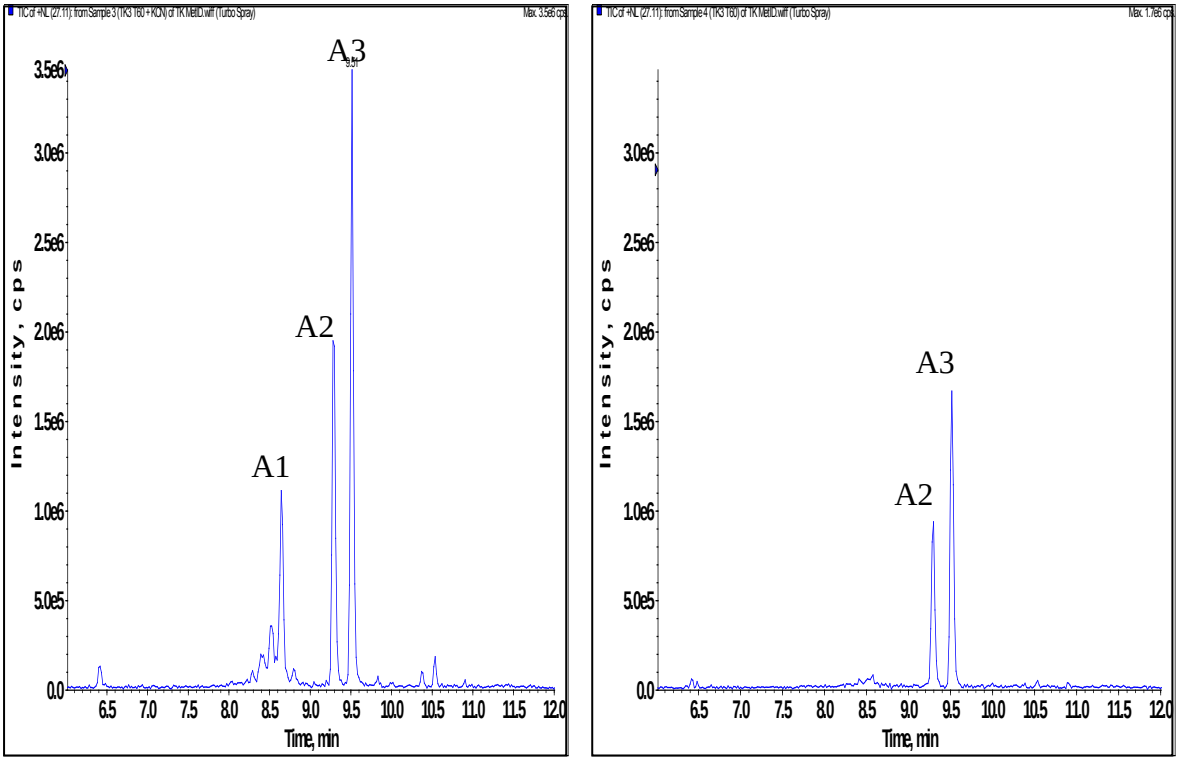

Figure 2.7: Total ion chromatogram of NL 27 in the +KCN and -KCN incubations

The fragmentation spectra of these adducts confirmed that they were parent related. The formation of cyanide adducts A2 and A3 even in the absence of the trapping agent could be due to reactions with cyanide produced from acetonitrile. Acetonitrile was used to stop the reactions and has been previously reported as the source of cyanide adducts formed in cycloalkylamine metabolism.[15] To confirm this hypothesis, the incubations were repeated with methanol in place of acetonitrile as the quenching reagent.

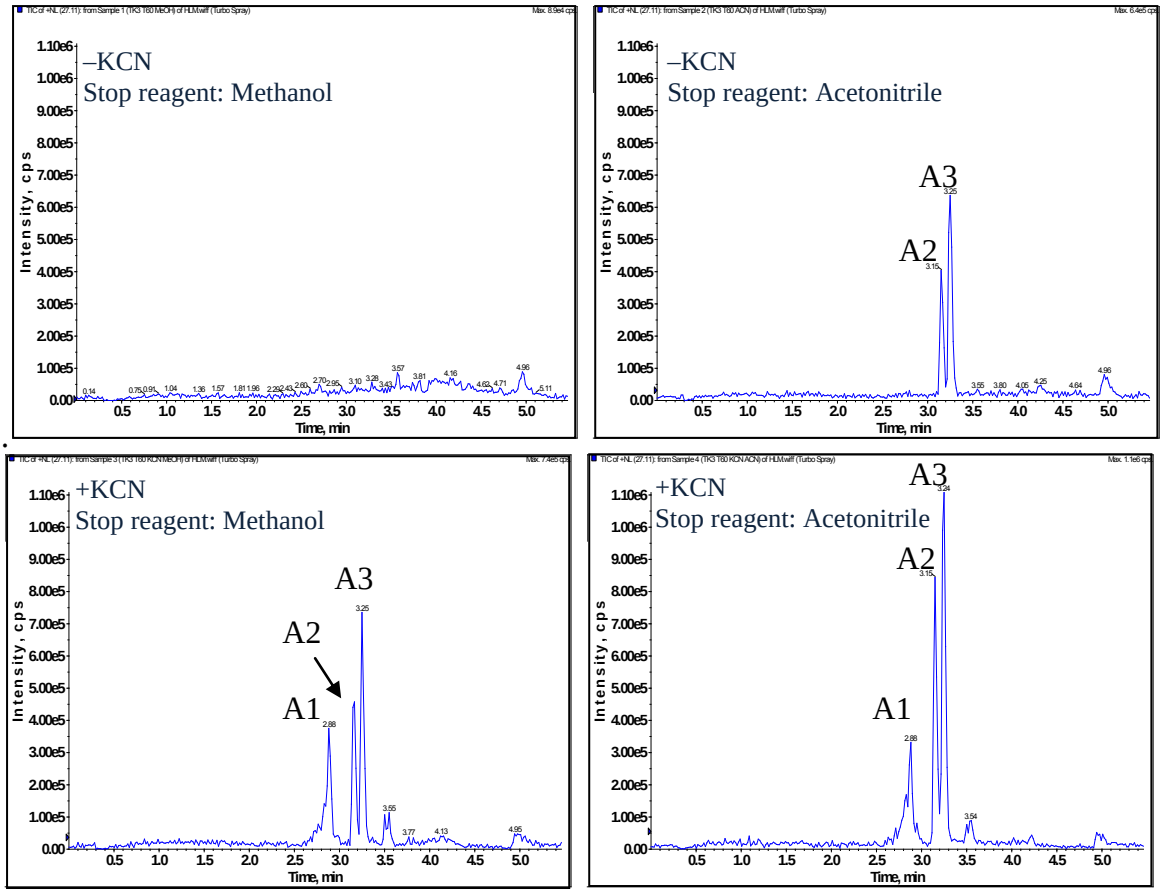

Figure 2.8: Total ion chromatogram of NL 27 in the presence and absence of cyanide, using different quenching reagents

A2 and A3 were absent in the incubation with no trapping agent, when methanol was used to stop the reaction. Even when acetonitrile is used, the intensity of A2 and A3 is slightly increased in the presence of potassium cyanide. These observations suggest that the same adducts are formed by potassium cyanide and acetonitrile and that the adducts are only formed when cyanide is present, whether from potassium cyanide, the trapping agent, or from acetonitrile, when it is used to quench the reaction.

2.2.2.3 Metabolite identification in hepatocytes

To further explore the metabolism of **TK3**, metabolite identification experiments were conducted in human and rat hepatocytes. In addition to the metabolites reported in Table 2.4, a number of glucuronides were also detected. However, unlike amodiaquine, no glutathione adducts were present.

Table 2.4: Hepatic metabolites of **TK3**

Code[a]	$M+H^+$	Proposed formula of $[M+H]^+$	Difference of measured mass of metabolite minus calculated mass (ppm)	Mass shift of $M+H^+$ after H/D exchange (Da)
M1	408	$C_{21}H_{23}N_7Cl$	-0.7	4
M2	478	$C_{25}H_{29}N_7OCl$	-2.7	3
M3	494	$C_{25}H_{29}N_7O_2Cl$	-4.2	4
M5	492	$C_{25}H_{27}N_7O_2Cl$	-3.7	3
M6	492	$C_{25}H_{27}N_7O_2Cl$	-1.0	3
M7	476	$C_{25}H_{27}N_7OCl$	-2.7	2
M8	458	$C_{25}H_{25}N_7Cl$	2.2	2
M9	584	$C_{27}H_{31}N_7O_6Cl$	-0.7	7
M10	510	$C_{25}H_{29}N_7O_3Cl$	3.3	5
M11	650	$C_{31}H_{25}N_7O_7Cl$	0.8	6
M12	654	$C_{31}H_{37}N_7O_7Cl$	-3.2	6
M13	670	$C_{31}H_{37}N_7O_8Cl$	-1.9	7
M14	670	$C_{31}H_{37}N_7O_8Cl$	1.2	7
M15	670	$C_{31}H_{37}N_7O_8Cl$	-2.8	7
M16	668	$C_{31}H_{35}N_7O_8Cl$	-2.8	6
M17	496	$C_{25}H_{31}N_7O_2Cl$	-3.2	5
M18	494	$C_{25}H_{29}N_7O_2Cl$	6.5	4
M19	494	$C_{25}H_{29}N_7O_2Cl$	5.9	4
M20	474	$C_{25}H_{25}N_7OCl$	-2.5	2
TK3	**462**	$C_{25}H_{29}N_7Cl$	**-5.8**	**2**

[a]For consistency, the same codes as in Table 2.3 were used and all newly detected metabolites were listed by retention time.

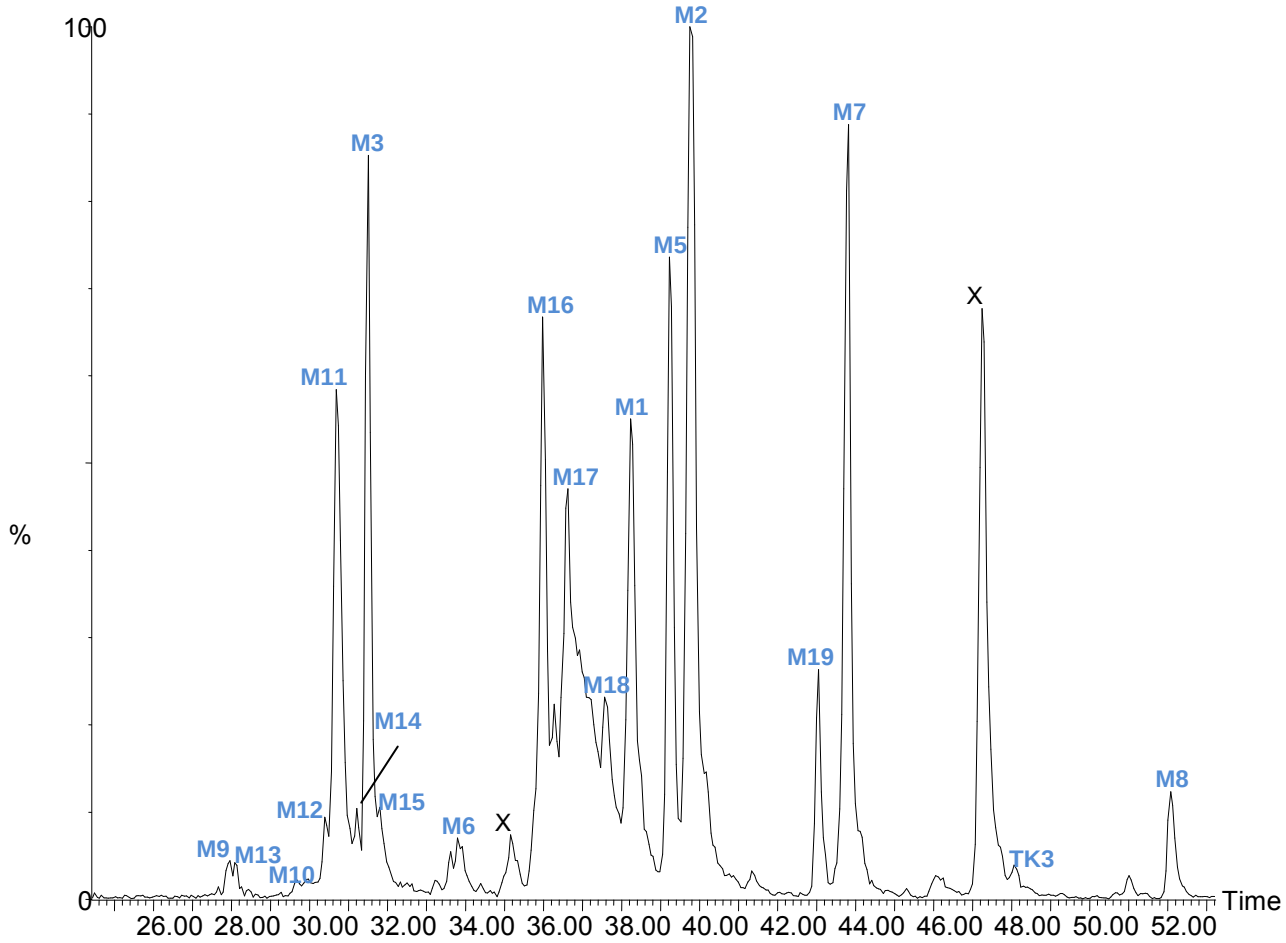

Figure 2.9: Hepatic metabolites of **TK3**

The two data sets can be interpreted together to elucidate the structures of the metabolites. As alluded to earlier, all the metabolites appear to form on the pyrrolidine ring. The involvement of an iminium ion intermediate suggests that M2, is the α-hydroxylated metabolite, most likely formed from the endocyclic iminium ion. The molecular formula of M12 and the 4 additional exchangeable protons relative to the parent, and a loss of 176Da on fragmentation imply that this metabolite is a glucuronide, most likely the O-glucuronide of M2.

.

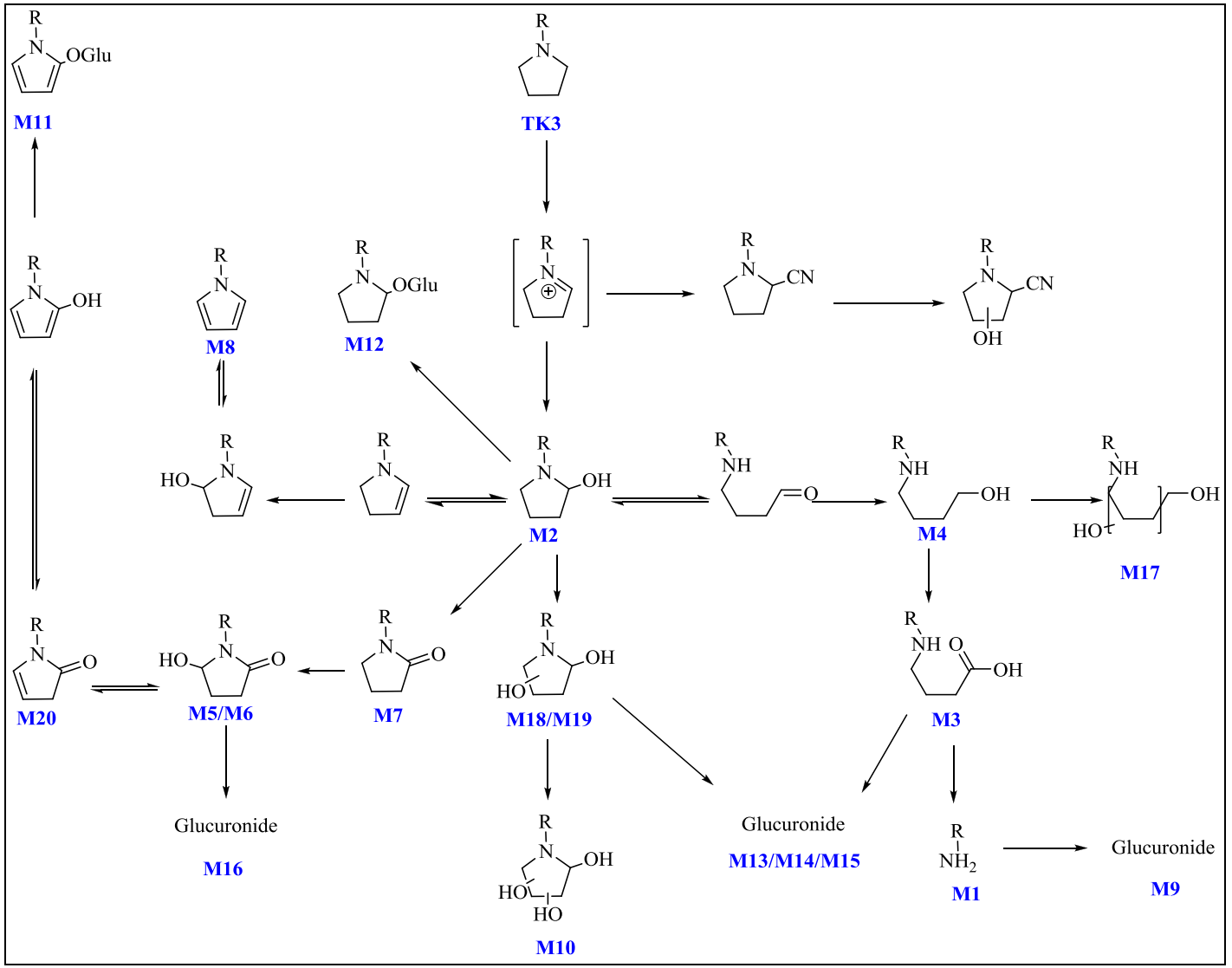

Figure 2.10: *In vitro* metabolism of **TK3**

While the fragmentation pattern of M17 is inconclusive, the additional 34Da and three exchangeable protons compared to the parent strongly imply that M17 is a hydroxylated aminoalcohol. M4, which is 16Da lower than M17, and 18Da higher than the parent could therefore be the aminoalcohol, produced through reduction of the aminoaldehyde.

M3, M18 and M19 are isobaric and their molecular formula suggests they are the dihydroxylation metabolites of **TK3**. The fragmentation is ambiguous but one of them should be the amino acid produced from M16, while the other two would be hydroxylations on the pyrrolidine ring. All three metabolites undergo glucuronidation to form M13-15.

The α-hydroxy group of M2 can be further oxidised to form the lactam M7, which can be further hydroxylated to give M5 and M6. This is suggested by the loss of 28Da from the MS/MS spectra of these metabolites, which probably results from the loss of CO following opening up of the lactam ring. M6/M7 finally undergo glucuronidation to form M11.

As proposed for other carbinolamines in Figure 2.7, M2 probably exists in equilibrium with the respective enamine. This equilibrium and further metabolism are proposed to result in M8 and M20.

Finally, any of the open chain metabolites can be dealkylated or undergo amide hydrolysis to give M1, the primary amine, which is then N-glucuronidated to give M9.

2.2.3 P450 inhibition

Current guidelines recommend the administration of antimalarials in combination, to forestall resistance selection. It is therefore important to consider the inhibition of metabolic enzymes, particularly P450s, by antimalarial agents in development. Such inhibition would interfere with plasma levels of any co-administered compounds metabolised by the inhibited enzyme.

TK2 and **TK3** were selected for P450 inhibition experiments with CYP450s and the results were as shown in table 4 below.

Table 2.5: CYP450 inhibition by **TK2** and **TK3**

		IC_{50} value (µM)	
CYP enzyme	**Probe reaction**	**TK2**	**TK3**
CYP1A2	phenacetin O-deethylation	4.33 ± 0.6	2.54 ± 0.2
CYP2A6	coumarin 7-hydroxylation	>20[b]	> 20[b]
CYP2B6	bupropion hydroxylation	16.89 ± 5.9	≈ 35.7 ± 6.2[a]
CYP2C8	paclitaxel 6α-hydroxylation	0.22 ± 0.0	0.12 ± 0.0
CYP2C9	diclofenac 4'-hydroxylation	2.43 ± 0.4	3.14 ± 0.4
CYP2C19	S-mephenytoin 4'-hydroxylation	12.20 ± 2.4	13.8 ± 1.8
CYP2D6	bufuralol 1'-hydroxylation	2.31 ± 0.1	3.46 ± 0.3
CYP2E1	chlorzoxazone 6-hydroxylation	24.94 ± 6.6[a]	≈ 32.9 ± 7.7[a]
CYP3A4	midazolam 1'-hydroxylation	0.006 ± 0.0	1.45 ± 0.1
CYP3A4	testosterone 6β-hydroxylation	0.01 ± 0.0	4.24 ± 0.6

[a]estimated by extrapolation of experimental data. [b]No inhibition seen in concetration range used

The experiments were carried out between 0-20µM because 20µM was the solubility limit of the compounds in the experimental conditions, as assessed by visual inspection of turbidity. For 2B6 and 2E1, the results were extrapolated from the available data because the IC_{50} was

above the concentration range used (See Figure 2.11C). These values are, however, above the solubility limit of the compounds and may therefore not be a true reflection of the IC_{50}. No curve inflection was seen in the concentration range used for CYP2A6 (See Figure 2.11D). Representative examples of the inhibition curves are shown below.

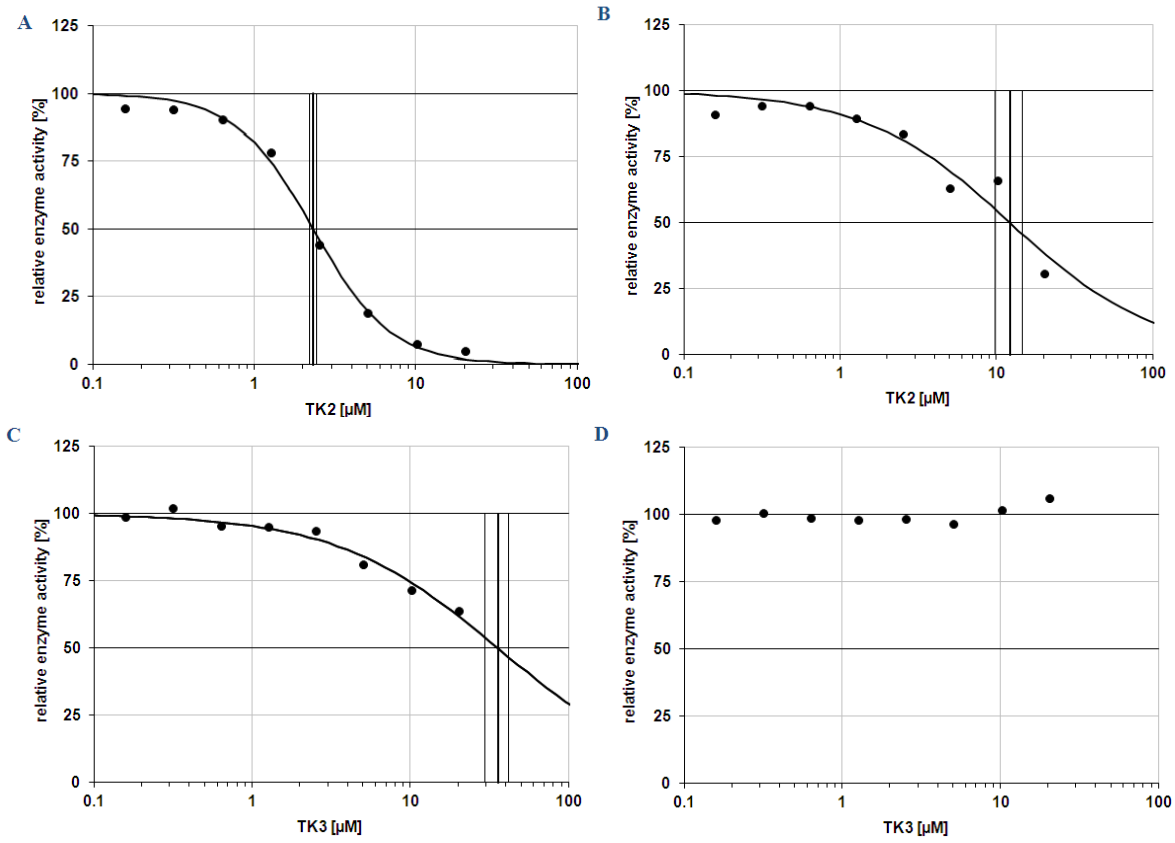

Figure 2.11: Selected inhibition curves

The results show that both compounds strongly inhibited CYP2C8 and CYP3A4 and were moderate to weak inhibitors of almost all other P450s tested. In most cases, inhibition by **TK2** was slightly stronger which may reflect its higher lipophilicity (4.96 vs 4.52).

Time dependent inhibition was investigated for CYP450s 1A2, 2C9, 2D6 and 3A4. **TK3** showed time dependent inhibition of CYP3A4 (Figure 2.12), with K_I (concentration of inhibitor giving half of maximum enzyme inactivation rate) 2.02µM and k_{inact} (maximum rate of inactivation) 0.019min^{-1}.

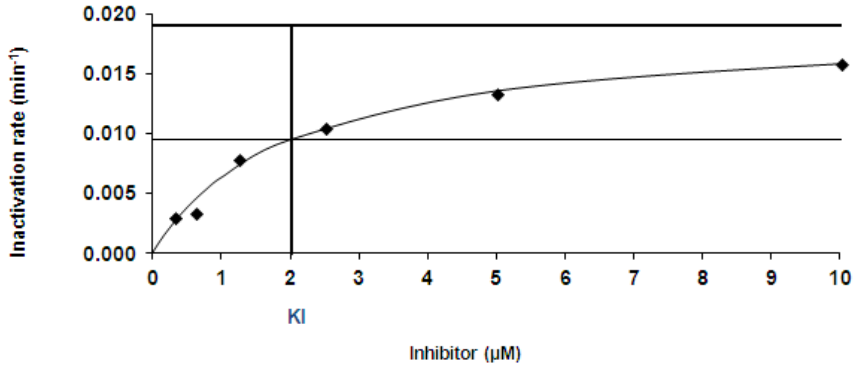

Figure 2.12: Time dependent inhibition of CYP3A4 by **TK3**

Further experimental work was conducted to investigate 3A4 inhibition in the entire compound set, in order to elucidate general trends in this property. Fluorescence inhibition with recombinant CYP3A4 was used because of its more rapid turnover. The results are presented in figure 2.15 below.

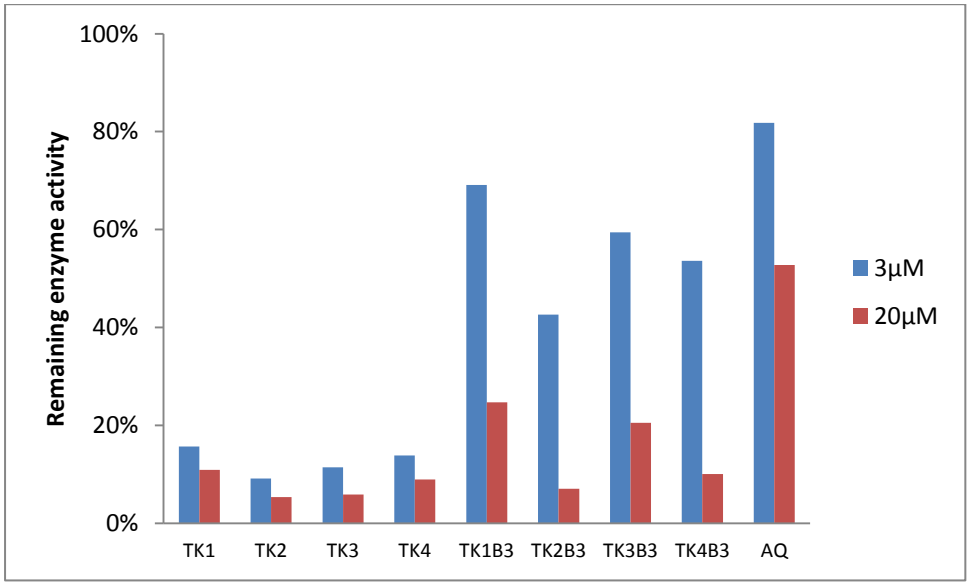

Figure 2.13: Fluorescence inhibition of recombinant CYP3A4 by the selected derivatives

2.2.3.1 In silico rationalisation of P450 inhibition

To understand the basis of the CYP3A4 inhibition by these compounds, the lowest energy conformations of **TK2**, **TK3** and amodiaquine were docked onto CYP3A4 (PDB ID: 2V0M) using Glide and Autodock 4.2.[16,17] The most favoured poses were similar for **TK2** and **TK3** but different from those of amodiaquine in both programs.

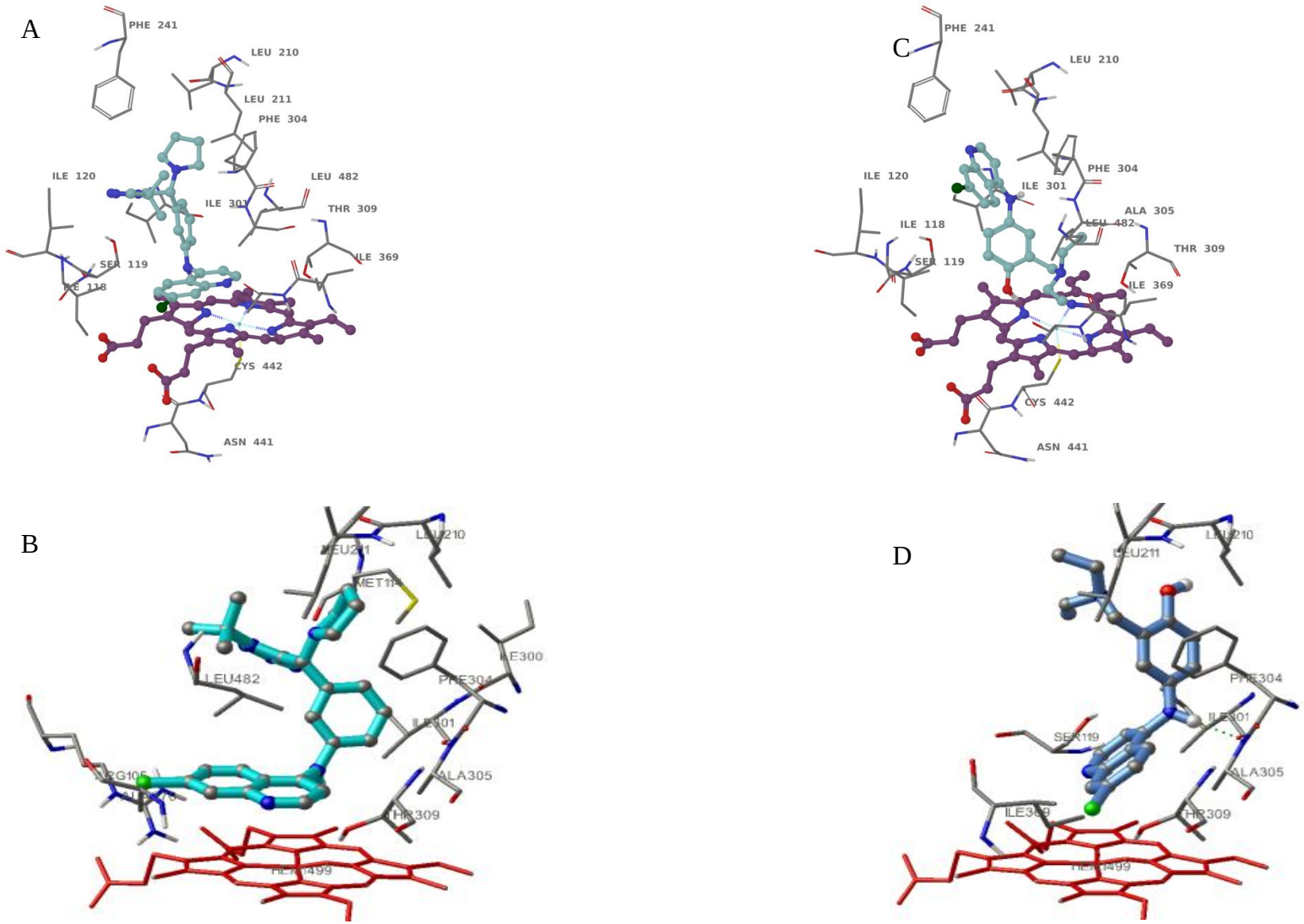

Figure 2.14: Lowest energy conformations of **TK3** (A, B) and Amodiaquine (C,D) in the active site of CYP3A4 (PDB ID: 2V0M). (A and C were generated in Glide, B and D were generated generated in Autodock 4.2)

The docked conformations are different in the two programs which may be expected because the large volume of the CYP3A4 active site allows molecules to rotate and may lead to multiple favoured conformations. However, a similarity in both cases for **TK3** (and for **TK2**, data not shown) is that the lowest energy conformation is docked such that the 7-chloro-aminoquinoline nucleus lies parallel to the heme. This would maximise π-π and π-cation interactions between this ring and heme. The rest of the molecule orients close to a number of hydrophobic residues and increased lipohilicity in this portion of the molecule could also contribute to hydrophobic interactions with these residues. In addition, Amodiaquine is smaller and less lipophilic and would therefore be expected to have less interaction with the heme and other active site residues.

2.2.4 Discussion

The most active compounds **TK1** – **TK4** were rapidly metabolised in both HLM and RLM. The site of metabolism for all compounds evaluated was the attachment on the tertiary nitrogen. **TK1** and **TK2** which have alkyl substituents on the tertiary nitrogen were metabolised by dealkylation and then didealkylation to the primary amine. The metabolism of **TK3** and **TK4**, which have cycloalkyl substituents (pyrrolidine and piperidine respectively), was mainly by hydroxylations on this ring.

Cycloalkylamine containing compounds are widely reported to undergo hydroxylation on the carbon adjacent to the nitrogen.[18] This hydroxylation is reported to proceed through a reactive iminium ion intermediate, which exists in equilibrium with the respective carbinolamine, enamine and aminoaldehyde.

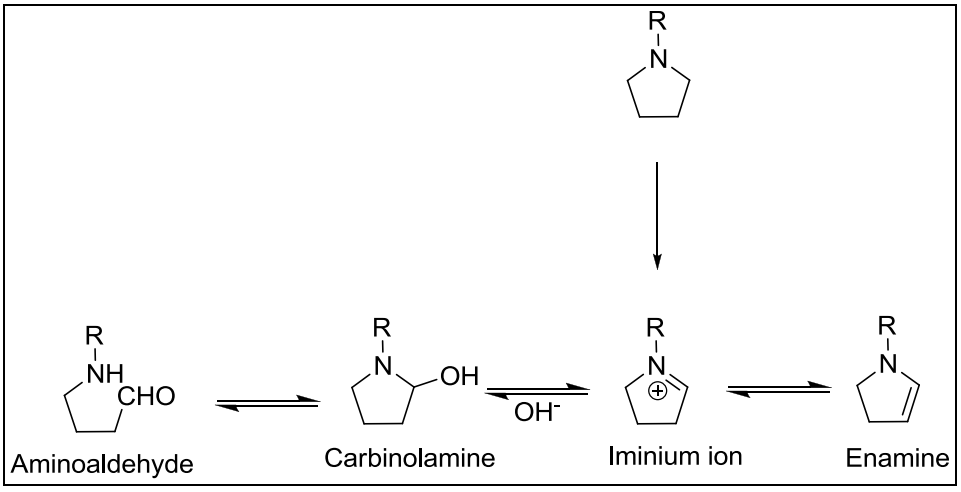

Figure 2.15: Iminium ion equilibrium for pyrrolidine and other cycloalkylamines[18]

The involvement of this pathway in the metabolism of **TK3** was confirmed by trapping the iminium ion using cyanide. Three cyanide adducts were identified for this compound. **TK3** contains two non-equivalent carbons α to the nitrogen, one endocyclic and one exocyclic. These are probably responsible for the formation of these adducts. The endocyclic iminium ion is more stable because it is stabilised by the equilibrium forms as shown in Figure 2.16

and is therefore the one that is further converted to the hydroxylated products. This preference for an endocyclic over an exocyclic pathway is precedented in literature.[18] More specifically for these compounds, this preference is demonstrated by the fact that **TK1** and **TK2**, which also have a carbon α to the nitrogen, but are not cyclic, do not form cyanide adducts, while adducts were detected for both **TK3** and **TK4** which are cyclic.

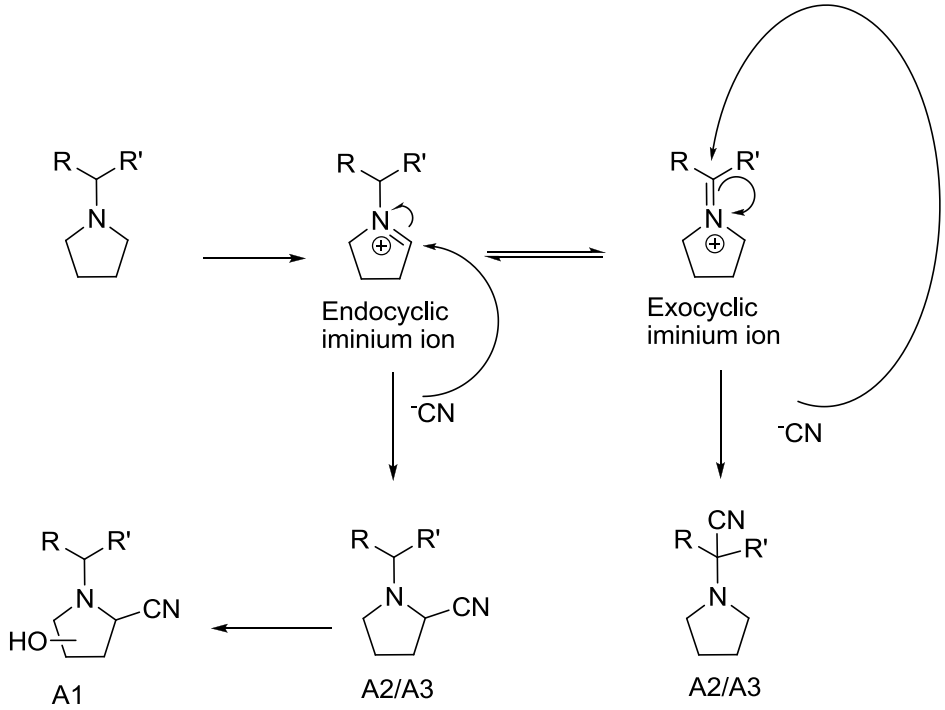

Figure 2.16: Proposed reactions in the formation of cyanide adducts A1 - A3

A similar metabolic pathway has been reported for pyronaridine, which also has a pyrrolidine ring. However, unlike **TK3** pyronaridine has a much longer half-life and the fraction metabolised is also much lower.[19,20]

The tetrazole deoxyamodiaquines were also found to be potent CYP450 inhibitors with **TK2** and **TK3** showing submicromolar IC_{50}s for CYP 2C8 and CYP 3A4 and moderate inhibition of most other CYP450s except CYP 2A6 and CYP 2E1. The weak inhibition of CYP2A6 and CYP 2E1 may reflect the difficulty of these two compounds in accessing the binding cavity of these enzymes, which is reported to be small, therefore favouring interactions with smaller

compounds.[21,22] Amodiaquine has been reported to competitively inhibit 2C8 and 2D6, with the latter inhibition reported to be strong enough to cause clinical interactions.[13,23] The inhibition of these two enzymes by these compounds could therefore be an extension of this effect with more lipophilic compounds.

CYP3A4 inhibition as measured using fluorescence assays was lower in the compounds lacking a *tert*-butyl substitution, an effect probably related to their lower lipophilicity (Figure 2.17).

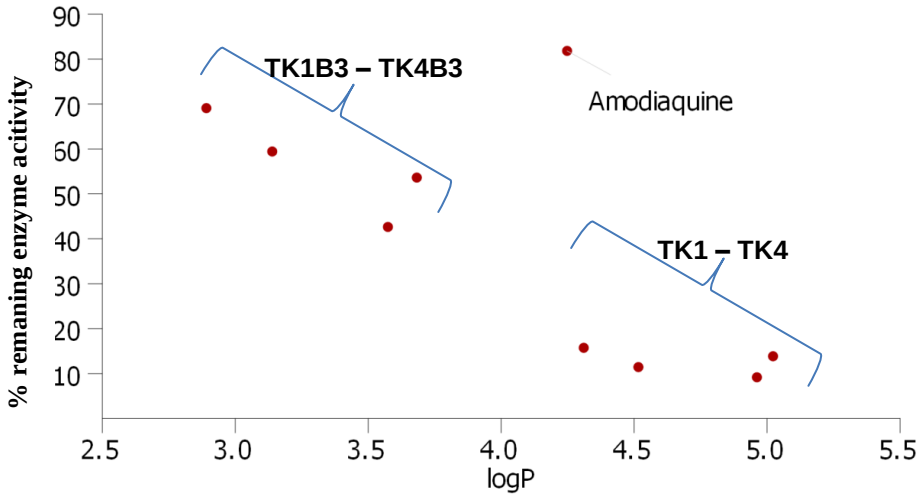

Figure 2.17: Variation in CYP3A4 inhibition with lipophilicity

This relationship between CYP3A4 activity and lipophilicity is reported for many other compound series.[24,25] Amodiaquine clearly differs from these compounds in its lack of 3A4 inhibition and even in literature, is reported to not inhibit CYP3A4. *In silico* work suggests that a difference in orientation and, therefore, interactions at the active site plays a part in this inhibition.

Because metabolic stability was identified as a significant liability for these compounds, the ability of StarDrop to predict the main sites of metabolism was assessed. A good correlation between the predicted and the observed sites of metabolism would indicate the utility of this tool in the *in silico* evaluation of other generations of these compounds synthesised to circumvent the metabolic lability.

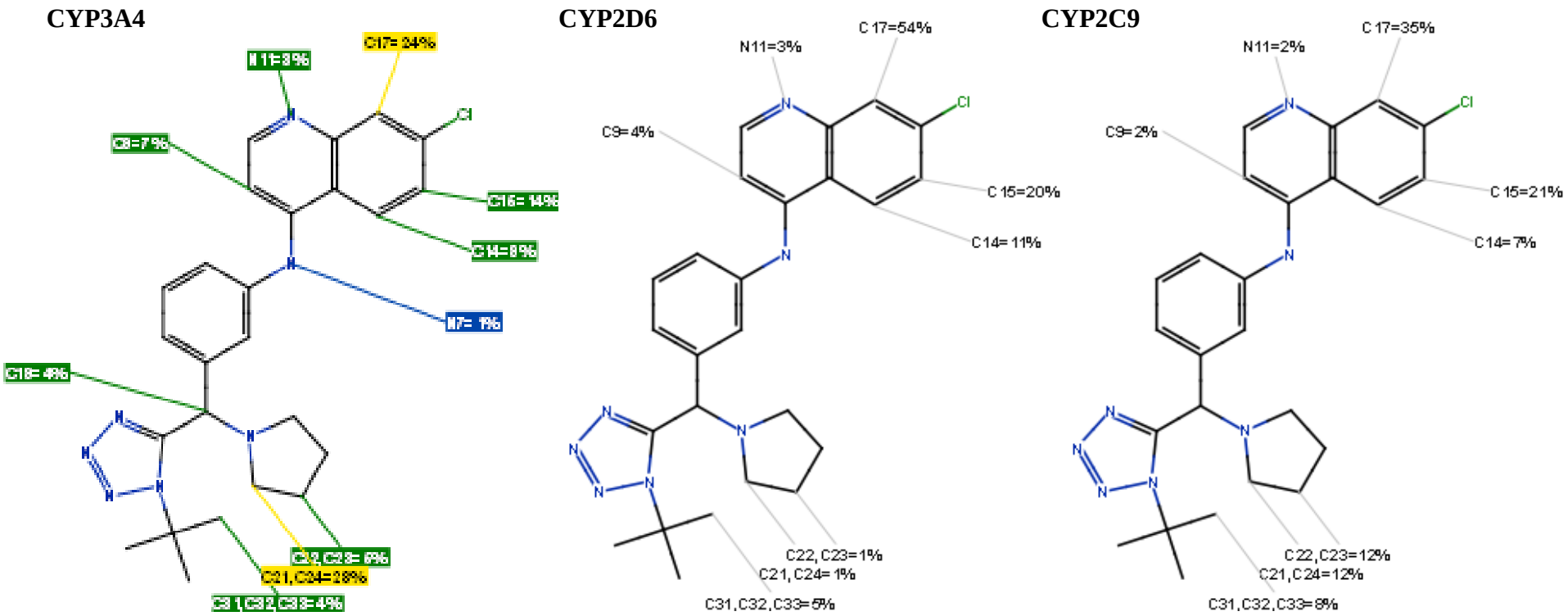

Figure 2.18: StarDrop predicted sites of metabolism for **TK3** assuming metabolism by CYP3A4, CYP2D6 or CYP2C9. (The percentages show the expected proportion of metabolites that would result from metabolism at the indicated position. For CYP3A4, the colors indicate the lability of the positions; red – labile, yellow – moderately labile, green – moderately stable, blue – stable)

From the experimental data, the metabolism of **TK3** involved α-hydroxylation of the pyrrolidine ring followed by formation of secondary metabolites by further metabolic and rearrangement reactions. The α-position on the pyrrolidine ring is indeed identified as the site that would contribute most (28%) to the metabolism of **TK3** by CYP3A4. In addition, this position is identified as moderately labile indicating the ease of proton abstraction at this position during CYP3A4 metabolism. Interestingly, both CYP2D6 and CYP2C9 predict position 8 of the aminoquinoline ring (C17 in Figure 2.18) as the major site of metabolism. No metabolites were observed in the experimental data on the aminoquinoline ring. The position is predicted to be metabolically labile by the CYP3A4 model and the absence of the corresponding metabolite in the experimental data may indicate poor accessibility in the active site of the enzyme. This may indicate that the correction factor for metabolic site accessibility is inadequately applied for this compound. Alternatively, the metabolism at the primary site (α-position of pyrrolidine) may be efficient and fast enough that it is formed preferentially over other sites of metabolism.

The same pattern of predictions was observed for **TK2** with CYP3A4 predicting metabolism α- to the tertiary nitrogen – in this case *N*-dealkylation, as the main metabolite. This was also predicted by the CYP2C9 model while the CYP2D6 model still had 8-hydroxylation as the main predicted metabolite.

For both compounds the CYP3A4 model offers a reasonable approximation of the experimental data regarding the identification of the major site of metabolism. This may partly be because CYP3A4 is more promiscuous, relying more heavily on the physicochemical characteristics of the compounds than on the presence of specific structural features in the compound. While StarDrop only has models for CYP3A4, CYP2D6 and CYP2C9, other CYP450s likely contribute to the metabolism of these compounds. In addition metabolism of cycloalkylamines following iminium ion formation is known to involve aldehyde oxidase and this enzyme is also a likely possible contributor to the rapid metabolism of these compounds.

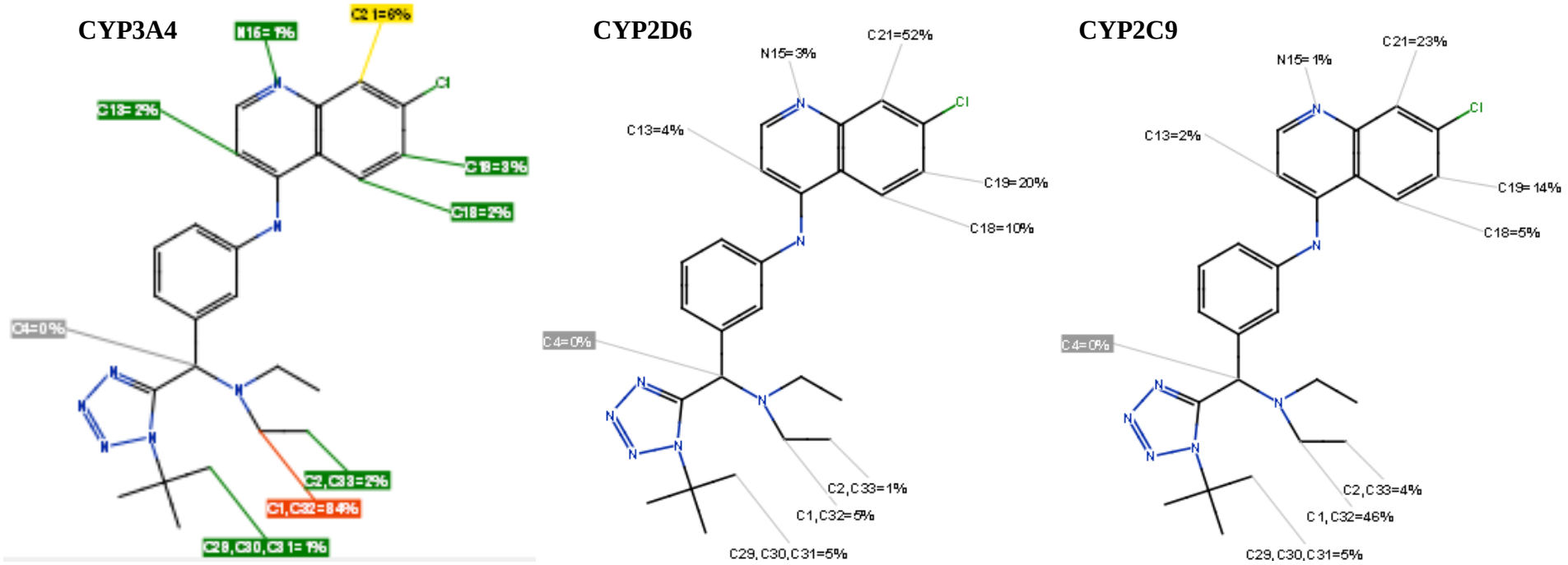

Figure 2.19: StarDrop predicted sites of metabolism for **TK2** assuming metabolism by CYP3A4, CYP2D6 or CYP2C9. (The percentages show the expected proportion of metabolites that would result from metabolism at the indicated position. For CYP3A4, the colors indicate the lability of the positions; red – labile, yellow – moderately labile, green – moderately stable, blue – stable)

StarDrop was also used to predict the physicochemical properties of the tentatively identified metabolites.

Table 2.6: Predicted physicochemical properties of the metabolites

Compound	MW	LogP	LogD	TPSA
TK3	462	4.52	1.99	72
Hydroxylation (M2)	478	3.94	1.56	92
Keto- formation (M7)	476	4.21	4.21	88
Amino acid (M3/M18/M19)	494	1.28	-0.36	118
Hydroxyketo O-glucuronidation (M16)	668	1.8	-0.18	205

The metabolite numbers correspond to those used in Figure 2.10 and elsewhere for these compounds

There were no large differences in physicochemical properties between the various isobaric metabolites (except the amino acid and dihydroxylation metabolites), and the structures used are therefore just representative of the possible metabolites. For example, the conclusions drawn do not change, if the β-position is hydroxylated on M16 rather than the α-position.

There is a progressive decrease in log P and log D as the compound is hydroxylated (to M2) then converted to the amino acid (M3/18/19). As expected, keto- formation (M7), increases the log D of the resulting metabolite, and glucuronidation of this metabolite (to M16) leads to a further drop in Log P and Log D. Overall though, M2 and M7 remain in the optimal zone for lipoidal permeability and their passive diffusion is possibly comparable to that of **TK3**. The amino acid metabolite and the glucuronide, however, have much lower log D and much higher TPSA and their ability to passively diffuse across membranes is likely to be significantly lower than the parent. This could have implications on their ability to reach the site of action and their contribution to *in vivo* antimalarial activity, might therefore be minimal, compared to the other two metabolites.

As discussed in Chapter I, the *in vivo* contribution of a metabolite depends not only on its intrinsic activity and lipoidal permeability, but also on the rate of its formation from the parent and its subsequent clearance through further metabolism or excretion. **TK3** is almost completely metabolised in both hepatocytes and microsomes. However, the presence of so many metabolites, coupled with the fact that most of these are second or third generation metabolites implies that the first and second generation metabolites are also liable to extensive metabolism. In each successive generation, the metabolites in general become more polar, less lipoidally permeable and therefore more likely to be excreted than to remain in circulation. In contrast, while amodiaquine is rapidly metabolised to desethylamodiaquine, the latter is quite metabolically stable and has a much longer half-life relative to amodiaquine (10days vs 12h).[26] The findings for these compounds suggest that most of the metabolites will have similar or only slightly higher half-lives relative to the parent. These compounds were therefore precluded from *in vivo* work pending the further optimisation of their metabolic stability.

2.3 Tetrazole chloroquines

2.3.1 Background

Chloroquine was the first of the synthetic aminoquinolines, synthesised based on the quinine template, and was once the most widely used antimalarial drug. The emergence of resistant strains has unfortunately greatly limited its usefulness.[27] The pharmacokinetics and metabolism of chloroquine have been reviewed by several authors.[1,28–30] The key points are that it is extensively distributed in tissues (Vd 200 – 800L/Kg), and has a very long half-life (20 – 60 days).[3030] Its main metabolic pathway *in vivo* is deethylation to mono- and dideseethyl metabolites. Monodesethylchloroquine retains some antiplasmodial activity, and is usually present at about 20-50% of the parent plasma concentration, while didesethylchloroquine is formed to about 10-15%.[31,32] This dealkylation pathway is driven mostly by CYP2C8, with contribution by CYP3A4 and CYP2D6.[31,32] This dealkylation pathway is driven mostly by CYP2C8, with contribution by CYP3A4 and CYP2D6. Side chain and aminoquinoline N-oxidation has also been reported. [32]

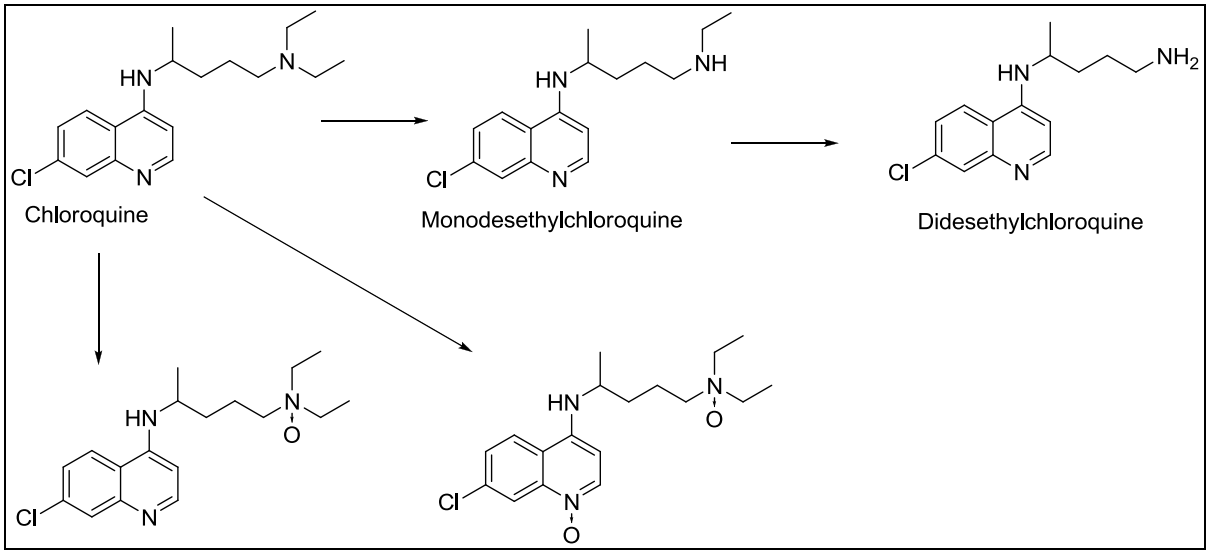

Figure 2.20: The metabolism of chloroquine in man[33,34]

Various approaches have been adopted to give derivatives with no cross-resistance with chloroquine.[1] The approach explored to produce the derivatives considered in this work involves shortening the side chain and incorporation of a bulky *N*-alkyl substituent fused to a tetrazole moiety.[3535] Shorter side chain analogues of chloroquine have been reported to retain the antiplasmodial activity of chloroquine and importantly, are also more active than chloroquine against chloroquine-resistant strains. Such derivatives are, however, reported to be more susceptible to *N*-dealkylation, and while the metabolites may retain antiplasmodial activity, the reduced lipid solubility is postulated to reduce activity against chloroquine resistant strains.[36] Bulkier *N*-substituents are therefore more common for these derivatives.

2.3.2 Compound selection

Several derivatives were selected, based on activity, and investigations on their metabolism conducted as reported in this section. Two derivatives without a *tert*-butyl substitution on the tetrazole ring were also selected to evaluate the effect of this group on the metabolism of the compounds. The derivatives considered are shown below.

Table 2.7: : Antiplasmodial activity of tetrazole chloroquines[35]

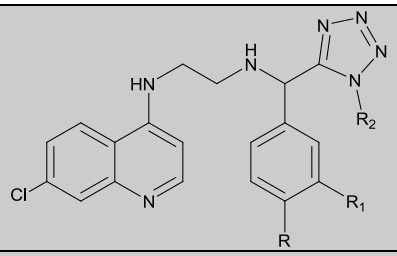

				P. falciparum IC50 (µM)		
Code	**R**	**R^1**	**R^2**	**3D7**	**K1**	**W2**
TK900A	H	H	t-Bu	0.005	0.038	0.069
TK900C	CH3	H	t-Bu	0.001	0.002	0.0311
TK900D	Cl	Cl	t-Bu	0.0004	0.008	0.0305
TK900E	Cl	H	t-Bu	0.002	0.001	0.0255
TK900DB3	Cl	Cl	H	nd	4.39	nd
TK900EB3	Cl	H	H	nd	2.38	nd
	Chloroquine			0.0052	0.036	0.059

2.3.3 Metabolism studies

The microsomal stability of the selected derivatives was determined in human and rat liver microsomes using a single point assay at 0.4mg/ml microsomal protein, for 30 minutes.[37]

Table 2.8: Microsomal metabolic stability of tetrazole chloroquines

Compound	**Microsomal stability (% remaining at 30 min)**		**Log P***
	HLM	RLM	
TK900A	38	8	4.49
TK900C	35	<5	4.85
TK900D	48	66	5.24
TK900E	52	55	4.88
TK900DB3	>99	80	3.83
TK900EB3	>99	92	3.42
Chloroquine	>99	76	4.63

In HLMs, chloroquine was stable with no reduction in the parent concentration observed, but its metabolism was faster in RLM, where only 76% of the initial concetration remained. For comparison, the data for chloroquine translates to a microsomal half-life >200min in HLMs and 77min in RLMs which is consistent with literature data for microsomal incubations.[38] **TK900A** – **TK900E** had poor to moderate stability in both species, while the derivatives lacking a *tert*-butyl were more stable.

2.3.3 Metabolite identification

Metabolite identification studies were conducted for the derivatives, first in microsomal incubations supplemented with NADPH, to understand the drivers of the microsomal instability observed, and subsequently in hepatocytes to gain a broader picture of the

metabolism of these compounds. For simplicity in presentation, **TK900E** will be discussed as the prototypical compound but significant deviations in the metabolism of the other compounds in the series will also be pointed out.

As a preamble to the metabolite identification work, the fragmentation of **TK900E** was evaluated.

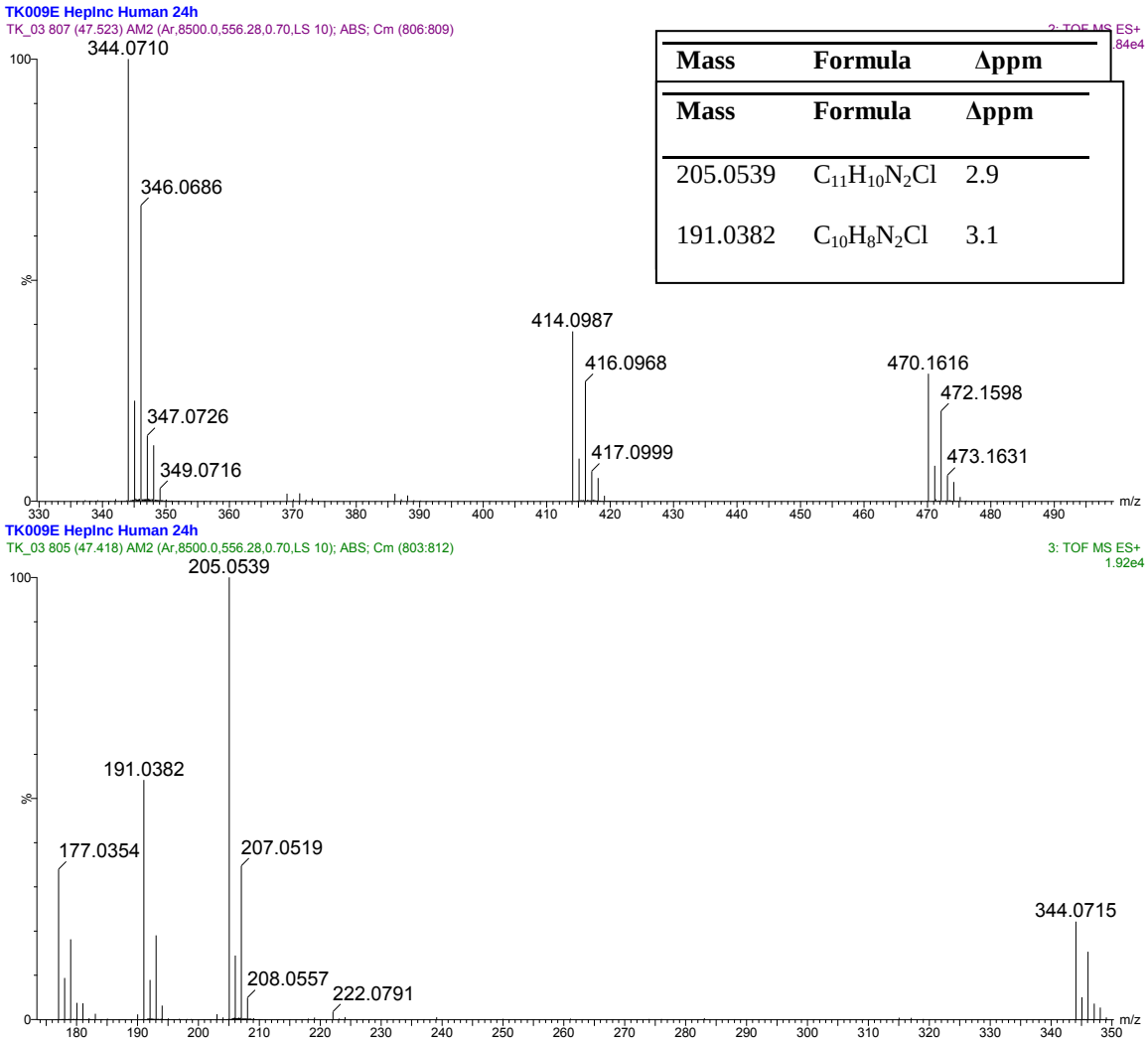

Mass	Formula	Δppm
205.0539	$C_{11}H_{10}N_2Cl$	2.9
191.0382	$C_{10}H_8N_2Cl$	3.1

Figure 2.21: MS^E spectra of **TK900E**

There are similarities between the fragmentation of **TK900E** and that of the tetrazole deoxyamodiaquines, especially regarding the fragmentation of the *tert*-butyl substituted tetrazole ring. This proceeds by a loss of the *tert*-buytl group, followed by, or in parallel with,

the loss of the tetrazole ring. The side chain nitrogen and its substituent are then lost with charge transfer to the methylene, to give the m/z 205 fragment, which then undergoes sequential methylene losses to give the remaining fragments.

2.3.3.1 Microsomal metabolism

Unlike the tetrazole deoxyamodiaquines, the peak corresponding to the unmetabolised parent, **TK900E**, was the major peak in the chromatogram. A number of mono-hydroxylated metabolites were also observed

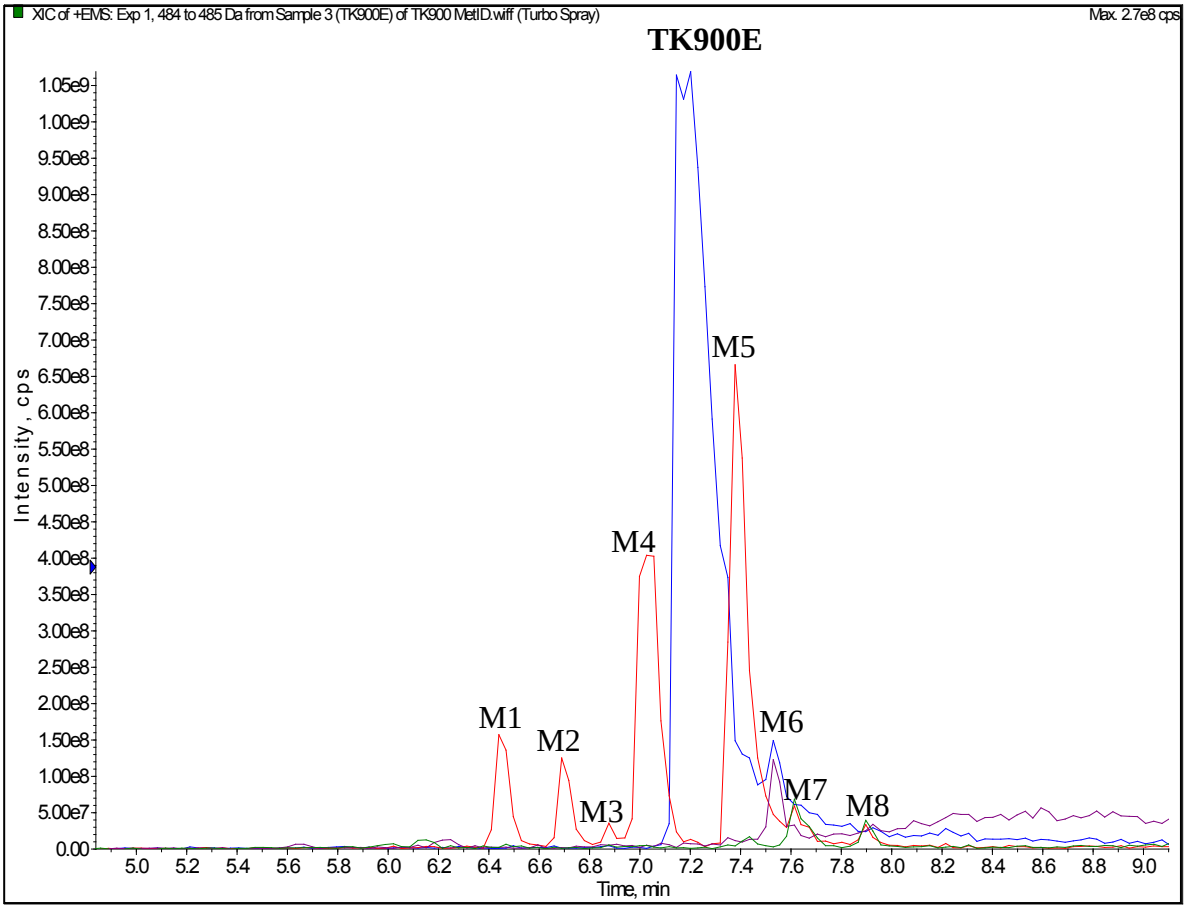

Figure 2.22: Extracted ion chromatograms of **TK900E** and its HLM metabolites

Similar metabolites were detected in rat liver microsomes. The collision induced dissociation of the metabolites was then considered in order to elucidate the metabolically labile positions.

All major fragments produced from M1 are similar to the fragments of the precursor ion of the parent compound. This suggests hydroxylation on the *tert*-butyl group, since this group is

the first to be lost during fragmentation, and any modifications occurring here would be lost together with this fragment.

Table 2.9: Microsomal metabolites of **TK900E**

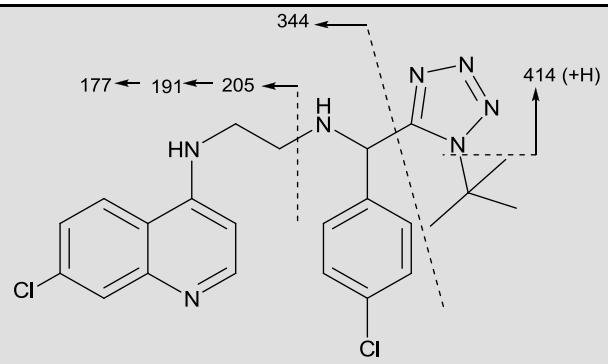

Code	Rt	m/z	Fragments			
			A	B	C	Others
			414	344	205	
M1	6.45	486	414	344	205	191, 177
M2	6.69	486	430	360	221	193, 207
M3	6.89	486	430	360	221	193, 207
M4	7.04	486	430	360	221	195, 166
M5	7.39	486	430	360	221	207, 191
M6	7.53	468	412	342	205	191, 177
M7	7.61	484	428	358	205	191,177
M8	7.90	484	428	358	205	400,354
Parent	7.19	470	414	344	205	191, 177

M2 – M5 all fragment to give m/z 430, 360 and 221, which are 16 Da higher than the corresponding fragments in the parent. This suggests that metabolism occurs on the left side of the molecule, on the ethylaminochloroquinoline. For M2 and M3, the sequential loss of methylene units to give the m/z 207 and 193 fragments, also higher than the corresponding

parent fragments by 16 Da, suggests that metabolism occurs on the 7-chloroaminoquinoline core. The position of metabolism for M4 is less clear; while the 221 fragment indicates that metabolism occurs somewhere on the ethylchloroaminoquinoline, the absence of fragments that would correspond to the methylene losses and/or the aminoquinoline core make it difficult to conclusively assign the metabolite. M5-M8 were similarly difficult to assign, beyond excluding the right side of the molecule as the metabolic site.

An additional route of metabolism in **TK900A** and **TK900C** is hydroxylation of the phenyl ring. This is particularly the case in **TK900C** where this metabolite accounts for more than 50% of the total metabolites present, as assessed by DAD peak area. A number of di hydroxylated metabolites were also detected. These additional metabolic routes possibly account for the reduced stability of these compounds relative to **TK900E**.

The metabolism of **TK900DB3** and **TK900EB3** is similar to that described for **TK900E**. The stability of these compounds is at least in part due to the absence of the *tert*-butyl group, which is a site of metabolism in **TK900D** and **TK900E**.

2.3.3.3 Metabolite identification in hepatocytes

The metabolism of **TK900E** was explored in rat and human hepatocytes.

In addition to the metabolites already described in microsomes, a number of glucuronides were detected, possibly resulting from O-glucuronidation of the hydroxylation metabolites described. N-glucuronidation to the side chain nitrogen was also observed, but at a much lower intensity. Metabolism was similar in both human and rat hepatocytes.

Table 2.10: Hepatic metabolites of **TK900E**

Component	$M+H^+$	Proposed formula of $[M+H]^+$	Δppm	Mass shift of $M+H^+$ after H/D exchange(Da)
M2	486	$C_{23}H_{26}N_7OCl_2$	3.2	4
M9	662	$C_{29}H_{34}N_7O_7Cl_2$	2.0	**7**
M10	646	$C_{29}H_{34}N_7O_6Cl_2$	0.5	nd
M11	791	$C_{33}H_{41}N_{10}O_7Cl_2S$	4.3	nd
M12	662	$C_{29}H_{34}N_7O_7Cl_2$	0.8	**nd**
M13	662	$C_{29}H_{34}N_7O_7Cl_2$	6.8	**nd**
M14	662	$C_{29}H_{34}N_7O_7Cl_2$	3.5	**7**
M7	484	$C_{23}H_{24}N_7OCl_2$	2.1	**3**
M4	486	$C_{23}H_{26}N_7OCl_2$	0.8	**4**
M5	486	$C_{23}H_{26}N_7OCl_2$	2.7	**3**
M1	486	$C_{23}H_{26}N_7OCl_2$	1.4	**4**
M8	484	$C_{23}H_{24}N_7OCl_2$	2.1	**2**
M3	486	$C_{23}H_{26}N_7OCl_2$	0.2	**4**
M6	468	$C_{23}H_{24}N_7Cl_2$	0.6	**2**
TK900E	470	$C_{23}H_{24}N_7Cl_2$	-2.3	3

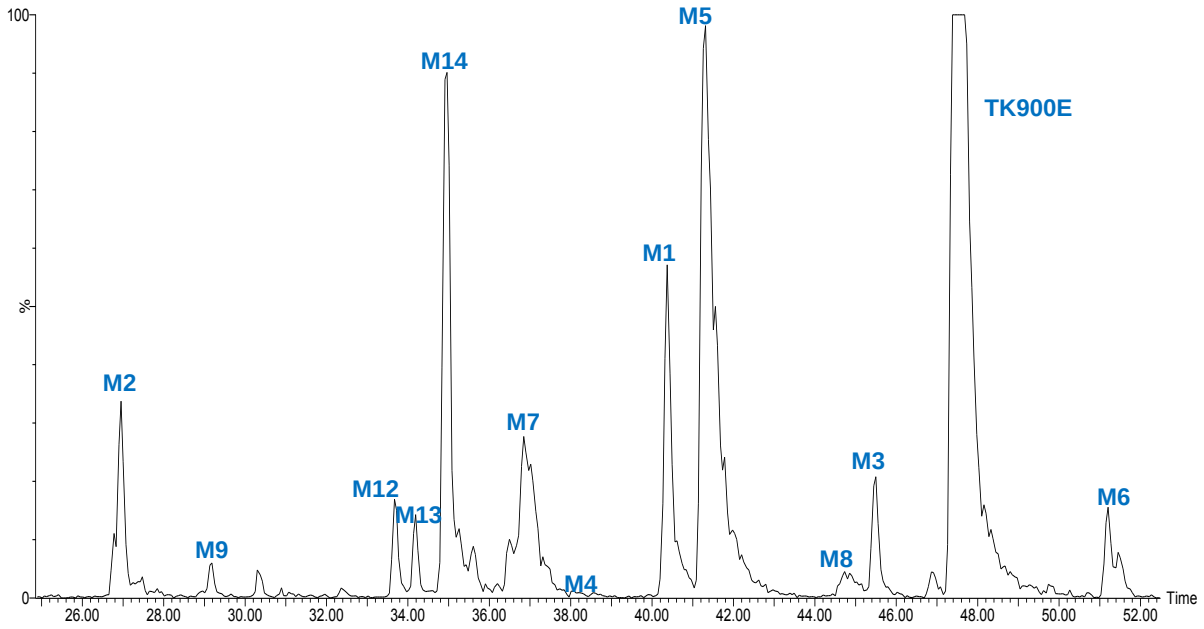

Figure 2.23: Extracted ion chromatogram of **TK900E** human hepatocyte metabolites

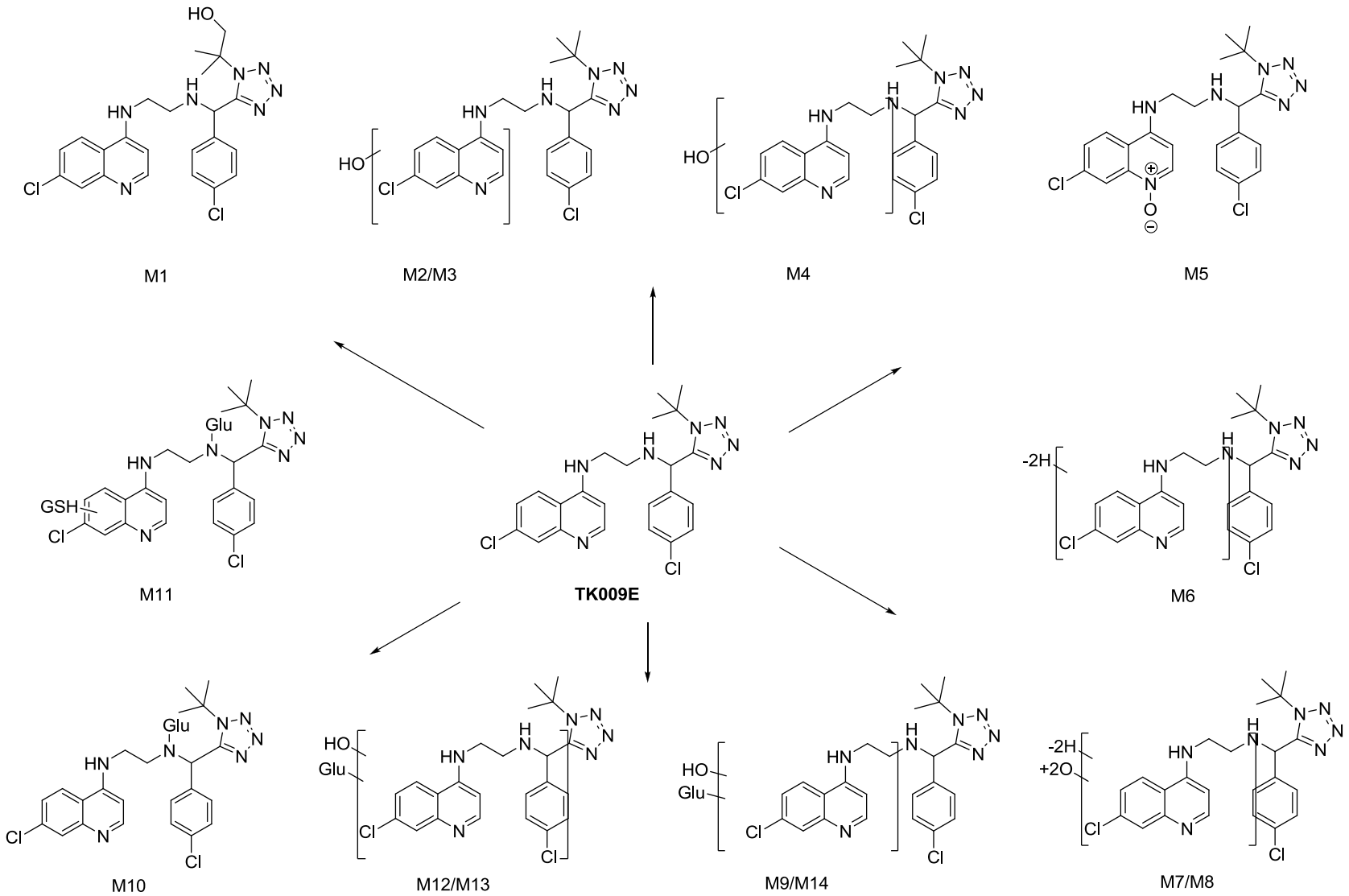

Figure 2.24: *In vitro* metabolites of **TK900E**

The H/D data for M5 shows that although it is a hydroxylation metabolite, it has the same number of exchangeable protons as the parent, suggesting that it is an *N*-oxide.[39] Quinoline *N*-oxidation is also reported for chloroquine and piperaquine and would therefore be plausible for this compound.[28,40]

The intensity of the glutathione adduct formed was not sufficient to give good fragmentation data. The experiment was, therefore, repeated in microsomes using a higher compound concentration. For comparison, **TK900A** was also incubated under the same conditions.

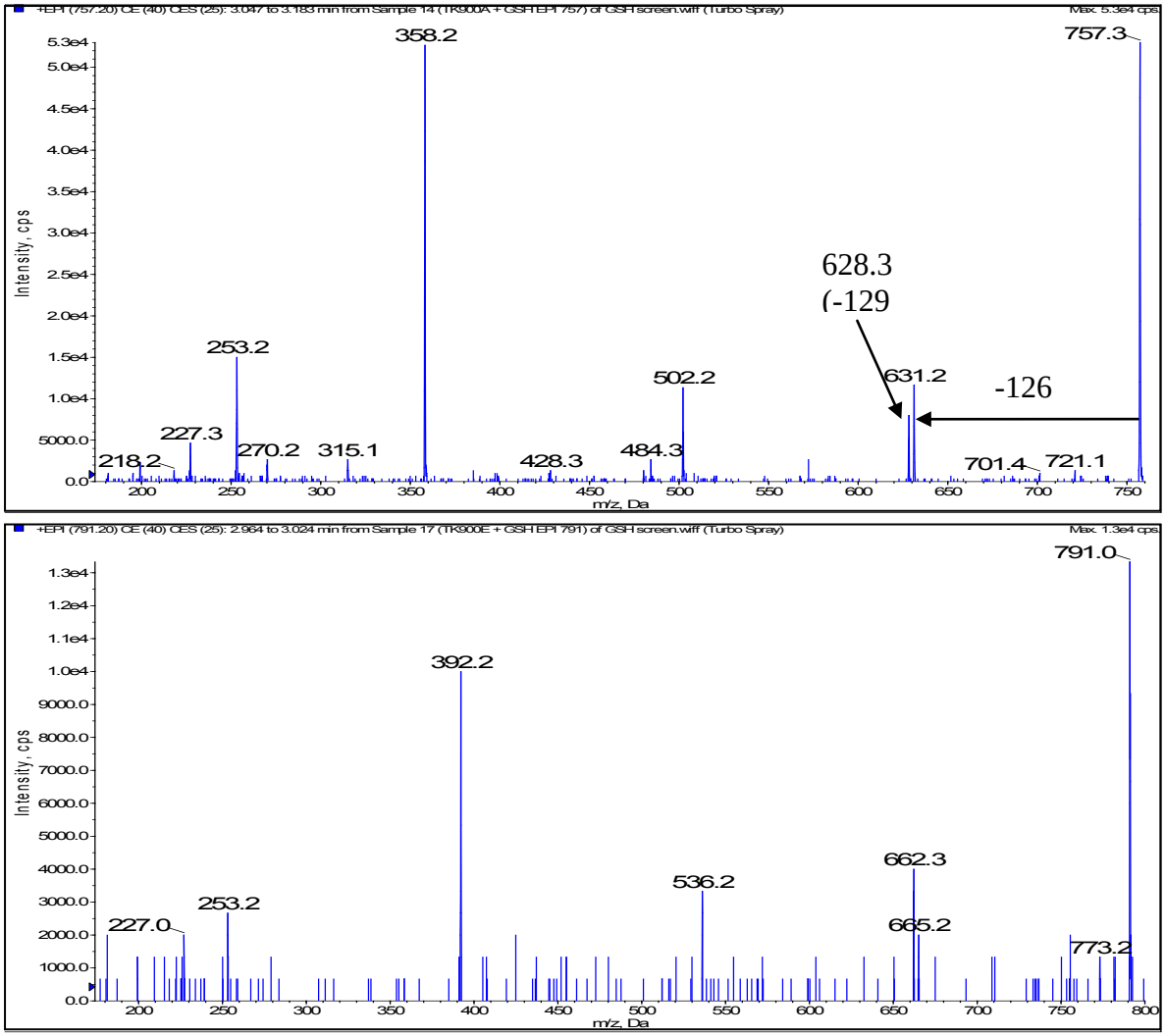

Figure 2.25: Product ion spectra of the glutathione adducts of **TK900A** and **TK900E**

In addition to the loss of 126 Da characteristic of these compounds, a loss of 129 Da (to give m/z 628 in **TK900A** and 662 in **TK900E**) is also observed. This neutral loss is considered diagnostic of glutathione adducts and is commonly used to screen for adducts.[41–43] The low intensity of these glutathione adducts led to inconclusive results with the neutral loss scan. The adducts could however be detected using EMS-IDA-EPI methods, and also when EPI scans were used in isolation as survey. The fragments of m/z 502 and 536Da in **TK900A** and **TK900E** respectively are produced from a loss of 129Da from m/z 628 and 662Da, which are produced as described earlier. The presence of these fragments means that the substituted tetrazole is not the site of conjugation.

It is postulated that m/z 358 and 392 (for **TK900A** and **TK900E** respectively) are produced by a loss of the cysteinyl moiety from m/z 628 and 662Da, leaving the sulfur attached to the aminoquinoline nucleus. This loss of 273Da is also characteristic of glutathione adducts.[41–43] In the product ion spectra obtained in the negative mode, the corresponding fragment of m/z 272 was also observed. The fragment with m/z 253 in both spectra probably corresponds to m/z 205 in the parent compound, produced by loss of the side chain nitrogen and its substituent. Finally, m/z 227, which is also in both spectra, is proposed to arise from cleavage of the entire alkyl side chain to give the mercaptoquinoline derivative. A summary of this fragmentation pathway is presented below.

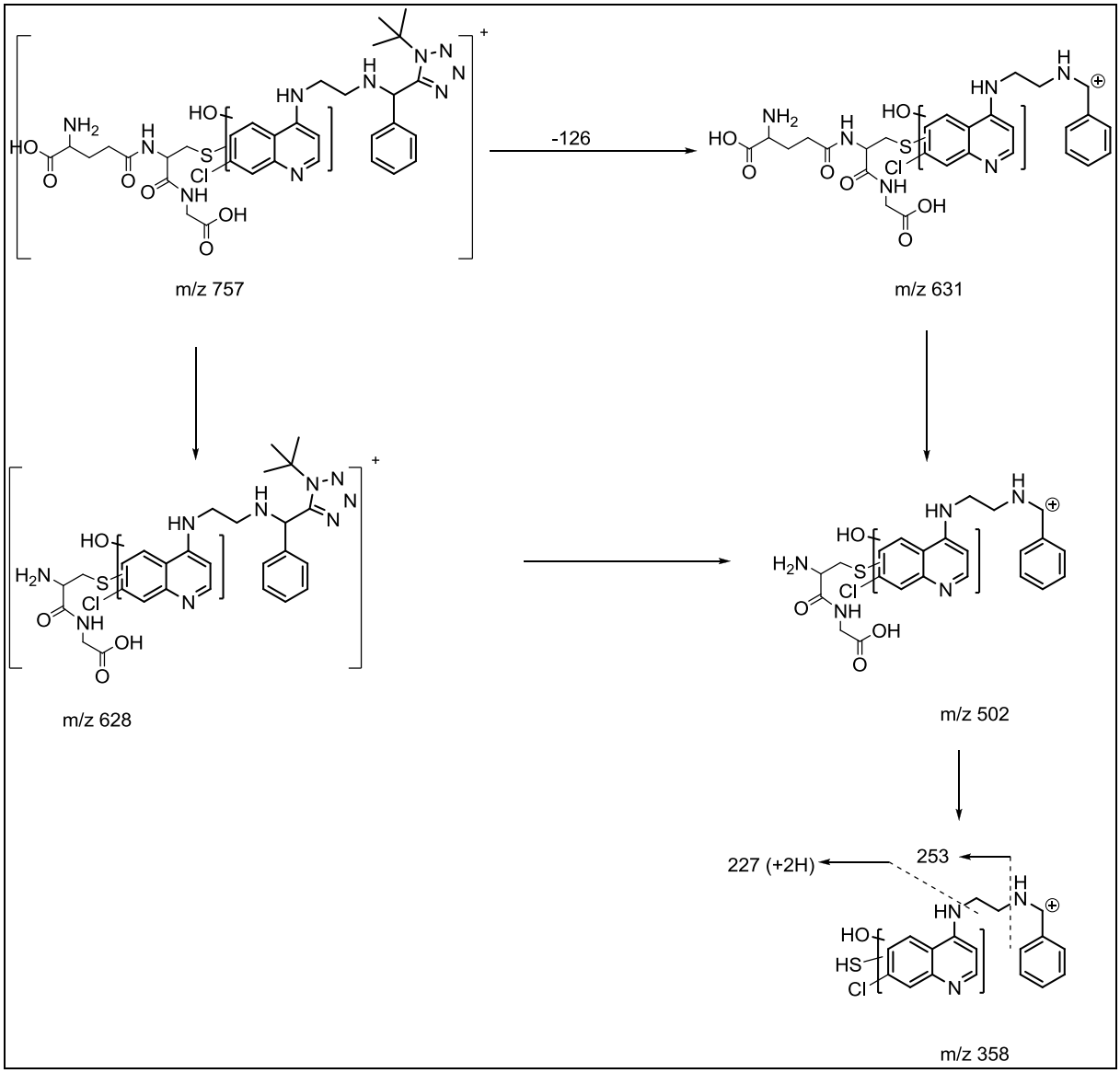

In addition to the loss of 126Da characteristic of these compounds, a loss of 129Da (to give m/z 628 in **TK900A** and 662 in **TK900E**) is also observed. This neutral loss is considered diagnostic of glutathione adducts and is commonly used to screen for adducts.[41–43] The low intensity of these glutathione adducts led to inconclusive results with the neutral loss scan. The adducts could however be detected using EMS-IDA-EPI methods, and also when EPI scans were used in isolation as the survey scans. The fragments of m/z 502 and 536Da in **TK900A** and **TK900E** respectively are produced from a loss of 129Da from m/z 628 and 662Da, which are produced as described earlier. The presence of these fragments means that the substituted tetrazole is not the site of conjugation.

It is postulated that m/z 358 and 392 (for **TK900A** and **TK900E** respectively) are produced by a loss of the cysteinyl moiety from m/z 628 and 662Da, leaving the sulfur attached to the aminoquinoline nucleus. This loss of 273Da is also characteristic of glutathione adducts.[41–43] In the product ion spectra obtained in the negative mode, the corresponding fragment of m/z 272 was also observed. The fragment with m/z 253 in both spectra probably corresponds to m/z 205 in the parent compound, produced by loss of the side chain nitrogen and its substituent. Finally, m/z 227, which is also in both spectra, is proposed to arise from cleavage of the entire alkyl side chain to give the mercaptoquinoline derivative. A summary of this fragmentation pathway is presented below.

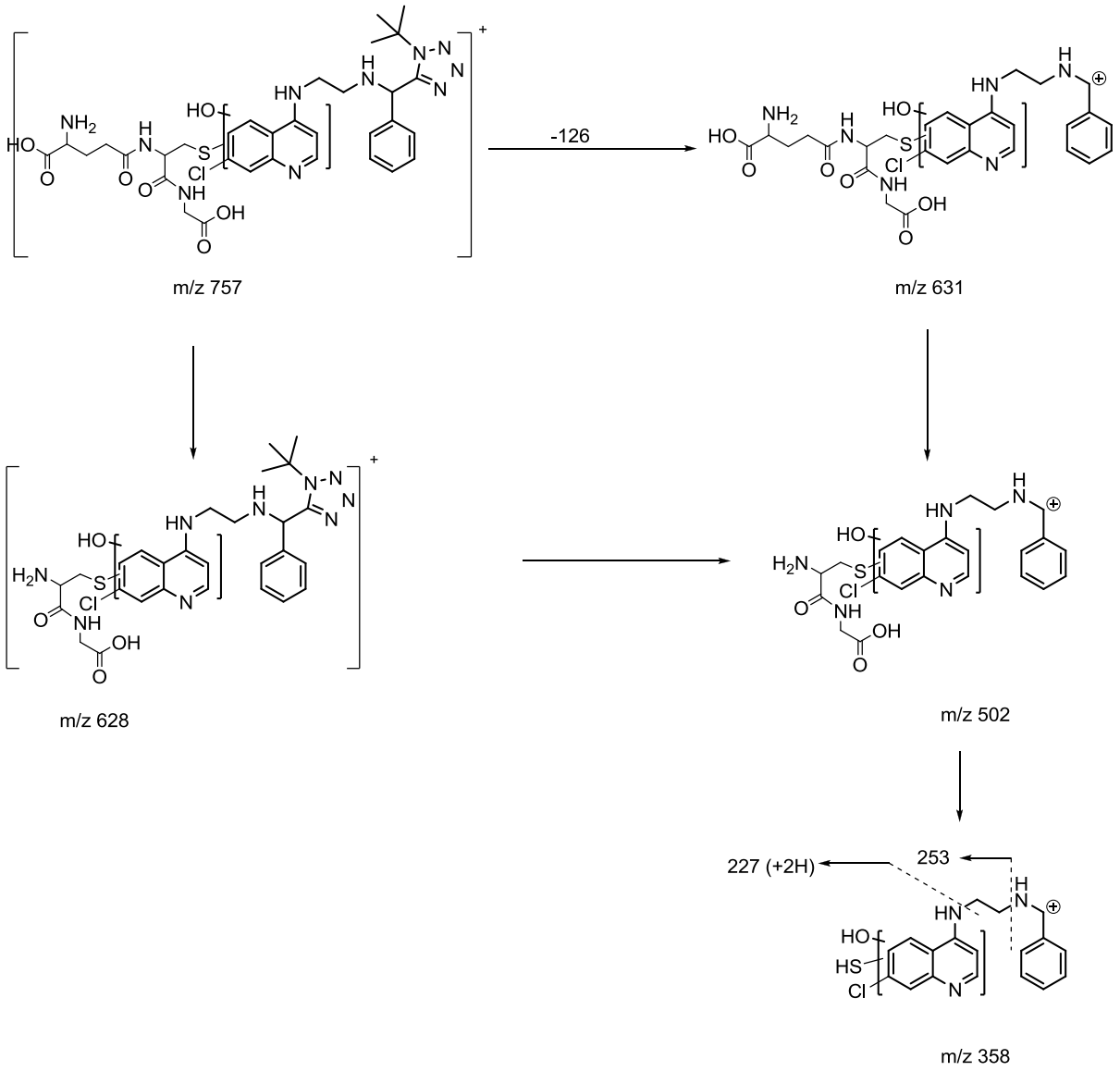

Figure 2.26: Proposed fragmentation pathway of the glutathione adduct of **TK900E**

2.3.4 CYP450 inhibition

The potential of these molecules to inhibit CYP450s was assessed using human liver microsomes. **TK900C** and **TK900E** were selected for the assay.

Unlike the tetrazole deoxyamodiaquines presented in Section 2.2, these compounds did not significantly inhibit any CYP450s, except CYP3A4, where the IC_{50} using both midazolam and testosterone as probe substrates was about 0.1µM. Time dependent inhibition was assessed for CYP1A2, CYP2C9, CYP2D6 and CYP3A4 but was not observed for any of these incubations.

Table 2.11: CYP450 inhibition profile of **TK900C** and **TK900E**

		IC_{50} value (µM)	
CYP enzyme	**Probe reaction**	**TK900C**	**TK900E**
CYP1A2	phenacetin O-deethylation	51.1 ± 19.4[a]	> 20[b]
CYP2A6	coumarin 7-hydroxylation	>20[b]	> 20[b]
CYP2B6	bupropion hydroxylation	32.58 ± 2.6[a]	≈ 30.62 ± 5.7[a]
CYP2C8	paclitaxel 6α-hydroxylation	3.98 ± 0.8	12.7 ± 0.8
CYP2C9	diclofenac 4'-hydroxylation	10.3 ± 2.9	8.91 ± 1.2
CYP2C19	S-mephenytoin 4'-hydroxylation	52.6 ± 27.5[a]	12.4 ± 1.9
CYP2D6	bufuralol 1'-hydroxylation	9.88 ± 2.1	4.0 ± 0.4
CYP2E1	chlorzoxazone 6-hydroxylation	>20[b]	≈ 21.9 ± 4.6[a]
CYP3A4	midazolam 1'-hydroxylation	0.17 ± 0.0	0.08 ± 0.0
CYP3A4	testosterone 6β-hydroxylation	0.31 ± 0.0	0.14 ± 0.0

[a]estimated by extrapolation of experimental data. [b]No inhibition seen in concentration range used

While chloroquine is known to inhibit CYP2D6, it does not inhibit CYP3A4.[23] The inhibition of CYP3A4 by all the selected molecules was therefore assessed using a fluorescent assay with recombinant CYP3A4.

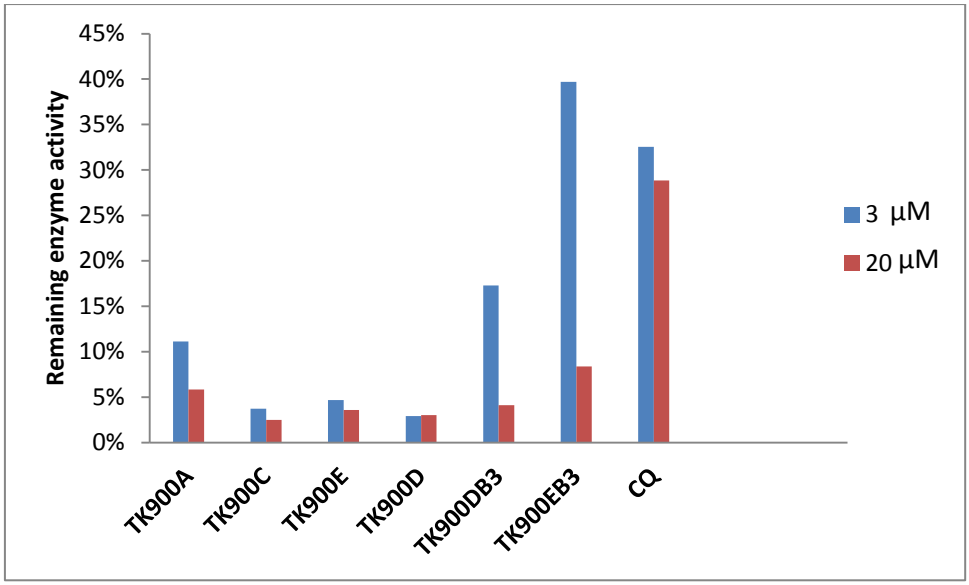

Figure 2.27: Percentage enzyme activity remaining after incubation of 3µm or 20µM compound with recombinant CYP3A4

It is interesting to note that in this assay, chloroquine shows moderate CYP3A4 inhibition. This is, however, not observed in the microsomal assay or clinically. The data for these compounds are consistent with the microsomal data with both **TK900C** and **TK900E** showing strong inhibition. The compounds lacking a *tert*-butyl substituent show less potent inhibition at the lower concentration and this could possibly be attributable to their lower lipophilicity. On this point, it is also useful to note that **TK900A**, which is the least lipophilic of the *tert*-butyl substituted compounds, showed the lowest inhibition amongst these compounds. The trends are more difficult to follow on the higher end of the lipophilic scale because the figures are smaller and experimental variations are likely to have a bigger effect.

Finally, the interaction of these compounds with 3A4 was modelled by docking **TK900C** and **TK900E** onto a crystal structure of CYP3A4 (PDB 2V0M, 2.8Å with ketoconazole) using glide. The docking protocol was validated by redocking the ketoconazole; the lowest energy conformation gave RMSD 1.48Å relative to the original ketoconazole.

In contrast to chloroquine, these compounds lie almost parallel to the heme. Like with the tetrazole deoxyamodiaquines, this orientation may maximise the π-π and π-cationic interactions with heme leading to inhibition. This is perhaps also suggested by the binding energies, which are about 1kcal/mol higher relative to chloroquine, and which approach the binding energy of ketoconazole.

Table 2.12: Binding energies of the most stable conformers

Compound	**GLIDE score (kcal/mol)**
TK900A	-7.891
TK900E	-7.774
Chloroquine	-6.646
Ketoconazole	-8.750

A B C

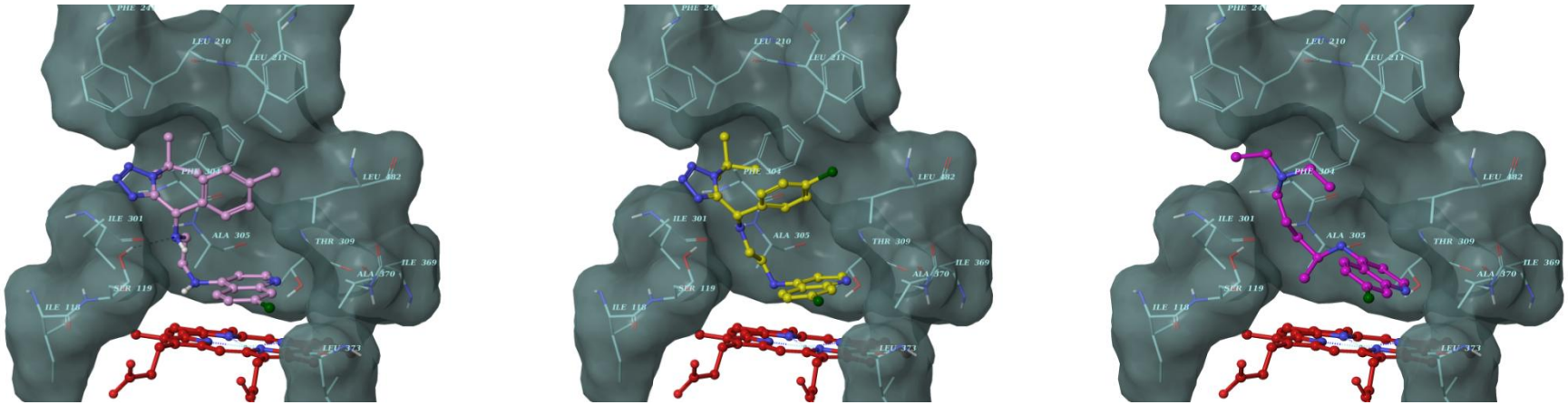

Figure 2.28: Lowest binding energy conformations for **TK900C** (A), **TK900E** (B) and Chloroquine (C) showing molecular surface binding site residues at a radius of 3A and heme

2.3.5 Discussion

The metabolism of the tetrazole chloroquines was mainly by hydroxylation on the *tert*—butyl group and by *N*-oxidation and hydroxylation on the aminoquinoline core. Compounds lacking a *tert*-butyl substitution were therefore more metabolically stable. A number of hydroxylation metabolites tentatively identified as being on the aminoquinoline ring were also observed.

The ability of StarDrop to predict the formation of these metabolites was evaluated using **TK900E** and **TK900C**. The major predicted metabolite using the CYP3A4 model is on the aminoquinoline ring (C31,

Figure 2.29). This site is also predicted to be the main site of metabolism by CYP2D6 and CYP2C9, and also as the most metabolically labile site in the CYP3A4 model. Various degrees of metabolism are predicted for all non-substituted positions on the aminoquinoline ring and on the 1,2-ethyldiamine linker. The fragmentation pattern suggests that M2 and M3 are hydroxylation products on the aminoquinoline ring, while for M4 – M8, the metabolic transformation could be on the 1,2-ethyldiamine linker or on the aminoquinoline ring. The predictions are therefore comparable to the experimental data. Aminoquinoline *N*-oxidation, and *t*-butyl oxidation, which are the other experimentally observed metabolites, are also predicted by all models but are generally lower than the aminoquinoline sites.

For **TK900C** where an additional metabolite accounting for more than 50% of the metabolites formed was observed, the StarDrop models, correctly identify the additional metabolite as forming on the toluyl substituent, just as the MS data suggested, but additionally suggest the *para*- methyl group as the site of metabolism, and also as the most labile position (CYP3A4).

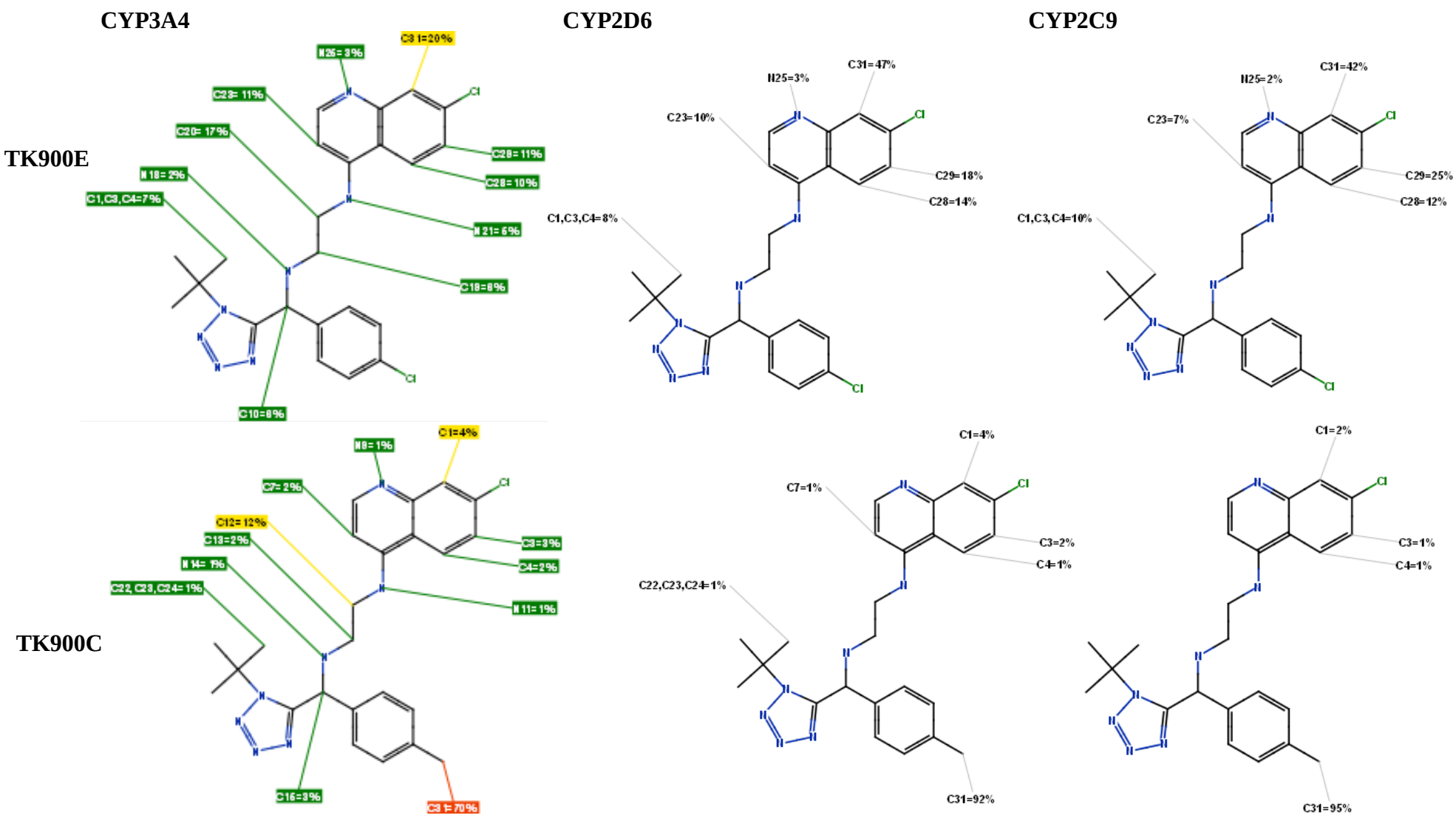

Figure 2.29: StarDrop predicted sites of metabolism for **TK009E** and **TK900C** assuming metabolism by CYP3A4, CYP2D6 or CYP2C9. (The percentages show the expected proportion of metabolites that would result from metabolism at the indicated position. For CYP3A4, the colors indicate the lability of the positions; red – labile, yellow – moderately labile, green – moderately stable, blue – stable)

A glutathione adduct was also observed with these compounds. This is a deviation from the known literature on the metabolism of chloroquine which does not form glutathione adducts. Nitrogen containing aromatic systems may be considered masked anilines and if hydroxylated may undergo further metabolism to form reactive quinone imine species. This is demonstrated by the bioactivation of chlorpromazine and mianserin as shown below.[44,45]

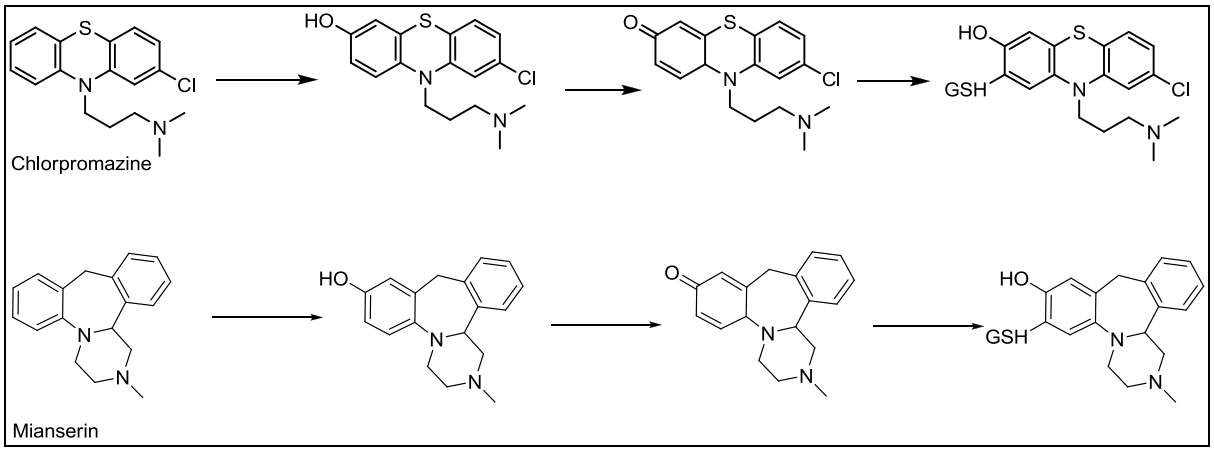

Figure 2.30: Reactive metabolite formation in Chlorpromazine and Mianserin[44,45]
: Reactive metabolite formation in Chlorpromazine and Mianserin[44,45]

While there does not appear to be any literature suggesting that glutathione adduct formation occurs on the 4-aminoquinoline nucleus, it is useful to note that other than *N*-oxidation, the site of metabolism usually lies elsewhere in the molecule. Since metabolism is shown to occur on the aminoquinoline ring in these molecules, with at least 3 metabolites (excluding *N*-oxidation) formed here, they are more likely to form glutathione adducts.

Finally, the physicochemical properties of the major metabolites in the hepatocyte incubations M1, M5, an aminoquinoline hydroxylation metabolite and its respective glucuronide, were determined in order to predict their possible contribution to the *in vivo* activity of the compound.

Table 2.13: Predicted properties of TK900E and its metabolites

Compound	MW	LogP	LogD	TPSA
TK900E	470	4.36	1.61	81
t-butylhydroxylation (M1)	486	3.46	1.07	101
N-oxidation (M5)	486	4.64	1.49	93
6-hydroxylation (M2/M3/M4)	486	3.97	1.20	101
6-O-glucuronidation (M9/M12/M13/M14)	662	0.003	-0.19	184

As expected, metabolism generally lowers the lipophilicity of the resulting metabolites. A known exception is the N-oxides which are usually more lipophilic than the parent molecules. For the three non-conjugated metabolites, log D is only slightly different relative to the parent and the TPSA is only 20Å higher. Lipoidal permeability is therefore unlikely to be substantially different compared to the parent.[46,4746,47] However, assuming that the three metabolites are formed at the same rate from **TK900E**, the next major factor in determining the circulating concentration of these metabolites is their rate of excretion and/or further metabolism. From the metabolite profiling done for this compound, it is instructive to note that while four O-glucuronides were detected, none of these were formed for the *tert*-butyl hydroxylation metabolite, despite this being amongst the major metabolites formed. It is therefore more likely that *in vivo* the aminoquinoline hydroxylated metabolites will be present in higher concentrations as the respective glucuronides. The model glucuronide in this case shows a drop of 1 unit in Log D and an increase by almost 100 units in TPSA. It would therefore be expected that this metabolite shows reduced lipid permeability. Glucuronides usually rely on transporters for excretion from the liver and depending on the

relative affinity of the glucuronide to the various transporters; it may be excreted into bile or back into circulation.

For antiplasmodial activity, the metabolites in circulation need to traverse the red blood cell membrane and the plasmodial membranes. Assuming passive mechanisms only, the glucuronide is unlikely to reach the site of action, and is therefore unlikely to contribute to the activity of this compound *in vivo*. Considering the 3 remaining metabolites, a few general conclusions can be drawn. While all three should be permeable enough to get to the site of action, modifications on the aminoquinoline nucleus have consistently been shown to result in a decrease in activity.[3636] The aromatic hydroxylation may therefore be less active than **TK900E**. An exception to this rule is *N*-oxidation which, for chloroquine, produces a more active metabolite.[36,48] The *N*-oxidation of this derivative could therefore also be active assuming a similarity in the mechanism of action.[36,48] The *N*-oxidation of this derivative could therefore also be active assuming a similarity in the mechanism of action. The hydroxylation of the *tert*-butyl group is remote enough from the aminoquinoline nucleus that it can be expected to not substantially affect antiplasmodial activity. Chloroquine and amodiaquine derivatives hydroxylated on the ethyl chain are indeed reported to be active with hydroxychloroquine actually being slightly more active and less toxic than chloroquine. [36,49,50] The *tert*-butyl oxidation is therefore also likely to be active.

However, despite the good *in vitro* activity of these compounds, the percentage reduction in parasitaemia plateaued at about 40%, giving no increases even at higher doses (Table 2.14).[35]

Table 2.14: In vivo antiplasmodial activity of **TK900D** in the *P. berghei* model (Day 7)[35]

Compound	Dose (mg/kg)	% Reduction in parasitaemia
TK900D	1 x 20	44.5
	1 x 10	41.4
	1 x 5	46.9
	1 x 1	22.7
Chloroquine	1 x 20	90.6

While this effect was postulated to arise, at least in part, from solubility-limited absorption – because of the poor solubility of these compounds, it remains unclear why better activity was not seen. This is despite moderate but reasonable *in vivo* PK parameters – $t_{½}$ 4hrs, Cmax 0.94µM and AUC 222min.µmol/L at 20mg/kg. Further work is therefore required to understand their poor *in vivo* activity.

2.4 Conclusions

The metabolism of a series of tetrazole aminoquinolines was investigated *in vitro*. The main site of metabolism of the tetrazole deoxyamodiaquines was the attachment to the tertiary nitrogen. Metabolism was by *N*-dealkylation in the case of simple alkyl substitutents and by hydroxylation through an iminium ion pathway, for cylcoalkyl substituted derivatives. The tetrazole chloroquines were metabolised by aminoquinoline N-oxidation, *tert*-butyl hydroxylation and by aminoquinoline hydroxylation. A glutathione adduct was also detected. Both series of compounds showed moderate – potent CYP450 inhibition and their inhibition of CYP3A4 was shown to result from the orientation in the active site of the enzyme. The main metabolites of both tetrazole deoxyamodiaquines and tetrazole chloroquines could be predicted using StarDrop and this software could therefore be useful in the further optimisation of these compounds.

2.5 References

(1) O'Neill, P. M.; Barton, V. E.; Ward, S. A.; Chadwick, J. 4-Aminoquinolines: Chloroquine, Amodiaquine and Next-Generation Analogues. In *Treatment and Prevention of Malaria*; Staines, H. M.; Krishna, S., Eds.; Springer Basel AG: Basel, 2012; pp. 19–44.

(2) Neftel, K. A.; Woodtly, W.; Schmid, M.; Frick, P. G.; Fehr, J. Amodiaquine Induced Agranulocytosis and Liver Damage. *BMJ* **1986**, *292*, 721–723.

(3) Schulthess, H. K.; von Felten, A.; Gmür, J.; Neftel, K. A. [Amodiaquine-Induced Agranulocytosis in Malaria Prevention: Demonstration of an Amodiaquine-Induced Cytotoxic Antibody against Granulocytes]. *Schweiz. Med. Wochenschr.* **1983**, *113*, 1912–1913.

(4) Olliaro, P.; Mussano, P. Amodiaquine for Treating Malaria. *Cochrane database Syst. Rev.* **2003**, CD000016.

(5) Naisbitt, D. J.; Williams, D. P.; O'Neill, P. M.; Maggs, J. L.; Willock, D. J.; Pirmohamed, M.; Park, B. K. Metabolism-Dependent Neutrophil Cytotoxicity of Amodiaquine: A Comparison with Pyronaridine and Related Antimalarial Drugs. *Chem. Res. Toxicol.* **1998**, *11*, 1586–1595.

(6) Harrison, A. C.; Kitteringham, N. R.; Clarke, J. B.; Park, B. K. The Mechanism of Bioactivation and Antigen Formation of Amodiaquine in the Rat. *Biochem. Pharmacol.* **1992**, *43*, 1421–1430.

(7) Shimizu, S.; Atsumi, R.; Itokawa, K.; Iwasaki, M.; Aoki, T.; Ono, C.; Izumi, T.; Sudo, K.; Okazaki, O. Metabolism-Dependent Hepatotoxicity of Amodiaquine in Glutathione-Depleted Mice. *Arch. Toxicol.* **2009**, *83*, 701–707.

(8) Tingle, M. D.; Jewell, H.; Maggs, J. L. L.; O'Neill, P. M. M.; Park, B. K. K. The Bioactivation of Amodiaquine by Human Polymorphonuclear Leucocytes in Vitro: Chemical Mechanisms and the Effects of Fluorine Substitution. *Biochem. Pharmacol.* **1995**, *50*, 1113–1119.

(9) Johansson, T.; Jurva, U.; Grönberg, G.; Weidolf, L.; Masimirembwa, C. Novel Metabolites of Amodiaquine Formed by CYP1A1 and CYP1B1: Structure Elucidation Using Electrochemistry, Mass Spectrometry, and NMR. *Drug Metab. Dispos.* **2009**, *37*, 571–579.

(10) Njoroge, M.; Njuguna, N. M.; Mutai, P.; Ongarora, D. S. B.; Smith, P. W.; Chibale, K. Recent Approaches to Chemical Discovery and Development Against Malaria and the Neglected Tropical Diseases Human African Trypanosomiasis and Schistosomiasis. *Chem. Rev.* **2014**,*114 (22)*, 11138

(11) O'Neill, P. M.; Harrison, A. C.; Storr, R. C.; Hawley, S. R.; Ward, S. A.; Park, B. K. The Effect of Fluorine Substitution on the Metabolism and Antimalarial Activity of Amodiaquine. *J. Med. Chem.* **1994**, *37*, 1362–1370.

(12) O'Neill, P. M.; Shone, A. E.; Stanford, D.; Nixon, G.; Asadollahy, E.; Park, B. K.; Maggs, J. L.; Roberts, P.; Stocks, P. A.; Biagini, G.; et al. Synthesis, Antimalarial Activity, and Preclinical Pharmacology of a Novel Series of 4'-Fluoro and 4'-Chloro Analogues of Amodiaquine. Identification of a Suitable "Back-up" Compound for N-Tert-Butyl Isoquine. *J. Med. Chem.* **2009**, *52*, 1828–1844.

(13) O'Neill, P. M.; Park, B. K.; Shone, A. E.; Maggs, J. L.; Roberts, P.; Stocks, P. A.; Biagini, G. A.; Bray, P. G.; Gibbons, P.; Berry, N.; et al. Candidate Selection and Preclinical Evaluation of N-Tert-Butyl Isoquine (GSK369796), an Affordable and Effective 4-Aminoquinoline Antimalarial for the 21st Century. *J. Med. Chem.* **2009**, *52*, 1408–1415.

(14) Tukulula, M.; Njoroge, M.; Mugumbate, G. C.; Gut, J.; Rosenthal, P. J.; Barteau, S.; Streckfuss, J.; Heudi, O.; Kameni-Tcheudji, J.; Chibale, K. Tetrazole-Based Deoxyamodiaquines: Synthesis, ADME/PK Profiling and Pharmacological Evaluation as Potential Antimalarial Agents. *Bioorg. Med. Chem.* **2013**, *21*, 4904–4913.

(15) Barbara, J. E.; Kazmi, F.; Muranjan, S.; Toren, P. C.; Parkinson, A. High-Resolution Mass Spectrometry Elucidates Metabonate (false Metabolite) Formation from Alkylamine Drugs during in Vitro Metabolite Profiling. *Drug Metab. Dispos.* **2012**, *40*, 1966–1975.

(16) Morris, G. M.; Huey, R.; Lindstrom, W.; Sanner, M. F.; Belew, R. K.; Goodsell, D. S.; Olson, A. J. AutoDock4 and AutoDockTools4: Automated Docking with Selective Receptor Flexibility. *J. Comput. Chem.* **2009**, *30*, 2785–2791.

(17) Friesner, R. A.; Murphy, R. B.; Repasky, M. P.; Frye, L. L.; Greenwood, J. R.; Halgren, T. A.; Sanschagrin, P. C.; Mainz, D. T. Extra Precision Glide: Docking and Scoring Incorporating a Model of Hydrophobic Enclosure for Protein-Ligand Complexes. *J. Med. Chem.* **2006**, *49*, 6177–6196.

(18) Sayre, L. M.; Engelhart, D. A.; Nadkarni, D. V; Manoj Babu, M. K.; Flammang, A. M.; McCoy, G. D. The Role of Iminium-Enamine Species in the Toxication and Detoxication of Cyclic Tertiary Amines. *NIDA Res. Monogr.* **1997**, *173*, 106–127.

(19) Lee, J.; Son, J.; Chung, S.; Lee, E.; Kim, D. In Vitro and in Vivo Metabolism of Pyronaridine Characterized by Low-Energy Collision-Induced Dissociation Mass Spectrometry with Electrospray Ionization. *J. Mass Spectrom.* **2004**, *39*, 1036–1043.

(20) Morris, C. A.; Dueker, S. R.; Lohstroh, P. N.; Wang, L.-Q.; Fang, X.-P.; Jung, D.; Lopez-Lazaro, L.; Baker, M.; Duparc, S.; Borghini-Fuhrer, I.; et al. Mass Balance and Metabolism of the Antimalarial Pyronaridine in Healthy Volunteers. *Eur. J. Drug Metab. Pharmacokinet.* **2014**, *In press*, doi: 10.1007/s13318–014–0182–0.

(21) DeVore, N. M.; Meneely, K. M.; Bart, A. G.; Stephens, E. S.; Battaile, K. P.; Scott, E. E. Structural Comparison of Cytochromes P450 2A6, 2A13, and 2E1 with Pilocarpine. *FEBS J.* **2012**, *279*, 1621–1631.

(22) *Drug Metabolism Handbook: Concepts and Applications*; Nassar, A. F.; Hollenberg, P. F.; Scatina, J., Eds.; John Wiley & Sons, Inc.: Hoboken, NJ, USA, 2009.

(23) Bapiro, T. E.; Egnell, A. C.; Hasler, J. A.; Masimirembwa, C. Application of Higher Throughput Screening (HTS) Inhibition Assays to Evaluate the Interaction of Antiparasitic Drugs with Cytochrome P450s. *Drug Metab. Dispos.* **2001**, *29*, 30–35.

(24) Ishigami, M.; Honda, T.; Takasaki, W.; Ikeda, T.; Komai, T.; Ito, K.; Sugiyama, Y. A Comparison of the Effects of 3-Hydroxy-3-Methylglutaryl-Coenzyme A (HMG-CoA) Reductase Inhibitors on the CYP3A4-Dependent Oxidation of Mexazolam in Vitro. *Drug Metab. Dispos.* **2001**, *29*, 282–288.

(25) Riley, R. J.; Parker, A. J.; Trigg, S.; Manners, C. N. Development of a Generalized, Quantitative Physicochemical Model of CYP3A4 Inhibition for Use in Early Drug Discovery. *Pharm. Res.* **2001**, *18*, 652–655.

(26) Rijken, M. J.; McGready, R.; Jullien, V.; Tarning, J.; Lindegardh, N.; Phyo, A. P.; Win, A. K.; Hsi, P.; Cammas, M.; Singhasivanon, P.; et al. Pharmacokinetics of Amodiaquine and Desethylamodiaquine in Pregnant and Postpartum Women with Plasmodium Vivax Malaria. *Antimicrob. Agents Chemother.* **2011**, *55*, 4338–4342.

(27) *Treatment and Prevention of Malaria: Antimalarial Drug Chemistry, Action and Use*; Staines, H. M.; Krishna, S., Eds.; Springer Basel AG: Basel, 2012.

(28) Essien, E. E.; Afamefuna, G. C. Chloroquine and Its Metabolites in Human Cord Blood, Neonatal Blood, and Urine after Maternal Medication. *Clin. Chem.* **1982**, *28*, 1148–1152.

(29) Krishna, S.; White, N. J. Pharmacokinetics of Quinine, Chloroquine and Amodiaquine. Clinical Implications. *Clin. Pharmacokinet.* **1996**, *30*, 263–299.

(30) Ducharme, J.; Farinotti, R. Clinical Pharmacokinetics and Metabolism of Chloroquine. Focus on Recent Advancements. *Clin. Pharmacokinet.* **1996**, *31*, 257–274.

(31) Fu, S.; Björkman, A.; Wåhlin, B.; Ofori-Adjei, D.; Ericsson, O.; Sjöqvist, F. In Vitro Activity of Chloroquine, the Two Enantiomers of Chloroquine, Desethylchloroquine and Pyronaridine against Plasmodium Falciparum. *Br. J. Clin. Pharmacol.* **1986**, *22*, 93–96.

(32) Projean, D.; Baune, B.; Farinotti, R.; Flinois, J.; Beaune, P.; Taburet, A.; Ducharme, J. In Vitro Metabolism of Chloroquine: Identification of CYP2C8, CYP3A4, and CYP2D6 as the Main Isoforms Catalyzing N-Desethylchloroquine Formation. *Drug Metab. Dispos.* **2003**, *31*, 748–754.

(33) Essien, E.; Afamefuna, G. Chloroquine and Its Metabolites in Human Cord Blood, Neonatal Blood, and Urine after Maternal Medication. *Clin. Chem.* **1982**, *28*, 1148–1152.

(34) McChesney, E. W.; Fasco, M. J.; Banks, W. F. The Metabolism of Chloroquine in Man during and after Repeated Oral Dosage. *J. Pharmacol. Exp. Ther.* **1967**, *158*, 323–331.

(35) Tukulula, M.; Njoroge, M.; Abay, E. T.; Mugumbate, G. C.; Wiesner, L.; Taylor, D.; Gibhard, L.; Norman, J.; Swart, K. J.; Gut, J.; et al. Synthesis and in Vitro and in Vivo Pharmacological Evaluation of New 4-Aminoquinoline-Based Compounds. *ACS Med. Chem. Lett.* **2013**, *4*, 1198–1202.

(36) O'Neill, P. M.; Bray, P. G.; Hawley, S. R.; Ward, S. A.; Park, B. K. 4-Aminoquinolines--Past, Present, and Future: A Chemical Perspective. *Pharmacol. Ther.* **1998**, *77*, 29–58.

(37) Di, L.; Kerns, E. H.; Gao, N.; Li, S. Q.; Huang, Y.; Bourassa, J. L.; Huryn, D. M. Experimental Design on Single-Time-Point High-Throughput Microsomal Stability Assay. *J. Pharm. Sci.* **2004**, *93*, 1537–1544.

(38) Li, X.-Q.; Björkman, A.; Andersson, T. B.; Gustafsson, L. L.; Masimirembwa, C. Identification of Human Cytochrome P(450)s That Metabolise Anti-Parasitic Drugs and Predictions of in Vivo Drug Hepatic Clearance from in Vitro Data. *Eur. J. Clin. Pharmacol.* **2003**, *59*, 429–442.

(39) Ohashi, N.; Furuuchi, S.; Yoshikawa, M. Usefulness of the Hydrogen--Deuterium Exchange Method in the Study of Drug Metabolism Using Liquid Chromatography-Tandem Mass Spectrometry. *J. Pharm. Biomed. Anal.* **1998**, *18*, 325–334.

(40) Tarning, J.; Bergqvist, Y.; Day, N. P.; Bergquist, J.; Arvidsson, B.; White, N. J.; Ashton, M.; Lindegårdh, N. Characterization of Human Urinary Metabolites of the Antimalarial Piperaquine. *Drug Metab. Dispos.* **2006**, *34*, 2011–2019.

(41) Xie, C.; Zhong, D.; Chen, X. A Fragmentation-Based Method for the Differentiation of Glutathione Conjugates by High-Resolution Mass Spectrometry with Electrospray Ionization. *Anal. Chim. Acta* **2013**, *788*, 89–98.

(42) Zhu, M.; Ma, L.; Zhang, H.; Humphreys, W. G. Detection and Structural Characterization of Glutathione-Trapped Reactive Metabolites Using Liquid Chromatography-High-Resolution Mass Spectrometry and Mass Defect Filtering. *Anal. Chem.* **2007**, *79*, 8333–8341.

(43) Zheng, J.; Ma, L.; Xin, B.; Olah, T.; Humphreys, W. G.; Zhu, M. Screening and Identification of GSH-Trapped Reactive Metabolites Using Hybrid Triple Quadruple Linear Ion Trap Mass Spectrometry. *Chem. Res. Toxicol.* **2007**, *20*, 757–766.

(44) Wen, B.; Zhou, M. Metabolic Activation of the Phenothiazine Antipsychotics Chlorpromazine and Thioridazine to Electrophilic Iminoquinone Species in Human Liver Microsomes and Recombinant P450s. *Chem. Biol. Interact.* **2009**, *181*, 220–226.

(45) Wen, B.; Fitch, W. L. Screening and Characterization of Reactive Metabolites Using Glutathione Ethyl Ester in Combination with Q-Trap Mass Spectrometry. *J. Mass Spectrom.* **2009**, *44*, 90–100.

(46) Loi, C.-M.; Smith, D. A.; Dalvie, D. Which Metabolites Circulate? *Drug Metab. Dispos.* **2013**, *41*, 933–951.

(47) Smith, D. A.; Dalvie, D. Why Do Metabolites Circulate? *Xenobiotica.* **2012**, *42*, 107–126.

(48) Elslager, E. F.; Gold, E. H.; Tendick, F. H.; Werbel, L. M.; Worth, D. F. Amodiaquine N-Oxides and Other 7-Chloro-4-Aminoquinoline N-Oxides. *J. Heterocycl. Chem.* **1964**, *1*, 6–12.

(49) McChesney, E. W.; McAucliff, J. . Laboratory Studies of the 4-Aminoquinoline Antimalarials I: Some Biochemical Characteristics of Chloroquine, Hydroxychloroquine and SN-7718. *Antibiot. Chemother.* **1961**, *11*, 800–810.

(50) McChesney, E. W. Animal Toxicity and Pharmacokinetics of Hydroxychloroquine Sulfate. *Am. J. Med.* **1983**, *75*, 11–18.

Chapter 3

METERGOLINE ANALOGUES

3.1 Chapter overview

In this Chapter, the microsomal metabolism of metergoline and metergoline analogues is investigated. The metabolites are tentatively identified using their product ion spectra, and additionally in the case of metergoline H/D exchange data. Differences in metabolic pathways among the compounds are discussed on the basis of their structure. CYP450 models on StarDrop are then used to predict the sites of metabolism of selected compounds and these are discussed relative to the experimentally observed metabolites.

3.2 Background

Metergoline is a semi-synthetic ergot-derived drug first described in 1965.[1] It has been used clinically to inhibit lactation in human and veterinary medicine, and for a variety of psychiatric uses.[2–4] These pharmacological actions draw mostly from its actions at serotonin and dopamine receptors, though it has also been reported to have high affinity for other CNS receptors.[5,6] It has mostly been overtaken by newer agents in the same class, though it is still marketed in several jurisdictions.[7,8]

More recently, metergoline has been reported to have anti-infective activity. Kang and co-workers reported potent antifungal activity for metergoline, and showed that cell death resulted from generation of reactive oxygen species and disturbance of mitochondrial homeostasis.[9,10] Metergoline has also been reported as a hit compound in various antiviral assays.[11,12]

The work herein described was motivated by a high-throughput screening conducted by the National Institutes of Health, under the Tuberculosis Antimicrobial Acquisition and Co-ordination Facility, which identified metergoline as a hit compound against *Mycobacterium tuberculosis* H37Rv (IC_{90} 15μM).[13] The increasing burden of tuberculosis and the dearth of novel drugs in the development pipelines have elevated the need for consideration of alternative drug discovery approaches, such as drug repositioning and repurposing. The derivatives were therefore screened with the aim of identifying derivatives with good antimycobacterial activity, whose development might be more feasible because of their similarity to a known clinical compound.

All derivatives were also screened for antiplasmodial activity. Various high-throughput screens have reported antiplasmodial activity in the 1 – 20μM range for metergoline, depending on the strain used.[14–17] This cross screening is an emerging practice in the discovery of drugs for neglected diseases; it maximises the value of the compound pool and the selectivity against various pathogens maybe of value in understanding the mechanism of action or toxicity of the compound.[18]

3.2.1 Metabolism of metergoline

Metergoline is almost completely absorbed when administered orally. It, however, undergoes considerable first-pass metabolism to 1-demethylmetergoline.[19] Both metergoline and its primary metabolite 1-demethylmetergoline have short plasma half-lives (50 minutes and 100 minutes respectively.[19] 12-Hydroxylation is also observed as a minor metabolite. In rats, 1,6-dimethyl-8 beta-aminomethylergoline produced by cleavage of the carbamate linker, and its 1-demethylation and N-acetylation metabolites are observed, together with a number of as yet unidentified polar metabolites (Figure 3.1).

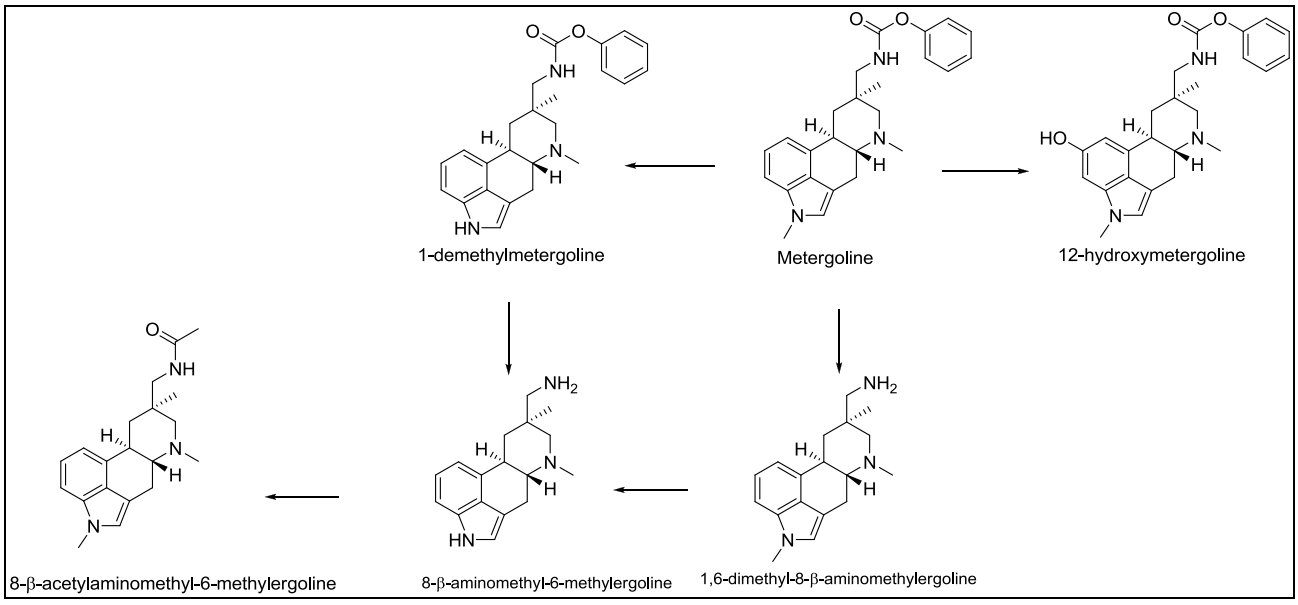

Figure 3.1: Metabolism of metergoline[19,20]

3.3 Compound selection

The compounds in this series were alkyl and aromatic amides, with the ergoline nucleus unchanged.[21] The selection of compounds for *in vitro* metabolism studies was based on their biological activity and on the expected diversity of metabolic reactions. Aromatic amides were also selected so as to represent each quadrant of the Craig plot; in order to assess any effects of the substituents on the metabolism of these compounds. Alkyl amides longer than the pentamidyl derivative selected were poorly soluble in DMSO and/or in the assay medium at the test concentrations and were therefore not included in this evaluation. The compounds and their biological activity are presented in Table 3.1.

Table 3.1: Biological activity of selected metergoline derivatives[21]

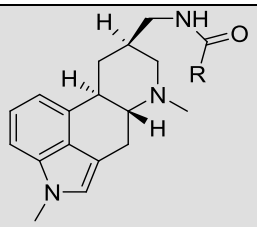

Code	R	*P.f* NF54[a] IC_{50} µM	*M.tb* H37Rv[b] MIC_{99}	Cytotox. – CHO[c] IC_{50} (µM)
FRM015	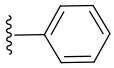	24.4	50	27.0
FRM004	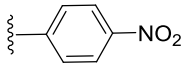	0.5	50	5.0
FRM001	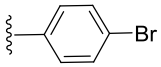	1.3	25	4.3
FRM003	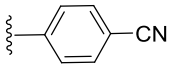	0.6	50	103.6
FRM010	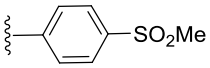	14.2	>50	221.5
FRM011	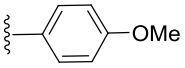	8.4	37	7.4
FRM007	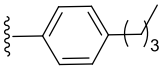	2.0	25	14.5
GKMG14		199	>50	ND
GKMG16	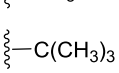	89.1	>50	ND
GKMG22	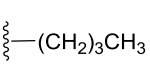	18.7	>50	105.0
Metergoline		3.7	25	16.6

[a]Drug sensitive strain of *Plasmodium falciparum*. [b]Drug sensitive strain of *Mycobacterium tuberculosis*. [c]Chinese Hamster Ovarian cell line

3.4 Metabolism studies

3.4.1 Microsomal stability

The microsomal stability of the derivatives was evaluated in human and mouse liver microsomes (HLM and MLM) using a single point assay at 0.4 mg/ml, for 30 minutes. The results are presented in Table 3.2 below**.**

Table 3.2: Microsomal metabolic stability of metergoline derivatives

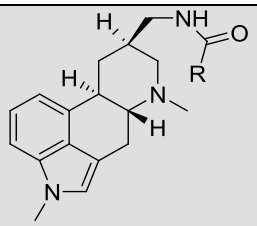

Code	R	Microsomal % remaining at 30min		LogP*
		HLM	MLM	
FRM015	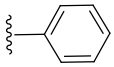	16	62	3.49
FRM004	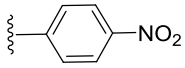	89	89	3.46
FRM001	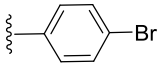	88	89	4.11
FRM003	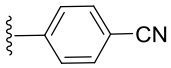	91	39	3.27
FRM010	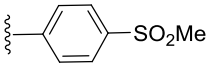	92	98	2.76
FRM011	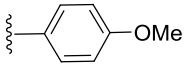	65	77	3.38
FRM007	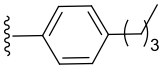	23	65	4.62
GKMG14		96	73	2.26
GKMG16	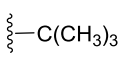	71	50	3.39
GKMG22	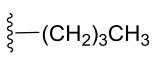	91	33	3.27
Metergoline		7	29	3.95

*Predicted using StarDrop v.5.5

Metergoline was rapidly metabolised in both HLM and MLM, with a projected half-life of 7 min in HLM and 17 min in MLM. The selected derivatives were more stable. Metabolite identification experiments were performed to understand the differences in metabolism between these compounds.

3.4.2 Metabolite identification

3.3.2.1 Fragmentation of metergoline and FRM015

The fragmentation of metergoline and one of the derivatives, **FRM015,** was evaluated to allow for tentative metabolite assignments. While no literature is available on the fragmentation pathways of metergoline, some work has been conducted on other ergolines and this can be extrapolated to elucidate the pathways for metergoline and its derivatives.[22–24]

Both metergoline and **FRM015** undergo cleavage of the carbamate/amide linker. In the case of metergoline, this appears to occur through dissociation of the carbamate C – O bond with charge retention on the carbonyl to give a fragment with m/z 296, followed by loss of CO to give the m/z 268 fragment. On the other hand, when the benzyl C-O bond is cleaved, the characteristic tropylium ion (m/z 91) is formed. A variant of this mechanism is observed for **FRM015**, dissociation of the amide C-N bond with charge retention on the carbonyl gives the m/z 105 fragment, which undergoes loss of CO to give the phenyl cation (m/z 77).

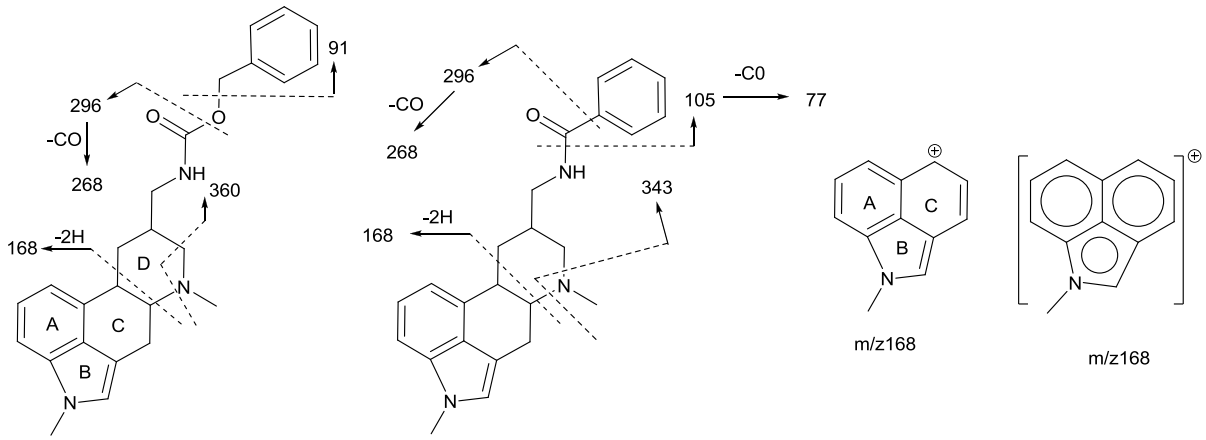

Figure 3.2: Major fragments of Metergoline and **FRM015**

A second pathway, also observed with lysergic acid and its analogues, involves cleavage of ring D by loss of CH_2=N-CH_3 in **metergoline**, and $HNCH_3$ in **FRM015** and the other amide derivatives to give m/z 360 in metergoline and m/z 343 for **FRM015**. The rest of ring D is eventually lost and combined with the linker cleavage, a stable aromatic system m/z 168 is formed. The proposed fragments are illustrated for **FRM015** and **metergoline** in Figure 3.2 , and the product ion spectrum of **FRM015** is shown in Figure 3.3.

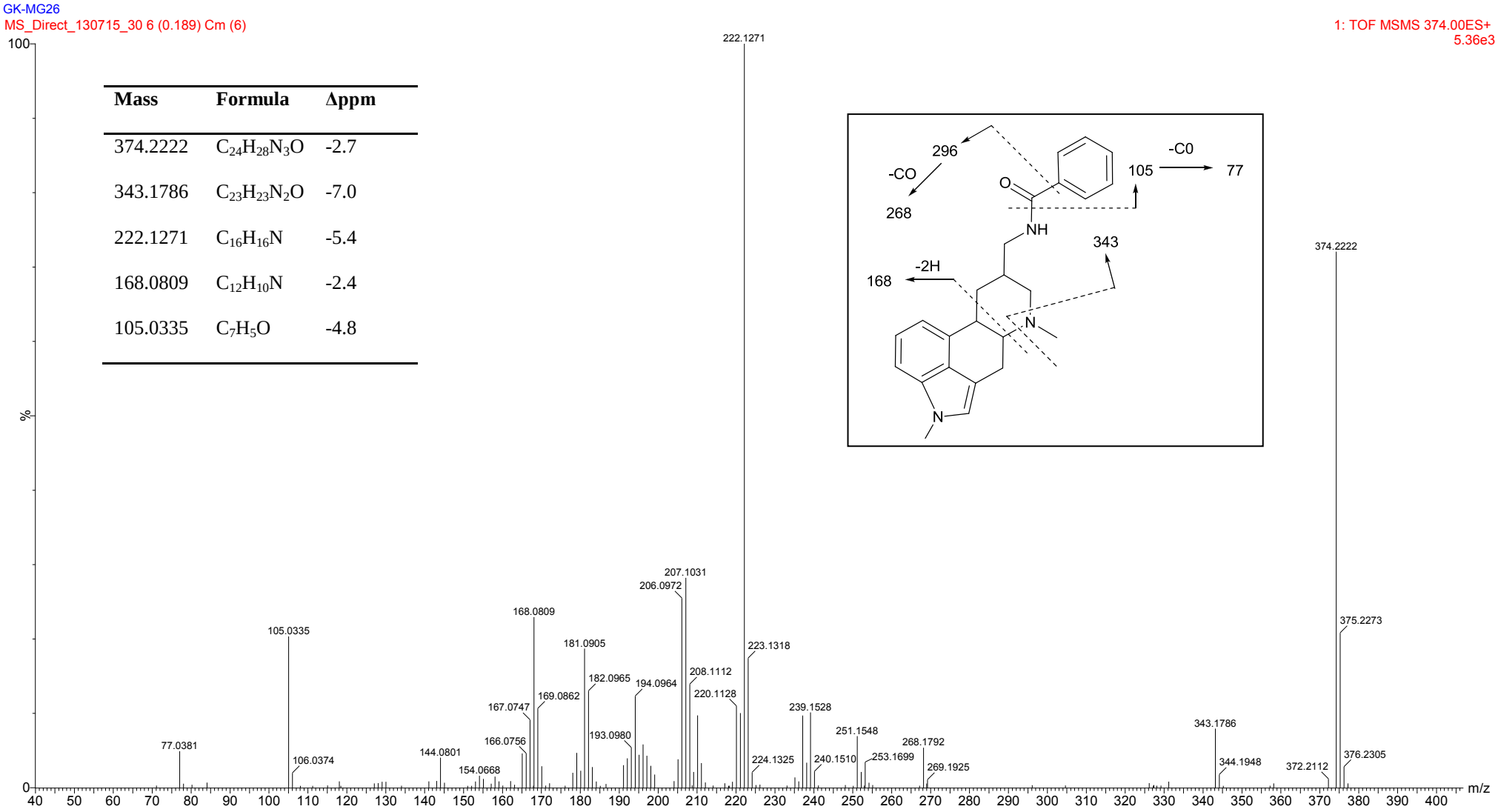

Mass	Formula	Δppm
374.2222	$C_{24}H_{28}N_3O$	-2.7
343.1786	$C_{23}H_{23}N_2O$	-7.0
222.1271	$C_{16}H_{16}N$	-5.4
168.0809	$C_{12}H_{10}N$	-2.4
105.0335	C_7H_5O	-4.8

Figure 3.3: Product ion spectrum of FRM015

3.3.2.2 Metabolite identification experiments for metergoline

Metabolite identification experiments were first performed with metergoline, to establish the chromatography and mass spectral characteristics that would be expected of the selected derivatives

Unlike the reported metabolism of metergoline *in vivo*, where 1-demethylmetergoline is the major metabolite, a hydroxylation product was formed as the major metabolite in both human and mouse liver microsomal metabolites (Figure 3.4).

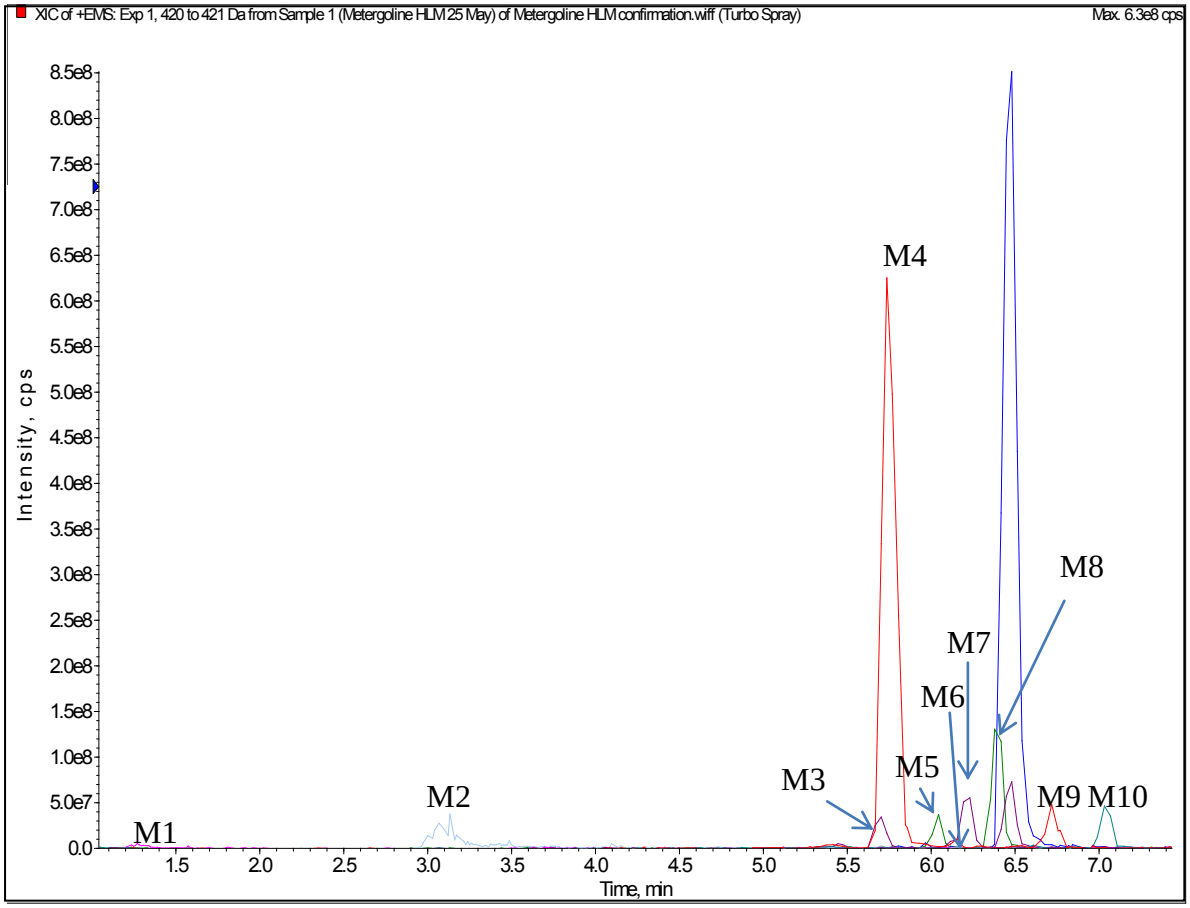

Figure 3.4: Extracted ion chromatogram of metergoline and its metabolites in HLM

The collision induced dissociation spectra of these metabolites show that all HLM metabolism occurs on the ergoline nucleus, as evidenced by the presence of the m/z 91 fragment in all metabolites (Table 3.3).

Table 3.3: HLM metabolites of metergoline and their diagnostic ions

Code	Rt	m/z	Fragments				
			A	B	C	Others	H/D
			360	168	91		
M1	1.27	286	-	184	-	-	nd
M2	3.13	270	-	168	-	-	3
M3	5.70	406	362	184	91	298, 270	nd
M4	5.74	420	376	184	91	312, 284	3
M5	6.04	390	346	154	91	282, 254	3
M6	6.15	420	-	184	91	-	nd
M7	6.21	416	372	-	91	308, 280	2
M8	6.39	390	346	168	91	282, 254	3
M9	6.72	420	-	-	91		2
M10	7.05	400	356	168	91	-, 264	nd
Parent	6.45	404	360	168	91	296, 268	2

The retention time and fragmentation of M2 corresponded to that of 1,6-dimethyl-8-β-aminomethylergoline, produced by Pd/C catalysed hydrogenolysis of metergoline.[21] Metabolism was similar between HLM and RLM incubations, with both producing hydroxylation and demethylation products on the ergoline nucleus, as the major metabolites. However, in MLM incubations, an additional hydroxylation metabolite was observed. This metabolite had a prominent m/z 107 fragment (in place of m/z 91, Figure 3.5), and the

fragments representing the ergoline skeleton were unchanged indicating metabolism on the benzyl group.

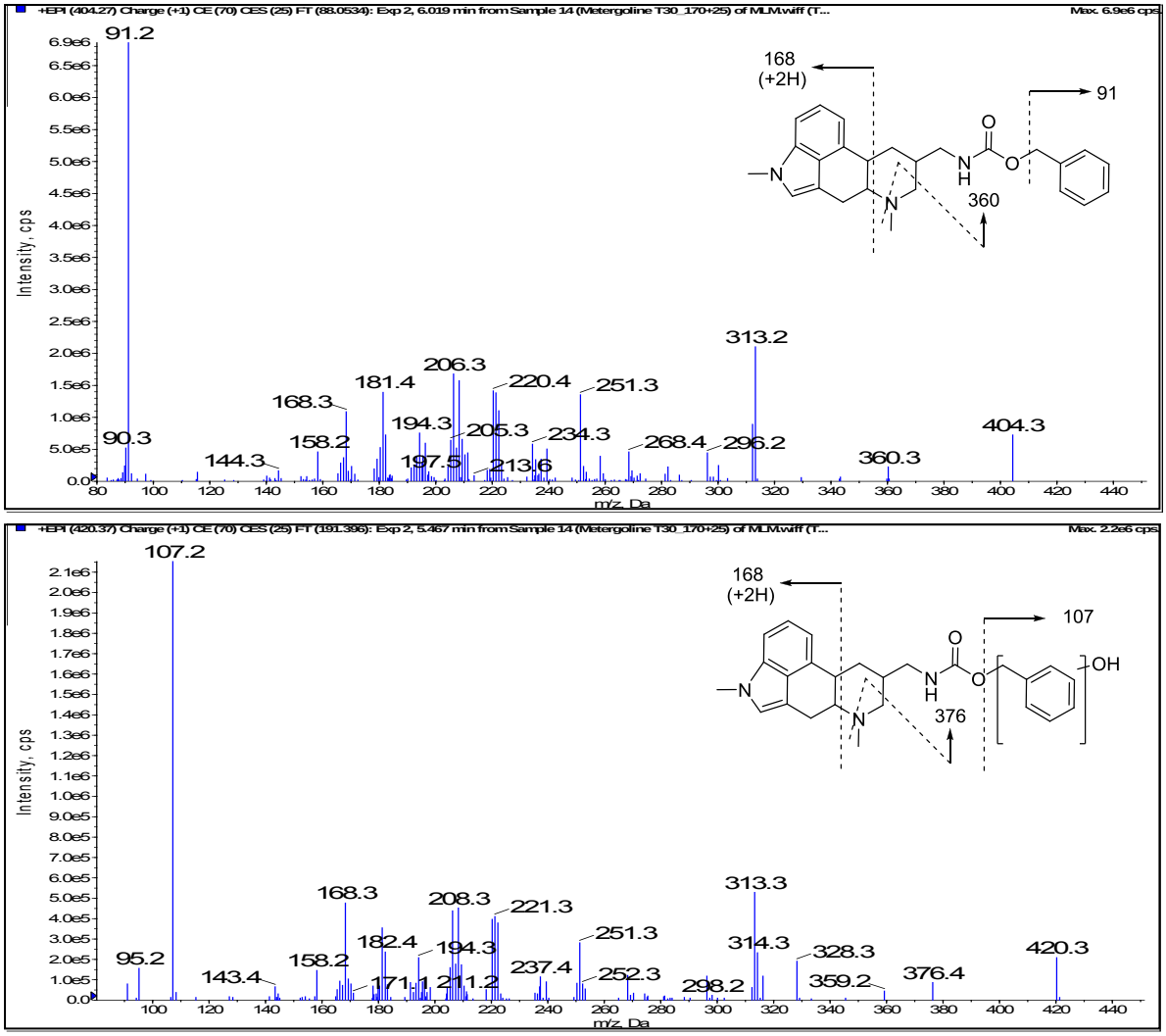

Figure 3.5: CID product ion spectrum of metergoline and its MLM hydroxylation metabolite

The mass shift on H/D exchange could only be conclusively established for the more intense metabolites. M9 has the same H/D mass shift as metergoline suggesting that it is an N-hydroxylation metabolite, which is also suggested by its later elution relative to metergoline.[25,26]

The remaining metabolites could be tentatively assigned based on the fragments shown in Table 3.3, and the H/D mass shift. For example, M4 could be identified as hydroxylation

somewhere on rings A, B or C because of the mass shift of the m/z 168 fragment in metergoline to m/z 184. The tentative structures of the metabolites are presented in Figure 3.6

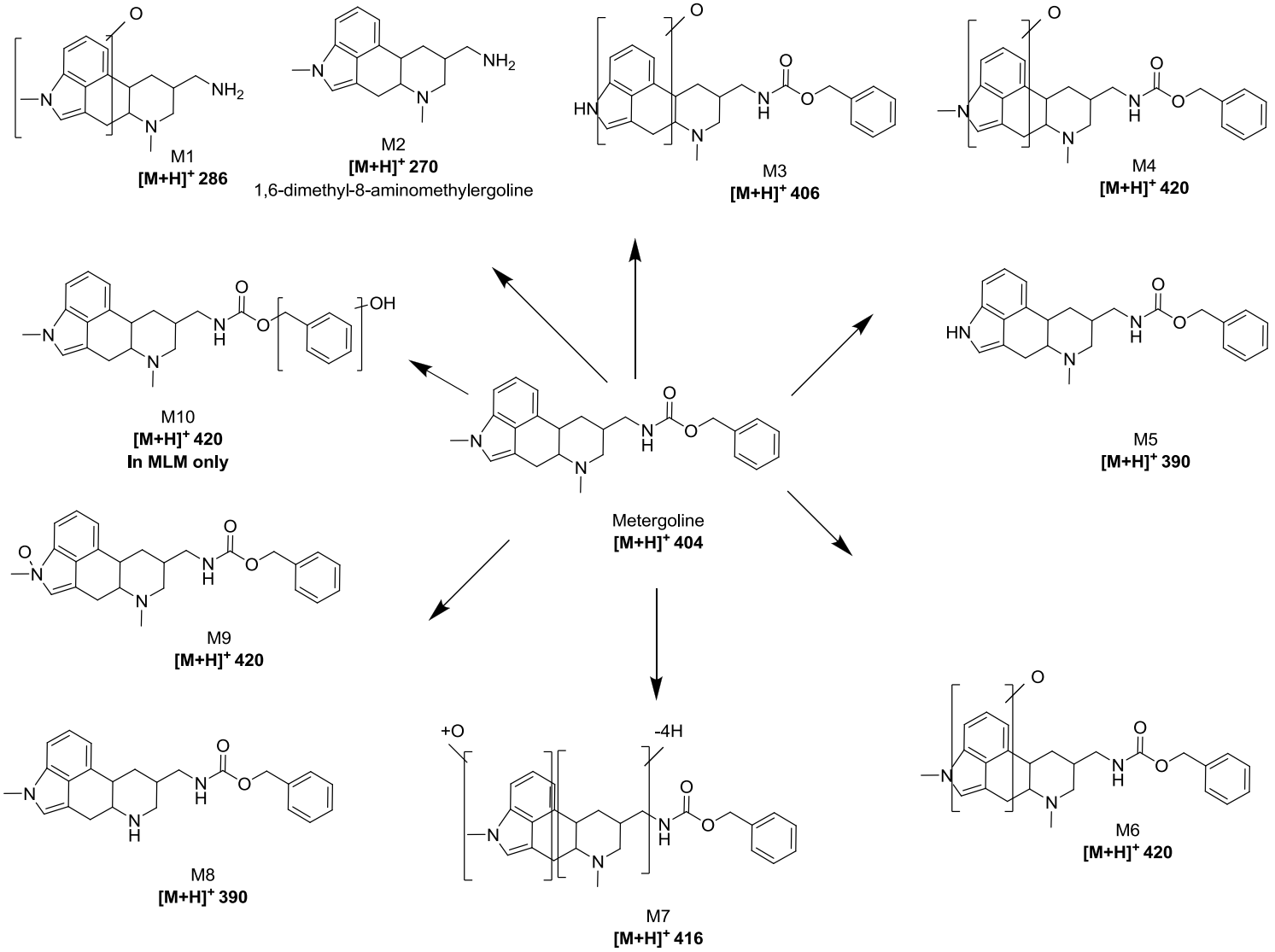

Figure 3.6: Microsomal metabolites of metergoline

3.3.2.3 Metabolism of metergoline derivatives

The metabolism of the metergoline analogues was evaluated in HLM and MLM. Their good MS sensitivity allowed the use of the metabolic stability incubations for metabolite identification experiments (1µM compound, 0.4mg/ml microsomal protein). The experiments were also performed at higher compound and microsomal protein concentrations (10µM compound, 1mg/ml microsomal protein) to allow for better characterisation of the minor metabolites.

A major difference in the metabolism of these derivatives, compared to metergoline, was that 1,6-dimethyl-8-β-aminomethylergoline (M2) was not observed. This is hypothesised to be as a result of the better stability of the amide bond, relative to the carbamate bond.

The metabolism of the aromatic amides was largely similar to that of metergoline. For **FRM015** for example, an ergoline hydroxylation metabolite, corresponding to M4, is observed as the major metabolite in both HLM and MLM. No metabolism is observed on the phenyl substituent.

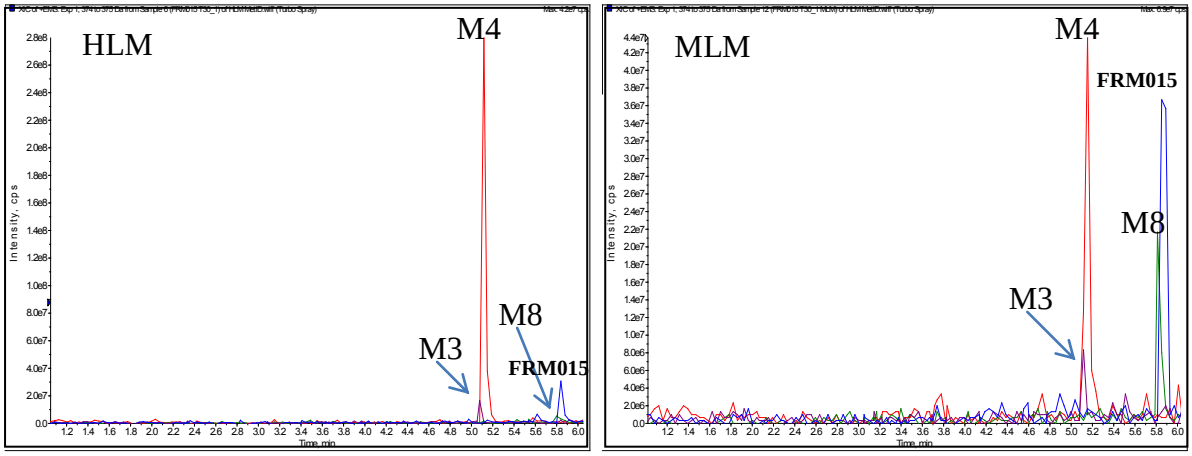

Figure 3.7: Extracted ion chromatograms of **FRM015** and its metabolites (The metabolite numbering represents the corresponding metabolite in metergoline)

However, for **FRM007**, which has a *para*-butyl substitution, the major site of metabolism was this butyl chain, with 3 hydroxylation and 1 dihydroxylation metabolites formed on this

chain (Figure 3.8). The ergoline hydroxylation metabolite was barely detectable. One of the butyl hydroxylation metabolites and the dihydroxylated metabolite were only detected in HLM incubations. This additional pathway contributes to the lower stability of this compound in HLM.

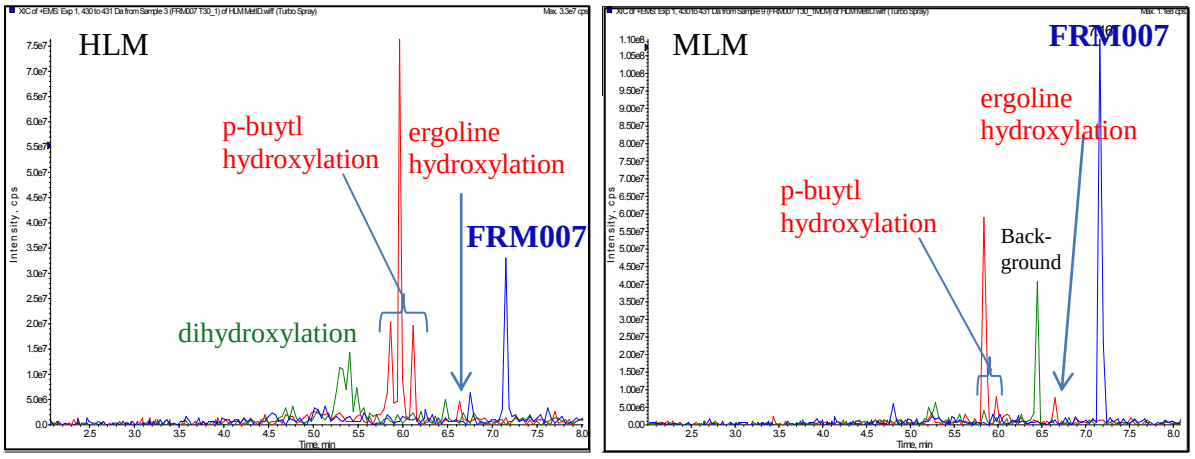

Figure 3.8: Extracted ion chromatograms of **FRM007** and its metabolites in HLM and MLM

For **FRM011,** the *O*-demethylated metabolite is observed in both HLM and MLM incubations (Figure 3.9)

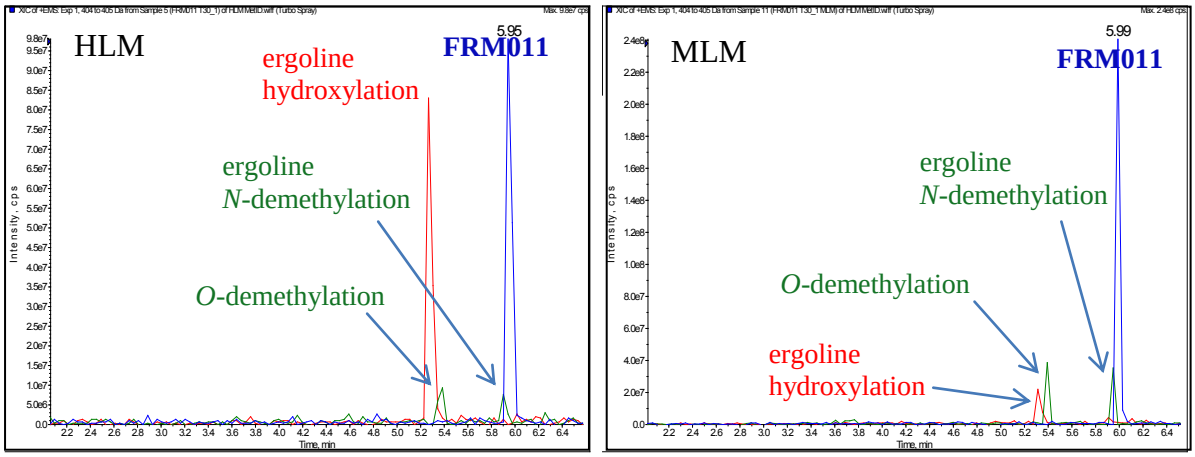

Figure 3.9: Extracted ion chromatograms of **FRM011** and its metabolites in HLM and MLM

Among the alkyl amides, **GKMG22** and **GKMG16** which have shorter chains are similar in their metabolism to metergoline, with ergoline hydroxylation (corresponding to M4) and

ergoline *N*-demethylation (corresponding to M8) as the main metabolites. **GKMG14**, with a butyl chain, is metabolised to 3 alkyl hydroxylation products in MLM, in addition to the ergoline hydroxylation metabolite (M4). However, in HLM only the ergoline hydroxylation metabolite is detected and this probably explains the better stability of this compound in HLM (Figure 3.10).

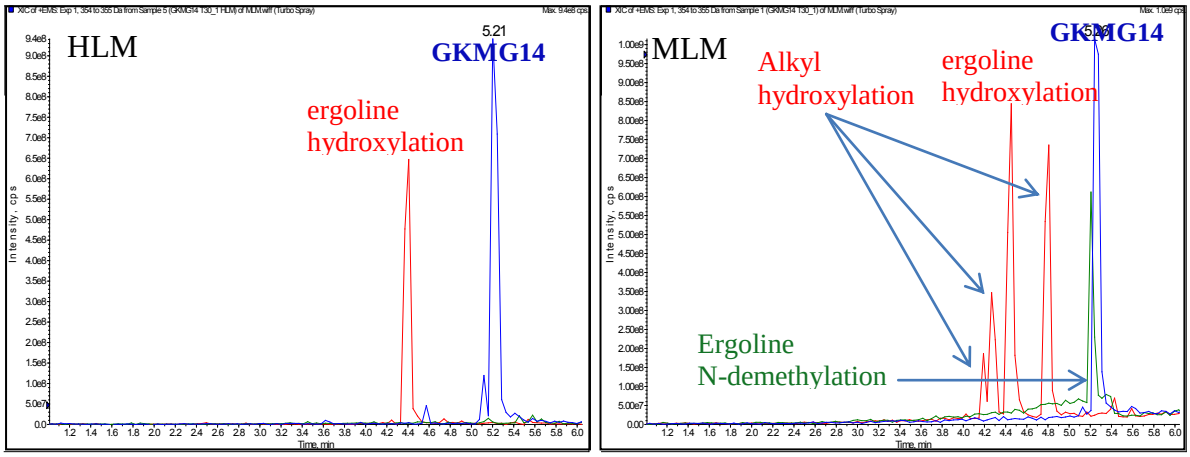

Figure 3.10: Extracted ion chromatograms of **GKMG14** and its metabolites

3.5 Discussion

The *in vitro* metabolism of metergoline proceeds by ergoline hydroxylation as the major pathway, in contrast to its reported metabolism *in vivo* where 1-demethylation is the major metabolite observed. A possible explanation could be the contribution of gut wall metabolism to the metabolite profile observed *in vivo.* This difference in metabolic pathways has no effect on the clearance of metergoline *in vitro* and rapid metabolism, as reported *in vivo* is still observed. It would however be of interest, for derivatives further along the development chain, to assess the clearance, metabolism and metabolite formation kinetics in intestinal fractions (microsomes/s9), to maximise the predictive value of *in vitro* data.

The derivatives selected were generally metabolised in a similar way to metergoline, with metabolism occurring on the ergoline nucleus. Among the aryl amides with no metabolically vulnerable groups (**FRM001, 003, 004, 010**) the metabolic stability was comparable regardless of the lipophilic or electronic properties of the substituent. These derivatives were more stable than metergoline. A derivative with a para-Fluoro substitution had a metabolic stability comparable to that of **FRM015** suggesting that the size of the substituent is important. Since metabolism of these derivatives exclusively occurs on the ergoline ring, the effects of the phenyl substituents is probably in changing the affinity of these compounds to the metabolising enzymes leading to lower metabolism and thus better microsomal stability. Metergoline itself is reported to be highly protein bound (>99%), so it is unlikely that the higher stability represents higher protein binding.[6] These compounds would therefore be projected to have better *in vivo* half-lifes compared to metergoline.

Alkyl hydroxylation was observed with **FRM007** and **GKMG14**. In the case of **FRM007** which has a p-butyl substituent, three hydroxylation products were detected in HLM. Assuming CYP450 involvement and hydrogen abstraction and stabilisation of the resulting electrophilic intermediate would be most favoured at the benzylic position, and benzylic

hydroxylation should therefore be the preferred metabolic pathway and should in any case be one of the three hydroxylation products detected. CYP450s are also known to catalyse hydroxylation at ω and ω-1 and these are probably the other two metabolites.[27] Incubations with **FRM002,** which has a *para*-ethyl substituent, gave one ergoline hydroxylation metabolite and only one hydroxylated metabolite on the substituted phenyl. Comparing **FRM002** and **FRM007**, it is probable that benzylic oxidation occurs in both cases but as the length of the alkyl chain increases, ω and ω-1 hydroxylation becomes easier, presumably because the chain is able to get closer to the active site of the enzyme. In the case of **GKMG14** alkyl hydroxylation was observed only in MLM, suggesting that an enzyme other than the one involved in **FRM002** and **007** metabolises this compound. A comparison with **GKMG22,** which has a shorter chain and where hydroxylation is only observed on the ergoline core, suggests that chain length has an effect on the ease of alkyl hydroxylation as would be expected.

M2 in metergoline was shown to be 1,6-dimethyl-8-b-aminomethylergoline by comparison of its retention time and fragmentation with an authentic compound. This metabolite, formed by carbamate hydrolysis was not detected for any of the amide derivatives, presumably because of the better stability of the amide bond. This metabolite was also detected in plasma incubations of metergoline showing a contribution by hydrolases in plasma to its formation.

The experimentally observed sites of metabolism were compared with those predicted by StarDrop (Figure 3.11) to determine the utility of this software in the optimisation of these compounds. For metergoline, the methyl group at N_1 is predicted to be the major site of metabolism by CYP3A4 and by CYP2C9, possibly by *N*-demethylation.

CYP3A4 **CYP2D6** **CYP2C9**

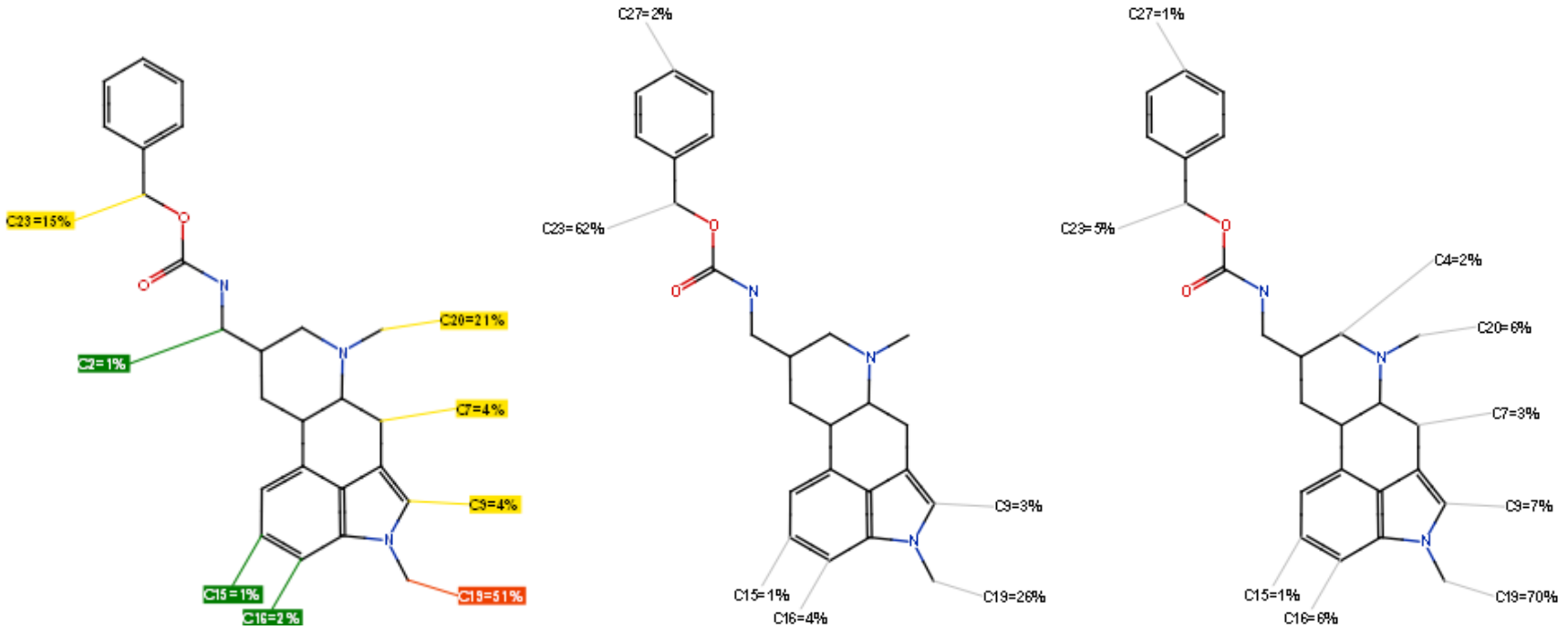

Figure 3.11: StarDrop predicted sites of metabolism for **Metergoline** assuming metabolism by CYP3A4, CYP2D6 or CYP2C9. (The percentages show the expected proportion of metabolites that would result from metabolism at the indicated position. For CYP3A4, the colors indicate the lability of the positions; red – labile, yellow – moderately labile, green – moderately stable, blue – stable)

While 1-demethylation is the major pathway *in vivo*, it was of less significance in HLM and MLM, with ergoline hydroxylation observed as the major metabolite. This position is also predicted to be the most metabolically labile by the CYP3A4 model. 12-hydroxylation, which is observed *in vivo*, is not predicted by this software, though a number of positions on the ergoline ring are suggested as sites of metabolism.

The alkyl hydroxylation pathway is well predicted in StarDrop. Focussing on CYP3A4 where both the site of metabolism and the relative lability are available, the ω and ω-1 positions in both **FRM007** and **GKMG14** and the benzyl $–CH_2$ in **FRM007** are predicted to be the major sites of metabolism of these compounds and are also predicted to be significantly labile.

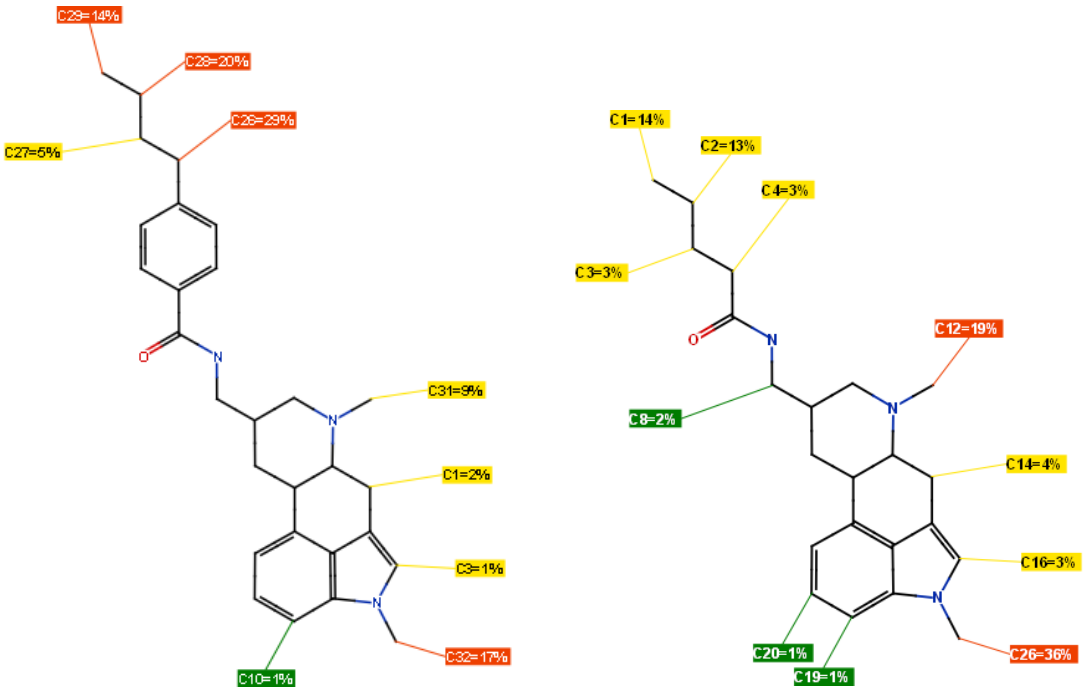

Figure 3.12: StarDrop predicted sites of metabolism for **FRM007** and **GKMG14** assuming metabolism by CYP3A4. (The percentages show the expected proportion of metabolites that would result from metabolism at the indicated position and the colors indicate the lability of the positions; red – labile, yellow – moderately labile, green – moderately stable, blue – stable)

As discussed in previous chapters, the physicochemical properties of the metabolites, specifically, lipophicity and TPSA are important determinants of the contribution of metabolites to *in vivo* activity. These properties are presented for metergoline and some of its metabolites below (Table 3.4).

Table 3.4: Physicochemical properties of metergoline and its metabolites

Compound	MW	LogP	Log D	TPSA
1-demethylmetergoline	389	3.74	2.72	57
12-hydroxymetergoline	419	3.54	2.27	67
1,6-dimethyl-8-β-aminomethylergoline	269	1.96	0.74	34
Metergoline	403	3.95	2.82	47

The lipophilicity (Log P and Log D) and TPSA of 1-demthylmetergoline and 12-hydroxymetergoline are only slightly changed compared to those of metergoline, suggesting that the passive diffusion of these metabolites is likely to be similar to that of metergoline. This is demonstrated by the observation that both metabolites possess *in vivo* antiserotonergic activity, and are indeed more active than metergoline.[28,29] 1-demethylmetergoline also has a longer plasma half-life compared to metergoline, possibly as a result of its reduced lipophilicity which reduces its affinity to metabolic enzymes. The contribution of these metabolites to *in vivo* antiplasmodial or antimycobacterial activity is difficult to predict since no information is available on the mechanism of action of these compounds. However, their *in vivo* antiserotonergic activity suggests that they are able to diffuse across cellular barriers to intracellular targets. The only unknown is how the structural modifications affect interaction with the biological target of these compounds in plasmodia and mycobacteria.

The structure and physicochemical properties of 1, 6-dimethyl-8-β-aminomethylergoline are quite different from those of metergoline and suggest significant differences in passive diffusion across membranes, relative to metergoline. This is also suggested by the observation that this compound was inactive in both the antiplasmodial and antimycobacterial assays. Therefore, while it is observed as a circulating metabolite, it is unlikely to contribute to the *in vivo* antiplasmodial or antimycobacterial activity of metergoline.

A complicating factor in the repositioning and repurposing of these agents is their CNS pharmacology, especially since the binding affinities against most of their target receptors is in the low nanomolar to high picomolar range, with their metabolites being upto 100 times more potent against certain receptor subtypes.[28,30] This is, however, surmountable because compounds can be designed such that they have poor blood brain barrier permeability. It may also be possible, with a larger compound set, to computationally determine the structural features required for activity and thus perform scaffold hoping to obtain compounds that retain the antiplasmodial or antimycobacterial activity but have no CNS activity.

While the first phase of this work was mostly exploratory and targeted only on amide derivatives of metergoline, the preliminary data shows that more extensive SAR work may yield derivatives that can be pursued as leads for the development of antiplasmodial and antimycobacterial agents.

3.6 Conclusion

The metabolism of metergoline and a number of its derivatives with antiplasmodial and/or antimycobacterial activity was investigated. The tentative structures of the metabolites could be assigned based on the similarities between the fragmentation patterns of these derivatives to more widely studied ergolines, and on the mass shift following H/D exchange. For metergoline, a hydroxymetergoline metabolite was identified as the main metabolite *in vitro,* in contrast to the *in vivo* metabolism where 1-demethylmetergoline is reported as the primary metabolite. The derivatives were more stable than metergoline in human and mouse liver microsomes, partly because of the stability of the amide bond, relative to the carbamate bond in metergoline. Their metabolism was broadly similar to that of metergoline but alkyl hydroxylation was also observed for two derivatives which had a butyl chain. This metabolic pathway showed species differences with *para*-butyl hydroxylation occurring only in HLM and hydroxylation of the pentyl chain observed in MLM only. These sites of metabolism were generally well predicted in StarDrop, particularly the ergoline demethylation and the alkyl hydroxylation. On the other hand, 12-hydroxylation, a known metabolite *in vivo*, was not predicted by the software. These preliminary data will be useful in further SAR expansion of these compounds.

3.7 References

(1) Beretta, C.; Ferrini, R.; Glasser, A. H. 1-Methyl-8 B-Carbobenzyloxy-Aminomethyl-10 A-Ergoline, a Potent and Long-Lasting 5-Hydroxytryptamine Antagonist. *Nature* **1965**, *207*, 421–422.

(2) Crosignani, P. G.; Lombroso, G. C.; Caccamo, A.; Reschini, E.; Peracchi, M. Suppression of Puerperal Lactation by Metergoline. *Obstet. Gynecol.* **1978**, *51*, 113–115.

(3) Gerstenberg, C.; Nöthling, J. O. The Effects of Metergoline Combined with PGF2α Treatment on Luteal Function and Gestation in Pregnant Bitches. *Theriogenology* **1995**, *44*, 649–659.

(4) Roca, C. A.; Schmidt, P. J.; Smith, M. J.; Danaceau, M. A.; Murphy, D. L.; Rubinow, D. R. Effects of Metergoline on Symptoms in Women with Premenstrual Dysphoric Disorder. *Am. J. Psychiatry* **2002**, *159*, 1876–1881.

(5) Eich, E.; Pertz, H. Ergot Alkaloids as Lead Structures for Differential Receptor Systems. *Pharmazie* **1994**, *49*, 867–877.

(6) Hooker, J. M.; Kim, S. W.; Reibel, A. T.; Alexoff, D.; Xu, Y.; Shea, C. Evaluation of [(11)C]metergoline as a PET Radiotracer for 5HTR in Nonhuman Primates. *Bioorg. Med. Chem.* **2010**, *18*, 7739–7745.

(7) Colao, A.; Savastano, S. Medical Treatment of Prolactinomas. *Nat. Rev. Endocrinol.* **2011**, *7*, 267–278.

(8) Metergoline - Drugs.com http://www.drugs.com/international/metergoline.html (accessed Jul 4, 2014).

(9) Kang, K.; Wong, K.-S.; Seneviratne, C. J.; Samaranayake, L. P.; Fong, W.-P.; Tsang, P. W.-K. In Vitro Synergistic Effects of Metergoline and Antifungal Agents against Candida Krusei. *Mycoses* **2010**, *53*, 495–499.

(10) Kang, K.; Wong, K.-S.; Fong, W.-P.; Tsang, P. W.-K. Metergoline-Induced Cell Death in Candida Krusei. *Fungal Biol.* **2011**, *115*, 302–309.

(11) Huang, Y.-C.; Han, Y.-S. Determining Anti-Betanodavirus Compounds through a GF-1 Cell-Based Screening Platform. *Antiviral Res.* **2014**, *105*, 47–53.

(12) Pubchem Bioassay: qHTS for inhibitors of binding or entry into cells for Marburg Virus http://pubchem.ncbi.nlm.nih.gov/assay/assay.cgi?aid=540276 (accessed Jul 8, 2014).

(13) Pubchem Bioassay: Highthroughput screening of inhibitors of Mycobacterium tuberculosis H37Rv http://pubchem.ncbi.nlm.nih.gov/assay/assay.cgi?aid=1332 (accessed May 7, 2014).

(14) Pubchem Bioassay: qHTS profiling for inhibitors of Plasmodium falciparum proliferation http://pubchem.ncbi.nlm.nih.gov/assay/asis.cgi?reqid=2312105874255158940&q=r&version=1.3 (accessed Jul 8, 2014).

(15) Pubchem Bioassay: qHTS for differential inhibitors of proliferation of Plasmodium falciparum line 3D7 http://pubchem.ncbi.nlm.nih.gov/assay/assay.cgi?aid=1876 (accessed Jul 8, 2014).

(16) PubChem BioAssay: qHTS for differential inhibitors of proliferation of Plasmodium falciparum line W2 http://pubchem.ncbi.nlm.nih.gov/assay/assay.cgi?aid=1883 (accessed Jul 8, 2014).

(17) Pubchem Bioassay: Primary qHTS for delayed death inhibitors of the malarial parasite plastid, 96 hour incubation http://pubchem.ncbi.nlm.nih.gov/assay/assay.cgi?aid=504834 (accessed Jul 8, 2014).

(18) Nwaka, S.; Besson, D.; Ramirez, B.; Maes, L.; Matheeussen, A.; Bickle, Q.; Mansour, N. R.; Yousif, F.; Townson, S.; Gokool, S.; et al. Integrated Dataset of Screening Hits against Multiple Neglected Disease Pathogens. *PLoS Negl. Trop. Dis.* **2011**, *5*, e1412.

(19) Martini, A.; Moro, E.; Marrari, P.; Pacciarini, M. A.; Sega, R.; Dell'Osso, L.; Bertelli, A.; Tamassia, V. Pharmacokinetics and Bioavailability of Metergoline in Healthy Volunteers after Single I.v. and Oral Administration. *Int. J. Clin. Pharmacol. Res.* **1983**, *3*, 27–34.

(20) Vicario, G. P.; Battaglia, R.; Bernardi, L.; Arcamone, F. Metabolism of Metergoline in the Rat. *Farmaco. Sci.* **1982**, *37*, 651–662.

(21) Singh, K.; Kaur, G.; Mjambili, F.; Smith, P. J.; Chibale, K. Synthesis of Metergoline Analogues and Their Evaluation as Antiplasmodial Agents. *Medchemcomm* **2014**, *5*, 165.

(22) Cai, J.; Henion, J. Elucidation of LSD in Vitro Metabolism by Liquid Chromatography and Capillary Electrophoresis Coupled with Tandem Mass Spectrometry. *J. Anal. Toxicol.* **1996**, *20*, 27–37.

(23) Lehner, A. F.; Craig, M.; Fannin, N.; Bush, L.; Tobin, T. Fragmentation Patterns of Selected Ergot Alkaloids by Electrospray Ionization Tandem Quadrupole Mass Spectrometry. *J. Mass Spectrom.* **2004**, *39*, 1275–1286.

(24) Mohamed, R.; Gremaud, E.; Tabet, J.; Guy, P. A. Mass Spectral Characterization of Ergot Alkaloids by Electrospray Ionization , Hydrogen / Deuterium Exchange , and Multiple Stage Mass Spectrometry : Usefulness of Precursor Ion Scan Experiments. *Rapid Commun. Mass Spectrom.* **2006**, *20*, 2787–2799.

(25) Ohashi, N.; Furuuchi, S.; Yoshikawa, M. Usefulness of the Hydrogen--Deuterium Exchange Method in the Study of Drug Metabolism Using Liquid Chromatography-Tandem Mass Spectrometry. *J. Pharm. Biomed. Anal.* **1998**, *18*, 325–334.

(26) Lu, Y.; He, Y.; Wang, M.; Zhang, L.; Yang, L.; Wang, Z.; Ji, G. Characterization of Nuciferine Metabolism by P450 Enzymes and Uridine Diphosphate Glucuronosyltransferases in Liver Microsomes from Humans and Animals. *Acta Pharmacol. Sin.* **2010**, *31*, 1635–1642.

(27) *Drug Metabolism Handbook: Concepts and Applications*; Nassar, A. F.; Hollenberg, P. F.; Scatina, J., Eds.; John Wiley & Sons, Inc.: Hoboken, NJ, USA, 2009.

(28) Arcamone, F.; Francesclii, G.; Glasser, A.; Dorigotti, L. US Patent US360046; 1,6-Dimethyl-10a-Ergoline Derivatives. US360046, 1972.

(29) Di Salle, E.; Praga, C.; Castegnaro, E. US Patent US 4151283A; 6-Methyl-and 1,6-Dimethyl-8β-Carbobenzyloxy-Aminomethyl-10α-Ergoline as Inhibitors of Prolactin Secretion. US 4151283 A, 1979.

(30) Cocchi, D.; Locatelli, V.; Carminati, R.; Müller, E. E. Mechanisms Underlying the Prolactin-Lowering Effect of Metergoline in the Rat. *Life Sci.* **1978**, *23*, 927–936.

Chapter 4

FUSIDIC ACID ANALOGUES

4.1 Background

Fusidic acid is a naturally occurring fusidane antibiotic produced by *Fusidium coccineum,* and various other fungi.[1,2] It has been in use since the 1960s for the management of gram positive infections, and more recently against methicillin resistant *Staphyloccus aureus.* While fusidic acid is the only fusidane antibiotic in clinical use, there are a number of naturally occurring fusidanes with antibiotic activity (Figure 4.1), including helvolic acid,[3] cephalosporin P1 and its analogues,[4] viridomidic acids (A, B, C)[5] and a number of fusidic acid co-metabolites (keto- ,anhydrofusidic acid analogues and their stereoisomers).[2,6,7] They are in general less active than fusidic acid or have activity against a narrower range of organisms, compared to fusidic acid.

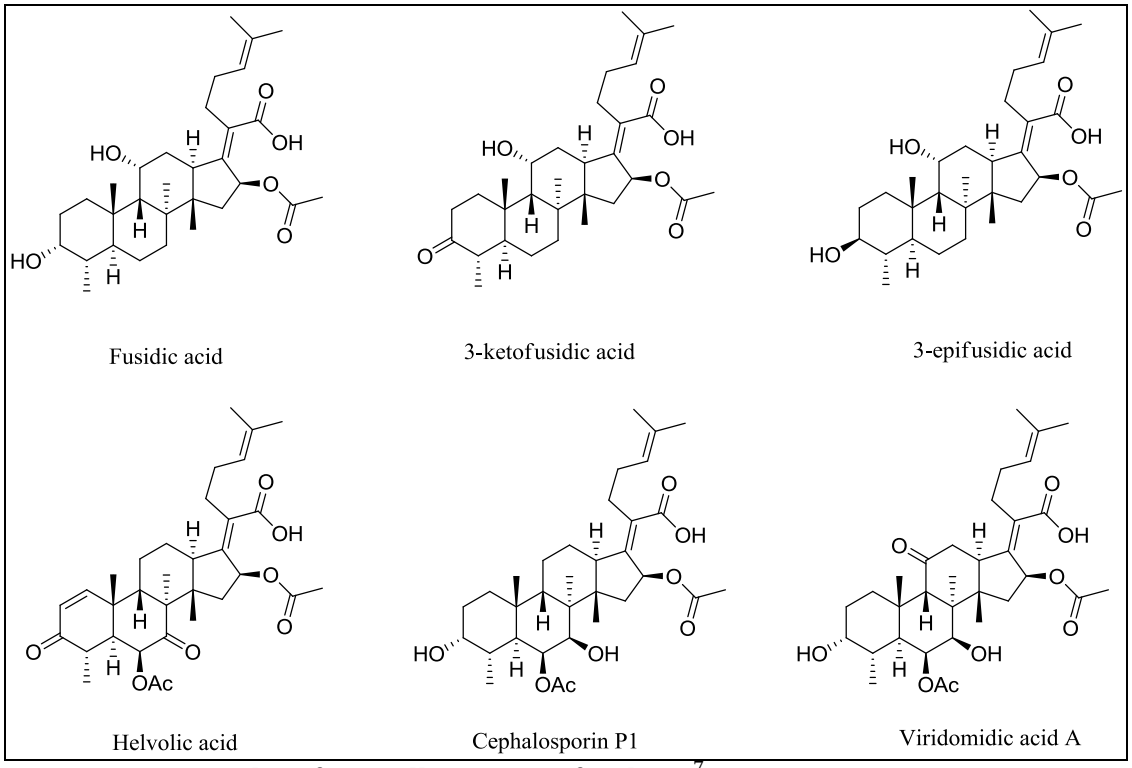

Figure 4.1: Examples of naturally occuring fusidanes[7]

The antibacterial activity of fusidic acid is thought to be a result of its inhibition of protein synthesis, by stabilisation of the elongation factor-GDP complex, therefore preventing peptide elongation.[8,9] This unique mode of action prevents cross resistance with commonly used antibiotics. Fusidic acid has also been reported to possess antiplasmodial activity through this mechanism.[10]

Various groups have also reported that fusidic acid has activity against *Mycobacetrium tuberculosis* (*M.tb*), with activity shown against common lab test strains and clinical isolates.[11–13] While this activity has been known for more than 2 decades now, no fusidic acid derivatives have been tested against *M.tb.* Given the slow pace of drug development in tuberculosis and the lack of cross resistance between fusidic acid against other antimycobacterial agents, the repurposing and repositioning of fusidic acid and its derivatives would represent a 'low-hanging fruit' in TB drug discovery. Moreover, fusidic acid has been widely used clinically in the management of antibacterial infections and is well tolerated by

patients.[14] This work is part of a larger project to explore the activity of fusidic acid derivatives and contribute to efforts for identification of potential anti-tuberculosis drugs.[15]

4.1.2 Metabolism of Fusidic acid

Hepatic metabolism, followed by excretion in bile, is the main clearance route for fusidic acid. The acyl glucuronide is the major metabolite produced, together with the 3-keto-, 27-carboxy-, and a hydroxylation metabolite as minor metabolites (Figure 4.2). These metabolites retain antibacterial activity but are less active than fusidic acid.[6,16]

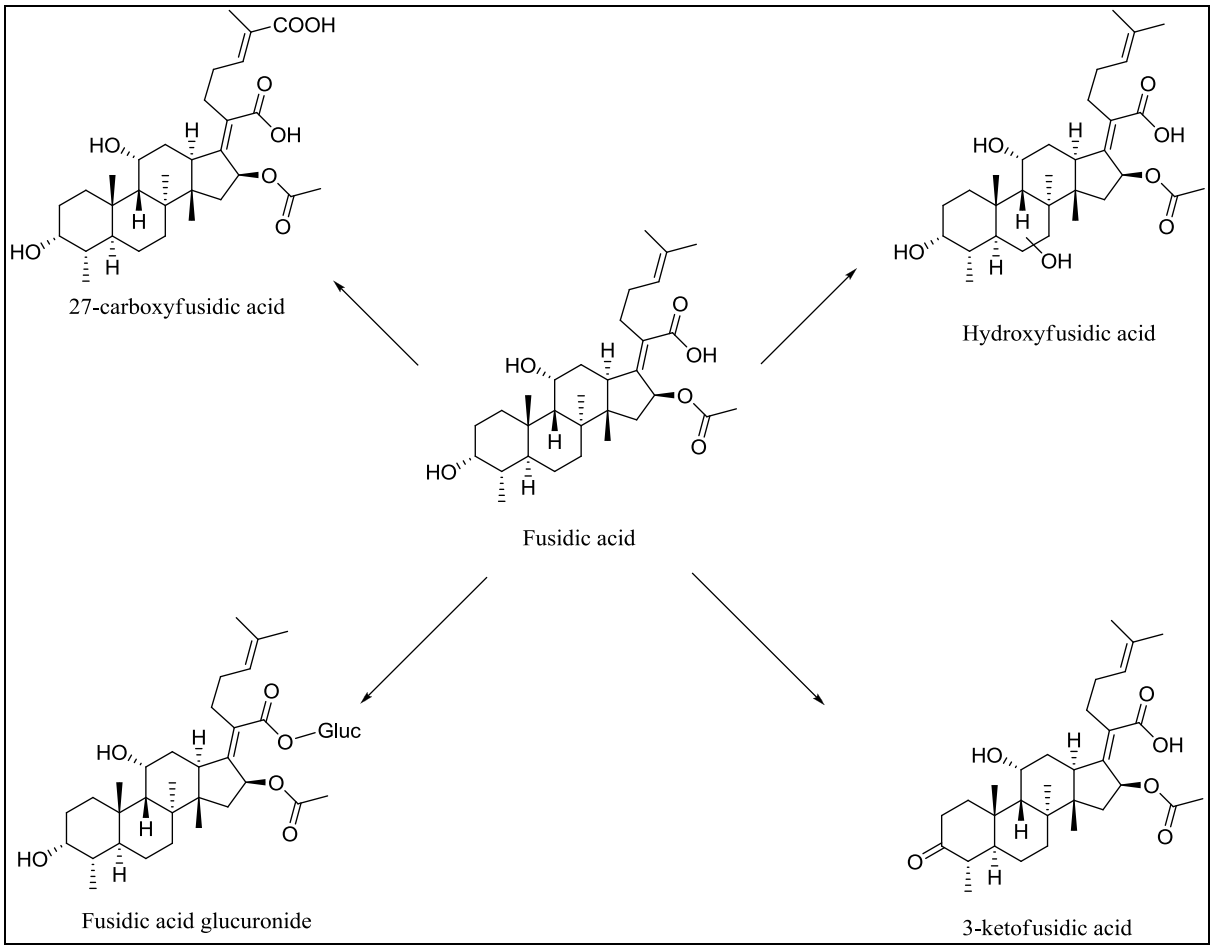

Figure 4.2: Metabolites of fusidic acid in man[16,17]

4.2 Metabolism studies

4.2.1 Compound selection

The compound set for the metabolic studies was selected based on biological activity and also on the availability of similar derivatives to allow for preliminary structure-metabolism work. The compounds are C-3 (esters, hydroxylamines) and C-21(esters, amides, hydrazines) derivatives with antimycobacterial and/or antiplasmodial activity. A summary of these compounds is presented in Figure 4.3 and their biological activity is presented in the relevant sections.

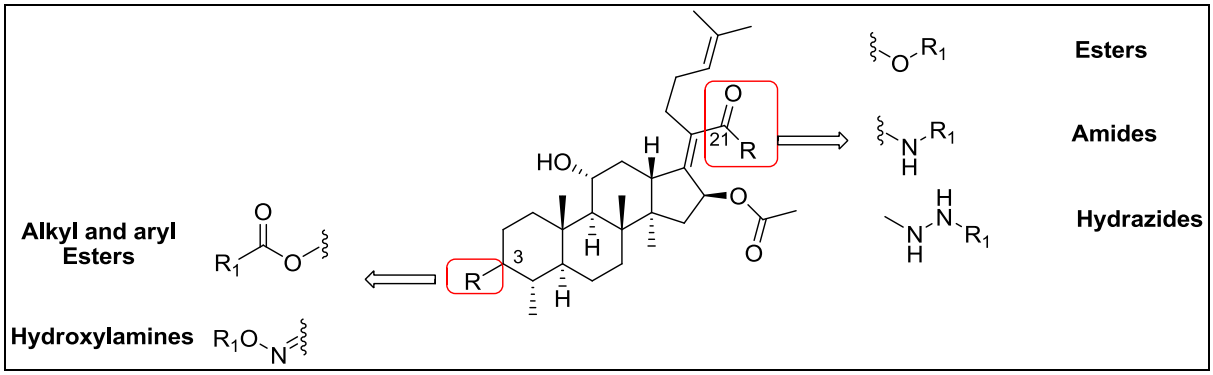

Figure 4.3: Summary of C-3 and C-21 derivatives for metabolic studies

A preliminary analysis of a number of derivatives showed that RLM and MLM metabolism was similar. Further, while there were some qualitative differences between the rodent microsomes and HLM, the metabolic stability was comparable. The data presented is therefore that for RLM stability. Important differences in the qualitative or quantitative data are, however, outlined where relevant. It was also anticipated that the 16-acetyl group of these derivatives, and the ester and amide functions of some of the derivatives might be unstable in plasma. Data on rat plasma stability is therefore also presented, with any differences between results in human and/or mouse plasma outlined.

4.2.2 Analytical considerations

Unlike the compounds presented in previous chapters, fusidic acid derivatives present a number of analytical challenges that are of relevance to the quality and nature of the data. First, the MS sensitivity of the respective precursor ions (M+H) is very poor in both positive mode electrospray ionisation, and is not greatly improved in negative mode. In its place, a number of adducts are detected (Figure 4.4).

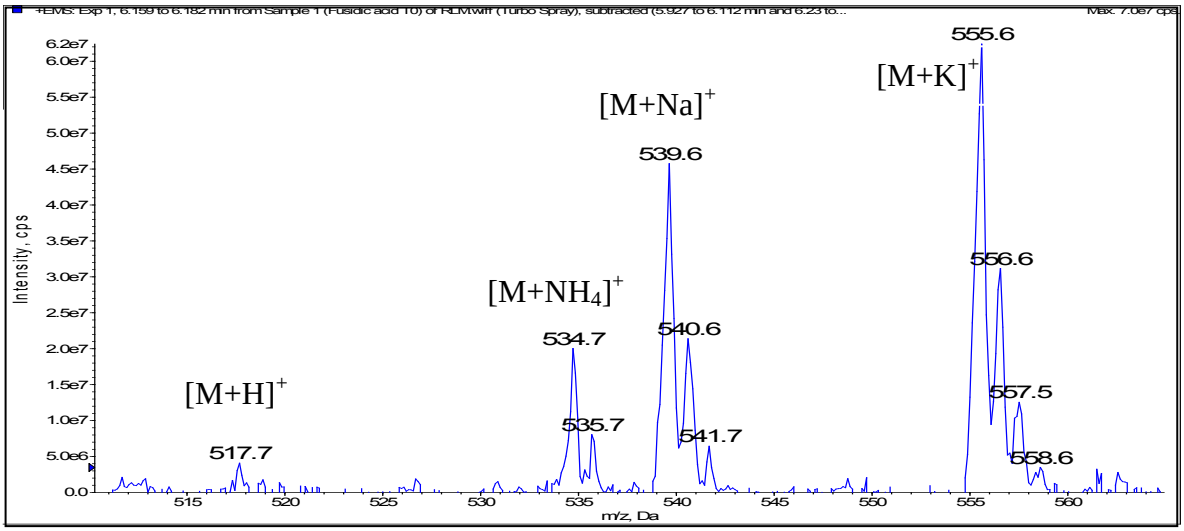

Figure 4.4: Mass spectrum of the precursor ion of fusidic acid and its commonly observed adducts in ESI positive mode

Both the sodium and potassium adducts showed poor CID fragmentation. In addition, it has been reported that the detection of these adducts is often irreproducible producing wide variations in quantitation.[18,19] However, in the presence of ammonium ions, an ammonium adduct was observed that also gave good CID spectra. The derivatives were therefore analysed in a mobile phase containing 5mM ammonium formate, to enhance formation of this adduct. The presence of the sodium and potassium adducts was used to confirm the molecular weight of the metabolites.

The second problem involves the in-source lability of these compounds leading to extensive in-source fragmentation. This was controlled slightly by using flow injection optimisation to optimise the source conditions for the detection of fusidic acid and a number of its most unstable derivatives. However, as can be seen in Figure 4, these conditions still produced significant fragmentation. However, this paralleled CID fragmentation and it was therefore used, together with the presence of adducts to confirm the presence and identity of the metabolites.

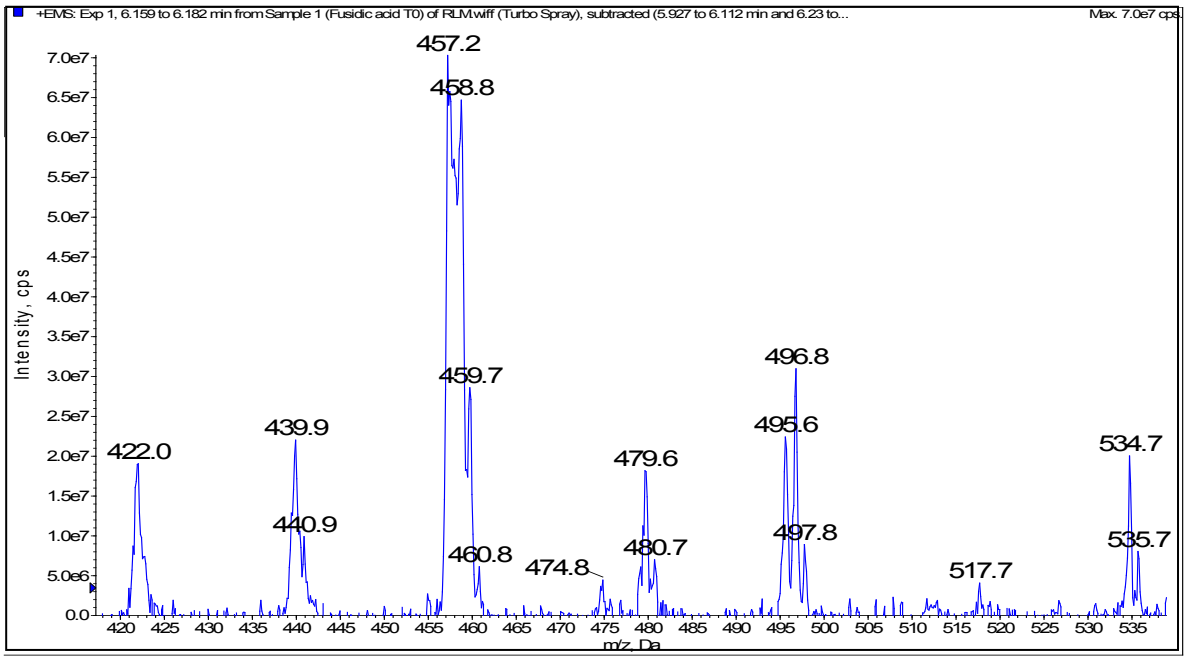

Figure 4.5: In-source fragmentation of fusidic acid

4.2.3 Fragmentation of fusidic acid

The fragmentation pattern of fusidic acid and its derivatives is generally quite ambiguous. Following loss of the 16-acetyl group (to give m/z 457 in fusidic acid), sequential losses of water (18Da) and finally the carbonyl produce the fragments from m/z 439 to m/z 393. From here, sequential losses of ethylene and other hydrocarbon fragments occur to give the rest of the fragments. It is therefore in general more difficult to pinpoint the region of metabolism using the data available.

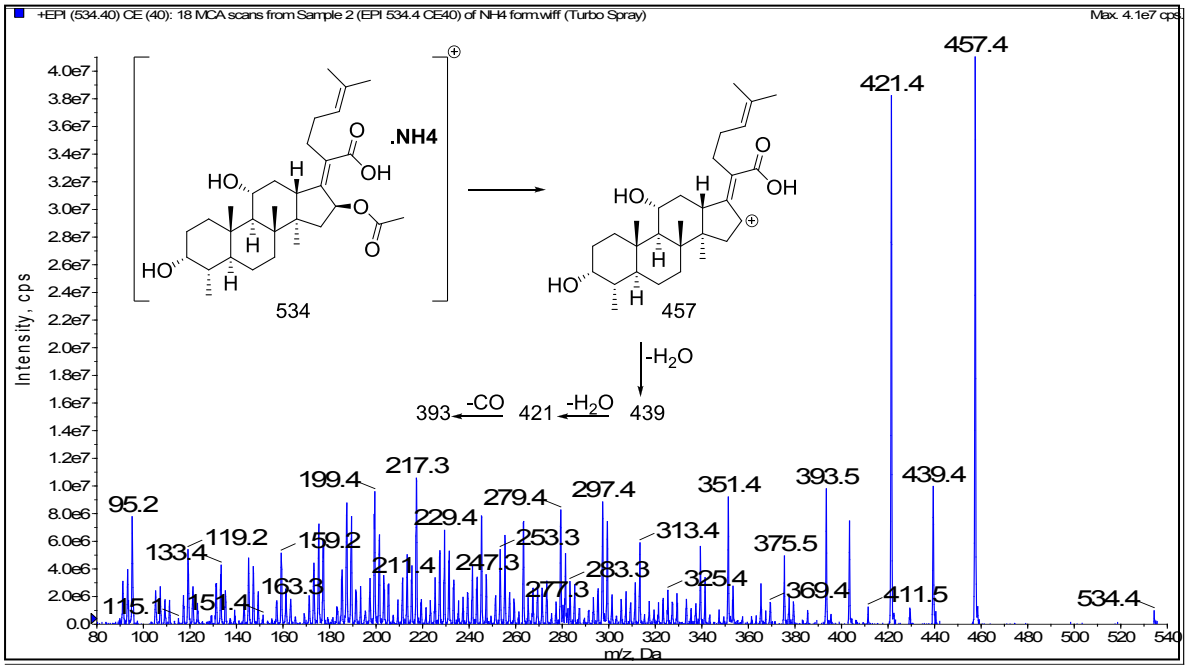

Figure 4.6: CID fragmentation of fusidic acid

4.2.4 Fusidic acid and other C-3 derivatives

Table 4.1: The biological activity and stability of fusidic acid and related C-3 derivatives

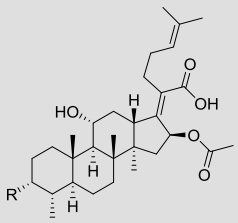

Code	R	*M.tb* H37Rv[a] MIC_{99}, µM	RLM[b] % Remaining	Rat plasma[c] % Remaining	Log P
Fusidic acid	–OH	<0.1563	61	74	4.45
GKFA37	=O	1.25	8	74	4.39
GKFA34	=N–OH	2.5	>99	80	4.68
GKFA46	=N–OMe	20	95	>99	4.96

[a]Drug sensitive strain of Mycobacterium tuberculosis.
[b] % remaining after 1hr incubation at 0.4mg/ml rat liver microsomes.
[c] % remaining after 3hrs incubation in rat plasma

The metabolism of **fusidic acid** in rat liver microsomes gave three products; two were tentatively identified as hydroxyfusidic acid, and ketofusidic acid.

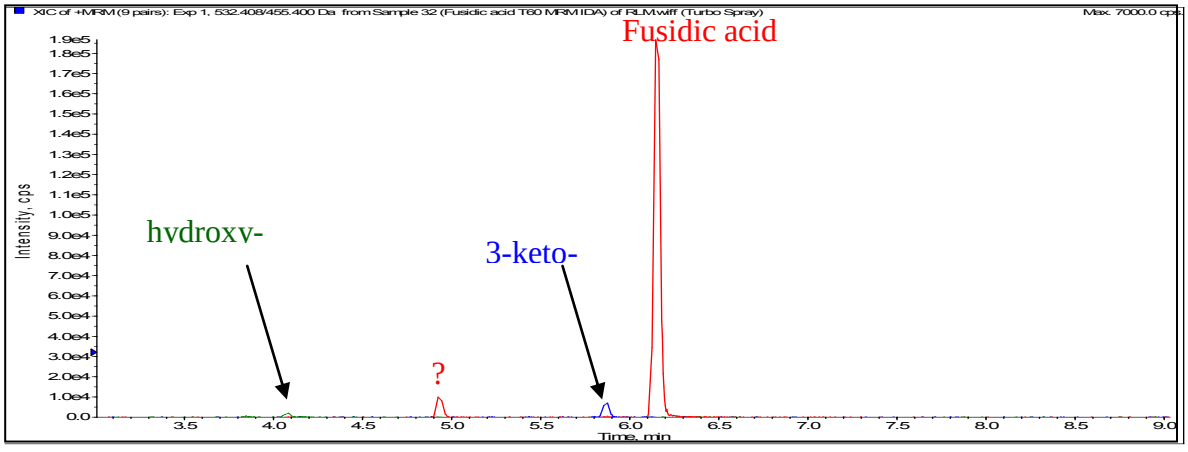

Figure 4.7: Extracted ion chromatogram of **fusidic acid** metabolites from the RLM+NADPH incubation

The specific position of metabolism is unclear from the fragmentation data. However, the ketofusidic acid had a retention time and fragmentation similar to **GKFA37** and is therefore proposed to be 3-ketofusidic acid. This would also be consistent with the reported *in vivo* metabolism of fusidic acid.

An additional metabolite was observed with the same m/z and fragmentation (both source and CID) as fusidic acid, but eluting about a minute earlier.

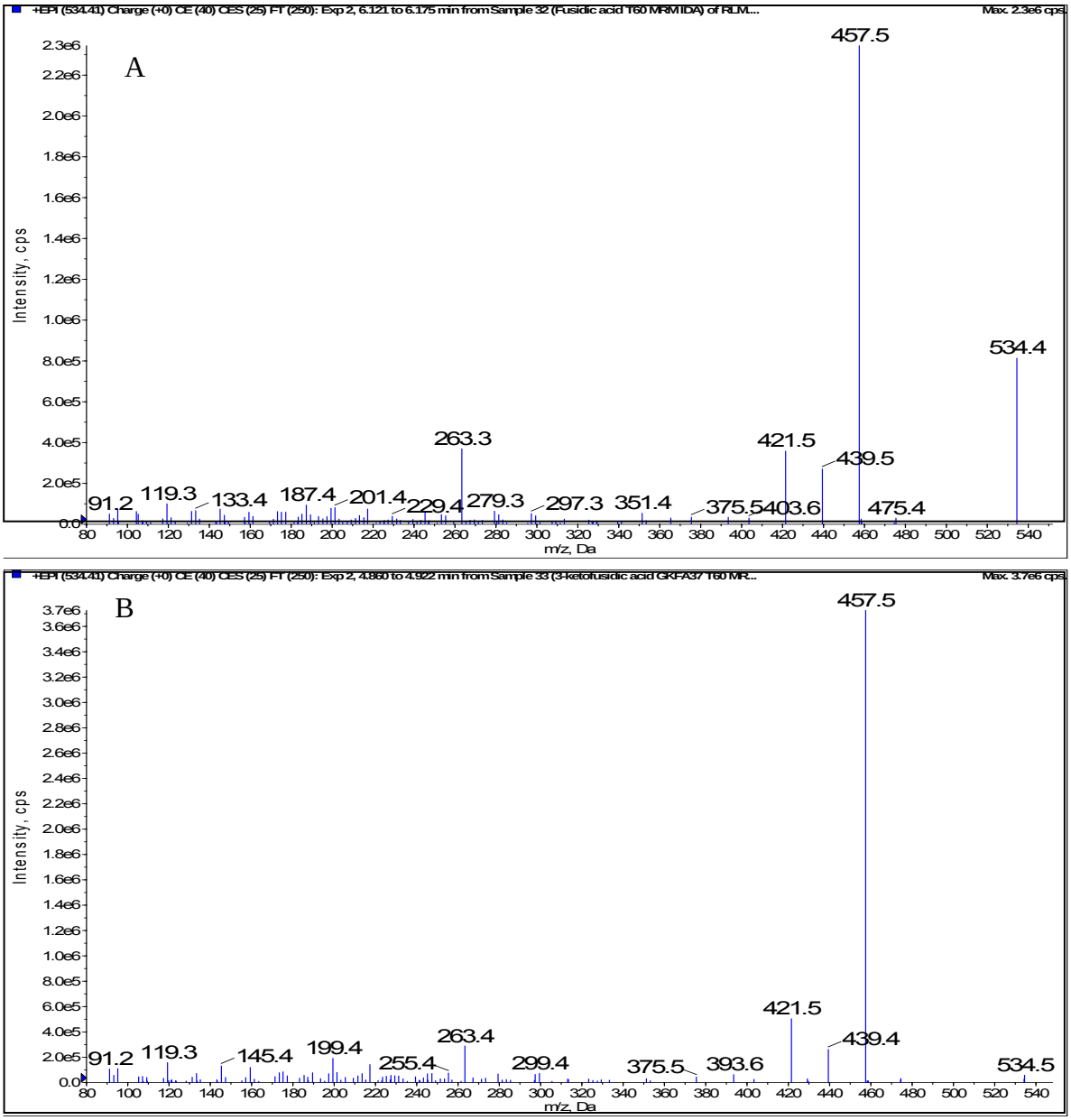

Figure 4.8: CID spectra of fusidic acid (A) and unknown metabolite (B)

The same metabolite was also observed in incubations of **GKFA37** (3-ketofusidic acid), where it was formed along fusidic acid as one of the metabolites. In the absence of NADPH, these metabolites formed in about equal proportion but the proportion of the unknown metabolite was higher in the presence of NADPH.

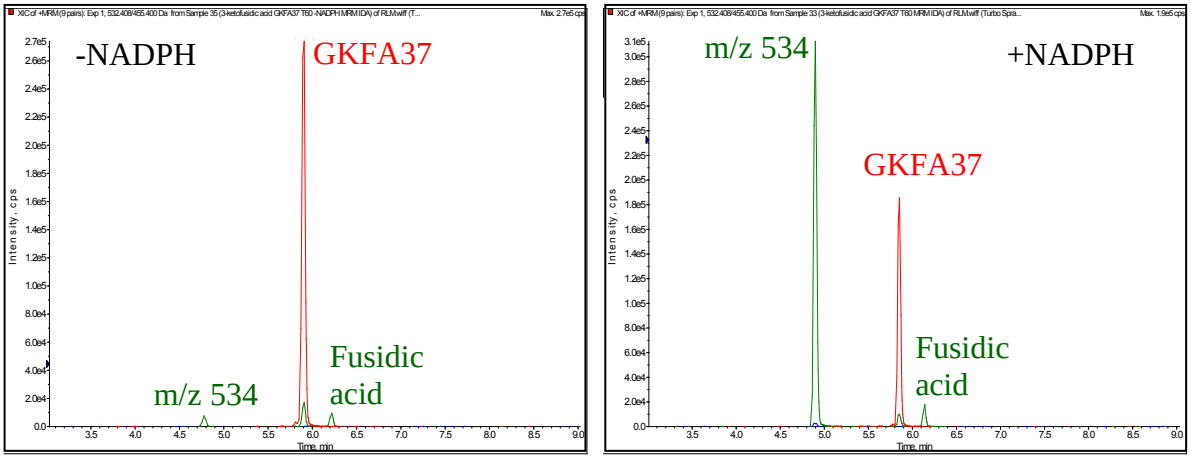

Figure 4.9: Extracted ion chromatogram of the two metabolites of **GKFA37**, in the absence and presence of NADPH

This metabolite is proposed to be 3-epifusidic acid. Based on its formation in incubations of 3-ketofusidic acid (**GKFA37**), it is proposed that in fusidic acid incubations, the metabolite is formed through oxidation of the C-3 OH to form the 3-keto, with the reverse reaction producing either fusidic acid or 3-epifusidic acid (Figure 4.10). This metabolite is reported to be have lower antibacterial activity than fusidic acid across a panel of test organisms.[20]

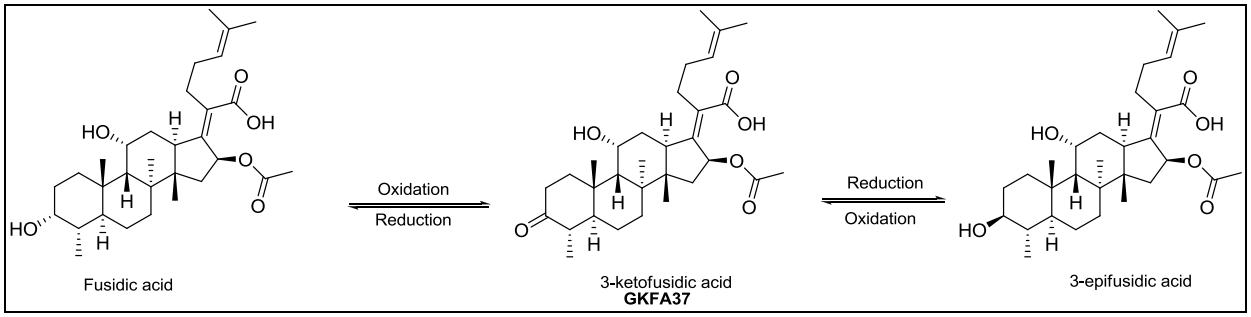

Figure 4.10: Proposed pathway for conversion of fusidic acid to 3-epifusidic acid in RLM

A similar pathway has been proposed for C-3 epimerisation in a number of steroids.[21] While the same pathway was observed in MLM, no C-3 epimerisation was observed in HLM. Instead, the proportion of 3-ketofusidic acid increases, and its hydroxylation metabolite is also observed.

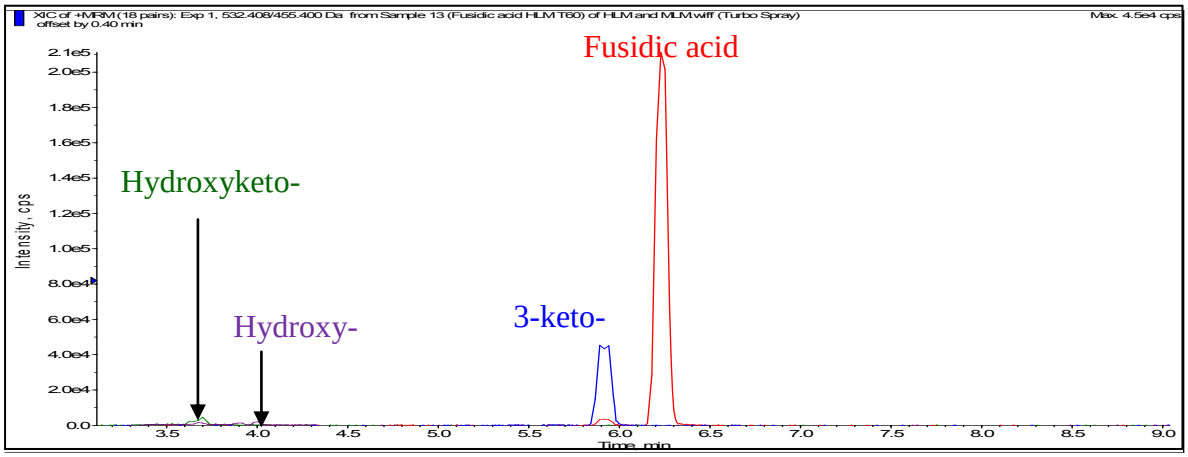

Figure 4.11: XICs of the HLM metabolites of fusidic acid

Despite this difference, the microsomal stability of fusidic acid under these experimental conditions was comparable in all three species (65% ± 5%, remaining).

O-dealkylation was detected for **GKFA46**, leading to formation of **GKFA34**. No metabolites were detected in incubations of **GKFA34**.

In plasma, hydrolysis of the 16-acetyl group followed by spontaneous lactonisation was observed as the only product. This process is reported even in aqueous solution, in formulations of fusidic acid.[22]

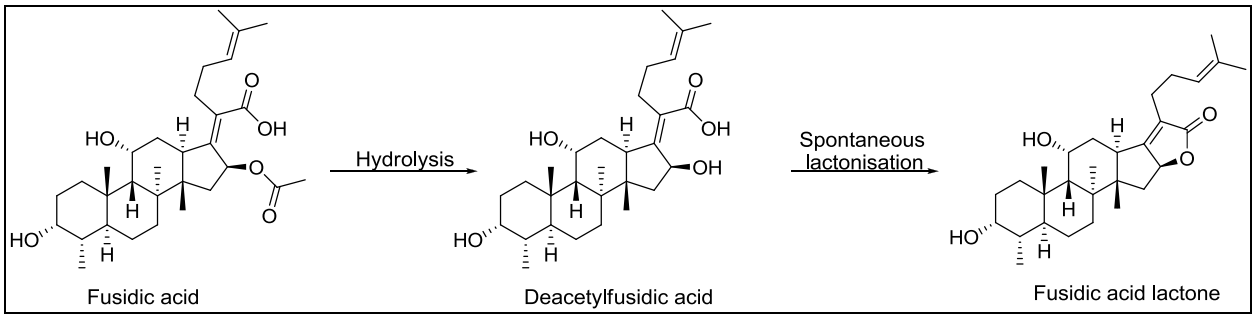

Figure 4.12: C-16 hydrolysis in fusidic acid

4.2.5 C-3 esters

Table 4.2: The biological activity and stability of fusidic acid C-3 esters

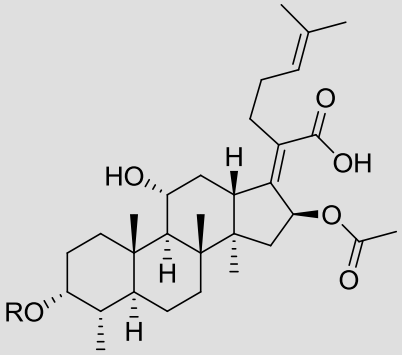

Code	R	*P.f* NF54[a] IC_{50}	*M.tb* H37Rv[b] MIC_{99}	% Remaining RLM[c]	% Remaining Rat plasma[b]	Log P
KSFA5	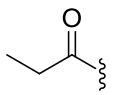	19.0	2.5	8	79	5.25
GKFA16	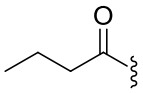	14.9	1.25	15	74	5.43
GKFA17	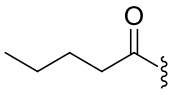	7.46	2.5	20	73	5.62
ME166	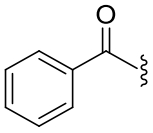	2.0	20	68	79	5.86
ME168	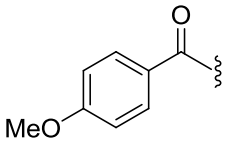	2.63	20	93	95	5.63
ME175	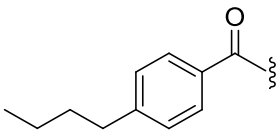	0.39	>160	>99	74	6.64
ME176	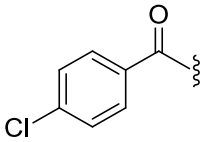	1.07	>160	93	>99	6.24
ME177	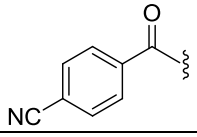	1.52	>160	70	81	5.62

[a]Drug sensitive strain of *Plasmodium falciparum*. [b]Drug sensitive strain of *Mycobacterium tuberculosis*.
[c] % remaining after 1hr incubation at 0.4mg/ml rat liver microsomes.
[d] % remaining after 3hrs incubation in 50% rat plasma

Both the alky and aryl esters are metabolised in RLM almost exclusively to fusidic acid. The alkyl esters are in general less stable than the aryl esters and their stability increases almost linearly with chain length and lipophilicity. Fusidic acid formation is observed in both cases , is not NADPH dependent and occurs quickly enough that it is detectable even in the T0 incubations.

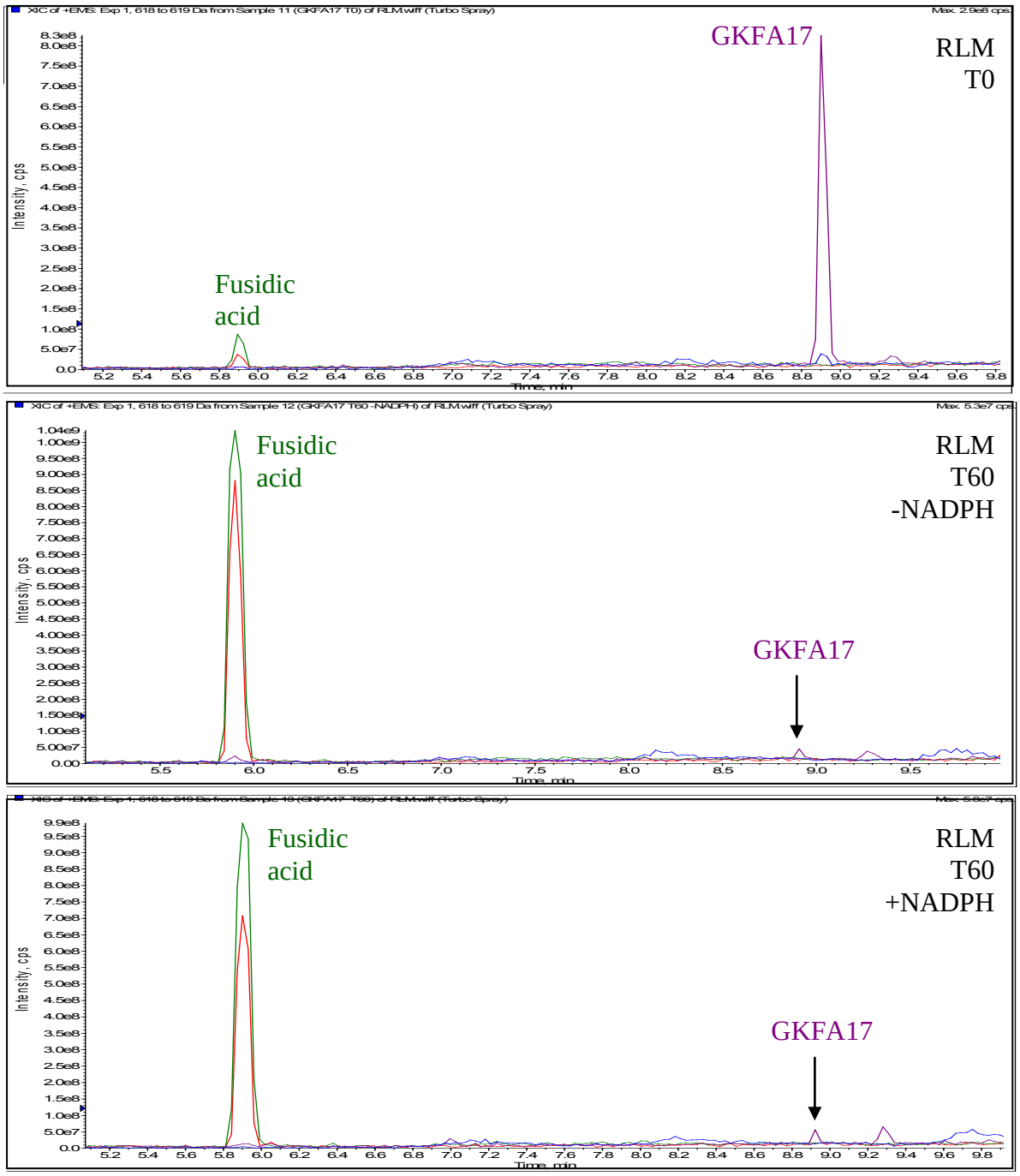

Figure 4.13: Metabolism of **GKFA17** in RLM incubations

Among the aryl esters, a hydroxylated metabolite is also produced. The CID fragmentation data show fragments that are 2Da lower than the corresponding fragments in the parent compound.

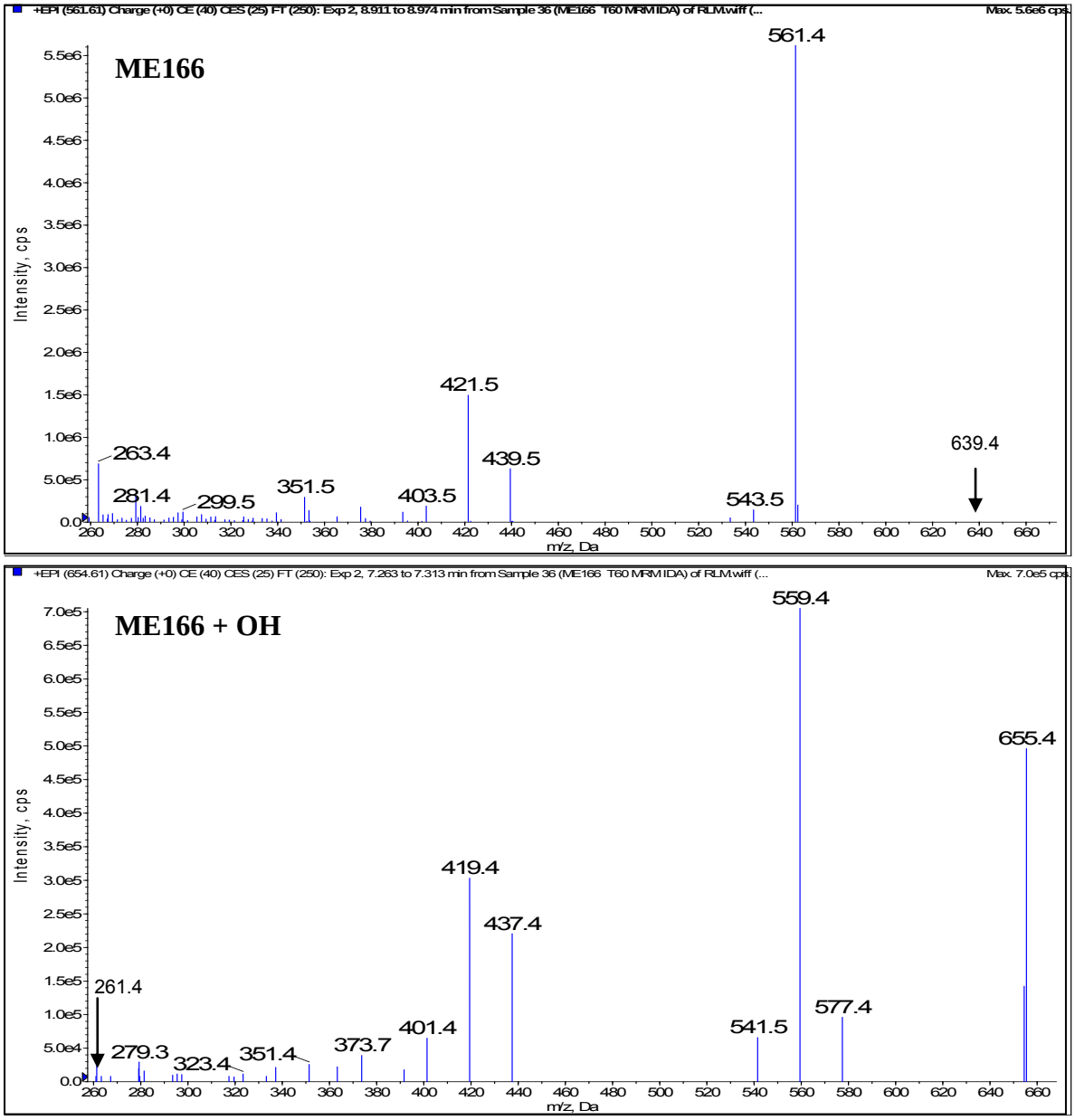

Figure 4.14: CID fragmentation of **ME166** and its hydroxylated metabolite

While the same fragments could also be interpreted as +16Da (for example 437.4 could either be 421 + 16 or 439 -2), the relative intensities of the peaks support the earlier interpretation. This suggests that hydroxylation occurs somewhere on the fusidic acid core, and that during

MS analysis the new hydroxyl group is lost as water with a double bond forming at this position, hence the loss of 2 Da.

Metabolism in plasma also produces fusidic acid, though the process is slower compared to RLM incubations. The differences between the alkyl and aryl esters are also less pronounced, which is expected since different enzymes are involved, as discussed later in this chapter. The plasma stability of **GKFA17** and **ME166** was further evaluated in human and in mouse plasma. Compared to their stability in rat plasma, both compounds were more stable in human plasma (>99% remaining at 3hrs) and drastically less stable in mouse plasma (<10% remaining at 3hrs, $t_{1/2}$ 30min). Hydrolysis in mouse plasma also produced fusidic acid.

4.2.6 C-21 aryl esters

Table 4.3: The biological activity and stability of fusidic acid C-21 aryl esters

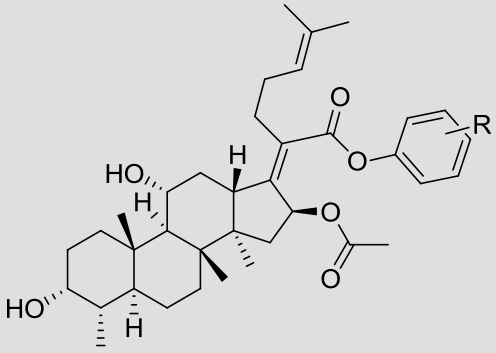

Code	R	*P.f* NF54[a] IC_{50} µM	*M.tb* H37Rv[b] MIC_{99} µM	% Remaining RLM[c]	% Remaining Rat plasma[d]	Log P
ME-29	H	2.40	>160	15	>99	5.71
ME-32	4-F	2.95	>160	14	96	5.86
ME-14	4-Cl	2.30	>160	68	>99	6.16
ME-19	4-Br	2.14	>160	68	67	6.31
ME-12	3-F	2.64	>160	21	>99	5.80
ME-11	3-Cl	1.39	160	63	86	6.10
ME-30	3-Br	2.64	>160	52	>99	6.24
ME-15	3-OMe	1.75	>160	3	>99	5.49
ME-23	3,4-Cl	3.56	>160	80	95	6.53
ME-25	2,4-Cl	3.51	>160	45	>99	6.53

[a]Drug sensitive strain of *Plasmodium falciparum*. [b]Drug sensitive strain of *Mycobacterium tuberculosis*.
[c] % remaining after 1hr incubation at 0.4mg/ml rat liver microsomes.
[d] % remaining after 3hrs incubation in 50% rat plasma

A preliminary examination of the data suggests that for comparing the non-substituted and the halogen-substituted derivatives, metabolic stability varies in the order -Br ≈ -Cl > F ≈ H at both the 3- and 4- positions. While these data may suggest that metabolism occurs on the ester substituent, the metabolism of these compounds is actually similar to the metabolism of fusidic acid with the 3-epi, 3-keto and hydroxy- metabolites in RLM and the 3-keto- and hydroxyfusidic acid in HLM. Similar to the metergoline derivatives presented in Chapter 4, the effect of the substituent may be in aligning the compound within the active site of the

CYP450s, with certain orientations resulting in more efficient metabolism. The increase in lipophilicity does play a role but as observed with the 2,4- and 3,4 diCl- derivatives (same lipophilicity, different metabolic stabilities), it is not the only factor influencing the patterns. **ME-15** is in addition also metabolised by *O*-dealkylation explaining its much lower metabolic stability.

Unlike the C-3 esters, fusidic acid is not observed as a metabolite in microsomal incubations or in plasma. This observation is discussed in more detail in later sections.

4.2.7 C-21 Alkyl esters and amides

Table 4.4: The biological activity and stability of fusidic acid C-21 alkyl esters and amides

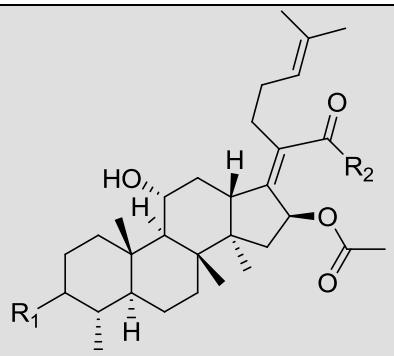

Code	R1	R2	*P.f* NF54[a] IC_{50} µM	*M.tb* H37Rv[b] MIC_{99} µM	% Remaining RLM[c]	% Remaining Plasma[d]	Log P
GKFA48	O	O	nd	40	<10	65	4.55
ME-81	HO	O	3.45	>160	<10	68	5.01
ME-83	HO	O$_2$	2.91	>160	<10	98	5.39
ME-84	HO	O$_6$	4.64	>160	<10	68	6.56
GKFA52	HO	N(H)OH	>10	10	2	84	3.57
GKFA54	HO	N OH	10.53	0.31	7	58	3.78
GKFA56	HO	N OH	2.96	20	5	83	4.00

[a]Drug sensitive strain of *Plasmodium falciparum*. [b]Drug sensitive strain of *Mycobacterium tuberculosis*.
[c] % remaining after 1hr incubation at 0.4mg/ml rat liver microsomes.
[d] % remaining after 3hrs incubation in 50% rat plasma

Unlike their aryl counterparts, all the alkyl esters are very unstable in RLM and are also less stable in rat plasma. Fusidic acid (and 3-ketofusidic acid for **GKFA48**) is observed as minor NADPH dependent metabolite, suggesting that just like for the C-21aryl esters, they do not undergo esterase dependent hydrolysis at C-21. No metabolism occurs in the absence of NADPH.

The metabolites are a variety of hydroxylation products as shown in Figure 4.15

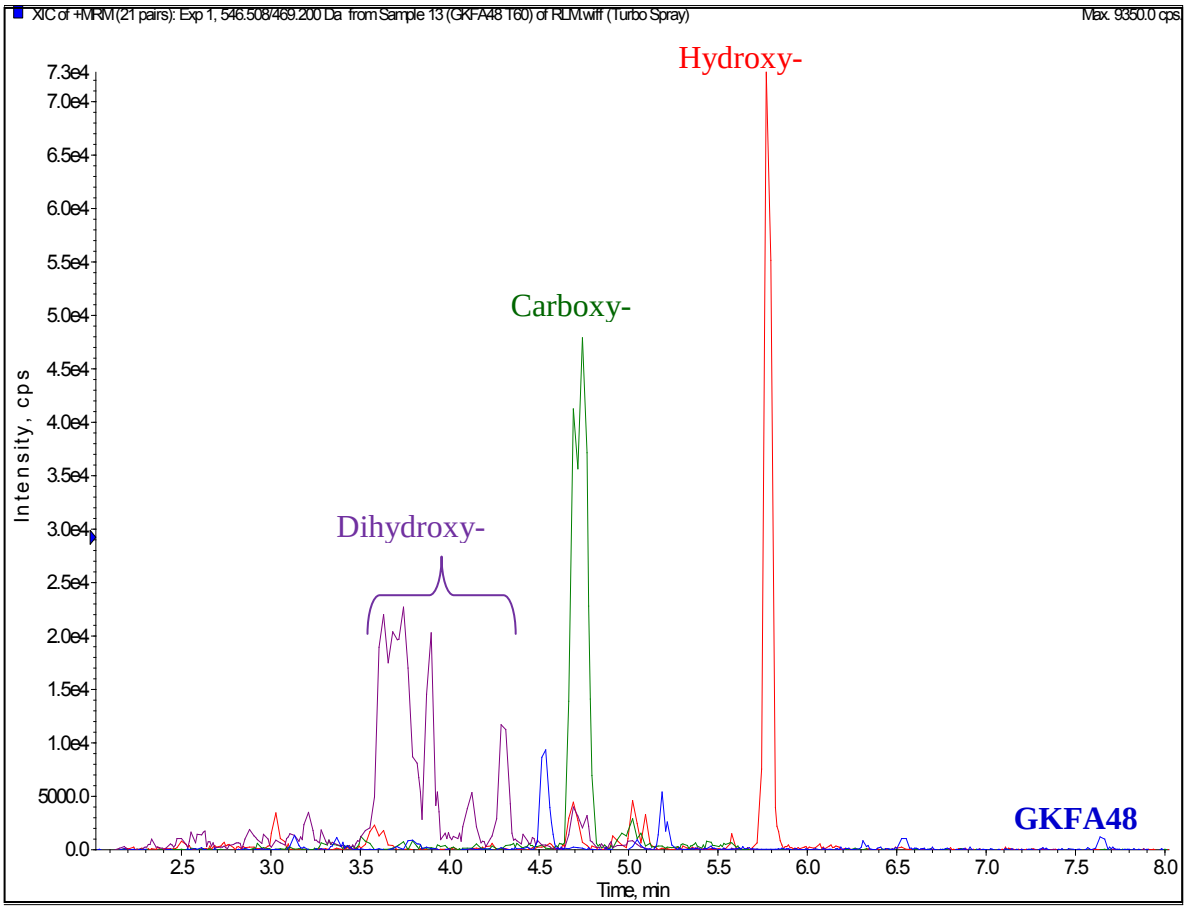

Figure 4.15: XICs of the RLM metabolites of **GKFA48**

An additional metabolite, whose ammonium adduct is 30Da higher than that of **GKFA48** is also observed. While the fact that this is 2Da lower than the dihydroxylation metabolite may suggest a keto- metabolite, the later elution relative to all the dihydroxylation metabolites is inconsistent with the observed pattern for the other fusidic acid derivatives where the keto- metabolites elute earlier than their respective parent compounds. In addition, the most common site of keto- formation, C-3, is already oxidised in this derivative. This metabolite is therefore proposed to be the carboxy- derivative of **GKFA48**.

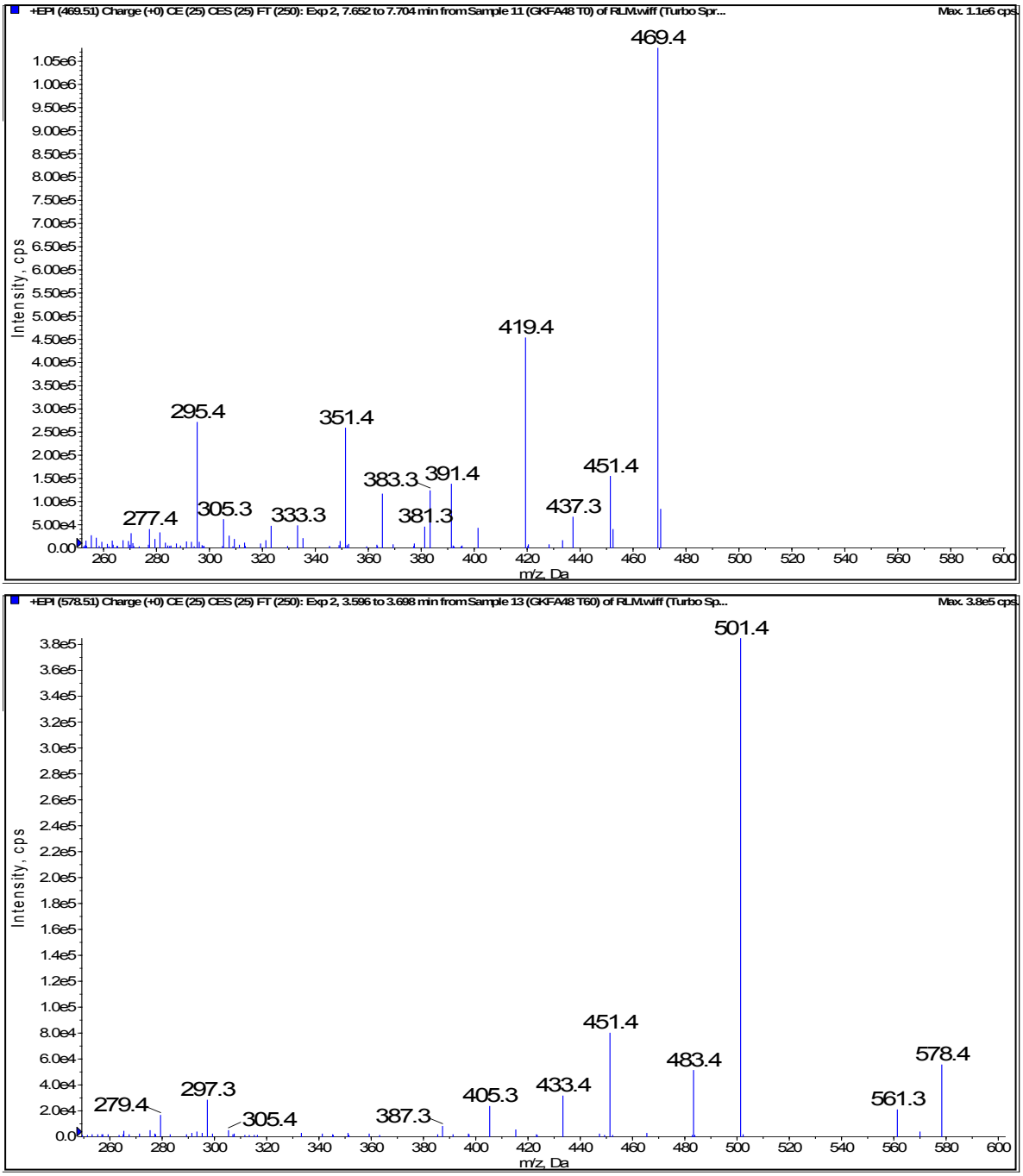

Figure 4.16: Enhanced product ion spectra of **GKFA48** and its carboxy- metabolite

While carboxyfusidic acid is reported as one of the *in vivo* metabolites of fusidic acid in man, it was not observed *in vitro* for fusidic acid and was only observed in incubations with **GKFA48** and **ME-81**.

The alkyl amides were detected as their M+H ions rather than as ammonium adducts observed with the previously discussed analogues. The precursor ions of the metabolites formed suggested hydroxylation and dehydrogenation (-2Da) metabolites.

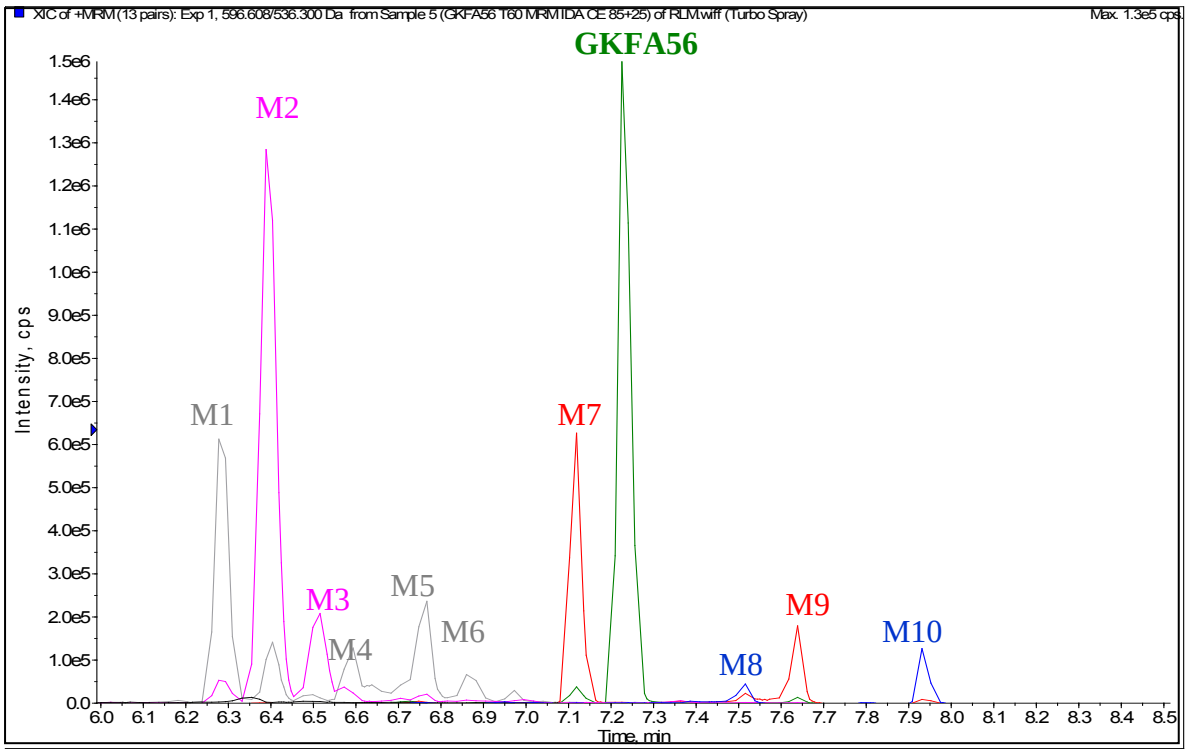

Figure 4.17: Extracted ion chromatograms of GKFA56 and its RLM metabolites

The tentative identification of the metabolites relied on the identification of the fragments resulting from the fusidane nucleus and those resulting from the amide substituent. This was more difficult to do for **GKFA52** and **-54** where the substituents were smaller and were generally not detected in the CID spectra. There was, however, some success with **GKFA56**. A higher collision energy (85V, compared 30 – 40V for other derivatives) was required to observe the fragment(s) resulting from the piperidinol substituent. A wide collision energy spread (25V) helped ensure that the low energy fragments were still observed. The main fragment observed from the piperidinol substituent was m/z 84, probably resulting from a loss of water following amide cleavage. This fragment was, however, not observed when metabolic transformation occurred on the piperidinol substituent but the site of metabolism

could be inferred from the mass changes (or lack thereof) on the fusidic acid core fragments.

A summary of the metabolites detected for **GKFA56** is presented in Table 4.5

Table 4.5: RLM metabolites of **GKFA56** and the tentative sites of metabolism

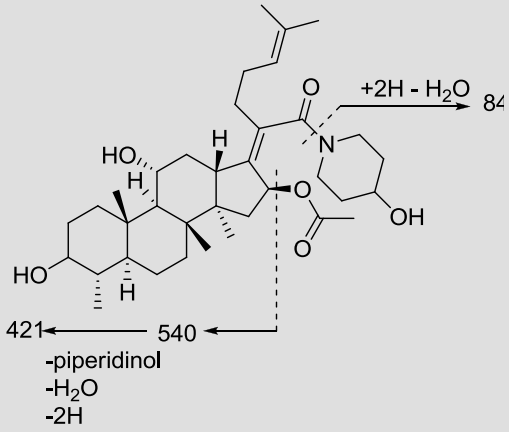

Code	m/z	Rt	$[M+H - OAC]^+$	421[a]	84[b]	Tentative identification
M1	614	6.28	554	435	84	Hydroxylation and -2H on fusidane core
M2	616	6.39	556	419[c]	84	Hydroxylation on fusidane core
M3	616	6.51	556	-	84	Hydroxylation on fusidane core
M4	614	6.59	554	-	-	Hydroxylation – 2H
M5	614	6.76	554	419	-	Hydroxylation on piperidinol, – 2H on fusidane,
M6	614	6.87	554	419	100	Hydroxylation on piperidinol, – 2H on fusidane,
M7	598	7.12	538	419	84	– 2H on fusidane
M8	596	7.52	536	419	-	– 2H on fusidane, -2H on piperidinol
M9	598	7.64	538	421	-	– 2H on piperidinol
M10	596	7.93	536	421	-	-4H on piperidinol
Parent	600	7.23	540	421	84	Parent

While it was not possible to process **GKFA54** and **GKFA52** metabolism to the same degree, the change in m/z of the metabolites relative to the respective parent compounds, (-4, -2, +14, +16) suggests a similar metabolic profile. The dehydrogenation site on the fusidane is most probably at C-3 to form the keto- metabolite. This is suggested by the retention time of M7 relative to the parent, which is consistent with the profile observed for the other 3-keto metabolites, for example for Fusidic acid (Figure 4.11) where the identity was confirmed with the authentic compound (**GKFA37**). This is in contrast to M9 which elutes after the parent, and for which the fragmentation data suggests dehydrogenation of the piperidinol. The site of dehydrogenation on the piperidinol is unclear from the data available, because of of its poor fragmentation, especially as alluded to earlier, when it undergoes any metabolic modification.

4.2.8 C-21 hydrazides

Table 4.6: The biological activity and stability of fusidic acid C-21 hydrazides

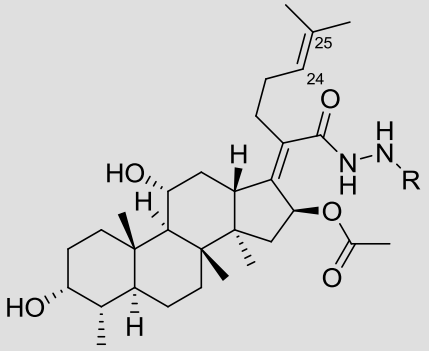

Code	R	*P.f* NF54[a] IC_{50} µM	*M.tb* H37Rv[b] MIC_{99} µM	% Remaining RLM[c]	% Remaining Plasma[d]	Log P
KSFA16	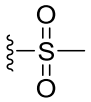	>10	10	34	>99	3.46
KSFA40	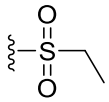	nd	40	20	>99	3.79
KSFA52[*]	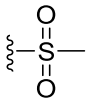	>10	10	39	>99	3.84
GKFA24	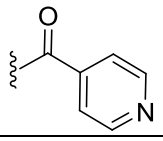	nd	10	84	>99	3.82

[*]24,25 double bond reduced.
[a]Drug sensitive strain of *Plasmodium falciparum*. [b]Drug sensitive strain of *Mycobacterium tuberculosis*.
[c] % remaining after 1hr incubation at 0.4mg/ml rat liver microsomes.
[d] % remaining after 3hrs incubation in rat plasma

The microsomal stability of the sulfonohydrazide derivatives was lower compared to the single carboxohydrazide (**GKFA24**) evaluated. The sulfonohydrazides underwent NADPH dependent cleavage of the linker to fusidic acid in the case of **KSFA16** and **-40** or to 24,24-dihydrofusidic acid in the case of **KSFA52**. The 3-keto derivative was also observed.

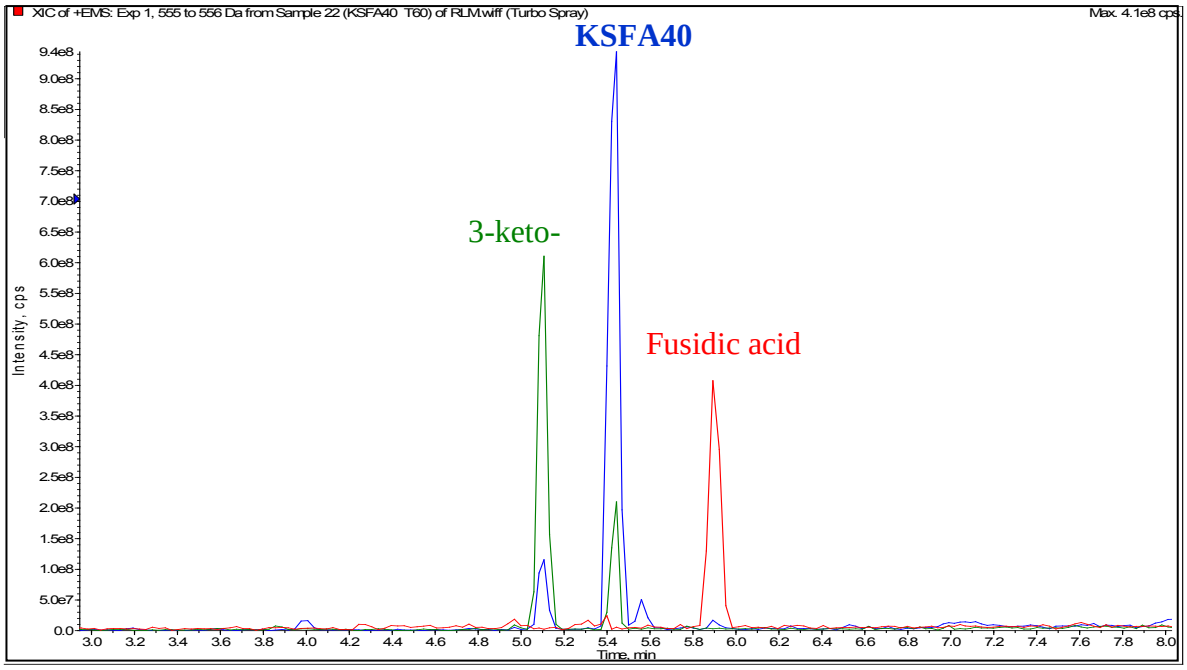

Figure 4.18: Extracted ion chromatogram of **KSFA40** and its RLM metabolites

Cleavage of the linker to release fusidic acid implies that the sulfonohydrazine group is also released. This could be considered a structural alert for these compounds since hydrazine derivatives are reported to mediate various organ toxicities through metabolic bioactivation to a variety of reactive intermediates which bind to biomolecules resulting in cell death or immune-mediated reactions.[23,24] These derivatives would therefore need to be evaluated further to investigate the possibility of their metabolic activation.

GKFA24 is basically an isoniazid-fusidic acid hybrid and isoniazid itself is implicated in hepatotoxicity following bioactivation. However, the microsomal metabolism of this compound (HLM, MLM, RLM) does not result in cleavage of this linker, as in the sulfohydrazides. Instead, just as with most of the fusidic acid derivatives discussed, the metabolites were tentatively identified as the 3-keto, 3-epi, and hydroxy- derivatives of the compound.

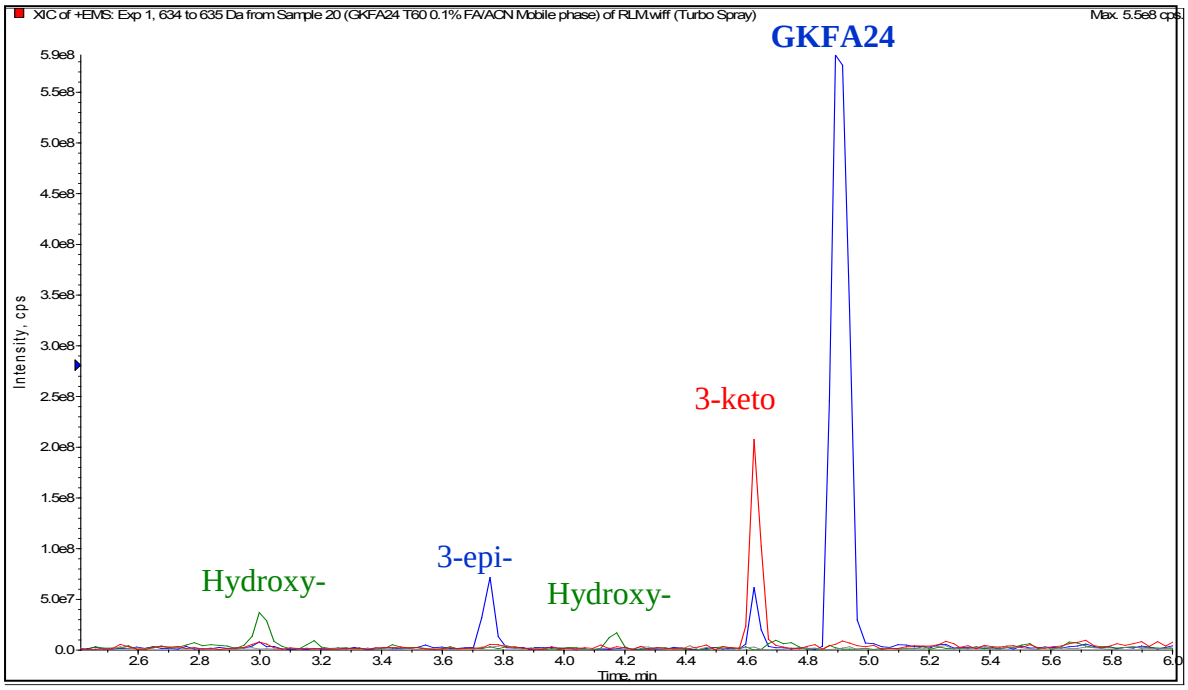

Figure 4.19: Extracted ion chromatogram of **GKFA24** and its RLM metabolites

4.3 *M. smegmatis* and *M. tb H37Rv* incubations

As has been alluded to in earlier sections, the 16-desacetyl derivative of fusidic acid and its lactone have much lower antibacterial activity compared to fusidic acid. Some *Nocardia* and *Streptomyces* species produce esterases that cleave this group and are consequently resistant to fusidic acid.[25,26]

Mycobacteria are reported to possess various hydrolases with activity against xenobiotics. Preliminary work was therefore perfomed to establish whether these have any activity towards fusidic acid. Incubations were performed with *M. smegmatis* lysate and the supernatant of *M. tuberculosis* H37Rv.

Under the conditions used, fusidic acid was stable in the buffer control and in the *M.tb* supernatant. However, its relative concentration reduced with time and the hydrolysis rate

could be described by (pseudo-)first order kinetics with a k of 3.8 x 10^{-3} min^{-1}, leading to a half-life of 182 min (± 20min).

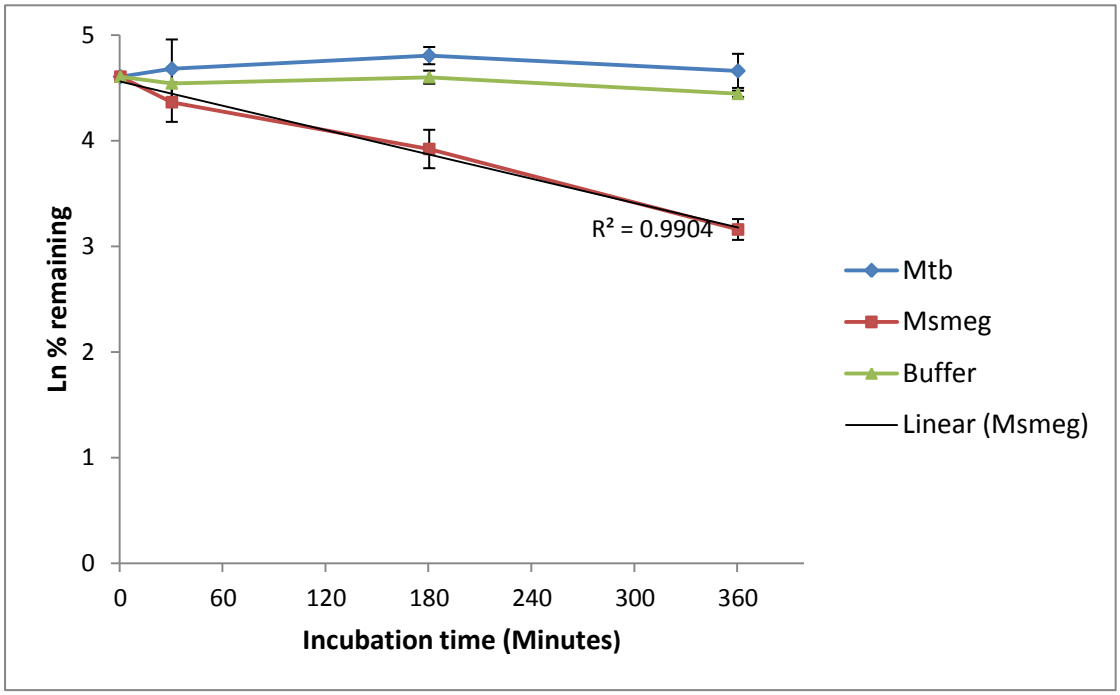

Figure 4.20: Stability of fusidic acid in incubations of *M. tb* supernatant, *M. Smeg* lysate and buffer control

In anticipation of the reported hydrolysis of fusidic acid in other bacteria, the MRM transitions of fusidic acid lactone were included in the analytical method, and this compound was detected in the *M. smegmatis* incubations but not in the *M. tb* or buffer control incubations. Its peak area increased with time and it was not formed in the absence of fusidic acid.

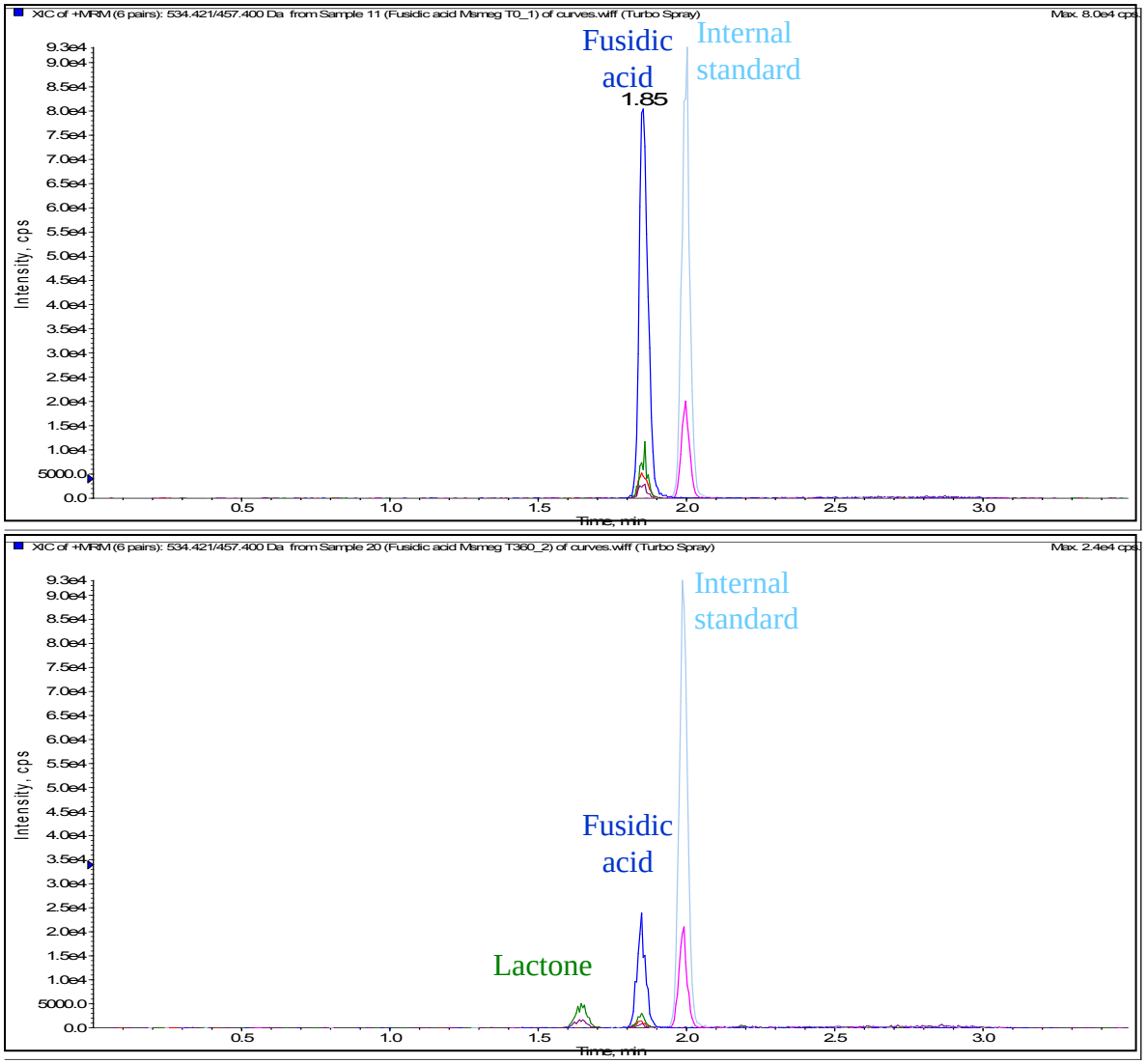

Figure 4.21: MRM total ion chromatogram of the T360min *M. smeg* incubation

This preliminary data shows that fusidic acid can undergo inactivation in the cytosol of *M. smegmatis* but is either not hydrolysed or is hydrolysed by a much slower process in *M. tb* H37Rv. It is of relevance to consider that *M. smegmatis* is a much faster growing organism than *M. tb* H37Rv and even a slow hydrolytic process may be of relevance to the longer compound incubation times in *M. tb* H37Rv. However, the fusidic acid is very active in *M.tb* (MIC_{99} < 0.1563µM) suggesting that the inactivation process is not of major significance to

this organism. This compares with a much higher MIC_{99} against *M. smegmatis* (≈ 40μM). While there are other biological differences between the two organisms that could contribute to this difference, the data presented show that the hydrolase activity is potentially one of the contributors.

16-Deacetylation was observed in all classes of derivatives presented but interestingly, was not observed at any other position in derivatives with hydrolysable groups. This implies that the hydrolases involved are specific for the 16- position in fusidic acid.

4.4 Discussion

The metabolism of fusidic acid in rat and mouse liver microsomes is different from the metabolism in human liver microsomes and from that reported in man. The main difference is in the formation of a metabolite tentatively identified as the C-3 epimer of fusidic acid. This metabolite was also observed in incubations of 3-ketofusidic acid, with the same species differences. It is proposed that this metabolite arises from fusidic acid by dehydrogenation at C-3 to form the 3-keto derivative, followed by the reverse reaction in a non-stereoselective way to produce both fusidic acid and 3-epifusidic acid. A similar mechanism has been proposed for another steroid cinobufagin.[27,28] Interestingly, C-3 epimerisation is also species specific in cinobufagin metabolism, with the 3-epi metabolite observed in rat (*in vitro* and *in vivo*) but not in the mouse or in man. The C-3 epimer was observed for most derivatives with a free C-3 OH and was only observed when the 3-keto metabolite was also present. While the clearance of fusidic acid is known to be faster in rodents than in man, there is no information to suggest that this is due to species specific metabolite pathways.[29] In addition, fusidic acid has been reported to autoinhibit its clearance at higher doses in man, through currently unelucidated mechanisms.[17,30,31] There is again no information on whether this autoinhibition is present in animal models and/or whether it contributes to the observed difference in

clearance. It will therefore be of interest as these derivatives are progressed to *in vivo* studies to see whether the 3-epi metabolite is observed and to assess its overall contribution to fusidic acid clearance in the animal models.

In plasma, fusidic acid was slowly hydrolysed to its lactone. This process was faster in rodent plasma but was unobserved in human plasma. Hydrolysis in plasma was additionally observed for the C-3 esters, which were hydrolysed to fusidic acid. The stability in plasma varied in the order, mouse>>rat>man which approximates the reported hydrolase activity of these species.[32] The hydrolytic activity is likely to be higher than reported here *in vivo* because of the contribution of esterases on red blood cells and leucocytes.[33]

C-3 ester derivatives were hydrolysed to fusidic acid in RLM, but this was not observed for the C-21 esters. Hydrolysis of the C-3 but not C-21 esters in RLM would appear to indicate carboxylesterase-2-like (CES-2) activity, as discussed in Chapter 1.[34] However, in rats, CES-2 is mostly located in the small intestines where it contributes to first pass metabolism, and is negligible in the rat liver.[35,36] It is more likely that the RLM hydrolysis of these compounds is by CES-1 esterases, which are known to catalyse the same reaction but at slower rates.[37] It has been reported that as CES-1 enzymes contribute as much as 95% of the carboxylesterase activity in the rat liver.[38] Hydrolysis should then be expected in C-21 derivatives, where there is the combination of a large acyl group (fusidane core) and small alcohol group, reported as the ideal substrate composition for CES-1.[39] However, even for compounds with comparatively small groups (e.g methyl **GKFA48**, ethyl **ME-81**) hydrolysis is not observed. Hydrolysis is also not observed at C-16 in microsomes of all species tested. This suggests that steric factors are at play, protecting these positions from hydrolytic activity. Metabolism at C-21 was only observed for the sulfonohydrazides which were metabolised to fusidic acid. However, this reaction was NADPH dependent.

C-16 hydrolysis was also observed in the *M. smegmatis* lysate but not in the *M.tb* H37Rv supernatant. The half-life of fusidic acid in the *M. smegmatis* lysate was about 3 hours. This observation is of interest because a similar phenotype in some *Nocardia* and *Streptomyces* species is associated with fusidic acid resistance. Mutant generation work is in progress for the larger fusidic acid project and it would be of interest to see whether this hydrolytic activity is observed in the fusidic acid resistant *M.tb* organisms generated.

A comparison of these experimentally observed metabolites with StarDrop predictions is complicated by the fact that unlike the compounds previously discussed, the fragmentation pathway is more ambiguous for fusidic acid complicating the identification of the sites of metabolism. Both C-27 (labelled as C33,34 in the StarDrop model) and C-3 were predicted by StarDrop as the main sites of metabolism by CYP3A4, 2D6, and 2C9, but also as the most inherently labile sites (CYP3A4). 27-carboxyfusidic acid and 3-ketofusidic acid are reported as metabolites of fusidic acid in man.[16,17]

CYP3A4 **CYP2D6** **CYP2C9**

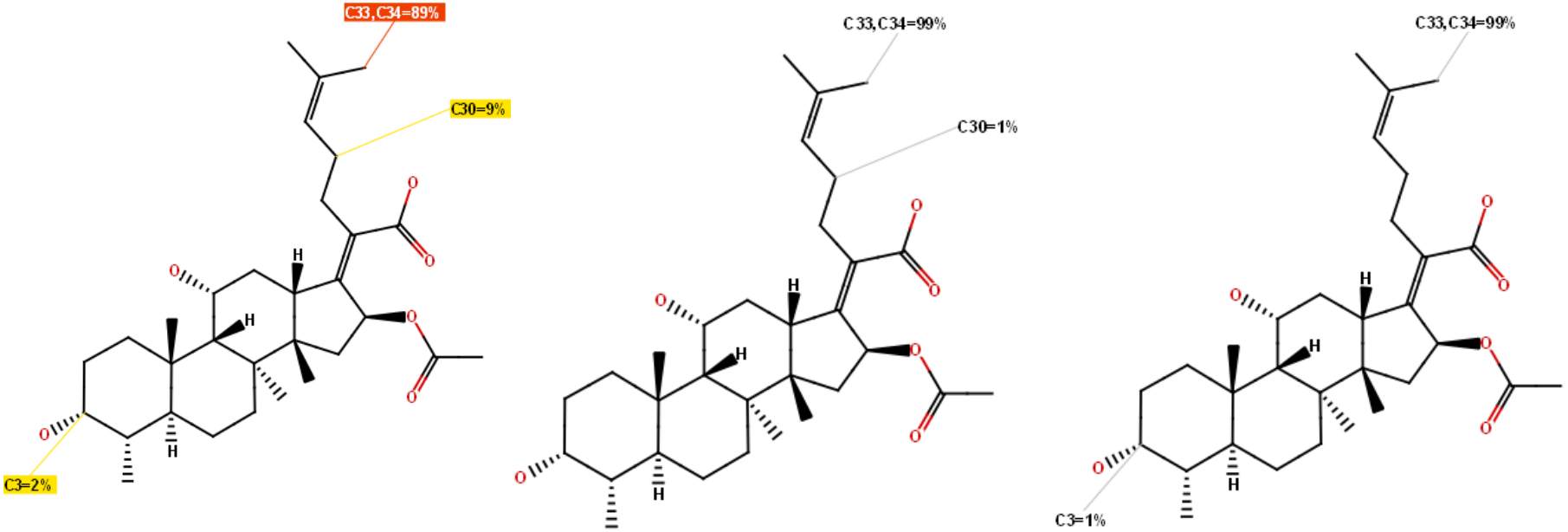

Figure 4.22: StarDrop predicted sites of metabolism for fusidic acid assuming metabolism by CYP3A4. (The percentages show the expected proportion of metabolites that would result from metabolism at the indicated position and the colors ndicate the lability of the positions; red – labile, yellow – moderately labile, green – moderately stable, blue – stable)

Finally, it is interesting to note that despite the close similarities between the physicochemical properties of fusidic acid and most of its metabolites, their biological activity is invariably lower than that of fusidic acid.

Table 4.7: Biological activity and physicochemical properties of fusidic acid and selected metabolites

Compound	*S. aureus* MIC_{50} [20]	*M.tb* MIC_{99}	LogP	LogD	TPSA
3-ketofusidic acid	0.622	1.25	4.39	1.56	101
Fusidic acid lactone	11.8	nd	4.35	4.35	67
3-epifusidic acid	12.2	nd	4.45	1.38	104
Fusidic acid glucuronide	17.3	nd	1.59	0.99	200
Fusidic acid	0.112	<0.156	4.45	1.38	104

This suggests that the structural characteristics required for binding to the target are very strict such that any modifications lead to loss of activity. Indeed, of all the structural analogues of fusidic acid synthesised, only 24,25-dihydrofusidic acid has antibacterial activity comparable to fusidic acid, with all others being less active. This is also illustrated by the fact that 3-epifusidic acid and fusidic acid glucuronide retain only 30 -40% of the activity of fusidic acid at the target[8]. It has been reported that 3-ketofusidic acid may accumulate in plasma to levels about 15% of the fusidic acid concentration and its Cmax is several times higher than its MIC against both *S. aureus* and *M.tb*.[17,40] Since this metabolite retains some of the activity of fusidic acid (against both *M. tb* and *S. aureus*) it would be expected to contribute to the *in vivo* activity of fusidic acid. While the properties of the glucuronide are

much more different compared to fusidic acid and the rest of the metabolites, it is notable that this metabolite retains activity against the target.[8] Therefore, if this metabolite could access the intracellular space, even through an active transport process, it could contribute to the activity of fusidic acid. However, the relevance of this metabolite is likely to be in maintaining fusidic acid levels through enterohepatic circulation. While no direct evidence of this has been shown, this metabolite is known to be cleavable in base and by β-glucuronidase.[16]

Finally, we have recently reported that drug metabolites may contribute to antimycobacterial activity when tested in combination with other antimycobacterials, even when their activity is lower than the parent drug.[41] Since antituberculosis regimens are invariably administered in combination, it would be of interest to investigate any synergism between these metabolites and other antimycobacterial compounds. This would be particularly interesting with 3-ketofusidic acid, whose levels in plasma are already established.

4.5 Summary

The microsomal and plasma metabolism of fusidic acid and its derivatives was evaluated. Fusidic acid was found to undergo species specific metabolism to a metabolite tentatively identified as 3-epifusidic acid. This metabolite was also found in all other derivatives with a free C3-OH and is hypothesised to result from oxidation at C-3 followed by non-stereoselective reduction to fusidic acid and 3-epifusidic acid. C-3 esters were metabolised almost exlusively by hydrolysis to fusidic acid. This process was observed in both microsomes and plasma and was faster in mouse plasma, compared to rat plasma and was hardly detectable in human plasma. Interestingly C-21 esters did not undergo hydrolysis to fusidic acid. The metabolism of the aryl esters paralleled that of fusidic acid and that of the alkyl esters involved multiple hydroxylations, including the formation of a metabolite tentatively identified as carboxyfusidic acid. The C-21 alkyl/cycloalkyl esters also underwent

multiple hydroxylations, both on the fusidic acid core and on the amide substituent. Among the hydrazides, metabolism was by NADPH dependent cleavage of the sulfonohydrazide linker to give fusidic acid. The isoniazid prodrug, however, underwent a different metabolic pathway that had more in common with that of fusidic acid. The 16-acetyl group of fusidic acid was cleaved in *M.smegmatis* but not *M. tb* H37Rv to give 16-deacetylfusidic acid and its lactone, both of which are reported to have less antibacterial activity compared to fusidic acid.

These data should be useful in the SAR expansion of fusidic acid and its derivatives.

4.6 References

(1) Godtfredsen, W. O.; Janhsen, S.; Lorck, H.; Roholt, K.; Tybring, L. Fusidic Acid: A New Antibiotic. *Nature* **1962**, *193*, 987.

(2) Perry, M. J.; Hendricks-Gittins, A.; Stacey, L. M.; Adlard, M. W.; Noble, W. C. Fusidane Antibiotics Produced by Dermatophytes. *J. Antibiot. (Tokyo).* **1983**, *36*, 1659–1663.

(3) Chain, E.; Florey, H. W.; Jennings, M. A.; Williams, T. I. Helvolic Acid, an Antibiotic Produced by Aspergillus Fumigatus, Mut. Helvola Yuill. *British Journal of Experimental Pathology*, 1943, *24*, 108.

(4) Burton, H. S.; Abraham, E. P. Isolation of Antibiotics from a Species of Cephalosporium; Cephalosporins P1, P2, P3, P4, and P5. *Biochem. J.* **1951**, *50*, 168–174.

(5) Kaise, H.; Munakata, K.; Sassa, T. Structures of Viridominic Acids A and B, New Chlorosis-Inducing Metabolites of a Fungus. *Tetrahedron Lett.* **1972**, *13*, 3789–3792.

(6) Godtfredsen, W. O.; Rastrup-Andersen, N.; Vangedal, S.; Ollis, W. D. Metabolites of Fusidium Coccineum. *Tetrahedron* **1979**, *35*, 2419–2431.

(7) Zhao, M.; Gödecke, T.; Gunn, J.; Duan, J.-A.; Che, C.-T. Protostane and Fusidane Triterpenes: A Mini-Review. *Molecules* **2013**, *18*, 4054–4080.

(8) Willie, G. R.; Richman, N.; Godtfredsen, W. O.; Bodley, J. W. Characteristics of and Structural Requirements for the Interaction of 24,25-Dihydrofusidic Acid with Ribosome Elongation Factor G Complexes. *Biochemistry* **1975**, *14*, 1713–1718.

(9) Okura, A.; Kinoshita, T.; Tanaka, N. Formation of Fusidic Acid-G Factor-GDP-Ribosome Complex and the Relationship to the Inhibition of GTP Hydrolysis. *J. Antibiot. (Tokyo).* **1971**, *24*, 655–661.

(10) Johnson, R. A.; Mcfadden, G. I.; Goodman, C. D. Characterization of Two Malaria Parasite Organelle Translation Elongation Factor G Proteins : The Likely Targets of the Anti-Malarial Fusidic Acid. **2011**, *6*.

(11) Hoffner, S. E.; Olsson-Liljequist, B.; Rydgård, K. J.; Svenson, S. B.; Källenius, G. Susceptibility of Mycobacteria to Fusidic Acid. *Eur. J. Clin. Microbiol. Infect. Dis.* **1990**, *9*, 294–297.

(12) Fuursted, K.; Askgaard, D.; Faber, V. Susceptibility of Strains of the Mycobacterium Tuberculosis Complex to Fusidic Acid. *APMIS* **1992**, *100*, 663–667.

(13) Cicek-Saydam, C.; Cavusoglu, C.; Burhanoglu, D.; Hilmioglu, S.; Ozkalay, N.; Bilgic, A. In Vitro Susceptibility of Mycobacterium Tuberculosis to Fusidic Acid. *Clin. Microbiol. Infect.* **2001**, *7*, 700–702.

(14) Kraus, C. N.; Burnstead, B. W. The Safety Record of Fusidic Acid in Non-US Markets: A Focus on Skin Infections. *Clin. Infect. Dis.* **2011**, *52 Suppl 7*, S527–37.

(15) Kigondu, E. M.; Wasuna, A.; Warner, D. F.; Chibale, K. Pharmacologically Active Metabolites, Combination Screening and Target Identification-Driven Drug Repositioning in Antituberculosis Drug Discovery. *Bioorg. Med. Chem.* **2014**.

(16) Godtfredsen, W. O.; Vangedal, S. On the Metabolism of Fusidic Acid in Man. *Acta Chem. Scand.* **1966**, *20*, 1599–1607.

(17) Turnidge, J. Fusidic Acid Pharmacology, Pharmacokinetics and Pharmacodynamics. *Int. J. Antimicrob. Agents* **1999**, *12 Suppl 2*, S23–34.

(18) Yang, X. J.; Qu, Y.; Yuan, Q.; Wan, P.; Du, Z.; Chen, D.; Wong, C. Effect of Ammonium on Liquid- and Gas-Phase Protonation and Deprotonation in Electrospray Ionization Mass Spectrometry. *Analyst* **2013**, *138*, 659–665.

(19) Mortier, K. A.; Zhang, G.-F.; van Peteghem, C. H.; Lambert, W. E. Adduct Formation in Quantitative Bioanalysis: Effect of Ionization Conditions on Paclitaxel. *J. Am. Soc. Mass Spectrom.* **2004**, *15*, 585–592.

(20) Godtfredsen, W. O.; Von Daehne, W.; Tybring, L.; Vangedal, S. Fusidic Acid Derivatives. I. Relationship between Structure and Antibacterial Activity. *J. Med. Chem.* **1966**, *9*, 15–22.

(21) Ma, X.-C.; Cui, J.; Zheng, J.; Guo, D.-A. Microbial Transformation of Three Bufadienolides by Penicillium Aurantigriseum and Its Application for Metabolite Identification in Rat. *J. Mol. Catal. B Enzym.* **2007**, *48*, 42–50.

(22) Pereira, D. E. Patent WO2012162439 A2 Compositions Comprising Fusidic Acid and Packages Therefor. WO2012162439 A2, November 29, 2012.

(23) Metushi, I. G.; Nakagawa, T.; Uetrecht, J. Direct Oxidation and Covalent Binding of Isoniazid to Rodent Liver and Human Hepatic Microsomes: Humans Are More like Mice than Rats. *Chem. Res. Toxicol.* **2012**, *25*, 2567–2576.

(24) Sinha, B.; Mason, R. Biotransformation of Hydrazine Dervatives in the Mechanism of Toxicity. *J Drug Metab Toxicol* **2014**, *5*, 30–31.

(25) Von Der Haar, B.; Schrempf, H. Purification and Characterization of a Novel Extracellular Streptomyces Lividans 66 Enzyme Inactivating Fusidic Acid. *J. Bacteriol.* **1995**, *177*, 152–155.

(26) Harada, K.; Tomita, K.; Fujii, K.; Sato, N.; Uchida, H.; Yazawa, K.; Mikami, Y. Inactivation of Fusidic Acid by Pathogenic Nocardia. *J. Antibiot. (Tokyo).* **1999**, *52*, 335–339.

(27) Ma, X.; Ning, J.; Ge, G.; Liang, S.; Wang, X.; Zhang, B.; Huang, S.; Li, J.; Yang, L. Comparative Metabolism of Cinobufagin in Liver Microsomes from Mouse, Rat, Dog, Minipig, Monkey, and Human. *Drug Metab. Dispos.* **2011**, *39*, 675–682.

(28) Zhang, J.; Sun, Y.; Liu, J.; Yu, B.; Xu, Q. Microbial Transformation of Three Bufadienolides by Nocardia Sp. and Some Insight for the Cytotoxic Structure-Activity Relationship (SAR). *Bioorg. Med. Chem. Lett.* **2007**, *17*, 6062–6065.

(29) Degenhardt, T. P.; Still, J. G.; Clark, K.; Fernandes, P. From Mouse to Man□: the Pharmacokinetics of CEM-102 (Fusidic acid) http://www.cempra.com/common/pdf/abstracts/From Mouse to Man-The Pharmacokinetics of CEM-102.pdf (accessed Jun 12, 2014).

(30) Tsuji, B. T.; Okusanya, O. O.; Bulitta, J. B.; Forrest, A.; Bhavnani, S. M.; Fernandez, P. B.; Ambrose, P. G. Application of Pharmacokinetic-Pharmacodynamic Modeling and the Justification of a Novel Fusidic Acid Dosing Regimen: Raising Lazarus from the Dead. *Clin. Infect. Dis.* **2011**, *52 Suppl 7*, S513–9.

(31) Bulitta, J. B.; Okusanya, O. O.; Forrest, A.; Bhavnani, S. M.; Clark, K.; Still, J. G.; Fernandes, P.; Ambrose, P. G. Population Pharmacokinetics of Fusidic Acid: Rationale for Front-Loaded Dosing Regimens due to Autoinhibition of Clearance. *Antimicrob. Agents Chemother.* **2013**, *57*, 498–507.

(32) Rudakova, E. V.; Boltneva, N. P.; Makhaeva, G. F. Comparative Analysis of Esterase Activities of Human, Mouse, and Rat Blood. *Bull. Exp. Biol. Med.* **2011**, *152*, 73–75.

(33) Cossum, P. A. Role of the Red Blood Cell in Drug Metabolism. *Biopharm. Drug Dispos.* **1988**, *9*, 321–336.

(34) Hosokawa, M. Structure and Catalytic Properties of Carboxylesterase Isozymes Involved in Metabolic Activation of Prodrugs. *Molecules* **2008**, *13*, 412–431.

(35) Masaki, K.; Hashimoto, M.; Imai, T. Intestinal First-Pass Metabolism via Carboxylesterase in Rat Jejunum and Ileum. *Drug Metab. Dispos.* **2007**, *35*, 1089–1095.

(36) Taketani, M.; Shii, M.; Ohura, K.; Ninomiya, S.; Imai, T. Carboxylesterase in the Liver and Small Intestine of Experimental Animals and Human. *Life Sci.* **2007**, *81*, 924–932.

(37) Imai, T.; Taketani, M.; Shii, M.; Hosokawa, M.; Chiba, K. Substrate Specificity of Carboxylesterase Isozymes and Their Contribution to Hydrolase Activity in Human Liver and Small Intestine. *Drug Metab. Dispos.* **2006**, *34*, 1734–1741.

(38) Sanghani, S. P.; Davis, W. I.; Dumaual, N. G.; Mahrenholz, A.; Bosron, W. F. Identification of Microsomal Rat Liver Carboxylesterases and Their Activity with Retinyl Palmitate. *Eur. J. Biochem.* **2002**, *269*, 4387–4398.

(39) Imai, T. Human Carboxylesterase Isozymes: Catalytic Properties and Rational Drug Design. *Drug Metab. Pharmacokinet.* **2006**, *21*, 173–185.

(40) Peter, J.; Pottecher, T.; Dupeyron, J.; Monteil, H.; Al, P. E. T. Pharmacokinetics of Intravenous Fusidic Acid in Patients with Cholestasis. **1993**, *37*, 501–506.

(41) Kigondu, E. M.; Njoroge, M.; Singh, K.; Njuguna, N.; Warner, D. F.; Chibale, K. Synthesis and Synergistic Antimycobacterial Screening of Chlorpromazine and Its Metabolites. *Medchemcomm* **2014**, *5*, 502.

Chapter 5

SUMMARY, CONCLUSIONS AND RECOMMENDATIONS FOR FUTURE WORK

5.1 Summary and conclusions

The broad aim of this work was to investigate the *in vitro* metabolism of tetrazole aminoquinolines, and derivatives of metergoline and fusidic acid. This work was carried out as part of medicinal chemistry exploration of these compounds as antiplasmodial and/or antimycobacterial agents.

The tetrazole deoxyamodiaquines with the best biological activity were also the most metabolically unstable. *In vitro* metabolite identification work in microsomes and hepatocytes showed that the metabolism occurred exclusively on the tertiary nitrogen substituent. Compounds with simple alkyl substituents were metabolised by *N*-dealkylation while those with cycloalkyl substituents were metabolised by multiple oxidations on the cycloalkyl ring. The latter derivatives also formed cyanide adducts implying that their metabolism follows the classical cycloalkylamine metabolic pathway involving iminium ion formation followed by α-hydroxylation on the cycloalkylamine. Compounds lacking a *tert*-butyl substitution on the tetrazole were more metabolically stable but also had lower biological activity. However, the tetrazole deoxyamodiaquines did not form glutathione adducts as reported for amodiaquine. This finding was expected because, as discussed in Chapter 2, glutathione adducts of amodiaquine are formed following formation of the reactive quinoneimine metabolite, which then reacts with glutathione (See Figure 2.1). These compounds are deoxyamodiaquines – in which the 4'-hydroxyl group required for

bioactivation is absent. Moreover, the phenyl ring is not a site of metabolism, and these compounds would therefore not be expected to form glutathione adducts.

StarDrop correctly predicted the top site of metabolism for both **TK2** and **TK3**. However, it also predicted the 8- position on the aminoquinoline ring as a site of metabolism – this was not observed experimentally. These compounds were also potent CYP450 inhibitors – **TK2** and **TK3** showed potent inhibition of CYP2C8 and CYP3A4 and moderate inhibition of most other CYP450s. Only CYP1A2 and CYP2E1 were not inhibited. Docking experiments with CYP3A4 suggest that these compounds orient in differently in the active site leading to stronger interactions, as suggested by their binding energies which are lower compared to amodiaquine.

The tetrazole chloroquines were in general less metabolically stable than chloroquine. Unlike the tetrazole deoxyamodiaquines, the *tert*-butyl substitution was one of the sites of metabolism in these compounds, with *N*-oxidation and hydroxylation of the aminouinoline ring also occurring. In **TK900A** and **TK900C** the aromatic ring on the tertiary nitrogen was also a site of metabolism. A glutathione adduct formed on the aminoquinoline ring was also observed, possibly because the aminoquinoline ring can be regarded as a masked aniline leading to formation of a reactive iminoquinone metabolite if the ring is appropriately hydroxylated. All sites of metabolism for these compounds were correctly predicted in StarDrop. While the CYP450 inhibition profile of the tetrazole chloroquines was better compared to that of the tetrazole deoxyamodiaquines, these compounds displayed sub-micromolar inhibition of CYP3A4. This inhibition was not time dependent. The docked conformations of these compounds suggest that, just like with the tetrazole aminoquinolines, they orient differently in the active site of CYP3A4 leading to more efficient interactions and lower binding energies.

Metergoline was metabolised mainly by hydroxylation on the ergoline nucleus in contrast to its metabolism *in vivo* where 1-demethylation is the main metabolite. Two demethylation products on the ergoline nucleus, presumably corresponding to the 1-demethylation and 6-demethylation metabolite were also observed, together with 1,6-dimethyl-8-β-aminomethylergoline, the carbamate hydrolysis metabolite. A hydroxylation metabolite on the benzyl substituent was observed only in mouse liver microsome incubations. The metergoline derivatives were in general metabolised in a similar way. A major exception was the absence of 1,6-dimethyl-8-β-aminomethylergoline, indicating the improved stability to metabolic hydrolysis of the amide compared to the carbamate linker. Derivatives with alkyl substituents longer than ethyl also underwent alkyl hydroxylations (e.g **FRM007** and **GKMG14**). Where the alkyl substituent was on a phenyl ring, as in the case of **FRM007**, hydroxylation of the benzyl –CH2 was also observed . StarDrop correctly predicted all of the major metabolites. In the case of metergoline where hydroxylation was observed on the benzyl group, StarDrop predicts that the benzyl –CH2 is metabolically labile and as the major site of metabolism by CYP2D6.

Fusidic acid underwent species specific metabolism in rat and mouse liver microsomes to give a metabolite tentatively identified as 3-epifusidic acid. This metabolite was formed in all derivatives with a free C-3 OH and in 3-ketofusidic acid and is hypothesised to form following metabolism at this position to form the C-3 keto which is then reduced in a non-stereospecific manner to give fusidic acid and 3-epifusidic acid. Fusidic acid was also metabolised to give 3-ketofusidic acid and a hydroxylation derivative. C-3, but not C-21, esters were hydrolysed to fusidic acid in both microsomes and plasma. In plasma, the rate of hydrolysis of the C-3 derivatives varied in the order mouse plasma>>rat plasma>human plasma. The acetyl group at C-16 was also hydrolysed in plasma in fusidic acid and its derivatives but at a much slower rate. This group was also hydrolysed in a lysate of *M.*

smegmatis but not *M. tuberculosis* H37Rv leading to formation of fusidic acid lactone. This process may contribute to the higher MIC_{99} of fusidic acid in *M. smegamtis* compared to *M. tuberculosis* H37Rv.

5.2 Recommendations for future work

In considering the work that could be performed to improve the metabolic stability issues identified with these derivatives, it is important to remember that most of these derivatives were synthesised as part of exploratory work into their antiplasmodial and/or antimycobacterial activity. This explains why most of the analogues were broadly similar and were generally derived from chemistry at one position. In general therefore, where the exploratory work yielded derivatives with good antiplasmodial and/or antimycobacterial activity, a more systematic medicinal chemistry campaign should yield a wider variety of derivatives which may allow the projects to progress to later drug discovery phases. However, the fact that metabolic liabilities were identifiable even at this stage, shows the value of early incorporation of drug metabolism work. The knowledge of the sites of metabolism gleaned during this exploratory work would be useful in the later, more systematic medicinal chemistry campaign.

While the most active tetrazole deoxyamodiaquines were also metabolically unstable, it is notable that no glutathione adducts were detected. This implies that appropriately substituted deoxyamodiaquine derivatives can give good antiplasmodial activity while avoiding the metabolic bioactivation reported for amodiaquine. This finding could be explored with other deoxyamodiaquine derivatives to give the optimal balance between activity, metabolic stability and toxicity.

The tetrazole chloroquines were found to be less metabolically stable than chloroquine itself and their *in vivo* activity was hypothesised to be subject to dose limited absorption. The

toxicity of chloroquine has been associated with its long half-life and less metabolically stable analogues are therefore not a disadvantage per se. More important will be the balance between *in vivo* activity and duration of action. Further medicinal chemistry work could focus on obtaining more water soluble derivatives to get better absorption. In addition, the increase in polarity would have effects on the metabolic stability and on reactive metabolite formation. Different formulations of the current derivatives could also be explored.

Metergoline and its analogues, in general, displayed low (>10μM) antimycobacterial activity, but the antiplasmodial activity of a number of derivatives would be worth exploring further, especially because most derivatives are more metabolically stable than metergoline. It was observed that metergoline was metabolised in microsomes to its 12-hydroxy derivative as the major metabolite, while 1-demethylation is reported to be the major metabolite *in vivo*. This difference would be interesting to explore with more active derivatives. Investigations could involve CYP450 phenotyping with microsomes and recombinant CYP450s to identify the main enzymes involved in formation of these metabolites. It would also be of interest to assess the contribution of gut wall metabolism to the formation of the metabolites, possibly by using intestinal microsomes and/or S9. These findings would be useful in predicting the contribution of metabolites to *in vivo* activity.

The preliminary data on the *in vitro* metabolism of fusidic acid raises a number of questions that are worth exploring as the project proceeds. First, the species specific metabolism of fusidic acid to 3-epifusidic acid, observed in mouse and rat liver microsomes, would be worth exploring *in vivo* because fusidic acid is known to have a shorter half-life in these species relative to man. Another possible contributor to the difference in clearance could be the difference in esterase activity in cleavage of the 16-acetyl group. While this pathway did not significantly contribute to *in vitro* clearance (in both microsomes and plasma), the *in vivo* environment has additional enzymes that could contribute to the hydrolysis of this group,

notably hydrolases in the wall of the small intestines and on the surface of red blood cells. These processes would need to be explored if fusidic acid lactone, the product of the 16-acetyl hydrolysis, is observed as a major metabolite *in vivo*. This could be performed using intestinal microsomes and fresh blood respectively. The difference in glucuronidation kinetics is also a possible reason for the difference in clearance if it is assumed that fusidic acid undergoes enterohepatic circulation. These hypotheses should be explored to enable a proper understanding of the difference in clearance in animal models relative to man, which would allow progression of fusidic acid derivatives through the drug discovery chain. Finally, the hydrolysis of fusidic acid in *M. smegmatis* but not *M. tuberculosis* H37Rv would be interesting to follow up. As discussed, this process is associated with fusidic acid resitance in certain species of *Nocardia* and *Streptomyces*. It would, therefore, be of interest to investigate the hydrolytic activity of fusidic acid resistant mutants of *M. tuberculosis*, in order to characterise the contribution, if any, of the hydrolytic process to the resistance phenotype.

Chapter 6

EXPERIMENTAL

6.1 Reagents and solvents

Microsomal preparations (Human, Rat, Mouse) were purchased from XenoTech (Kansas, USA) through their African distributor, African Institute of Biomedical Sciences and Technology (Harare, Zimbabwe). The human liver microsomal preparations were pooled (50 individuals) mixed gender, and the rat liver microsomes were from male IGS rats (pool of 433), while the mouse liver microsomes were from male BALB/c mice (pool of 800). All microsomal preparations were provided as 20mg/ml suspensions transported in liquid nitrogen and were stored at -80°C until use. Each individual vial was used for a maximum of three times, to eliminate any variation due to freeze-thaw stability. NADPH (as β-Nicotinamide adenine dinucleotide 2′-phosphate reduced tetrasodium salt hydrate) was purchased from Merck (Johannesburg, South Africa) and was divided to 5 -10mg aliquots and stored at -80°C until use. Reduced L-glutathione, UDPGA (as Uridine 5′-diphosphoglucuronic acid trisodium salt) and potassium cyanide were purchased from Sigma-Aldrich (Johannesburg, South Africa).

All solvents and additives for chromatography work were purchased from Merck (Johannesburg, South Africa) or from Sigma-Aldrich (Johannesburg, South Africa) and were of at least HPLC grade. Deionised water (18Ω) for buffer preparation and HPLC mobile phases was collected from a Millipore Synergy water purification system (Microsep, Tygervalley, South Africa).

A different set of reagents and solvents was used for the hepatocyte incubations and for the CYP450 inhibition experiments as outlined in the relevant sections.

6.2 Instrumentation

Except where otherwise indicated, all LC-MS analysis was performed on an Agilent 1200 Rapid Resolution (600 bar) HPLC system consisting of a binary pump, degasser, auto sampler and temperature controlled column compartment coupled to an AB SCIEX 4000 QTRAP mass spectrometer. Analyst (vl.4, 1.5, 1.6, AbSciex, Johannesburg, South Africa) was used for LC-MS control and data acquisition.

6.3 Compounds for analysis

The procedures and data for synthesis, characterisation and biological evaluation of the aminoquinoline tetrazoles (Chapter 2), and the metergoline analogues (Chapter 3) have already been published.[1–3] Synthetic procedures and data for the fusidic acid analogues will appear in publication soon (Kawaljit Singh, Marlene Espinoza, Gurminder Singh *et al*., manuscript in preparation). Metergoline HCl, Chloroquine diphosphate and Amodiaquine HCl were purchased from Sigma-Aldrich (Johannesburg, South Africa) while fusidic acid was purchased from Avachem Scientific (Texas, USA).

All compounds were received as dry powders and were reconstituted in DMSO (HPLC grade, Sigma-Aldrich, Johannesburg, South Africa) as 10mM stocks and frozen at -80°C until required for the assays, when they were thawed at room temperature.

6.4 Mass spectrometry conditions

Purified air was used as the nebuliser gas (gas 1) and heater gas (gas 2) and both were in general set to 50psi and 60psi respectively. Curtain gas (N_2) was generally set at 30psi and collision gas (N_2) was set to ‘medium’ for MRM experiments and ‘high’ for EMS IDA experiments. In general, ionspray voltage was set at 5000V and source temperature at 500°C. Compound dependent parameters were optimised by infusing at 10µl/min, a 50nM (aminoquinoline tetrazoles, metergoline derivatives) or 500nM (fusidic acid analogues)

solution of the compound in 50% mobile phase A/B. No further optimisation was required for the aminoquinoline tetrazoles and the metergoline derivatives. For the fusidic acid analogues, significant source fragmentation was observed and flow injection analysis (FIA) experiments were set up to optimise all source parameters. The parameters used for a representative compound in each of the classes analysed for this work is provided in Table 5.1.

Table 6.1: MS source parameters for representative compounds

	TK3	TK900E	Metergoline	Fusidic acid
Curtain gas (psi)	30	30	30	40
Ionspray voltage (V)	5000	5000	5000	5000
Source temperature	500	500	500	350
Gas 1 (psi)	50	50	50	40
Gas 2 (psi)	60	60	60	40

6.5 Chromatography

The mobile phase for the work in Chapter 2 and 3 was 0.1% formic acid containing 5% Acetonitrile (A) and Acetonitrile with 0.1% formic acid (B). Because of the need to use ammonium adducts for the identification and quantitation of the fusidic acid analogues, the mobile phase used was 5mM ammonium formate containing 5% acetonitrile (A) and 5mM ammonium formate in 95% acetonitrile (B).

The column used for the metabolic stability work was a Kinetex C18 2.1mm x 50mm, with 2.6µM particles, while a Kinetex C18 2.1mm x 150mm, with 2.6µM was used for the metabolite identification work.

The mobile phase flow rate was 500µl/min and the run time was 3 minutes for metabolic stability methods and 400µl/min with a run time of 15 minutes for metabolite identification methods.

The general gradient used for the stability assays in Chapter 2 and 3 is provided in Table 6.1 while that for the fusidic acid analogues is shown in Table 6.2. Modifications were only made when the compound of interest co-eluted with the internal standard.

Table 6.2: General gradient for metabolic stability work in Chapter 2 and 3

Time	% B
0	10
1.4	90
1.58	90
1.60	10
3.00	10

Table 6.3: General gradient for metabolic stability work in Chapter 4

Time	% B
0	40
1.5	100
2.08	100
2.1	40
3.5	40

The gradients for the metabolite identification work were similar in nature but as alluded to, the run time and flow rate were different. In general, the gradient above was ramped up over 9 min, held at the highest % B for 3 min and then immediately lowered for re-equilibration over the last 3minutes. Because of the qualitative nature of this work and the ability of the 4000Q to give detailed spectra even for co-eluting metabolites, no detailed chromatography

method development work was performed other than to check that the compounds did not elute too early or too late (first or last 4 minutes in the 15 minute ran) in the gradient.

6.6 Metabolic stability experiments

The microsomal stability of the test compounds was evaluated using a single point metabolic stability assay.[4] Incubation mixtures contained microsomes and 1µM compound in 0.1M phosphate buffer and were pre-incubated at 37°C for 3 minutes. The reactions were started by adding 1mM NADPH and were incubated at 37°C for 30min in the case of the compounds in Chapter 2 and 3, and 60 minutes for the fusidic acid derivatives in Chapter 4. Ice-cold acetonitrile (-20°C) containing the internal standard was added to stop the reaction at T0 (before addition of NADPH) and at T30 min. The samples were then centrifuged at 4°C, 4000g for 30minutes and then filtered through a 0.2µM polyvinylidene difluoride (PVDF) filter. The decrease in parent concentration was monitored using MRM methods. Data were processed on Analyst v1.5 and analysed on Microsoft Excel 2007.

6.7 Plasma stability

Human, rat and mouse plasma was provided courtesy of the Division of Pharmacology, University of Cape Town. The procedure for this assay broadly was based on the optimised parameters suggested by Di et al.[5] Compounds were tested at 1µM in a 50% dilution of plasma in Phosphate buffered saline (0.1M, PBS pH 7.4) and the negative controls in PBS only. Incubations were performed at 37°C for 3 hours and stopped by addition of ice cold acetonitrile containing the internal standard. The processing and analysis was then carried out as for metabolic stability above. Albendazole and Benfluorex were used as positive controls.[5]

6.8 *Mycobacterium smegmatis* and *Mycobacterium tuberculosis* lysate hydrolysis experiments

The *Mycobacterium smegmatis* mc^2155 lysate and the *Mycobacterium tuberculosis* H37Rv supernatant were provided courtesy of the Molecular Mycobacteriology Research Unit, Institute of Infectious Disease and Molecular Medicine, University of Cape Town. The lysate was prepared according to a previously published procedure.[6] Because of the biological hazard associated with *M.tb*, the procedure above was modified to include a centrifugation step at the end, followed by filtration through a 0.2µM membrane to ensure that no intact cells would end up in the supernatant. This preparative work was carried out in a Biosafety Level 3 (BSL3) lab. The analytical work could, however, be safely performed in an ordinary analytical lab (BSL1/2).

Benfluorex, which was used as a positive control for plasma stability, was used here to confirm the hydrolytic ability of the *M.smeg* lysate and *M.tb* supernatant.

The fusidic acid experiments involved a 20-fold dilution of the lysate/supernatant in 0.1M phosphate buffered saline, pH 7.4 (PBS) mixed with 1µM of fusidic acid and incubated at 37°C. Aliquots of the reaction were stopped at 0, 30, 180 and 360min with acetonitrile containing an internal standard, as discussed in the metabolic stability work. The rest of the procedure including the instrumental and data analysis are also as discussed under metabolic stability.

6.9 Microsomal metabolite identification experiments

6.9.1 Incubations

The test compound (10 μM) was incubated at 37 °C with 1mg/ml microsomes (human, rat or mouse) in phosphate buffer (100 mM, pH 7.4) which contained magnesium chloride (5 mM). Reactions were started after a 5 minute pre-incubation by adding 1mM NADPH (1 mM) and were incubated with shaking in a water bath at 37°C for 1 hour. An equal volume of ice cold acetonitrile was added to stop the reaction and to precipitate the proteins. After centrifuging the mixture at 14000 rpm for 30 minutes the supernatant was transferred to a HPLC vial. Control samples with no NADPH, no microsomes and a T0 sample were also included and processed in a similar way to the samples.

Where necessary, Glutathione (5mM), UDPGA (7.5 mM) or potassium cyanide (1mM) were added before the pre-incubation and the necessary controls included.

6.9.2 LC-MS analysis

The LC-MS method was created using Lightsight v2.1 which relied on Analyst method files created during direct infusion of the compounds.[7] The methods generally consisted of survey scans were coupled through information dependent acquisition to enhanced product ion scans. For all compounds, a method with an enhanced mass spectrum scan coupled to an enhanced product ion scan (EMS-IDA-EPI) was used as the method for the primary data acquisition and subsequently, MRM, neutral loss, or precursor ion scans, with or without dependent EPI scans were used to get more data on the metabolites. The scan range was selected to include the masses of the expected metabolites and their common adducts, and also such that the cycle time of the method did not significantly exceed 1s. The collision energy and collision energy spread were suggested by Lightsight based on the optimised collision energy of the ions selected during direct infusion. This tended to be optimal for most

compounds but was adjusted as necessary, depending on the fragment ions required for tentative metabolite identification.

6.9.3 Data analysis

Metabolites formed in the incubations were identified by comparison of their respective chromatograms with chromatograms at T0, in the control without NADPH or in the buffer only control using Lightsight. The type of metabolites formed were deduced from the mass shift of their $[M+H]^+$ ions relative to the parent. Tentative identification of the site of metabolism was determined by comparison of the product ion spectra of the parent and the metabolite. Neutral loss and precursor fragment ion filtering was also performed, post-acquisition, using the IDATraceExtractor script in Analyst 1.5 using precursor ions or neutral losses common to the metabolites and their respective parents.[8]

6.10 Hepatocyte metabolite identification experiments for tetrazole aminoquinolines

Cryopreserved hepatocytes were thawed and viable cells enriched by centrifugation in the presence of percoll (GE Healthcare biosciences, Uppsala, Sweden) according to the supplier's instructions. The cells were resuspended in HepatoZYME culture medium (Gibco Invitrogen, Carlsbad, USA) and their viability determined using a Guava EasyCyte Minisystem Viacount assay, as described by the supplier. The cells were diluted to $1x10^6$ viable cells/ml with HepatoZYME and aliquoted into 500µl portions for the reactions. The test compounds were added to a final concentration of 5µM, with 0.1% DMSO. The incubations were performed for 6 hours under a humidified atmosphere containing 5% CO_2. The test compounds were also incubated in HepatoZYME only, under the same conditions to identify products of chemical instability.

The reactions were stopped by adding an equal volume of acetonitrile. They were then stored at -20°c for 4hrs to fully precipitate the proteins before centrifugation at 4000g for 30min.

The supernatant was transferred to analysis vial and evaporated with nitrogen then reconstituted with 5µM ammonium acetate in water containing 10% acetonitrile. 250µl of this solution was injected for analysis. LC-MS/MS analyses were performed on an Agilent 1100 HPLC (Agilent technologies, USA) coupled to a Q-Tof Premier mass spectrometer (Waters, Manchester, UK).The MS data was acquired in positive electrospray ionisation mode, with a Z-spray interface. Data were acquired from 50 to 1000Da with a 1s cycle time. Collision energy was set to 5V, 20V and 40V (Function 1, 2 and 3 respectively). The desolvation temperature used was 200°C, while the source temperature was 100°C. During acquisition, the reference chanel of the LockSpray interface was operated with a solution of leucine-enkephalin (200pg/ml), with a reference ion of 556.2771.

6.11 CYP450 inhibition experiments for tetrazole aminoquinolines (Chapter 2)

The P450 inhibition potential of the compounds was assessed by incubating 0.078–20 lM of the compoundswith known specific P450 isoform substrates in human liver microsomes.The probe substrate concentrations were less than or equal to their Km. The percentage decrease in formation of the specific metabolites was monitored by LC/MS using a triple quadrupole Quattro Ultima mass spectrometer (Waters, Milford, USA). The probe substrate reactions monitored were; phenacetin O-deethylation (CYP1A2), coumarin 7-hydroxylation (CYP2A6), bupropion hydroxylation (CYP2B6), paclitaxel 6a-hydroxylation (CYP2C8), diclofenac 40-hydroxylation (CYP2C9), S-mephenytoin 40-hydroxylation (CYP2C19), bufuralol 10-hydroxylation (CYP2D6), chlorzoxazone 6-hydroxylation (CYP2E1), midazolam 10-hydroxylation and testosterone 6b-hydroxylation (3A4). Known specific P450 isoform inhibitors were used as positive controls. Further details of the methodology, including references to the probe substrate concentrations used and their Km are as previously published.[9]

6.12 Docking experiments for tetrazole aminoquinolines

The docking experiments relied on a crystal structure CYP3A4 in complex with its inhibitor, ketoconazole, with a resolution of 2.80 Å (PDB ID: 2V0M). Details of the docking protocol have previously been published.[1,2]

6.13 StarDrop predictions of physicochemical properties and CYP450 sites of metabolism

Chemical structures were drawn directly in StarDrop 5.5 or imported in the smiles format from ChemBioDraw Ultra 11.0. There were no user adjustable settings. The CYP450 models took about 5-10min per compound. Predictions of physicochemical properties were based on QSAR models and therefore only required a few seconds for the entire compound set.[10]

6.14 References

(1) Tukulula, M.; Njoroge, M.; Mugumbate, G. C.; Gut, J.; Rosenthal, P. J.; Barteau, S.; Streckfuss, J.; Heudi, O.; Kameni-Tcheudji, J.; Chibale, K. Tetrazole-Based Deoxyamodiaquines: Synthesis, ADME/PK Profiling and Pharmacological Evaluation as Potential Antimalarial Agents. *Bioorg. Med. Chem.* **2013**, *21*, 4904–4913.

(2) Tukulula, M.; Njoroge, M.; Abay, E. T.; Mugumbate, G. C.; Wiesner, L.; Taylor, D.; Gibhard, L.; Norman, J.; Swart, K. J.; Gut, J.; et al. Synthesis and in Vitro and in Vivo Pharmacological Evaluation of New 4-Aminoquinoline-Based Compounds. *ACS Med. Chem. Lett.* **2013**, *4*, 1198–1202.

(3) Singh, K.; Kaur, G.; Mjambili, F.; Smith, P. J.; Chibale, K. Synthesis of Metergoline Analogues and Their Evaluation as Antiplasmodial Agents. *MedChemComm* **2014**, *5*, 165.

(4) Di, L.; Kerns, E. H.; Gao, N.; Li, S. Q.; Huang, Y.; Bourassa, J. L.; Huryn, D. M. Experimental Design on Single-Time-Point High-Throughput Microsomal Stability Assay. *J. Pharm. Sci.* **2004**, *93*, 1537–1544.

(5) Di, L.; Kerns, E. H.; Hong, Y.; Chen, H. Development and Application of High Throughput Plasma Stability Assay for Drug Discovery. *Int. J. Pharm.* **2005**, *297*, 110–119.

(6) Valente, E.; Simões, M. F.; Testa, B.; Constantino, L. Development of a Method to Investigate the Hydrolysis of Xenobiotic Esters by a Mycobacterium Smegmatis Homogenate. *J. Microbiol. Methods* **2011**, *85*, 98–102.

(7) Jones Jr, E.; Bramwell, C. Automated Software for QQQ/LIT Method Creation and Data Reduction. *Drug Metab. Rev.* **2006**, *38*, 195–195.

(8) Jian, W.; Liu, H.-F.; Zhao, W.; Jones, E.; Zhu, M. Simultaneous Screening of Glutathione and Cyanide Adducts Using Precursor Ion and Neutral Loss Scans-Dependent Product Ion Spectral Acquisition and Data Mining Tools. *J. Am. Soc. Mass Spectrom.* **2012**, *23*, 964–976.

(9) Fasinu, P. S.; Gutmann, H.; Schiller, H.; James, A.-D.; Bouic, P. J.; Rosenkranz, B. The Potential of Sutherlandia Frutescens for Herb-Drug Interaction. *Drug Metab. Dispos.* **2013**, *41*, 488–497.

(10) StarDrop - Optibrium www.optibrium.com/StarDrop (accessed Jun 12, 2014).